# Arginine metabolism in immunity and cancer




**Andreas Hadjinicolaou**

**Radcliffe Department of Medicine**

**Merton College**

**University of Oxford**

**This thesis is submitted for the degree of**

***Doctor of Philosophy***

**Trinity 2018**

# Abstract

Amino acid catabolism causing nutritional stress has emerged as a key immune escape mechanism in cancer to suppress tumour-specific lymphocytes. Here, we show that Arginase-2, the enzyme that breaks down arginine, is released in the blood of acute myeloid leukaemia (AML) patients and mouse models to deplete systemic arginine and inhibit T-cell proliferation and effector function, effects that are abrogated by use of Arginase inhibitors. Importantly, we reveal that the genetic reprogramming in response to arginine starvation differs between cancer cells and activated T-cells in a way that only cancer cells continue to proliferate in the absence of arginine by taking up and converting citrulline to arginine. This dichotomy is accounted for by the cancer-specific ability to upregulate ASS1, the enzyme controlling conversion of citrulline to arginine. ASS1 knockdown in cancer cells completely abrogates proliferation in arginine-free conditions. Furthermore, we show that ASS1 upregulation is regulated by the transcription factor ATF4, which binds an internal enhancer in the ASS1 locus, along with its partner CEBPβ. ATF4/CEBPβ binding at this enhancer is high in cancer cells and augmented further upon amino acid depletion, whereas it is absent in T-cells. This discrepancy is explained by the presence of DNA methylation, H3K27me3 and H3K9me2/3, epigenetic modifications that create repressive chromatin at the ASS1 enhancer in T-cells but not cancer cells. ATF4 knockdown or deletion of the ATF4-binding site in the ASS1 enhancer abolishes the proliferative advantage displayed by cancer cells in arginine-free conditions. Finally, we reveal the citrulline transporters used by cancer cells and confirm that our findings are clinically relevant since, compared to healthy controls, AML patients have higher serum citrulline levels and possess leukaemic blasts with greater ASS1 and ATF4 expression. In conclusion, we identify arginine metabolism as a cancer immune evasion strategy and elucidate the adaptive mechanisms by which cancer cells, but not T-cells, resist arginine depletion in the tumour microenvironment. Our findings identify the epigenetic basis of a clinically relevant phenotype and reveal potential targets for cancer immunotherapy.

# Acknowledgements

Firstly, I would like to thank my supervisors, Professors Enzo Cerundolo and Paresh Vyas for their continuous support and for the opportunity to work in their labs. I am particularly grateful to Enzo for his trust, scientific guidance, inspiration and friendship that have allowed me to fulfil my potential and grow not only as a scientist but also as a person. I am also grateful to Paresh for his co-supervision and his invaluable scientific insight that have made me a better academic clinician. I would also like to thank all the members of the Cerundolo lab, past and present, that have helped me during difficult times and shared my joy during moments of success. I have learnt something from each and every one of them and for this I am grateful. Special thanks go to Mashiko, Uzi, Gennaro, Ji-Li, Corinna, Laura, Claudia, Prathiba, Anne, Mao, Elina, Mike, Hemza and Dawn. I would also like to thank all of our collaborators especially Nick and Tom for believing in my work and empowering me to take it to a higher level as true advocates of a multidisciplinary approach to science. Their attitude has inspired me to take this collaborative spirit with me to my future endeavours. Furthermore, I have to express my gratitude to the Wellcome Trust for generously sponsoring my work through a PhD Fellowship for clinician-scientists. This work would not have been possible with this funding. I would also like to thank the Medical Research Council (MRC) Human Immunology Unit, Cancer Research UK, the Harry Mahon Cancer Research Trust, the Ludwig Institute of Cancer Research and the A.G. Leventis Foundation for further funding this work. Finally, I would like to express my eternal gratitude to my family who have been by my side throughout this tough challenge. As such I would like to dedicate this work to my parents, my sister and my wife, Lina, for their unconditional love and support for as long as I can remember. Although this was a tough test of perseverance and endurance, I never felt I was alone during my DPhil journey.

# Statement of authorship

I declare that this thesis represents my own work, except where stated below and in the text. This work has not been submitted for any other degree. The following parts of this thesis have been executed in collaboration with other scientists:

- Plasma from AML patients was obtained in collaboration with Jessica Doondea[1] (Paresh Vyas group).
- Serum from mouse models was obtained in collaboration with Dr Chris Booth[2] (Adam Mead group; spontaneous AML model), Dr Amit Grover[3] and Mr Alexander Thomas[3] (Claus Nerlov group; inducible AML model) and Dr Tom Riffelmacher[4] (Katja Simon group; autophagy-deficient myeloproliferative disease model).
- RNA extraction and RNA-seq analysis of human AML blasts and healthy control myeloid cells was performed in collaboration with Dr Lynn Quek[1].
- Illumina gene expression microarray was carried out with help from the High-Throughput Genomics Group at the Wellcome Trust Centre for Human Genetics (funded by Wellcome Trust grant reference 090532/Z/09/Z) and analysed in collaboration with Dr Steve Taylor[5] and Dr Lars Rønn Olsen[6].
- DeepBind computational analysis for identification of transcription factor-binding motifs within the *ASS1* locus was done in collaboration with Dr Hashem Koohy[5].

---

[1] Normal and Malignant Haematopoiesis Lab (Vyas group), MRC Molecular Haematology Unit, Weatherall Institute of Molecular Medicine, University of Oxford, Oxford, United Kingdom
[2] Haematopoietic Stem Cell Biology Lab (Mead group), MRC Molecular Haematology Unit, Weatherall Institute of Molecular Medicine, University of Oxford, Oxford, United Kingdom
[3] Haematopoietic Stem Cell Genetics Lab (Nerlov group), MRC Molecular Haematology Unit, Weatherall Institute of Molecular Medicine, University of Oxford, Oxford, United Kingdom
[4] Autophagy in the Immune System Lab (Simon group), MRC Human Immunology Unit, Weatherall Institute of Molecular Medicine, University of Oxford, Oxford, United Kingdom
[5] MRC WIMM Centre for Computational Biology, Weatherall Institute of Molecular Medicine, University of Oxford, Oxford, United Kingdom
[6] Center for Biological Sequence Analysis, Department of Systems Biology, Technical University of Denmark, Lyngby, Denmark

- The transduction procedure to generate ASS1-expressing T-cells as well as the analysis of the proliferation of these cells by flow cytometry were carried out in collaboration with Dr Uzi Gileadi[7].
- The Incucyte-based killing assay was carried out in collaboration with Dr Ji-Li Chen[7] who also provided the NY-ESO-1-specific $CD8^+$ T cell clone (4D8) used in the assay.
- CRISPR silencing of SLC7A5 (LAT1) in HeLa was performed by Dr Hemza Ghadbane[7] and Dr Elina Timosenko[7].
- CRISPR silencing of the ATF4 binding motif within the ASS1 intronic enhancer was carried out in collaboration with Dr Nicholas Crump[8] (Tom Milne group).
- Experiments to measure intracellular amino acid concentrations and heavy-labeled amino acid influx by LC-MS were carried out in collaboration with Dr Zhanru Yu[9] (Benedikt Kessler group).
- ChIP-qPCR, ChIP-seq, ATAC-seq and bisulfite sequencing experiments were carried out in collaboration with Dr Nicholas Crump[8] and Prof Tom Milne[8] (Tom Milne group) and Dr Mashiko Setshedi[7].

[7] Cerundolo group, MRC Human Immunology Unit, Weatherall Institute of Molecular Medicine, University of Oxford, Oxford, United Kingdom
[8] Epigenetics and Gene Regulation in Leukaemia Lab (Milne group), MRC Molecular Haematology Unit, Weatherall Institute of Molecular Medicine, University of Oxford, Oxford, United Kingdom
[9] Mass Spectrometry Lab (Kessler group), Target Discovery Institute, Nuffield Department of Medicine, University of Oxford, Oxford, United Kingdom

# Table of Contents

**INDEX OF FIGURES** ..... **14**

**INDEX OF TABLES** ..... **21**

**CHAPTER 1: INTRODUCTION** ..... **25**

1.1 OVERVIEW OF THE IMMUNE SYSTEM ..... 25

1.1.2 Innate immunity ..... 25

1.1.3 Adaptive immunity ..... 26

1.2 CANCER IMMUNOSURVEILLANCE AND ANTI-TUMOUR IMMUNITY ..... 27

1.2.1 Tumour-specific immune responses ..... 27

1.2.2 Immunoediting theory ..... 27

1.3 MECHANISMS OF CANCER IMMUNE EVASION AND THE TUMOUR MICROENVIRONMENT 28

1.3.1 Immune evasion by hijacking antigen presentation ..... 28

1.3.2 Tumour microenvironment ..... 28

1.3.2.1 Immune evasion by hijacking immune checkpoint molecules ..... 28

1.3.2.2 Immune evasion by recruitment of immunosuppressive cell populations ..... 29

1.3.2.3 Immune evasion by release and expression of inhibitory immune mediators ..... 30

1.3.2.4 Immune evasion by generation of metabolic stress through nutritional starvation ..... 30

1.4 ARGININE PHYSIOLOGY ..... 31

1.4.1 Arginine function ..... 31

1.4.2 Arginine metabolism ..... 31

1.4.2.1 Arginine sources and arginine synthesis ..... 31

1.4.2.2 Arginine catabolism and the Arginase isoenzymes ..... 32

1.4.2.3 Arginase-1 (ARG1) ..... 33

1.4.2.4 Arginase-2 (ARG2) ..... 33

1.5 THE ROLE OF ARGINASE IN PHYSIOLOGY AND PATHOLOGY ..... 34

1.5.1 Neutralisation of toxic substances through the hepatic urea cycle ..... 34

1.5.2 Regulation of nitric oxide biosynthesis ..... 35

1.5.3 Regulation of ornithine, proline and polyamines biosynthesis ..... 36

1.5.4 Modulation of immune responses ..... 36

1.5.4.1 Role in macrophage function ....36
1.5.4.2 Role in infection ....37
1.5.4.3 Role in regulation of T-cell function ....38
1.5.4.4 Role in autoimmunity ....38
1.5.4.5 Role in pregnancy ....39
1.5.4.6 Role in antigen presentation ....39
1.6 ARGINASE IN THE TUMOUR MICROENVIRONMENT ....40
1.6.1 The role of Arginase as a pro-tumourigenic enzyme ....40
1.6.2 Arginase utilization by cancers ....40
1.6.3 Arginase utilization by cancer-promoting cell populations ....41
1.6.3.1 Myeloid-derived suppressor cells (MDSCs) ....41
1.6.3.2 Tumour -associated macrophages (TAMs), ....42
1.6.3.3 Cancer-associated fibroblasts (CAF) ....42
1.7 THERAPEUTIC AVENUES IN CANCER IMMUNOTHERAPY BY TARGETING ARGINASE ....43
1.8 THE FUNCTION AND REGULATION OF ARGININOSUCCINATE SYNTHASE (ASS1) ....44
1.8.1 Role in the urea cycle and conversion of citrulline to arginine ....44
1.8.2 Sub-cellular localization of ASS1 ....44
1.8.3 Regulation of expression of ASS1 ....45
1.8.4 The physiological role of ASS1 ....46
1.8.5 The role of ASS1 in cancer ....47
1.9 SENSING OF AMINO ACID STARVATION: THE GCN2-ATF4 AND MTOR PATHWAYS ....48
1.9.1 The GCN2-ATF4 pathway ....48
1.9.2 The mTOR pathway ....49
1.10 ARGININE TRANSPORT AND THE CATIONIC AMINO ACID TRANSPORTER FAMILY ....50
1.10.1 The solute carrier (SLC) super-family of transmembrane amino acid transporters ....50
1.10.2 The diversity in SLC localisation, function and specificity ....50
1.10.3 system y+L: The cationic amino acid transporters ....50
1.10.3.1 The SLC7A1 (CAT1) transporter ....51
1.10.4 System L: the neutral large amino acid transporter system ....52
1.10.4.1 The SLC7A5 (LAT1) transporter ....52
1.10.5 System $x^-_c$ : the neutral small amino acid transporter system ....52
1.10.5.1 The SLC1A5 (ASCT2) transporter ....53

1.10.6 The role of SLC transporters in cancer ..... 53
1.11 ACUTE MYELOID LEUKEMIA (AML) ..... 54
1.11.1 Introduction and epidemiology of AML ..... 54
1.11.2 Diagnosis and Treatment of AML ..... 54
1.11.3 Anti-leukaemic immunity and the role of the immune system in AML treatment ..... 55
1.12 PROJECT AIMS ..... 56
**CHAPTER 2: MATERIALS AND METHODS ..... 60**
2.1 CELL LINES AND CULTURE MEDIA ..... 60
2.2 REAGENTS ..... 61
2.2.1 Antibodies for Western blotting ..... 61
2.2.2 Antibodies for Fluorescence-activated cell sorting (FACS) ..... 62
2.2.3 Chemicals ..... 63
2.3 HUMAN SAMPLES ..... 64
2.3.1 Generation and activation of human $CD4^+$ and $CD8^+$ T cells ..... 65
2.4 MICE ..... 66
2.4.1 AML mouse models ..... 66
2.4.2 Mouse serum preparation ..... 67
2.5 DIFFERENTIAL GENE EXPRESSION ANALYSIS ..... 67
2.5.1 Microarray ..... 67
2.5.1.1 Differential gene expression analysis of microarray data ..... 68
2.5.1.2 Gene set enrichment analysis ..... 68
2.5.2 Real-time quantitative reverse transcription PCR (q-RT-PCR) ..... 68
2.5.3 Transcriptome sequencing (RNA-seq) ..... 69
2.6 GENERATION OF ARG2-OVEREXPRESSING THP1 CELLS ..... 70
2.6.1 Cloning of ARG2 gene ..... 70
2.6.2 Transformation of bacteria ..... 73
2.6.3 Transfection and Lentiviral Transduction ..... 73
2.7 GENERATION OF RECOMBINANT HUMAN ARGINASE-2 (RHARG2) ..... 74
2.8 OVEREXPRESSION OF ASS1 GENE IN PRIMARY HUMAN T-CELLS ..... 75
2.9 CRISPR-CAS9-MEDIATED GENE SILENCING ..... 76
2.10 SHRNA-MEDIATED GENE KNOCKDOWN ..... 76
2.11 ARGINASE ACTIVITY ASSAY ..... 77

2.12 ELISA (ENZYME-LINKED IMMUNOSORBENT ASSAY) ..... 79
2.12.1 Arginase-1 and Arginase-2 measurements ..... 79
2.12.2 Interferon-gamma (IFN-γ) measurements ..... 79
2.12.3 Arginine measurements ..... 81
2.12.4 Citrulline measurements ..... 81
2.13 PROTEIN EXPRESSION ANALYSIS ..... 82
2.13.1 Cell lysis ..... 82
2.13.2 Quantification of protein concentration ..... 82
2.13.3 Western blotting ..... 82
2.14 FLOW CYTOMETRY ..... 84
2.14.1 Live-Dead staining ..... 84
2.14.2 CFSE and CTV staining ..... 84
2.14.3 Cell surface marker staining ..... 84
2.14.4 Intracellular (cytoplasmic) staining ..... 85
2.14.5 Running of samples ..... 85
2.15 INCUCYTE KILLING ASSAY ..... 86
2.16 BIOENERGETIC PROFILING TO EVALUATE CANCER CELL GLYCOLYSIS AND OXIDATIVE PHOSPHORYLATION ..... 87
2.16.1 Sample preparation and overview of metabolic experiments ..... 87
2.16.2 Glycolysis stress test analysis ..... 88
2.16.3 Mitochondrial respiration stress test analysis ..... 89
2.17 METABOLOMIC ANALYSIS ..... 91
2.17.1 Intracellular amino acid measurements by liquid-chromatography mass-spectrometry (LC-MS) ..... 91
2.17.2 Heavy-labeled amino acid influx measurements for amino acid cellular uptake ..... 93
2.18 CHROMATIN IMMUNOPRECIPITATION (CHIP) ..... 94
2.18.1 DeepBind analysis to identify transcription factor binding sites ..... 96
2.19 EVALUATION OF DNA ACCESSIBILITY USING ASSAY FOR TRANSPOSASE-ACCESSIBLE CHROMATIN WITH HIGH THROUGHPUT SEQUENCING (ATAC-SEQ) ..... 97
2.19.1 Sequencing process for ChIP and ATAC analysis ..... 97
2.20 ASSESSMENT OF DNA METHYLATION BY BISULFITE SEQUENCING ..... 98
2.21 STATISTICAL ANALYSIS ..... 99

**CHAPTER 3: ARGINASE-MEDIATED ARGININE DEGRADATION IN AML: EFFECTS ON T-CELLS AND THERAPEUTIC TARGETS FOR CANCER IMMUNOTHERAPY ..... 100**

3.1 INTRODUCTION ..... 100

3.2 ARGINASE-2 PROTEIN LEVELS AND ENZYMATIC ACTIVITY ARE HIGH IN AML PATIENT PLASMA ..... 100

3.3 ARGINASE-2 PROTEIN LEVELS AND ENZYMATIC ACTIVITY ARE ALSO HIGH IN AML MOUSE MODELS LEADING TO SYSTEMIC ARGININE DEPLETION ..... 102

3.3.1 A spontaneous AML mouse model shows higher Arginase activity and lower serum arginine levels than healthy control mice ..... 102

3.3.2 High Arginase activity in the spontaneous AML mouse model is purely due to the presence of high serum concentration of Arginase-2 with no contribution from Arginase-1 ..... 104

3.3.3 Serum Arginase activity in the spontaneous AML mouse model is closely linked to clinical indices of disease ..... 108

3.3.4 An inducible AML mouse model also shows high serum Arginase activity that increases over time with enhanced disease burden ..... 109

3.3.5 Serum Arginase activity is closely linked to clinical indices of disease in the inducible AML mouse model too ..... 111

3.3.6 A mouse model of myeloproliferative disease also shows high serum Arginase activity because of high serum levels of the Arginase-2 enzyme ..... 114

3.4 GENERATION OF RECOMBINANT HUMAN ARGINASE-2 PROTEIN ..... 118

3.5 EVALUATION OF NOVEL ARGINASE INHIBITORS TO BLOCK ARGINASE-2 ACTIVITY ..... 123

3.5.1 Novel small molecule Arginase inhibitors can effectively block the enzymatic activity of the synthetic rhARG2 ..... 123

3.5.2 Novel small molecule Arginase inhibitors can effectively block the enzymatic activity of Arginase-2 from the mitochondria of human cancer cells in culture ..... 125

3.6 ARGINASE-2 INHIBITS PROLIFERATION OF STIMULATED T-CELLS, AN EFFECT THAT IS REVERSIBLE WITH USE OF NOVEL SMALL MOLECULE ARGINASE INHIBITORS ..... 129

3.6.1 The novel small molecule Arginase inhibitor, OAT-081, can rescue T-cell proliferation in the presence of recombinant human Arginase-2 (rhARG2) ..... 129

3.6.2 The novel small molecule Arginase inhibitor, OAT-081, can rescue T-cell proliferation in the presence of human mitochondria expressing Arginase-2 ..... 131

3.7 Recombinant human Arginase-2 (rhARG2) and arginine starvation cause downregulation of surface CD3 in stimulated T-cells .....135
3.8 Recombinant human Arginase-2 (rhARG2) and arginine starvation inhibit the mTOR pathway in stimulated T-cells .....136
3.9 Recombinant human rhARG2 inhibits T-cell effector function by suppressing production of interferon gamma (IFN-γ) .....138
3.10 AML plasma-derived Arginase-2 suppresses the cancer killing ability of effector CD8+ T-cells .....139
3.11 Discussion .....141

**CHAPTER 4: THE EFFECT OF (ARGINASE-DEPENDENT) ARGININE STARVATION ON THE EXPRESSION PROFILE OF GENES INVOLVED IN AMINO ACID METABOLISM AND TRANSPORT IN CANCER CELLS AND T-CELLS.....146**

4.1 Introduction.....146
4.2 The signatures of differential gene expression in cancer cells and T-cells upon arginine deprivation show both similarities and differences.....147
4.3 Arginine starvation induces a genetic reprogramming in cancer cells but not T-cells that involves upregulation of proteins involved in arginine metabolism and might be driven by the ATF4 transcription factor .....150
4.4 ASS1 is upregulated in response to arginine starvation in cancer cells but not T-cells although an ATF4-based response is mounted in both cell types154
4.5 ASS1 is required for citrulline metabolism to promote cancer cell growth in the absence of arginine.....157
4.6 Arginine starvation does not induce ASS1 upregulation in monocytes suggesting that ASS1 upregulation in THP1 cells is a cancer-specific rather than a lineage-specific effect .....158
4.7 Analysis of the ASS1 upregulation kinetics .....160
4.8 Treatment with Arginase-2 has similar transcriptional and translational effects in THP1 cancer cells as their exposure to arginine starvation .....161
4.9 ASS1 upregulation in response to arginine starvation is an effect that occurs globally in multiple cancer cell lines .....163
4.10 Citrulline uptake in THP1 cancer cells is dependent on the SLC7A5 (LAT1) and SLC1A5 amino acid transporters .....167

4.11 UPTAKE OF EXTRACELLULAR CITRULLINE IS NECESSARY FOR DE NOVO ARGININE SYNTHESIS INTRACELLULARLY BY THP1 CANCER CELLS ..... 171
4.12 ARGININE DEPRIVATION ALSO AFFECTS GLUCOSE METABOLISM IN CANCER CELLS BY REVERSING THE WARBURG EFFECT ..... 173
4.13 UPREGULATION OF ATF4 AND ASS1 TO UTILIZE EXTRACELLULAR CITRULLINE IS CLINICALLY RELEVANT IN THE CONTEXT OF AML ..... 178
4.13.1 ASS1 and ATF4 show higher expression in AML blasts compared to healthy myeloid cells ..... 178
4.13.2 Plasma citrulline levels are higher in AML patients compared to healthy controls ..... 179
4.13.3 Mouse AML blasts behave similar to human ones in that they can utilize citrulline to grow in arginine-depleted conditions ..... 180
4.14 DISCUSSION ..... 181

**CHAPTER 5: THE DISCREPANCY BETWEEN CANCER CELLS AND T-CELLS IN ADAPTING TO ARGININE STARVATION CAN BE EXPLAINED BY DIFFERENCES IN EPIGENETIC REGULATION OF ASS1 EXPRESSION..... 188**

5.1 ATF4-DEPENDENT ASS1 EXPRESSION IS REQUIRED FOR CITRULLINE UTILISATION TO PROMOTE THP1 GROWTH IN ARGININE-DEPRIVED CONDITIONS ..... 188
5.2 ATF4-DEPENDENT ASS1 EXPRESSION IS REQUIRED FOR THE GROWTH OF SOLID TUMOUR HELA CELLS IN THE ABSENCE OF ARGININE SUGGESTING IT IS A PHENOMENON APPLICABLE TO A VARIETY OF CANCERS ..... 192
5.3 GAIN-OF-FUNCTION STUDIES SHOW THAT ASS1 EXPRESSION IS SUFFICIENT TO PERMIT T-CELL PROLIFERATION IN THE ABSENCE OF ARGININE AND PRESENCE OF CITRULLINE ..194
5.4 ASS1 EXPRESSION IS DEPENDENT ON EPIGENETICALLY REGULATED BINDING OF ATF4 TO AN INTERNAL ENHANCER ..... 198
5.5 EXPRESSION OF ASS1 IN THP1 AND T-CELLS IS REGULATED BY CHANGES IN CHROMATIN ACCESSIBILITY ..... 208
5.6 THE ASS1 INTERNAL ENHANCER IS EPIGENETICALLY REPRESSED IN T CELLS ..... 213
5.7 THE REPRESSIVE H3K9ME2/3 MAY BE REGULATED BY KDM4C ..... 219
5.9 EPIGENETICALLY-REGULATED ATF4 BINDING AT THE ASS1 INTRONIC ENHANCER MIGHT BE A PHENOMENON PRESENT IN MANY CANCERS INCLUDING SOLID TUMOURS AND IN RESPONSE TO VARIOUS TYPES OF NUTRITIONAL STRESS ..... 233

5.10 THE EPIGENETIC REGULATION OF ASS1 APPEARS TO BE A CANCER-SPECIFIC ATTRIBUTE RATHER THAN A LINEAGE-RELATED EFFECT ....236
5.11 THE UPREGULATION OF CITRULLINE TRANSPORTERS SLC1A5 AND SLC7A5 UPON ARGININE STARVATION IN THP1 CANCER CELLS MIGHT ALSO BE REGULATED BY ATF4/CEBPB BINDING AT INTERNAL ENHANCERS ....238
5.12 DISCUSSION ....245
**CHAPTER 6: SUMMARY AND CONCLUSIONS ....252**
**REFERENCES ....259**

# Index of Figures

Figure 1 - 1. Arginase-mediated arginine depletion creates an immunosuppressive tumour microenvironment. ....43

Figure 2 - 1. Cloning of *ARG2*-HA into the pHR-SIN-IRES-GFP expression vector ....71
Figure 2 - 2. Representative Glycolysis Stress Test profile of the key parameters of glycolytic function. ....90
Figure 2 - 3. Representative Stress Test profile of the key parameters of mitochondrial respiration. ....91

Figure 3 - 1. Plasma Arginase activity is significantly higher in AML patients compared to healthy controls....101
Figure 3 - 2. Plasma levels of Arginase-2 (ARG2) protein are significantly higher in AML patients compared to healthy controls....102
Figure 3 - 3. Serum Arginase activity is significantly higher in mice with AML compared to healthy control mice....103
Figure 3 - 4. Serum arginine levels are significantly lower in AML mice compared to healthy control mice....104
Figure 3 - 5. Serum levels of Arginase-2 (ARG2) protein are significantly higher in AML mice compared to healthy control mice. ....105
Figure 3 - 6. Arginase-1 (ARG1) protein is not detected in the serum of AML mice or healthy control mice and so cannot be the source of Arginase activity in the AML context. ....106
Figure 3 - 7. Arginase-2 specific activity is most likely responsible for depletion of arginine levels in the serum of AML mice....107
Figure 3 - 8. Arginase activity is associated with clinical indices of AML disease severity. ....109
Figure 3 - 9. Serum Arginase activity is significantly higher in our 'inducible' AML mouse model compared to healthy control mice. ....110
Figure 3 - 10. Serum Arginase activity correlates with disease progression over time....111

Figure 3 - 11. Arginase activity is associated with clinical indices of AML disease severity in an inducible AML mouse model. .....114
Figure 3 - 12. Serum Arginase activity is significantly higher in autophagy-deficient mice with myeloproliferative disease compared to healthy control mice. .....115
Figure 3 - 13. Serum levels of Arginase-2 protein are significantly higher in autophagy-deficient mice with myeloproliferative disease compared to healthy control mice. .....116
Figure 3 - 14. Arginase activity in the serum of mice with myeloproliferative disease does not source from Arginase-1, which has undetectable levels in both diseased and healthy control mice. .....117
Figure 3 - 15. Arginase activity seems to be purely due to the presence of Arginase-2 protein in the serum of mice with myeloproliferative disease. .....118
Figure 3 - 16. De novo generation of a highly purified and active recombinant human Arginase-2 (rhARG2) protein.....122
Figure 3 - 17. The hydrolytic reaction of arginine breakdown. .....124
Figure 3 - 18. Small molecule inhibitors OAT081 and OAT090 can inhibit rhARG2. ....124
Figure 3 - 19. Small molecule inhibitor OAT081 can inhibit rhARG2 at various concentrations. .....125
Figure 3 - 20. ARG2-overexpressing THP1 cells have significant Arginase activity that originates in the mitochondria. .....127
Figure 3 - 21. ARG2-overexpressing THP1 cells express significant amounts of Arginase-2 protein that originates in the mitochondria. .....127
Figure 3 - 22. Intact mitochondria from ARG2-overexpressing THP1 cells can break down and thus deplete arginine in culture medium.....128
Figure 3 - 23. Novel Arginase-specific small molecule inhibitors can block Arginase-2 present in mitochondria from ARG2-THP1 cells. .....129
Figure 3 - 24. rhARG2 can inhibit proliferation of stimulated T-cells, an effect that can be abrogated by Arginase inhibitors. .....131
Figure 3 - 25. Gating strategy used to select and analyse live CD8+ T-cells. .....133
Figure 3 - 26. Free intact mitochondria from THP1 overexpressing Arginase-2 can inhibit proliferation of stimulated murine T-cells, an effect that can be abrogated by Arginase inhibitors.....134

Figure 3 - 27. rhARG2 treatment and arginine starvation inhibit lead to downregulation of the CD3 co-receptor in stimulated T-cells, an effect that can be prevented by Arginase inhibitors.....135
Figure 3 - 28. Treatment of stimulated T-cells with rhARG2 or arginine-depleted culture medium abolishes the phosphorylation of S6, a surrogate marker of the mTOR pathway activation involved in cell proliferation. .....137
Figure 3 - 29. rhARG2 suppresses interferon gamma (IFN-γ) release suppressing CD4+ T-cell effector function. .....139
Figure 3 - 30. Arginase in AML plasma suppresses the cancer killing ability of effector CD8+ T-cells. .....141

Figure 4 - 1. The signature of differential gene expression upon arginine starvation differs between cancer cells and T-cells. .....148
Figure 4 - 2. Comparison of up- and down-regulated genes in THP1 and T-cells following arginine starvation.....149
Figure 4 - 3. A significant number of genes upregulated upon arginine starvation in THP1 cells but not T-cells belong to the arginine biosynthesis pathway and contain binding motifs for the transcription factor ATF4. .....152
Figure 4 - 4. Forest plot showing changes of expression of key genes involved in arginine uptake and metabolism.....153
Figure 4 - 5. Stimulated T-cells downregulate the expression of ARG2 in response to arginine to starvation.....154
Figure 4 - 6. Schematic diagram showing the roles of key genes in arginine uptake and metabolism. .....155
Figure 4 - 7. Arginine starvation induces upregulation of ASS1 RNA only in THP1 cells but upregulation of ATF4 RNA in both THP1 and T-cells.....156
Figure 4 - 8. Arginine starvation induces upregulation of ASS1 protein only in THP1 cells but upregulation of ATF4 protein in both THP1 and T-cells. .....157
Figure 4 - 9. THP1 cells can use citrulline as an alternative arginine source and can thus proliferate in arginine-free conditions whereas T-cells fail to do so. .....158
Figure 4 - 10. Arginine starvation does not induce upregulation of ASS1 RNA in CD14+ monocytes unlike THP1 cells suggesting this is a cancer-specific rather than a lineage-specific effect.....159

Figure 4 - 11. ASS1 protein levels in THP1 cells increase with time to a maximum at 96hr after exposure to arginine starvation whereas the presence of citrulline can partially drive ASS1 expression even in sufficient arginine levels.....160
Figure 4 - 12. Arginine-starvation-induced upregulation of ASS1, ATF4, SLC7A1 and SLC7A5 in THP1 cells is recapitulated by incubation of cells with recombinant human Arginase-2 (rhARG2). .....162
Figure 4 - 13. THP1 cells display elevated ASS1 protein levels upon incubation of with rhARG2 and can thus utilize exogenous citrulline and proliferate despite rhARG2-induced arginine depletion in culture.....162
Figure 4 - 14. ASS1 upregulation upon arginine depletion is also observed in human solid tumour cell lines, such as HeLa (cervical cancer) and LNCAP (prostate cancer), where it allows cancer cells to utilise citrulline and proliferate in the absence of arginine. .....164
Figure 4 - 15. ASS1 upregulation, at gene and protein level, upon arginine depletion is also observed in the human bladder cancer cell line RT112, where it allows cancer cells to utilise citrulline and proliferate in the absence of arginine. .....165
Figure 4 - 16. ASS1 upregulation upon arginine depletion is also observed in various human leukaemic cell lines, such as MOLM-13 (AML), OCI-AML (AML) and HL-60 (APML) where it allows cancer cells to utilise citrulline and proliferate in the absence of arginine.....166
Figure 4 - 17. ASS1 upregulation, at gene and protein level, upon arginine depletion is also observed in the human acute promyelocytic leukaemia (APML) cell line NB-4, where it allows cancer cells to utilise citrulline and proliferate in the absence of arginine. .....167
Figure 4 - 18. Extracellular citrulline is imported into THP1 cancer cells through the transmembrane amino acid transporters SLC7A5 and SLC1A5, which are upregulated in response to arginine starvation. .....169
Figure 4 - 19. Deletion of the SLC7A5 gene, which is upregulated in response to arginine starvation in HeLa cells, reduces the rate of citrulline-dependent cancer cell growth. .....170
Figure 4 - 20. Citrulline is taken up by THP1 cancer cells and in its presence, newly-formed arginine is detected intracellularly.....172
Figure 4 - 21. In response to arginine starvation, citrulline is taken up by THP1 cancer cells and converted to *de novo* arginine intracellularly.....173
Figure 4 - 22. Arginine starvation inhibits the glycolytic activity of cancer cells an effect that is reversed by citrulline supplementation. .....175

Figure 4 - 23. Arginine starvation promotes mitochondrial respiration in cancer cells an effect that is reversed by citrulline supplementation. .....176
Figure 4 - 24. Forest plot showing arginine starvation leads to downregulation in expression of key genes involved in the glycolysis and gluconeogenesis pathway in THP1 and T-cells. .....177
Figure 4 - 25. ATF4 and ASS1 are overexpressed in AML blasts from patients compared to myeloid cell populations from healthy controls. .....178
Figure 4 - 26. Citrulline levels are higher in plasma from AML patients compared to healthy controls and are sufficient to support THP1 cell proliferation in the absence of arginine.....180
Figure 4 - 27. Similar to THP1 cancer cells, primary AML blasts from our CEBPα mouse model can also use citrulline as an alternative arginine source to proliferate in arginine-free conditions. .....181

Figure 5 - 1. ASS1 upregulation in response to arginine starvation is dependent on the transcription factor ATF4.....190
Figure 5 - 2. Citrulline-dependent growth of THP1 cells under arginine starvation is dependent on both ASS1 and ATF4. .....191
Figure 5 - 3. ASS1 upregulation in HeLa cells is also abrogated by ATF4 knockdown...193
Figure 5 - 4. Citrulline-dependent growth of HeLa cells under arginine starvation is dependent on ATF4.....193
Figure 5 - 5. Genetic modification of T-cells to achieve exogenous expression of ASS1 enables citrulline-dependent growth under arginine starvation.....197
Figure 5 - 6. ATF4 and CEBPβ have more binding sites in THP1 cells than T-cells and a large proportion of these sites are shared by the two transcription factors. .....201
Figure 5 - 7. ATF4 and CEBPβ ChIP-seq in THP1, HeLa and T-cells reveals the presence of a tumour-preferred enhancer within the first intron of the ASS1 locus.....203
Figure 5 - 8. ATF4 and CEBPβ ChIP-seq in THP1, HeLa and T-cells reveals the presence of a global, non-tumour-specific enhancer near the promoter of the SLC7A1 and ASNS loci.....205
Figure 5 - 9. ATF4 ChIP-qPCR shows that ATF4 binding at the ASS1 intronic enhancer only occurs in THP1 cells but not T-cells and is augmented in response to arginine starvation. .....205

Figure 5 - 10. Deletion of the ATF4-binding motif sequence in the ASS1 intronic enhancer in THP1 abolishes ATF4 binding, ASS1 expression and citrulline utilization. ..... 208
Figure 5 - 11. ATAC-Seq reveals decreased chromatin accessibility for ATF4/ CEBPβ transcription factors to bind at the ASS1 intronic enhancer in T-cells compared to THP1 cancer cells. ..... 211
Figure 5 - 12. ATAC-Seq reveals no differences between THP1 and T-cells in chromatin accessibility at the ATF4-binding sites in the promoter region of the SLC7A1 and ASNS genes. ..... 213
Figure 5 - 13. Lack of chromatin accessibility and ATF4 binding at the ASS1 intronic enhancer in T-cells is the result of conspicuous repressive heterochromatic histone modifications H3K9me2 and H3K9me3 ..... 216
Figure 5 - 14. High levels of the repressive heterochromatic histone modification H3K27me3 also lead to reduced chromatin accessibility and ATF4 binding at the ASS1 intronic enhancer in T-cells. ..... 216
Figure 5 - 15. DNA methylation at the ASS1 intronic enhancer is more pronounced in T-cells than THP1 cells further restricting chromatin accessibility and ATF4/ CEBPβ binding ..... 219
Figure 5 - 16. SD70 inhibits KDM4C-mediated H3K9 demethylation abrogating ATF4 binding at the ASS1 intronic enhancer in cancer cells. ..... 220
Figure 5 - 17. SD70 inhibits ATF4-mediated ASS1 upregulation in response to arginine starvation in THP1 cells. ..... 221
Figure 5 - 18. KDM4C is overexpressed in AML blasts from patients compared to myeloid cell populations from healthy controls. ..... 222
Figure 5 - 19. The transcription factors ATF4, CEBPβ, Xbp1 and RUNX2 have specific binding sites within the *ASS1* enhancer. ..... 225
Figure 5 - 20. The transcription factors MYC and Xbp1 have specific binding sites within the *ASS1* promoter. ..... 226
Figure 5 - 21. Binding Specificity Score (BSS) analysis confirms strong binding signal for transcription factors ATF4, CEBPβ, Xbp1 and RUNX2 within the *ASS1* enhancer and strong biding signal for transcription factors c-MYC and Xbp1 within the ASS1 promoter. ..... 229

Figure 5 - 22. Sequence analysis confirms an ATF4/CEBPβ binding motif within the *ASS1* intronic enhancer at the exact region where ATF4 and CEBPβ ChIP-seq reveal an overlapping binding site for the two transcription factors. .....230
Figure 5 - 23. CEBPβ ChIP-qPCR shows that CEBPβ binding at the ASS1 intronic enhancer only occurs in THP1 cells but not T-cells and is augmented in response to arginine starvation.....231
Figure 5 - 24. Deletion of the ATF4/ CEBPβ-binding motif sequence in the ASS1 intronic enhancer in THP1 cells abolishes CEBPβ binding in a similar manner that ATF4 binding was abolished.....232
Figure 5 - 25. ATF4 binding at the *ASS1* enhancer is a phenomenon observed not only in THP1 but also HeLa cancer cells and occurs in response to tryptophan starvation in addition to arginine starvation. .....236
Figure 5 - 26. The epigenetic regulation of ASS1 through ATF4/CEBPβ seems to be a cancer-specific attribute rather than a lineage-related effect as monocytes show the same features as T-cells rather than THP1 cancer cells.....238
Figure 5 - 27. ATF4/CEBPβ ChIP-seq, ATAC-seq for chromatin accessibility and histone modification analysis in THP1 cells reveal the presence of an arginine-sensitive intronic enhancer near the promoter of the *SLC1A5* gene locus. .....242
Figure 5 - 28. ATF4/CEBPβ ChIP-seq, ATAC-seq for chromatin accessibility and histone modification analysis in THP1 cells reveal the presence of an arginine-sensitive intronic enhancer near the promoter of the *SLC7A5* gene locus. .....244
Figure 5 - 29. ATF4 ChIP-qPCR shows that ATF4 binding at the *ASNS* promoter and at the *SLC7A5* and *SLC1A5* intronic enhancers occurs in both THP1 cells and T-cells and but is stronger and more significantly augmented in response to arginine starvation in the former. .....244

Figure 6 - 1. Proposed model of the ATF4-dependent cellular response to arginine depletion in the tumour microenvironment.....258

# Index of Tables

Table 2 - 1. Primary antibodies used for Western blotting. .....62
Table 2 - 2. Primary antibodies used for Fluorescence-activated cell sorting (FACS). .....63
Table 2 - 3. Chemicals used for the purposes of this work. .....64
Table 2 - 4. TaqMan® probes used for q-RT-PCR gene expression analysis. .....69
Table 2 - 5. Primers used for cloning and sequencing for generation of ARG2 overexpressing THP1 cells and recombinant human ARG2 (rhARG2) enzyme. .....72
Table 2 - 6. Sequences of shRNA used for gene knockdown and silencing. .....77
Table 2 - 7. PCR primers used in ChIP experiments. .....96
Table 2 - 8. PCR primers used in bisulfite sequencing experiments. .....99

# Abbreviations

| | |
|---|---|
| 2-DG | 2-deoxy-glucose |
| AML | Acute Myeloid Leukaemia |
| ANOVA | Analysis of variance |
| APC | Antigen presenting cell |
| ARG1 | Arginase-1 |
| ARG2 | Arginase-2 |
| ASL | Argininosuccinate lyase |
| ASNS | Asparagine synthetase |
| ASS1 | Argininosuccinate synthase |
| ATAC | Assay for Transposase-Accessible Chromatin |
| ATP | Adenosine triphosphate |
| BBB | Blood brain barrier |
| BCH | 2-Amino-2-norbornanecarboxylic acid |
| BET | Bromo- and Extra-Trminal domain |
| BTLA | B and T-lymphocyte attenuator |
| CAF | Cancer-associated fibroblasts |
| CAM | Cell adhesion molecule |
| cAMP | Cyclic adenosine monophosphate |
| CAR | Chimeric antigen receptor |
| cas9 | CRISPR associated protein 9 |
| CAT | cationic amino acid transporter |
| CCL | CC chemokine ligand |
| CD | Cluster of differentiation |
| CDK | Cyclin-dependent kinase |
| cDNA | complementary DNA |
| CEA | Carcinoembrynogenic antigen |
| CEBP | CCAAT-enhancer-binding proteins |
| CFSE | Carboxyfluorescein succinimidyl ester |
| ChIP | Chromatin Immunoprecipitation |
| COX | Cyclo-oxygenase |
| CRISPR | Clustered Regularly Interspaced Short Palindromic Repeats |
| CTLA-4 | Cytotoxic T-Lymphocyte Associated Protein 4 |
| CTV | Cell tracker violet |
| DMEM | Dulbecco's Modified Eagle's Medium |
| DMSO | Dimethyl sulfoxide |
| ECAR | Extracellular acidification rate |
| EDTA | Ethylenediaminetetraacetic acid |
| ELISA | Enzyme-Linked Immunosorbent Assay |
| *Ezh2* | Enhancer of Zeste homologue2 |
| FACS | Fluorescence-activated cell sorting |
| FBS | Foetal bovine serum |
| FCCP | Carbonyl cyanide-4-(trifluoromethoxy)phenylhydrazone |
| FLT3 | Fms-related tyrosine kinase 3 |
| FMO | Fluorescence minus one |
| Fwd | Forward (primer) |

| | |
|---|---|
| GAPDH | Glyceraldehyde 3-phosphate dehydrogenase |
| GCN2 | General control nondepressible protein 2 |
| GFP | Green fluorescent protein |
| GLUT | Glucose transporter |
| GPNA | L-γ-Glutamyl-p-nitroanilide |
| GVHD | Graft versus host disease |
| HDAC | Histone deacetylase |
| HEK | Human embryonic kidney |
| HIF | Hypoxia-induced factor |
| HLA | Human leukocyte antigen |
| HPLC | High-performance liquid chromatography |
| HRP | Horseradish peroxidase |
| HSCT | Haematopoietic stem cell transplantation |
| IBD | Inflammatory Bowel Disease |
| IDH | Isocitrate dehydrogenase |
| IDO | Indoleamine 2,3-dioxygenase |
| IFN | Interferon |
| Ig | Immunoglobulin |
| IL | Interleukin |
| iNOS | inducible Nitric Oxide Synthase |
| IRES | Internal ribosomal entry site element |
| ITD | Internal Tandem Duplication |
| KD | Knockdown |
| KDM4C | Lysine Demethylase 4C |
| KO | Knockout |
| LAT | L-type amino acid transporter |
| LB | Lysogeny broth |
| LC-MS | Liquid chromatography-mass spectrometry |
| LMP | Latent membrane protein |
| LPS | Lipopolysaccharide |
| M-CSF | Macrophage colony-stimulating factor |
| mAb | Monoclonal Antibody |
| MACS | Magnetic-activated cell sorting |
| MDSC | Myeloid-derived suppressor cells |
| MHC | Major histocompatibility complex |
| MRC | Medical Research Council |
| mTOR | mammalian target of rapamycin |
| NHLA | N-hydroxy-nor-L-arginine |
| NK | Natural Killer |
| NO | Nitric Oxide |
| NOHA | N-hydroxy-L-arginin |
| OAT | Ornithine aminotransferase |
| OCR | Oxygen consumption rate |
| ODC | Ornithine decarboxylase |
| OVA | Ovalbumin |
| PAGE | polyacrylamide gel electrophoresis |
| PAMP | Pathogen-associated molecular patterns |
| PBMC | Peripheral blood mononuclear cell |
| PBS | Phosphate buffered saline |
| PCR | Polymerase chain reaction |

| | |
|---|---|
| PD-1 | Programmed cell death-1 |
| PD-L1 | Programmed cell death ligand-1 |
| PFA | Paraformaldehyde |
| PG | Prostaglandin |
| PML | Promyelocytic leukaemia |
| PRR | Pattern-recognition receptors |
| q-RT-PCR | quantitative Real-Time Polymerase Chain Reaction |
| RCC | Renal cell carcinoma |
| Rev | Reverse (Primer) |
| rhARG2 | recombinant human Arginase-2 |
| ROS | Reactive oxygen species |
| RPMI | Roswell Park Memorial Institute (medium) |
| RUNX1 | Runt-related transcription factor 1 |
| SDS | sodium dodecyl sulfate |
| SEM | Standard error of the mean |
| Seq | Sequencing |
| SFFV | Spleen focus-forming virus |
| shRNA | short hairpin RNA |
| SLC | Solute carrier |
| SLE | Systemic lupus erythematosus |
| STAT | Signal transducer and activator of transcription |
| TAM | Tumour-associated macrophages |
| TAP | Transporter associated with antigen processing |
| TCR | T cell receptor |
| TGF | Transforming growth factor |
| Th | T-helper |
| TIL | Tumour-infiltrating lymphocytes |
| TLR | Toll-like receptor |
| TNF | Tumour necrosis factor |
| Treg | regulatory T-cells |
| TSS | Transcription start site |
| VEGF | Vascular endothelial growth factor |
| WB | Western blotting |
| WCL | Whole cell lysate |
| WHO | World Health Organisation |
| WT | Wild-type |

# Chapter 1: Introduction

Parts of Chapter 1 are based on my own work from my personal contribution to our published literature review (Timosenko E*, Hadjinicolaou AV* and Cerundolo V, immunotherapy, 2017 - * denotes equal contribution as first co-authors) [1].

## 1.1 Overview of the immune system

### 1.1.1 Components of the immune system

We are constantly exposed to various organisms and material that have the potential to cause disease. What controls the outcome of the host-pathogen interaction, in addition to the culprit's pathogenicity, is the host immune system. The immune system is multifaceted consisting of various components, from invisible molecules and cells to various organs such as the spleen, lymph nodes, thymus and bone marrow. The latter is the source of haematopoietic stem cells from which different types of immune cells originate. From a lineage point of view, the main arms are myeloid cells and lymphoid cells. The former play a major role in the inflammatory response seen in innate immunity, and comprise of mainly phagocytes such as macrophages and dendritic cells and granulocytes such as neutrophils, basophils, eosinophils and mast cells. Lymphoid cells include the major players of adaptive immunity, namely T-cells, B-cells and NK cells [2].

### 1.1.2 Innate immunity

From a functional perspective, the immune system is divided into innate and adaptive aspects. Innate immunity protects the host in a rapid, non-specific manner and is heavily evolutionary conserved suggesting a crucial role in survival of even the simplest organisms. It comprises of physical barriers such as the skin and mucosal membranes, chemical barriers such the complement cascade, cytokines, acute phase inflammatory

proteins and enzymes, microbiological barriers such as the natural gut flora and antimicrobial factors and cellular barriers such as phagocytes and granulocytes. Discrimination of pathogen from self by the innate immune cells occurs via pattern-recognition receptors (PRRs), which recognize fairly generic pathogen-associated molecular patterns (PAMPs) [3].

### 1.1.3 Adaptive immunity

Adaptive immunity comprises of B-cells and T-cells and is only found in complex organisms such as mammals and protects the host in a very specific manner through antigen-driven responses. B-cells are responsible for production of antibodies that drive humoral immune responses whereas T-cells, categorised in cytotoxic cluster of differentiation (CD)8 and helper CD4 subsets, drive the cellular arm of adaptive immune responses [4]. In contrast to innate immunity, adaptive immunity takes longer to develop but has memory, is more elegant and precise thus causing minimal damage to the host itself. Going hand-in-hand with this specific, targeted effect is diversity that also characterizes adaptive immunity. In the case of T-cells, this stems from the highly variable T-cell receptor (TCR) that is made up of one of many combinations of α and β chains [5]. Bridging innate to adaptive immunity, antigen-presenting cells (APC) display peptides from pathogenic organisms or anomalous proteins from cancers in the context of major histocompatibility complex (MHC) to T-cells [6]. MHC class I is found on all nucleated cells and recognized by CD8 T-cells whereas MHC class II is only found on professional APCs, such as dendritic cells, and recognized by CD4 T-cells [4]. Antigen presentation and recognition by the TCR, occurring in the right circumstances and with the appropriate co-stimulatory signals, allows activation, expansion and effector status acquisition for specific T-cells that perpetuate and orchestrate the necessary adaptive immune response.

## 1.2 Cancer immunosurveillance and anti-tumour immunity

### 1.2.1 Tumour-specific immune responses

The tumour immunosurveillance hypothesis suggests that host immune cells can distinguish mutant, aberrant, misbehaving cells from healthy ones and try to clear them before they develop into malignant tumours with clinical manifestations [7]. Initially proposed by Ehrlich in 1909, the idea that the immune system has the ability to naturally recognise cancers and mount a response against them was strongly advocated for again by Burnet in 1957 and Thomas in 1982 and has been around and challenged for years [7, 8]. Although controversial, the concept of anti-tumour immunity has had a lot of findings in its support such as the higher incidence of cancers observed in immunosuppressed individuals or spontaneous tumours in mice lacking T-cells or NK cells and the link between increased survival rates for cancer patients with tumour-infiltrating lymphocytes (TILs) [9, 10]. Current evidence suggests that immune-mediated tumour destruction is initiated by recognition of tumour-associated antigens by cytotoxic immune cells such as CD8 T-cells and NK cells. Tumour-associated antigens develop as a result of accumulating mutations in tumours and can be physiological proteins that are overexpressed or inappropriately expressed by cancer cells, tumour-specific neoantigens that arise as a result of mutated genes, tissue differentiation antigens, oncofetal (tumour germline) antigens and proteins from oncogenic viruses [11].

### 1.2.2 Immunoediting theory

According to the tumour immunoediting theory, the relationship between cancer and the host immune system is complex and in fact, anti-tumour immunity and cancer progression occur simultaneously as part of a dynamic process. In the initial stages, in line with cancer immunosurveillance, TILs reach the site of the tumour and eliminate cancer cells (elimination phase) but only partially, until an intermediate stage of equilibrium

(equilibrium phase) is reached where the rate of tumour destruction by the immune system equals the rate of tumour expansion [12, 13]. In time, tumours mutate further, become more heterogeneous and eventually escape the immune system to grow uncontrollably (escape phase) [14]. The escape phase relies on the ability of cancer cells to develop immune evasion mechanisms, compromising the effector function of TILs. All in all, the immune system ends up assisting tumour progression by permitting the survival of poorly immunogenic cancer cells that can successfully withstand anti-tumour immune responses.

## 1.3 Mechanisms of cancer immune evasion and the tumour microenvironment

### 1.3.1 Immune evasion by hijacking antigen presentation

Evasion of the anti-tumour immune response is now formally recognized as a hallmark of cancer in the revised criteria by Hanahan and Weinberg [15]. Thus, it is not surprising that tumours have evolved various strategies to achieve this. Certain tumours compromise cancer antigen presentation by impairing their own antigen processing (immunoproteasome) system (e.g. TAP, LMP2, LMP7 mutations), downregulating their own MHC molecules, or those of APCs [16-23]. In hampering tumour antigen presentation, cancers prevent initiation of anti-tumour immune responses.

### 1.3.2 Tumour microenvironment

#### 1.3.2.1 Immune evasion by hijacking immune checkpoint molecules

Further immune evasion strategies take advantage of the host's naturally existing immunosuppressive mechanisms to regulate effector T-cell function and it has now emerged that cancer immunoediting and immune escape are strongly linked to the generation of an immunosuppressive, tolerant tumour microenvironment [24]. Many

cancer cells exploit inhibitory checkpoint molecules such as PD-1, CTLA-4 and BTLA present on stimulated T-cells to induce apoptosis, anergy or reduced effector function [25-27]. Cancer cells in the tumour microenvironment maintain expression of these receptors on TILs and also constitutively express or upregulate proteins of the B7 family that act as ligands to these receptors, such as PD-L1 [28-30]. PD-L1 expression has been shown to correlate with poor prognosis in various cancer contexts [31]. The biological findings determining this immune escape mechanism have been translated to the clinic through the development of immune checkpoint inhibitors (anti-CTLA4 and anti-PD1 mAbs) that have displayed tremendous survival benefit for cancer patients, alone and in combination [32-35].

**1.3.2.2 Immune evasion by recruitment of immunosuppressive cell populations**

Another frequent phenomenon within the tumour microenvironment is the expansion of and/or recruitment of immunosuppressive cells such as regulatory T-cells (Tregs), myeloid-derived suppressor cells (MDSCs) and tumour-associated macrophages (TAMs). These cells can inhibit T-cells, NK cells and APCs. MDSCs are a heterogeneous population of immature myeloid cells comprising of macrophage, granulocyte and dendritic cell precursors that are characterized by the expression of the surface markers Gr1 and CD11b, and the ability to cause immunosuppression [36]. Both Tregs and MDSCs have been shown to be enriched in tumour sites and peripheral blood of cancer patients and their presence has been linked to poor survival outcomes [31, 37, 38]. Furthermore, depletion of Tregs or MDSCs in tumour-bearing mice led to spontaneous tumour regression highlighting the key role of these immunosuppressive populations in cancer immune evasion [31, 37, 39]. Infiltration and expansion of these immunosuppressive cells depends on factors released by tumour cells; Tregs are expanded by TGF-b and PGE2 and recruited by the CCL5 and CCL22 chemokines whereas MDSCs are activated and

expanded by IL-1β, IL-6 and PGE and TAMs accumulation depends mainly on IL-4, IL-13, CSF1 and CCL2 [40-46].

#### 1.3.2.3 Immune evasion by release and expression of inhibitory immune mediators

Additionally, tumour immune escape is often achieved by production and release of anti-inflammatory mediators that have direct inhibitory effects on APCs as well as the activation, proliferation, effector function/cytotoxicity and survival of TILs mainly CTLs. Such factors originate either from tumour cells or the cancer-associated immune cells mentioned earlier and include reactive oxygen species (ROS), nitric oxide (NO), IDO, TGF-β, IL-10, prostaglandin $E_2$ ($PGE_2$), vascular endothelial growth factor (VEGF), sialomucins [47, 48] Interestingly, the majority of anti-tumour effects of these secreted factors seem to act via STAT3, making this transcription factor a good target for cancer immunotherapy [49, 50]. Induction of apoptosis through secretion of glycans like galectins (mainly Galectin-1) and expression of cell death receptor ligands such as FasL and TRAIL, is another mechanism to inhibit anti-tumour immunity [49].

#### 1.3.2.4 Immune evasion by generation of metabolic stress through nutritional starvation

Finally, metabolic stress achieved through nutrient starvation, oxygen deprivation or acid-base imbalance is another strategy adapted by tumours to escape immune-mediated damage [51]. Nutritional stress, of crucial relevance to this work, is physiologically used by complex organisms to control actively proliferating cells including stimulated immune cells during inflammation. Evidence now suggests that infectious agents and cancers can apply the same strategy to escape immune responses. One way for tumour cells, MDSCs and sometimes even cancer-associated stromal cells such as fibroblasts to deplete amino acids and generate nutritional stress in the tumour microenvironment, is by expression and/or secretion of indoleamine 2,3-dioxygenase (IDO), iNOS and Arginase, the enzymes

that degrade tryptophan and arginine respectively [1]. Tryptophan metabolism in the tumour microenvironment has been extensively studied and there is clear evidence that inhibition of IDO, expressed by many cancers, leads to stronger anti-tumour immune responses [52]. Consequently, multiple IDO inhibitors and other regulators of the kyneurine pathway are already being tested in cancer immunotherapy clinical trials as single agents or in combination with chemotherapy or immune checkpoint inhibitors [53]. Interestingly, there is less work on the link of arginine metabolism with cancer immune evasion, which is the focus of this work and discussed next.

## 1.4 Arginine physiology

### 1.4.1 Arginine function

Arginine is an extremely versatile, dibasic, cationic amino acid that is involved in multiple physiological processes as it acts as precursor to essential compounds such as creatine, citrulline, nitric oxide, proline, ornithine and polyamines [54-56]. The diverse functions of arginine include modulation of various physiological processes such as immune function [57], wound healing [58], hormone secretion ([59], vascular tone [60], insulin sensitivity [61] and endothelial function [62].

### 1.4.2 Arginine metabolism

#### 1.4.2.1 Arginine sources and arginine synthesis

Arginine can be derived both exogenously through diet or endogenously through *de novo* synthesis or turnover of cellular protein [63]. *De novo* synthesis accounts for 5-15% of endogenous supply and occurs in the kidney and liver [64]. Glutamine is first broken down in the small intestine forming citrulline which is then absorbed and converted to arginine in the kidney by the action of argininosuccinate synthase (ASS1) and argininosuccinate lyase

(ASL) [63, 65]. The intestinal-renal axis accounts for 60% of de novo synthesis with the remaining 40% of arginine coming through the hepatic urea cycle [63, 66, 67]. Arginine is considered a semi-essential amino acid which means that although in healthy states, endogenous biosynthesis is sufficient to satisfy cellular metabolic requirements, in cases of nutritional stress such as trauma [68] pregnancy, or sepsis [69] or conditions of hyperproliferation (inflammation, cancer) or organ dysfunction (bowel disease, renal disease) dietary intake becomes necessary in order to meet the additional amino acid demands [64, 70]. Normal levels of arginine in human plasma differ with age and sex and range from around 50 to 120μM although intracellular concentrations are much higher reaching up to 1mM [71]. The reference range for murine plasma arginine is approximately 90-210μM [72]. Physiological amounts of arginine are necessary for protein synthesis, tissue repair and, of most relevance to this work, immune function preservation. The fine balance between intracellular and extracellular concentrations of arginine is tightly regulated through the action of catabolic enzymes, the enzymatic pathway responsible for de novo synthesis and the arginine cell membrane transporter system [73].

#### 1.4.2.2 Arginine catabolism and the Arginase isoenzymes

Arginase is the binuclear metalloenzyme that catalyses the hydrolytic conversion of arginine to ornithine and urea, first discovered by Kossel and Dakin more than 100 years ago in mammalian liver as part of the ammonia-urea cycle [74, 75]. There are two Arginase isoforms, Arginase-1 (ARG1) and Arginase-2 (ARG2) that catalyse the same chemical reaction but differ in terms of their regulation, subcellular localization and cellular/tissue expression [75-78]. They are encoded by two distinct genes, found on different chromosomes and controlled independently from one another.

#### 1.4.2.3 Arginase-1 (ARG1)

The human *ARG1* gene is located on chromosome 6q23 whereas *ARG2* maps to chromosome 14q24.1 [79, 80]. Human ARG1 is a cytosolic enzyme consisting of 322 amino acids, primarily and abundantly found in liver hepatocytes where it plays a crucial role in ammonia detoxification by catalysing the final part of the urea cycle [75, 81]. It is also constitutively expressed in erythrocytes and in the granules of polymorphonuclear neutrophils from which it is liberated in an inactive form (activated upon extracellular release) during inflammation [82-84]. ARG1 mRNA expression in murine macrophages can be induced by IL-4, IL-10 and IL-13, the cytokines of the Th2 signature [85-89]. In fact, this seems to be characteristic of all murine myeloid populations as granulocytes and dendritic cells also show upregulated ARG1 expression upon Th2 cytokine mediated stimulation [90-92]. ARG1 expression is also enhanced by IL-21 which causes the upregulation of IL-4Rα and IL-13Rα on the surface of murine macrophages [93] and inhibited by the iNOS intermediate N-hydroxy-L-arginine (NOHA) in line with the antagonistic relationship of these two enzymes which compete for the same substrate [94, 95]. Ornithine, a product of the Arginase reaction, also acts as a competitive inhibitor of the enzyme and can also diminish arginine transport into cells suggesting a fine balance in the regulation of Arginase activity and arginine breakdown [96-99]. Furthermore, in murine macrophages ARG1 is induced by lipopolysaccharide (LPS) and oxidative lipoproteins whereas in rat alveolar macrophages, it is induced by hydrogen peroxide [86, 100, 101].

#### 1.4.2.4 Arginase-2 (ARG2)

On the other hand, ARG2 is a mitochondrial protein (usually found in the outer membrane [92%] and matrix [8%] of mitochondria) with a global constitutive expression in various tissues most prominently kidney, prostate, brain, pancreas and small intestine but also

skeletal muscle, monocytes, macrophages, airway alveolar and epithelial cells, endothelial cells and the lactating mammary gland [64, 83, 102-106]. It is synthesized as a 354-amino acid pre-protein and imported to mitochondria, via a mitochondrial-targeting signal peptide, where it is processed to the mature form by protelolysis [64, 106, 107]. The regulation of *ARG2* is relatively understudied compared to the *ARG1* gene, but it has been suggested that Toll-like receptor (TLR) ligands such as LPS and oligodeoxynucleotides containing high amounts of unmethylated cytosine guanine motifs (CpG) induce ARG2 expression in murine macrophages with dexamethasone and dibutyryl cAMP enhancing this induction and IFN-γ inhibiting it [102]. Despite early observations suggesting an inhibitory effect on ARG2 expression, the role of IFN-γ remains controversial as more recent studies imply a positive regulation through priming [108].

Although the two human Arginase isoforms show a 58% homology in their amino acid sequence, human ARG2 shares 71% sequence identity with xenopus ARG2 suggesting that gene duplication preceded the mammal-amphibian divergenece [109]. Furthermore, there are multiple conserved regions where 92% homology exists in the human isoforms and more specifically seven residues, crucial for enzymatic activity and arginine breakdown, are conserved with full homology across species in all types of Arginase [102, 106, 109]. Additionally, the two human Arginase isoforms share key features of their crystal structure including the formation of a homotrimer (ARG1: 34,700 Da; ARG2: 36,100 Da) and a binuclear manganese cluster necessary for activity [75].

## 1.5 The role of Arginase in physiology and pathology

### 1.5.1 Neutralisation of toxic substances through the hepatic urea cycle

The physiological explanation for the existence of two distinct Arginase isoenzymes catalysing the same chemical reaction in distinct subcellular locations remains to be

elucidated. Emphasizing the important role of ARG1 in the hepatic urea cycle to clear excess toxic nitrogenous waste, mice lacking this gene die within 14 days of age as a result of the poisonous effects of hyperammonaemia [110, 111]. ARG1 deficiency in humans also leads to hyperarginaemia, low ornithine and excess ammonia with ensuing cirrhosis, neurological disease and mental/developmental retardation justifying why the enzyme is normally constitutively expressed at high levels in the liver [112]. Its role in stomach, pancreas, lung and other extrahepatic tissues where it is expressed, remains unknown [113].

### 1.5.2 Regulation of nitric oxide biosynthesis

In contrast to *ARG1*, *ARG2* knockout mice have no obvious phenotype with the exception of elevated levels of arginine and reduced levels of ornithine in blood [110]. Thus, although ARG2 does not substantially participate in the hepatic urea cycle, it is still involved in maintaining the appropriate circulating arginine concentration. Its physiological function is still poorly understood but evidence suggests that it might be the regulation of arginine concentration within cells and in the extracellular spaces and thus, control of substrate availability for the biosynthesis of key substances such as nitric oxide, proline and polyamines from the arginine precursor [114]. The main tissue where the biological role of ARG2 has been investigated is vascular endothelium where it acts to limit the amounts of arginine that can be used as substrate by endothelial nitric oxide synthetase (eNOS) [115]. This leads to reduced nitric oxide (NO) and enhanced superoxide production, causing oxidative stress, upregulation of inflammatory and adhesion molecules, such as VCAM-1 and ICAM-1, and endothelial dysfunction [116-118]. Upregulation of Arginase prevents NOS activity whereas inhibition of Arginase causes enhanced iNOS expression and leads to increased NO production [119]. The ARG-NOS balance is important in the pathophysiology of endothelial dysfunction [120], regulation of

airway dilatation and thus pathology of asthma [121], regulation of vascular tone [60], wound healing [58] and modulation of hormone release and function such as induction of insulin sensitivity [61].

### 1.5.3 Regulation of ornithine, proline and polyamines biosynthesis

In addition to the metabolic effects mediated by regulation of NO production, Arginase also affects cellular functions through regulation of arginine and ornithine availability for downstream conversion to other amino acids. Ornithine serves as substrate to either ornithine decarboxylase (ODC) to produce polyamines, fundamental for cell proliferation, inflammation control and membrane transport, or ornithine aminotransferase (OAT) to generate proline, the building block of collagen whose synthesis is indispensable to tissue repair, fibrosis and healing [64, 122, 123]. As eluted to earlier, these functions appear to be heavily based on the main extrahepatic isoenzyme, ARG2, rather than ARG1 [114].

### 1.5.4 Modulation of immune responses

Another important physiological function of Arginase is the modulation of immune responses [57] but its precise role currently remains ambiguous as it can lead to both beneficial and detrimental outcomes.

#### 1.5.4.1 Role in macrophage function

Firstly, the competition between Arginase and NOS also occurs in macrophages where the former regulates the production of NO from inducible NOS (iNOS) by limiting the availability of the common substrate of the two enzymes, arginine [88, 124, 125]. Alternatively activated M2 macrophages expand in response to Th2 cytokines such as IL-4 and IL-13 as well as IL-10 and TGF-b to upregulate ARG1, inhibit iNOS, and thus, enhance humoural immunity, allergic and anti-helminth immune responses and also to assist in resolution of inflammation and promotion of tissue repair and healing [89, 91,

126, 127]. This is in contrast to classically activated M1 murine macrophages, which arise as a result of Th1 cytokines such as IFN-g and strongly express iNOS to foster and propagate inflammation [128, 129]. Polarization of myeloid populations into tolerogenic phenotypes seems to be driven, at least partly by low arginine levels [130].

#### 1.5.4.2 Role in infection

Arginine is crucial during infections as it provides the substrate for generation of NO, which is a strong antimicrobial agent and allows the invaded host cells, especially macrophages, to clear intracellular pathogens such as mycobacterium tuberculosis, salmonella, leishmania major and extracellular microbes such as Escherichia coli [131]. Consequently, iNOS expression, mainly in macrophages, is strongly induced by various pro-inflammatory cytokines released during infection, such as TNF-a and IFN-g. This renders the aforementioned competition between Arginase and iNOS crucial in deciding the outcome of bacterial or parasitic infections and suggests that Arginase activity might suppress the immune response to tilt the balance in favour of pathogens and lead to poor clinical outcomes [64, 132]. Indeed, it has been demonstrated that the immunomodulatory or polyamine-producing capacity of pathogen-induced Arginase in host cells, primarily macrophages, is detrimental in Salmonella Typhimurium [133], Mycobacterium tuberculosis [134], Helicobacter pylori [135, 136], Toxoplasma gondii [137, 138], schistosoma mansoni [139], trypanosome cruzii or bruceii [140-143], leishmania [144, 145] and even hepatitis C virus infections where it promotes the development of HCV-associated hepatocellular carcinoma [146]. Furthermore, toll-like receptor (TLR) mediated induction of Arginase-1 in murine macrophages reduced arginine availability and NO production leading to reduced survival in Toxoplasma gondii infection and enhanced mycobacterial load in the host's lungs in tuberculosis [137]. Interestingly, there are microorganisms, such as Helicobacter pylori, Leishmania and Schistosoma that possess

their own Arginase, to make urea and at the same time deplete the arginine within the host cell and the extracellular space [147-150]. Overall, modulation of the host Arginase activity by invading pathogens, to divert the arginine reserves away from NO production is strategically important for the survival of invading pathogens. NO regulation is only one of the ways arginine breakdown favours pathogens; arginine deprivation from immune cells and polyamine production for pathogens have an equal contribution to this effect.

#### 1.5.4.3 Role in regulation of T-cell function

Arginase-mediated arginine depletion is an effective way to keep adaptive immune responses in check. Adequate levels of arginine in the extracellular milieu are crucial for T cell proliferation and functional T cell activity [77, 151]. Profoundly depleted arginine levels in plasma, between 0 and 50 μmol/L, are accompanied by loss of CD3z chain expression and dysregulation of cyclin D3 and cyclin-dependent kinase 4 (CDK4) leading to arrest at the G0-G1 phase of the cell cycle and T-cell anergy [151-155]. In vitro, arginine concentrations below 60 μmol/L decreased CD3z expression, cell proliferation, and cytokine production [68, 156-158]. Downregulation of CD3, a crucial co-factor of the T-cell receptor (TCR) is part of the T-cell inactivation signature that occurs through induction of transcriptional and translational effects regulated by GCN2, a protein that directs the global cellular response to nutritional stress, linking cell proliferation to the abundance of amino acids [159].

#### 1.5.4.4 Role in autoimmunity

Arginase involvement in autoimmunity can be either positive or negative. Negative effects have been demonstrated in the central nervous system where Arginase promotes autoimmune inflammation [160], in rheumatoid arthritis (RA) where ARG2 upregulation was observed in synovial fluid inflammatory cells [161] and systemic lupus erythematosus

(SLE) where enhanced ARG1 in patient serum leads to Arginase-dependent Th17 differentiation and correlates with disease severity [162]. ARG1 in myeloid-derived suppressor cells (MDSC) has been shown to have positive effects through depleting arginine to inhibit T-cell proliferation and resolve inflammation in murine collagen induced arthritis [163].

#### 1.5.4.5 Role in pregnancy

Pregnancy is one of the many settings that the immune system needs to be closely regulated. Arginase activity is significantly enhanced in peripheral blood (through hrelease of the enzyme from cells), term placentae of pregnant women and myometrium of pregnant guinea pigs as part of a physiological mechanism to provisionally suppress maternal T-cell function and ensure materno-fetal tolerance during pregnancy [152, 164]. Elahi and colleagues have shown that CD71+ erythrocytes physiologically expand in neonatal mice and human cord blood and express high amounts of ARG2 that makes them immunosuppressive [165]. Abrogation of the Arginase activity of these cells or arginine supplementation restored immune responses and protection against perinatal pathogens such as Listeria monocytogenes and Escherichia coli suggesting a crucial role for ARG2 in neonatal susceptibility to infection.

#### 1.5.4.6 Role in antigen presentation

The regulation of amino acid metabolism is crucial to monitor physiological antigen presentation [166]. ARG2 is the principal Arginase isoenzyme in dendritic cells (DC) where it is downregulated by microRNA-155 upon maturation in order for DC to effectively stimulate T-cell proliferation following antigen presentation [167]. DCs deficient in microRNA-155 showed high ARG2 activity with consequent depletion of extracellular arginine leading to impaired antigen-specific T-cell responses [167].

## 1.6 Arginase in the tumour microenvironment

### 1.6.1 The role of Arginase as a pro-tumourigenic enzyme

The presence of Arginase in the tumour microenvironment can have a variety of detrimental effects: i) inhibition of production of tumouricidal NO by inflammatory macrophages, ii) generation of polyamines (via ornithine) that support cancer cell proliferation and iii) arginine depletion locally within the tumour microenvironment or systemically causing T-cell dysfunction and immunosuppression [168].

### 1.6.2 Arginase utilization by cancers

Arginine deprivation is now a recognized strategy for cancer cells to keep anti-tumour lymphocyte responses in check. Therefore, it is no surprise that Arginase expression has been demonstrated in many cancer cell lines including non-small lung cancer, breast cancer, prostate cancer and renal cell carcinoma [168-172]. Tumour Arginase consumes arginine depriving it from immune cells within the local tumour microenvironment rendering them dysfunctional. In prostate cancer, ARG2 (and iNOS) expression is aberrantly high suppressing tumour-infiltrating lymphocytes (TILs) an effect that can be reversed through pharmacological inhibition of the two enzymes [173, 174]. ARG2 expression is further enhanced by androgens explaining why androgen depletion therapy, that diminishes ARG2 activity, is often followed by an immunological boost (enhanced T-cell activation and IFN-g secretion) in vivo, a result that mirrors the effects of Arginase knockdown in prostate cancer cells in vitro [169]. Arginase activity is enhanced in gastric cancer when compared to healthy gastric tissue [175-177] and the enzyme is released in vitro by gastric cancer cell lines and in vivo in the serum of patients with gastric cancer [178]. Arginase activity, attributed to ARG2 levels, was significantly higher in breast cancer tissue when compared to healthy control tissue as well as in peripheral blood of breast cancer patients compared to healthy donors [179].

### 1.6.3 Arginase utilization by cancer-promoting cell populations

In addition to direct amino acid degradation by the cancer cells, tumours are also able to hijack surrounding stromal cells or incoming immune cells, such as tumour-associated macrophages (TAM) and myeloid-derived suppressor cells (MDSC) programming them towards immunosuppression **(Figure 1-1)**. Amongst other actions, these cancer-associated cells (CAC) overexpress and secrete Arginase to deplete arginine in the microenvironment and provide one of the main mechanisms to induce T-cell anergy and facilitate cancer immune evasion [180].

#### 1.6.3.1 Myeloid-derived suppressor cells (MDSCs)

Myeloid-derived suppressor cells (MDSCs) are immature monocytes or granulocytes that are physiologically present in bone marrow but frequently expand within solid tumours, spleens, lymph nodes and peripheral blood of human patients with various cancers or cancer mouse models to suppress T-cell function and promote cancer spread thus aggravating disease and leading to poor clinical outcomes [181-186]. MDSCs can impair immune responses through a number of ways including production of reactive nitrogen and oxygen species [187] but the most recognized one is through Arginase- and iNOS-mediated arginine depletion [185, 188]. ARG1 expression can be induced by various tumour-releasing soluble factors such as prostaglandins (synthesized as a result of COX-2 overexpression in tumours) or via activation of the transcription factor STAT3 [189] and STAT6 [190]to generate an-arginine depleted microenvironment to starve T-cells and prevent their activation and proliferation [186, 191]. Enhanced ARG1 activity in peripheral blood as a result of the expansion of MDSC has so far been demonstrated in renal cell carcinoma (RCC) [154, 185], breast cancer [192], head and neck squamous cell carcinomas (within tumours, draining lymph nodes and peripheral blood) [189]. In addition to their intracellular Arginase activity, MDSCs also store ARG1 in granules that can be

released in the extracellular space to directly deplete arginine in the microenvironment [92, 193]. Ochoa and colleagues have in fact demonstrated that the release of ARG1 in the plasma of RCC patients is enough to reduce systemic arginine levels below the threshold at which T-cells fail to proliferate [154]. We have recently shown that circulating AML blasts are phenotypically similar to MDSCs and are able to release ARG2 (rather than ARG1) in peripheral blood, to inhibit not only T-cell proliferation but also proliferation of haematopoietic progenitor and stem cells and additionally, to polarize monocytes towards expanding into an ARG1-expressing, immunosuppressive M2 population [130]

**1.6.3.2 Tumour-associated macrophages (TAMs),**

Another type of cancer-associated cells, are tumour -associated macrophages (TAMs), which comprise a significant proportion of the expanding tumour and have been shown to correlate with poor clinical outcomes [194-196]. This is not just due to the capacity of M2-polarised TAMs to promote tumour angiogenesis, invasion and metastasis but also their high ARG1 activity, which leads to depletion of arginine in the tumour microenvironment and suppresses T-cell activation and proliferation to escape the anti-tumour immune response [186, 197]. Overexpression of ARG1 in M2 macrophages, although, as aforementioned, is beneficial to the host through protection from excess inflammation, has also been shown to promote tumour growth in prostate cancer and renal carcinoma [154, 186, 198]. Consistent with a prominent role of TAMs and MDSCs in assisting immune-mediated evasion of cancer, inhibition of ARG1 blocked the growth of lung carcinoma in mice suggesting that Arginase is an attractive therapeutic target to boost anti-cancer immune responses [186].

**1.6.3.3 Cancer-associated fibroblasts (CAF)**

More recently, ARG2 expression was demonstrated in cancer-associated fibroblasts (CAF) in the context of the hypoxic environment of pancreatic cancer [184]. The presence of

ARG2-expressing CAFs correlated with poor overall and disease-free survival in patients and suggests that tumour-associated stromal cells are key players in the regulation of the tumour microenvironment.

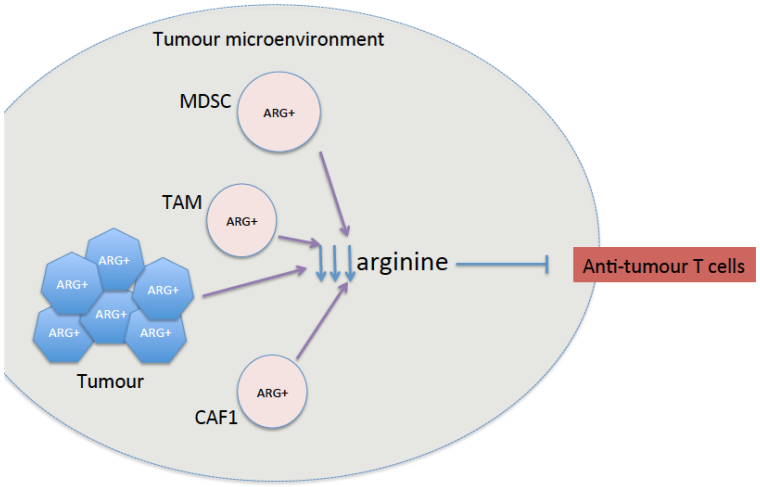



**Figure 1 - 1. Arginase-mediated arginine depletion creates an immunosuppressive tumour microenvironment.**
Tumour cells and cancer-associated cells (MDSC, TAM and CAF) express and release Arginase (ARG+) and are thus able to deplete arginine in the tumour microenvironment to immunosuppress tumour infiltrating lymphocytes.

## 1.7 Therapeutic avenues in cancer immunotherapy by targeting Arginase

Modulation of the immunosuppressive, tumour-promoting activity of MDSCs or TAMs through global depletion or specific targeting of Arginase could clearly have significant therapeutic implications. Various reports have shown that antibody-mediated chelating of MDSCs allowed CD8 T-cells to mount anti-tumour responses [199-201]. Addition of small-molecule Arginase inhibitors such as nor-NOHA abrogated the arresting effects of Arginase on T-cell proliferation and allowed lymphocyte-dependent tumour reduction [186]. As MDSC are also able to polarize macrophages towards the M2 phenotype, at least

partially through ARG1 activity, Arginase inhibitors could have a double effect in favour of T-cells by preventing the expansion of immunosuppressive TAMs [130, 201]. In the case of circulating Arginase, chelators that would specifically bind and mob up only one of the two isoenzymes, depending on which is most prominent in each context, could provide stronger and safer effects with their increased specificity, enhanced bioavailability and reduced toxicity. Arginase inhibitors are currently being tested in a few clinical trials and results are awaited.

More evidence of how this therapy might work comes from extensive data with IDO inhibitors many of which are currently in clinical trials as part of combination therapy regimes [53].

## 1.8 The function and regulation of argininosuccinate synthase (ASS1)

### 1.8.1 Role in the urea cycle and conversion of citrulline to arginine

Although often thought as an enzyme of the hepatic urea-ammonia cycle, argininosuccinate synthase (ASS1) is increasingly recognized to have an integral role in other cellular and metabolic processes. As described earlier in the Introduction, arginine can be synthesized de novo by the sequential action of argininosuccinate lyase (ASL) and ASS1 enzymes on citrulline [202]. More precisely, ASS1 catalyses the ATP-dependent conversion of aspartate and citrulline, to argininosuccinate [202, 203]. Being the direct precursor of arginine, argininosuccinate is then metabolised to fumarate and arginine itself by ASL.

### 1.8.2 Sub-cellular localization of ASS1

The intracellular localization of the ASS1 enzyme varies according to tissue, being around and/or associated with the outer mitochondrial membrane in hepatocytes in order to take part in the urea cycle, within caveolae and around Golgi apparatus in endothelial cells to

control NO production with endothelial NOS (eNOS) and free in the cytoplasm in kidney cells [202, 204-207].

### 1.8.3 Regulation of expression of ASS1

ASS1 expression usually correlates with the need for arginine; expression is high in hepatocytes where arginine is continuously broken down by Arginase whereas in vascular endothelium, where NO production needs to be tightly regulated, expression is low so that levels of arginine (as a precursor of NO) are closely monitored [63, 208]. There are 14 copies of the ASS1 gene across the genome, of which 13 are pseudogenes [202]. The ASS1 gene located on chromosome 9 appears to be the only functional one given that mutations in this gene copy are sufficient to cause citrullinaemia [209-211]. Regulation of expression is mainly by the availability of substrate (citrulline) and product (arginine), as well as nutrients such as proteins and hormonal factors such as glucocorticoids, insulin, glucagon and cAMP [63, 212, 213]. Activation of the ASS1 promoter seems to be controlled by the complicated action of multiple transcription factors including Sp1, Sp4, AP-2, c-Myc and HIF-1α also depending on the levels of arginine in the surrounding environment [214-217]. A cAMP response element has instead been identified approximately 10kb upstream of the transcription start site (TSS) rather than within the ASS1 promoter [212]. Although transcriptional control of ASS1 has been studied extensively, translational, post-translational and localization regulation remain to be elucidated. Additionally, and perhaps more relevant to this work, little is known about co-activating and co-repressing factors acting at the promoter or at non-promoter regions to regulate or fine-tune the expression of ASS1. Identification of such players will lead to understanding of the complex interplay between transcription factors to control ASS1 expression globally, in response to metabolic changes and at a tissue- or cell-specific level, components that are critical and will in fact be studied as part of this work.

### 1.8.4 The physiological role of ASS1

As one of the enzymes controlling the biosynthesis of arginine, ASS1 is involved in the regulation of various metabolic pathways where arginine has a crucial role. These include alongside conversion of ammonia to urea, the generation of NO, polyamines synthesis, and creatine production. ASS1 has been shown to be essential in the citrulline-NO cycle in vascular endothelium where abrogation of the enzyme led to the inability of endothelial cells to maintain basal NO levels and thus their dysfunction [218]. The recycling of citrulline to arginine has also been shown to be bottleneck for the generation of NO in vascular smooth muscle and pulmonary endothelium, suggesting that the function of ASS1 might be the rate-limiting factor in this pathway [219, 220].

ASS1 is also crucial at maintaining physiological levels of arginine in the blood. Significant ASS1 expression is seen in the gut only in neonates, a developmental stage at which arginine becomes an essential amino acid given the low levels of the amino acid in maternal milk [221]. The presence of ASS1 in the neonatal intestine allows enterocytes to produce arginine for the first 2-3 years of life before this task is taken over by the kidneys [222]. Finally, ASS1 appears to be necessary to provide a source of arginine for production of creatine necessary for muscle tissue [223] and polyamines essential for living cells to survive, grow and proliferate [224]. At the level of the entire organism, ASS1 deficiency, as a result of mutations in the *ASS1* gene, leads to type I citrullinaemia, a disease characterized by high levels of serum citrulline with onset in childhood [209]. Type II citrullinaemia is most often seen in adults and relates to low level of the ASS1 enzyme as a result of defects in the *SLC25A13* gene that encodes for a mitochondrial calcium ion-dependent aspartate-glutamate transporter that is necessary for the stabilization and degradation protection of ASS1 [211].

### 1.8.5 The role of ASS1 in cancer

The importance of ASS1 in cancer has recently been highlighted with various reports suggesting that expression of the gene is altered in transformed tumour cells. In a range of malignant tumours including hepatocellular carcinoma [225], glioblastoma [226, 227], pancreatic cancer [228], endometrial cancer [229], ovarian cancer [230], melanoma [225], mesothelioma [231] and osteosarcoma [232], the gene is downregulated or even silenced, in many cases by CpG island methylation of the *ASS1* promoter [227, 230, 233]. Although this causes arginine auxotrophy, making these tumours vulnerable to arginine starvation [234, 235], ASS1 also behaves like a tumour-suppressor gene as its downregulation or silencing have been linked to poor patient prognosis and in some cases, resistance to chemotherapy and enhanced invasive potential [228-230, 232, 236-239]. However in other cases such as epithelial ovarian cancer [240] gastric cancer [241, 242] and colorectal cancer [243], ASS1 is in fact overexpressed and seems to behave as an oncogene since its upregulation has been linked to increased pathogenicity and enhanced cancer cell ability to become malignant and metastasize [241, 242]. It is clear that the global role of ASS1 in cancer is dubious and remains to be elucidated. Different cancers utilize the enzyme in different ways leading to a variety of expression levels amongst tumours. One way or another ASS1 is certainly an interesting target for cancer therapy with significant clinical implications for patients. Although results of targeting ASS1 in vitro have been promising, there has not been any success in vivo so far. One could hypothesize that inhibition of ASS1, whether overexpressed or underexpressed in a tumour, could have beneficial effects by making cancer cells less able to adapt and thus more vulnerable to certain metabolic changes as well as making them less aggressive.

## 1.9 Sensing of amino acid starvation: the GCN2-ATF4 and mTOR pathways

There are two pathways that can sense amino acid depletion; the (general control nondepressible protein 2 (GCN2) kinase pathway and the mammalian target of rapamycin (mTOR) pathway.

### 1.9.1 The GCN2-ATF4 pathway

The GCN2 pathway is directly activated by the accumulation of uncharged tRNA, which occurs due to lack of an amino acid [244-246]. Normally during translation, each amino acid is attached to their corresponding specific tRNA by a covalent bond by the action of aminoacyl-tRNA synthetases. In the absence of an amino acid, such as arginine, this reaction fails to occur and the arginine-specific tRNA remains uncharged causing activation of the GCN2 kinase which in response autophosphorylates and dimerises [247-249]. The activated GCN2 kinase subsequently phosphorylates serine 51 residue of the alpha subunit of translation initiation factor (eIF2α), which promotes cessation of protein synthesis [250]. One of the few genes that continue to be translated under such conditions is activating transcription factor 4 (ATF4), a master regulator of the integrated stress response by which cells can adjust to metabolic changes [251, 252]. By binding to specific motifs of its target genes (often at the promoter region), ATF4 leads to upregulation of enzymes and proteins involved in amino acid biosynthesis, amino acid transport, adaptation to oxidative stress and regulation of apoptosis, assisting the cell to survive [251, 252]. In terms of its role in cancers, the GCN2-ATF4 pathway has been shown to be active in a range of tumours, both human and murine, and necessary in order to enable tumour cell proliferation and survival in amino acid-depleted environments [253].

### 1.9.2 The mTOR pathway

In contrast to the GCN2-ATF4 pathway, the mTOR pathway is in fact inhibited by amino acid deprivation. Although multiple inducers of the mTOR pathway exist, including hypoxia, DNA damage, growth factors and cytokines [254], none of these can actually activate the pathway when the cell is starved of amino acids, a finding that suggests that amino acid availability is a necessary and the most potent stimulus of the mTOR pathway [255, 256]. Following sensing of sufficient amino acid levels, a process governed by vacuolar ATPase and bidirectional amino acid transport, the mTORC1 kinase translocates from a feebly-defined cytoplasmic region to the lysosome surface membrane by the action of the Ragulator-Rag GTPase complex [255, 257-259]. The sensing mechanism seems to depend on the specific amino acid sensed e.g. the lysosomal arginine transporter SLC38A9 and the cytosolic proteins CASTOR1/2 are crucial in arginine sensing whereas the proteins Sestrin1/2 and cytosolic leucyl-tRNA-synthetase are crucial in leucine sensing [260-267]. Following activation by Ras homologue enriched in brain (Rheb) at the lysosome, the functional mTORC1 kinase phosphorylates downstream targets within the mTOR pathway, namely 4E-BP1/eIF4E and p70-S6 kinase (the latter of which phosphorylates its own targets including eEF2 and the risobomal protein S6), a cascade of events that trigger mRNA translation to proteins [268-270]. Activation of the mTORC1 pathway is not essential for just T-cell activation and function but has also been shown to drive differentiation of naïve CD4+ T-cell to Th1 effectors rather than Treg. This is likely via the action of amino acid-related immunometabolites such as α-ketoglutarate, which decreases within activated T-cells in the absence of glutamine thus failing to activate mTORC1 [271].

## 1.10 Arginine transport and the cationic amino acid transporter family

### 1.10.1 The solute carrier (SLC) super-family of transmembrane amino acid transporters

Cellular import-export of nutrients and other metabolic factors, including amino acids, ion exchange and waste product elimination is carried out by a large superfamily of transmembrane transporters known as solute carriers (SLCs) located at membranes at the cell surface and around subcellular organelles [272]. There are currently 456 recognised members sorted into 52 SLC subfamilies, each with unique structure, function and specificity range for one or more substrates [273]. The majority of these transporters are facilitative as they rely on electrochemical or ion gradients (often sodium) created by ATP-dependent pumps in order to push their substrates across membranes [274].

### 1.10.2 The diversity in SLC localisation, function and specificity

According to various reports the SLC diversity is so vast that there are multiple subfamilies catalysing multiple functions including transport of inorganic ions (SLC4, SLC8, SLC9, SLC12, SLC20, SLC24, SLC25, SLC26 and SLC34 subfamilies), neurotransmitters (SLC1, SLC5, SLC6, SLC17 and SLC25), glucose (SLC2/GLUT, SLC5, SLC37 and SLC45), nucleotide sugars (SLC35), fatty acids (SLC27), metal ions (SLC11, SLC30, SLC31, SLC39, SLC40 and SLC41) and vitamins (SLC19, SLC25, SLC46 and SLC52) [275, 276]. In the case of amino acids, transport is mediated by protein belonging to the SLC1, SLC6, SLC7, SLC15, SLC16, SLC17, SLC32, SLC36, SLC38 and SLC43 subfamilies [277]. For the purposes of this work we focus mainly on the SLC1 and SLC7 amino acid transporter subfamilies.

### 1.10.3 system y+L: The cationic amino acid transporters

The $Na^+$-independent $y^+L$ transporters are a subfamily of SLC transporters that include cationic amino acid transporter (CAT)1 (SLC7A1), CAT2 (SLC7A2) and CAT3

(SLC7A3), mainly responsible for arginine uptake in most mammalian cell types and controlling the concentration of arginine intracellularly [73, 278-280]. Although the aforementioned transporters are able to function on their own, others in the same subfamily, such as SLC7A6 and SLC7A7 need to link with the chaperone protein CD98/4F2hc in order to work [279]. Overall, the $y^+L$ transporters are characterized by high affinity for cationic amino acids, pH and $Na^+$ independence, and the ability of substrate on the opposite (*trans*) side of the membrane to increase transport activity [281].

#### 1.10.3.1 The SLC7A1 (CAT1) transporter

Although the CAT2B splice variant is the transporter mainly linked to regulation of immune responses, such as macrophage routing to classical rather than alternative activation, NO production, inflammation and infection [280, 282, 283] inducible CAT1 has also been shown to be necessary for human T-cell proliferation emphasizing the crucial role of arginine in this context [284]. Furthermore, the role of CAT1 appears to be more than just arginine import from the extracellular environment as it has been suggested that its multi-level localization at various sub-cellular organelle membranes is crucial in the intracellular sorting and distribution of arginine for use in the appropriate metabolic processes [73]. Unlike CAT3, which is primarily expressed in the brain and unlike CAT2, whose expression is dynamically regulated, CAT1 is mainly considered to be constitutively and widely expressed in the majority of tissues and cells [285-287]. However, CAT1 is still regulated at the gene level as suggested by the fact that hepatocytes lack any expression as a result of high levels of miR-122, a microRNA acting as a negative regulator of CAT1 [288]. Indeed, as we will see in the results section of this work, *SLC7A1*, the gene encoding for CAT1 can in fact be regulated and transcribed in response to arginine deprivation in cancer cells and T-cells.

### 1.10.4 System L: the neutral large amino acid transporter system

System L amino acid transporters show ubiquitous expression in the human body and function in a $Na^+$-independent manner to mediate the movement of large neutral amino acids, mainly leucine [289]. They are a group of heterodimeric transporters, where CD98 (SLC3A2/4F2hc) a membrane chaperone glycoprotein is attached to one of many reporter light chains such as LAT1 (SLC7A5) or LAT2 (SLC7A8) by bisulfide covalent bonds [279, 290-295]. Their function is obligatory in that they depend on other amino acid transporters for the generation of amino acid gradients, such as by the accumulation of intracellular glutamine, which can then be exchanged for large neutral amino acids that system L transporters can import [257, 295].

#### 1.10.4.1 The SLC7A5 (LAT1) transporter

LAT1 (SLC7A5) functions in a $Na^+$-independent manner to transport essential large neutral amino acids such as leucine, valine, tryptophan, tyrosine, methionine, histidine, phenylalanine and isoleucine by forming a heterodimer with CD98 (SLC3A2 or 4F2hc), a glycoprotein that acts as a chaperone for transporter stability, appropriate trafficking and correct subcellular localization [296-298]. Although found in various tissues, LAT1 is selectively highly expressed at the blood brain barrier (BBB) where it supplies the central nervous system (CNS) with nutrients and other compounds [299].

### 1.10.5 System $x^-_c$ : the neutral small amino acid transporter system

Unlike system L, the SLC1 subfamily mediates transport of small neutral amino acids with the majority of its members (SLC1A1, SLC1A2, SLC1A3, SLC1A6 and SLC1A7) expressed mainly in the nervous system where they are responsible for glutamate homeostasis in neurons [290]. On the other hand, SLC1A4 and SLC1A5 are alanine, serine, cysteine and threonine transporters (ASCT) that perform their function in a $Na^+$-dependent manner [290]. SLC1A5 is special in that it facilitates transport of a much

broader spectrum of amino acids including gluatamate, valine, lycine, leucine, methionine, glutamine and tryptophan [290, 300, 301].

#### 1.10.5.1 The SLC1A5 (ASCT2) transporter

SLC1A5 is physiologically found in a range of major organs including lung, kidneys, brain, large bowel and skeletal muscle [300]. It is a $Na^+$-dependent transporter that mediates the exchange of small neutral amino acids whose main function is thought to be the regulation of glutamine levels [302]. Amongst its roles, it has been shown to determine the lineage commitment of haematopoietic stem cells in association with the availability of glucose and glutamine in the microenvironment [303].

### 1.10.6 The role of SLC transporters in cancer

It has already been established that amino acid transporters have a role in various diseases such as inflammatory bowel disease (IBD), lupus, and Parkinson's disease [304-306]. Amino acid transporters also have a role in cancer. When cancer cells reprogram to go into glycolysis, they automatically become increasingly dependent on the uptake of not just glucose but also amino acids that can be used to eventually generate energy, especially glutamine and leucine. This means that cancer cells start relying on SLC7A5 (LAT1) and SLC1A5 (ASCT2) for neutral amino acids as well as GLUT1 for glucose. Furthermore, cancer cells tend to have higher metabolic rate and growth needs than healthy cells, an effect that leads to the need for more amino acids to trigger the mTOR pathway, especially in the hypoxic tumour microenvironment [307]. This means that cancer cells have to increase the expression of amino acid transporters, either via oncogenic mutations or in response to stress pathway, in order to take in as many amino acids as possible [296, 308-310]. This feature is now considered one of the new metabolic hallmarks of cancer [310]. Many amino acid transporters have now been reported to be upregulated in tumours. The cysteine-glutamate transporter SLC7A11 is overexpressed in triple-negative breast cancer

[311] as well as tumour-associated MDSC [312] to protect cancer cells from oxidative stress [313] whereas SLC7A1 (CAT1) is overexpressed in colorectal cancer to promote arginine uptake and cancer cell proliferation [314]. More relevant to our work, SLC7A5 and SLC1A5 have been show to cooperate in order to generate bidirectional amino acid movement [315] in an effort to provide sufficient nutrients for energy and cellular proliferation in cancer cells and as such, it is no surprise that they have been found to be upregulated and associated with poor patient prognosis in a range of cancers including prostate cancer [316-318], breast cancer [319, 320], melanoma [321-323], lung cancer [324-326] and colorectal cancer [327]. For this reason, many amino acid transporters, and notably SLC7A5 and SLC1A5, are now considered pro-tumoural players and are interesting targets for cancer therapies as their knockdown in cancer cell lines reduces tumour growth and proliferation [296, 328].

## 1.11 Acute Myeloid Leukaemia (AML)

### 1.11.1 Introduction and epidemiology of AML

Acute Myeloid Leukaemia (AML) is the most common leukaemia in adults and its incidence rate has been increasing steadily in the past 20 years. The disease affects men and women equally, rarely presents before 45 years of age and usually after the age of 55 years with an average patient age of 68 years. It is an extremely heterogeneous disease both clinically an biologically, with the leukaemic blasts stemming from almost any developmental stage along the sequence of differentiation from myeloid, pro-myelocyte and myelocyte, to monocyte, erythroid, and megakaryocyte precursors giving rise to main subtypes of AML.

### 1.11.2 Diagnosis and Treatment of AML

The gold standard for diagnosis is bone marrow biopsy and disease categorization

universally uses the WHO classification system [329]. Treatment options include radiation therapy, chemotherapy with combination of the agents daunorubicin, cytarabine and etoposide (ADE), autologous or allogeneic haematopoietic stem cell transplant (HSCT) often with an aim to induce graft versus host disease (GVHD), other agents such as all-trans retinoic acid with arsenic trioxide for patients with acute promyelocytic leukaemia that carries the (15;17) translocation and finally targeted therapies such as inhibitors of epigenetic modifiers (such as HDACs, IDH and BET) and cell cycle proteins (such as CDK, Hedgehog and MDM2) [330].

### 1.11.3 Anti-leukaemic immunity and the role of the immune system in AML treatment

Despite the plethora of treatments, a significant proportion of patients relapse. This highlights the need to identify novel therapeutic avenues such as AML immunotherapy. The strongest advocate for the role of an anti-leukaemic immune response initially came from harnessing the graft-versus-leukaemia effect observed in allo-HSCT, which supported a role for the immune system, and more specifically T-cells and NK cells, in recognising and clearing leukaemic blasts [331, 332]. Further support for the role of the host immune system in eradicating AML comes from observations of spontaneous AML remission following infections with pathogenic organisms and the association of low relapse rates and lymphocyte revival post-chemotherapy [333, 334]. T-cell-mediated immune responses against AML have been reported in various disease subtypes either against neoantigens or existing aberrant antigens but appear inadequate in globally controlling tumour burden [335-338]. Despite the lack of a strong endogenous anti-AML immune response (as a result of low immunogenicity due to low mutational burden in AML blasts) and the failure to identify AML-specific antigens to target, there has been significant momentum in the AML immunotherapy field [339]. Consequently, various

immunotherapies have been successfully tried for AML treatment including Anti-CD19 CAR T-cells, checkpoint inhibitors, DC vaccination and T-cell recruiting antibody constructs mainly targeting CD33 and CD123 [340]. Nevertheless, it is now clear that like solid tumours, AML has various immune evasion mechanisms to resist anti-leukaemic immune responses, which might explain the inability of host immune cells to eradicate the disease. These are similar to those seen in solid tumours and include dysregulation of immune checkpoints, release of immunosuppressive cytokines and other factors, recruitment of immunosuppressive cell populations, compromise of leukaemic antigen presentation and promotion of T-cell and NK cell apoptosis/death [331]. Of relevance to this work, we have recently demonstrated that AML blasts might be able to release Arginase in the blood of patients to systemically suppress T-cell proliferation [130]. Therefore, in this work we try to understand whether this finding can be translated to a clinical application and how the leukaemic cells, and other solid tumour cancer cells, themselves are able to survive and proliferate in an arginine-depleted environment.

## 1.12 Project Aims

Cancer immunology has gained tremendous momentum in recent years with novel biological discoveries proving that the immune system is able to recognise tumour cells and mount a response against them to keep them in check or even clear them. Despite significant clinical success with immunomodulatory drugs to boost the anti-tumour immune responses, not all patients achieve good outcomes and many that initially respond well to immunotherapies, end up relapsing. This suggests that cancers are able to evade the immune system by inducing a highly dynamic immunosuppressive microenvironment. Generation of nutritional stress, by starving immune cells of amino acids such as arginine and tryptophan is one way of inducing this immunosuppressive tumour microenvironment

and escaping anti-tumour immune responses. Our suggestion that AML blasts might secrete Arginase in patients with AML, a disease characterized by global immunocompromise, raises the possibility of systemic arginine depletion and systemic immunosuppression in leukaemias, as opposed to the local immunosuppression seen in solid tumours. What remains elusive is the ability of cancer cells to survive and thrive within the arginine-depleted suppressive environment they create, within which host cells, and more importantly T-cells, the main drivers of the anti-tumour immunity, suffer. We hypothesized that cancer cells, and more specifically AML blasts, must possess an adaptation strategy that allows them to adjust to low levels of arginine, and in fact other amino acids or nutrients, in order to continue to proliferate and function within the tumour microenvironment. We hypothesized that this adaptation mechanism might be through enhanced transport or increased de novo synthesis of the missing amino acid, in this case, arginine or its precursors. We also hypothesized that this mechanism is tightly regulated in a cancer-specific manner driven by mediators that are not active in normal healthy immune cells and other host cells. Furthermore, we hypothesized that abolition of this adaptation mechanism would render cancer cells vulnerable to their own suppressive microenvironment, creating opportunities for cancer therapies. In similar manner, identification of this adaptation mechanism could allow manipulation of T-cells, to equip them with the same ability to resist amino acid starvation, thus improving adaptive T-cell transfer therapies for cancer. Finally, we hypothesized that blocking the action of Arginase in the context of tumours and liquid cancers would relieve the immunosuppression imposed on T lymphocytes, and other immune cells, opening new avenues for cancer immunotherapy in the context of AML and other cancers.

To address these hypotheses, this project aimed to achieve the following:

1. to investigate whether Arginase is released in the bloodstream of AML patients and

whether this effect is reproduced in AML mouse models

2. to study the effects of Arginase-mediated arginine depletion on T-cells
3. to generate recombinant human Arginase-2 (rhARG2) and use it to test the efficacy of novel Arginase-specific inhibitors and their ability to rescue T-cells from Arginase effects
4. to investigate the effect of arginine starvation on the transcriptomic profile of cancer cells and T-cells, especially focusing on enzymes involved in amino acid metabolism/biosynthesis and transporters involved in amino acid cellular exchange
5. to study the biological function and importance of the most interesting and relevant genes upregulated in cancer cells but not T-cells in response to arginine starvation
6. to evaluate whether upregulation of proteins involved in arginine biosynthesis and transport confers a functional adaptation advantage for cancer cells over T-cells, in order to survive and proliferate in an arginine-depleted microenvironment
7. to test whether genetically modifying T-cells to mimic the transcriptional reprogramming observed in cancer cells, equips them with the ability to adapt to arginine starvation in the same way as cancer cells
8. to investigate whether arginine starvation has any metabolic effects on cancer cells, other than cessation of protein synthesis and suppression of cell growth and proliferation, and establish whether these effects can be prevented by any functional adaptation mechanisms the cancer cells might possess
9. to establish the regulatory networks, (genetic, epigenetic, transcriptional or translational) governing the upregulation of amino acid transporters and biosynthetic enzymes involved in the adaptation mechanisms employed by cancer cells in response to arginine starvation.
10. to explore the molecular mechanisms that give rise to any identified discrepancies

between cancer cells and T-cells in terms of their ability to adapt to arginine starvation or deprivation of other amino acids.

# Chapter 2: Materials and Methods

## 2.1 Cell lines and culture media

The human tumour cell lines THP1, NB4, HL60, MOLM13, OCI-AML, RT112, LNCaP and HeLa were obtained from Cancer Research UK or kindly gifted by collaborators at the Weatherall Institute of Molecular Medicine, University of Oxford. Cell lines were kept frozen and were passaged in the user's laboratory for fewer than 6 months after resuscitation. All leukaemic cell lines were cultured in Roswell Park Memorial Institute (RPMI) 1640 medium (Gibco) supplemented with 10% fetal bovine serum (FBS), 1% penicillin/streptomycin (100U/mL penicillin, 100µg/ml streptomycin; Gibco), 2mM L-glutamine (Gibco), 10 mM HEPES (Gibco), 1mM sodium pyruvate, and 0.1mM 2-mercaptoethanol to generate what will be referred to as R10 medium from now on. To generate D10 medium for appropriate cell lines such as HeLa, LNCaP and RT112 the equivalent supplements were added to Dulbecco's Modified Eagle Medium (DMEM). For arginine metabolic experiments, customized RPMI medium depleted of glutamine, lysine and arginine (Gibco) was supplemented with 10% dialysed FBS (Life Technologies, #26400044), 1% penicillin/streptomycin (100U/mL penicillin, 100µg/ml streptomycin; Gibco), 2mM L-glutamine (Gibco), 10 mM HEPES (Gibco), 1mM sodium pyruvate, 0.1mM 2-mercaptoethanol and the missing amino acids except arginine to generate arginine-depleted R10 medium. For tryptophan metabolic experiments, customized DMEM depleted of tryptophan, glutamine, arginine, leucine, isoleucine, glycine and serine (Life Technologies) was supplemented with 10% dialysed FBS (Life Technologies), 1% penicillin/streptomycin (100U/mL penicillin, 100µg/ml streptomycin; Gibco), 2mM L-

glutamine (Gibco), 10 mM HEPES (Gibco), 1mM sodium pyruvate, 0.1mM 2-mercaptoethanol and the missing amino acids except tryptophan to generate tryptophan-depleted D10 medium.

## 2.2 Reagents

### 2.2.1 Antibodies for Western blotting

Primary antibodies for Western blot were used as shown in **Table 2-1**:

| **Target** | **Catalogue number** | **Source** | **Species origin** |
|---|---|---|---|
| ASS1 | sc-365475 | Santa Cruz | mouse |
| GAPDH | sc-166574 | Santa Cruz | rabbit |
| ATF4 | 11815 | Cell Signalling Technology | rabbit |
| ATF4 | sc-390063 | Santa Cruz | mouse |
| β-actin | 8457 | Cell Signalling Technology | rabbit |
| SLC7A5 (LAT1) | 5347 | Cell Signalling Technology | rabbit |

| | | | |
|---|---|---|---|
| β-tubulin | 86298 | Cell Signalling Technology | mouse |
| S6 | 2217 | Cell Signalling Technology | rabbit |
| pS6 | 5364 | Cell Signalling Technology | rabbit |
| LC3 (I+II) | ABC929 | Sigma-Aldrich | rabbit |
| LAT1 (SLC7A5) | 5347 | Cell Signalling Technology | rabbit |

**Table 2 - 1. Primary antibodies used for Western blotting.**

All primary antibodies were used at a dilution of 1:1000 with the exception of GAPDH that was used at 1:500. For conventional western blotting, donkey anti-rabbit horseradish peroxidase (HRP)-conjugated affinity purified F(ab')2 Fragment (H+L) secondary antibody (Jackson ImmunoResearch laboratories; #711-036-152) was used at a dilution of 1:10,000. For fluorescent western blot, two fluorophore-conjugated secondary antibodies, Alexa Fluor® 680 goat anti–mouse IgG (ThermoFisher Scientific) and Alexa Fluor® 790 goat anti–rabbit IgG (ThermoFisher Scientific), were used simultaneously at a dilution of 1:20,000 to detect two targets at once.

### 2.2.2 Antibodies for Fluorescence-activated cell sorting (FACS)

The primary anti-human antibodies used for flow cytometry are shown in **Table 2-2**:

| **Target** | **Conjugated** | **Catalogue** | **Source (clone)** | **Dilution** |
|---|---|---|---|---|

| | **fluorophore** | **number** | | **(final)** |
|---|---|---|---|---|
| CD3 | PECy7 | 300420 | Biolegend (UCHT1) | 1:25 |
| CD3 | PE-Dazzle | 317345 | Biolegend (OKT3) | 1:25 |
| CD4 | FITC | 11-0348-41 | eBioscience (OKT4) | 1:25 |
| CD8 | APC-H7 | 560179 | BD Biosciences (SK1) | 1:25 |
| CD14 | BV510 | 301842 | Biolegend (M5E2) | 1:50 |
| CD19 | Unconjugated | 4349181 | Invitrogen | 1:20 |
| CD25 | PE | 12-0259-71 | eBioscience (BC96) | 1:50 |
| CD33 | PE | 12-0338-42 | eBioscience (WM53) | 1:25 |
| CD69 | APC | 17-0699-42 | eBioscience (FN50) | 1:50 |
| ASS1 | Unconjugated | MA5-17033 | Invitrogen/ThermoFisher Scientific | 1:200 |
| Live/Dead (405-450/50) | Violet Fluorescent Reactive dye | L34955 | Life Technologies | 1:100 |

**Table 2 - 2. Primary antibodies used for Fluorescence-activated cell sorting (FACS).**

Secondary antibodies used included donkey anti-mouse IgG conjugated to AlexaFluor®647 (ThermoFisher Scientific; A31571; 1:500 dilution), goat anti-rabbit IgG conjugated to AlexaFluor®647 (ThermoFisher Scientific; A21245; 1:500 dilution) and goat anti-mouse IgG conjugated to BV605 (Biolegend; 405327; 1:50 dilution).

### 2.2.3 Chemicals

The following chemicals were used as shown in **Table 2-3**:

| **Chemical** | **Catalogue number** | **Source** |
|---|---|---|
| L-citrulline | C7629 | Sigma-Aldrich |
| SD70 | M60194 | Xcess Biosciences |
| 2-aminobicyclo-(2,2,1)-heptane-2-carboxylic acid (BCH) | A7902 | Sigma-Aldrich |
| L-γ-Glutamyl-p-nitroanilide (GPNA) | G2505 | Sigma-Aldrich |

| | | |
|---|---|---|
| O-Benzyl-L-serine (Benser) | 13900 | Sigma-Aldrich |
| L-arginine | A5006 | Sigma-Aldrich |
| L-lysine | L5501 | Sigma-Aldrich |
| Isotope-labelled L-arginine-HCl (13C6, 15N4) | 89990 | ThermoFisher Scientific |
| Isotope-labelled citrulline (13C5, 2H4) | CDLM-7139-MPT-PK | Cambridge Isotope Laboratories |

**Table 2 - 3. Chemicals used for the purposes of this work.**

The novel Arginase-selective small molecule inhibitors, OAT081 and OAT090, were a gift from OncoArendi Therapeutics.

## 2.3 Human samples

Bone marrow or blood was obtained from healthy donors and AML patients as part of projects in the Cerundolo and Vyas labs and processed on the same day. All volunteer donors gave written informed consent in accordance to the declaration of Helsinki. Data and sample collection was approved by the Oxford Research Ethics Committee (MDSBio Study, MREC 06/Q1606/110; Oxford Musculoskeletal Biobank, MREC 09/H0606/11: South Central Oxford C Research Ethics Committee). Some of the samples were collected as part of the approved AML17 clinical trial (MREC 08/MRE09/29: Wales Research Ethics Committee). Peripheral blood or bone marrow mononuclear cells were isolated by the Ficoll-Hypaque density centrifugation method. Briefly, samples were diluted in R10 medium at a 1:1 volume ratio. 30mL of this diluted blood sample was overlaid carefully onto 15mL of Lymphoprep (AxisShield) and centrifuged for 30 min at 300g without brake or acceleration. Following centrifugation, the layer of mononuclear cells was collected carefully using a Pasteur pipette. Platelets and debris were removed by two subsequent

centrifugations, at 1500rpm and 1200rpm, each for 10 min. When necessary, the pellet was suspended in Red Blood Cell Lysis buffer (Qiagen) and left to stand for 5 min at room temperature to remove contaminant red blood cells. The mixture was then washed with R10 medium to obtain a clean cell pellet for further applications. Mononuclear cells were used to isolate either AML blasts or haematopoietic stem cells or to isolate CD4+ and CD8+ T-cells, which were used in various experiments. In the case of AML and healthy control bone marrow and peripheral blood samples, CD34+ and CD34- cells were further characterised and sorted using lineage depletion and appropriate antibodies as described in the published work from the Vyas laboratory [341]. For CD4+ and CD8+ T-cells, isolation was performed by magnetic-activated cell sorting (MACS) purification using CD4 or CD8 Microbead kits (Miltenyi Biotec) respectively and MACS separation columns (Miltenyi Biotec). Where appropriate, plasma from AML patients or healthy controls was also obtained by Ficoll separation of bone marrow or peripheral blood as described above by collecting the layer of plasma following the first centrifugation step after the lymphoprep application (in collaboration with Jessica Doondea).

AML blasts were identified by xenograft assays where leukaemic propagating cells were selected by their ability to engraft in irradiated NOD scid gamma (NSGS) mice (The Jackson Laboratory) [341].

### 2.3.1 Generation and activation of human $CD4^+$ and $CD8^+$ T cells

Peripheral blood mononuclear cells (PBMCs) were isolated from commercially available leukocyte cones (NHS Blood and Transplant, Bristol) by density gradient centrifugation in collaboration with Dr Mashiko Setshedi. $CD4^+$ and $CD8^+$ T cells were purified from PBMCs by positive or negative selection using magnetic cell separation – human CD4 MicroBeads or human $CD8^+$ T Cell Isolation Kit (Miltenyi Biotec), respectively. Pre-coating with anti-human CD3 and CD28 antibodies (eBioscience), both used at 5µg/ml

(1:1 ratio), was used for stimulation.

## 2.4 Mice

### 2.4.1 AML mouse models

The spontaneous AML mouse model used in this work, was generated by Dr Chris Booth (Mead group) as described in the literature [342]. Briefly, in the first instance, mice with *Ezh2* and *Runx1* deletions in early thymic progenitors were generated using the Rag1Cre-loxP system ($Ezh2^{fl/fl}Runx1^{fl/fl}Rag1Cre^{+}$). These double knockout mice were then crossed with mice that had $Flt3^{ITD/+}$ knocked in, as internal tandem duplications (ITD) of FLT3 are very common in human leukaemias. $Ezh2^{fl/fl}Runx1^{fl/fl}Rag1Cre^{+}Flt3^{ITD/+}$ mice developed a very aggressive form of acute, predominantly myeloid leukaemia that showed full penetrance and some lymphoid lineage features. With a median survival of approximately 9 weeks as a result of disease burden, mice were anaesthetised and sacked by terminal bleeding by cardiac puncture in collaboration with Dr Chris Booth who was breeding the mice. For the inducible AML mouse model, 50,000 fetal liver cells (CD45.2 allotype) carrying CEBPα mutant alleles 'K' and 'L' (K/L) along with wild-type helper CD45.1 competitor bone marrow cells (CD45.1 allotype) were used to inject the tail vein of sub-lethally irradiated B6SJL recipient mice (CD45.1 allotype) as previously described [343, 344]. Mice were terminally bled by cardiac puncture at 3, 4 and 5 weeks post-transplantation in collaboration with Dr Amit Grover and Alex Thomas who had recreated the model in the Nerlov lab. The mouse model of myeloproliferative disease had been generated by Dr Monika Mortensen and Prof Katja Simon by conditionally deleting the autophagy gene *Atg7* in the hematopoietic system to create Vav-$Atg7^{-/-}$mice that had autophagy-deficient haematopoietic stem cells as described in the literature [345, 346].

Serum from these mice was obtained in collaboration with Dr Tom Riffelmacher (Simon group) who was breeding these mice.

### 2.4.2 Mouse serum preparation

For the generation of serum, 1mL of whole blood obtained from each mouse was initially collected in Eppendorf tubes and allowed to clot undisturbed at room temperature for 30 min. The clotted portion was then removed by centrifugation at 1500 x g at 4$^{o}$C for 10 min. The resulting supernatant was collected using a Pasteur pipette, without disturbing the clotted bottom, aliquoted in new polypropylene tubes and stored in a freezer at -20$^{o}$C.

## 2.5 Differential gene expression analysis

### 2.5.1 Microarray

THP1 cells and primary activated CD4 T-cells obtained from three different healthy donors, were seeded at a density of 1 x10$^{5}$ cells per ml in 30ml of R10 or arginine-depleted R10 for 72hr before RNA was extracted using the RNeasy minikit (Qiagen; 74104) for RNA isolation according to the manufacturer's instructions. Each experimental condition was set up in biological triplicates and samples were randomized before gene expression analysis. Following RNA level normalization using nanodrop, a quality control analysis was carried out using a Bioanalyser before RNA was converted into biotin-labelled cRNA, used for hybridization. The hybridized and washed chips were then scanned using iScan Scanner (Illumina). A whole genome gene expression analysis was performed on the 12 RNA samples of human origin, utilizing the Human HT12v4.0 Expression Beadchip (Illumina, Cambridge) and GenomeStudio® software (Illumina, Cambridge) with help from the High-Throughput Genomics Group at the Wellcome Trust Centre for Human Genetics (funded by Wellcome Trust grant reference 090532/Z/09/Z). The data will be deposited in the GEO database following publication of this work.

#### 2.5.1.1 Differential gene expression analysis of microarray data

Differential expression of genes between THP1 cells and CD4 T cells grown in full medium and arginine depleted medium was estimated using the R package 'limma' [347]. An adjusted p-value threshold of 0.05 (multiple testing corrected using Benjamini-Hochberg) and a log2 fold change (log2FC) cutoff of <-1.5 or >1.5 were applied. Before running limma, samples were quantile-normalized using the R package 'preprocessCore'. Analysis of differential gene expression was performed in collaboration with Dr Steve Taylor and Dr Lars Rønn Olsen.

#### 2.5.1.2 Gene set enrichment analysis

Gene set enrichment analysis was performed with default parameters using javaGSEA version 2.2.4. [348]. Canonical pathways were evaluated based on GO term analysis.

### 2.5.2 Real-time quantitative reverse transcription PCR (q-RT-PCR)

RNA was extracted using the RNeasy minikit (Qiagen; 74104) for RNA isolation, including removal of genomic DNA, according to the manufacturer's instructions. cDNA was generated from the isolated RNA using the RETROscript® kit (Ambion) according to the manufacturer's instructions and using oligo-dT primers.

Final mRNA expression analysis was performed using commercially available Taqman® probes defined in **Table 2-4** (all obtained from Life Technologies) to detect genes of interest according to the manufacturer's instructions. Probes were specifically chosen to span exons within a gene when possible. All PCR reactions were performed on the 7500 Fast Real-Time PCR System (Applied Biosystems).

| Target gene (all human) | Amplicon length | Catalogue number |
|---|---|---|
| 18S | 187 | Hs99999901_s1 |
| GAPDH | 122 | Hs99999905_m1 |

| | | |
|---|---|---|
| ACTB | 171 | Hs99999903_m1 |
| HPRT | 100 | Hs99999909_m1 |
| ATF4 | 68 | Hs00909569_g1 |
| ASS1 | 94 | Hs01597989_g1 |
| SLC7A5 | 78 | Hs01001189_m1 |
| SLC1A5 | 68 | Hs01056542_m1 |
| KDM4C | 104 | Hs00909577_m1 |
| SLC7A11 | 57 | Hs00921938_m1 |
| ASNS | 69 | Hs04186194_m1 |
| ARG1 | 86 | Hs00163660_m1 |
| ARG2 | 62 | Hs00982833_m1 |
| OAT | 119 | Hs00236852_m1 |
| OTC | 95 | Hs00166892_m1 |
| ODC | 85 | Hs00159739_m1 |

**Table 2 - 4. TaqMan® probes used for q-RT-PCR gene expression analysis.**

### 2.5.3 Transcriptome sequencing (RNA-seq)

RNA was isolated from the different FACS-characterised cell populations from AML patients and healthy controls using an RNeasy Micro kit (74004; QIAGEN). Sequencing libraries were prepared as previously described [341] using the SeqCap EZ (v3; Nimblegen) or the SureSelect All Exon Enrichment kit (V5; Agilent Technologies). Sequencing was carried out on HiSeq2000 (Illumina) to produce 100 bp pair-end reads. Reads were mapped to the NCBI Human Reference Genome Build hg19 using a Burrows-Wheeler aligner (Stampy) [341]. Analysis was performed using R (Version 3.0.1) after

duplicates were removed and reads filtered for uniquely mapping reads (aiming for a mapping quality score (MAPQ) >3) using SAMtools (version 0.1.19) [349]. Gene expression was evaluated on edgeR [350]. Results were normalised as counts per million (cpm) and log2 transformed. Data have been deposited on ArrayExpress (Accession E-MTAB-2672). RNA-seq and its analysis were carried out in collaboration with Dr Lynn Quek.

## 2.6 Generation of ARG2-overexpressing THP1 cells

### 2.6.1 Cloning of ARG2 gene

The parental vector pHR-SIN-IRES-GFP **(Figure 2-1)** was used for the overexpression of ARG2. This vector contains the spleen focus-forming virus (SFFV) promoter and an internal ribosomal entry site element (IRES) to drive the expression of green fluorescent protein (GFP) as a reporter gene. Genes of interest, in this case *ARG2,* can be cloned between restriction sites and thus inserted downstream of the SFFV promoter which will then strongly drive their expression [351] **(Figure 2-1)**. In brief, following vector digestion with restriction enzymes *BamH*I and *Xho*I (New England Biolabs) for 1.5hr at 37ºC, the digested genetic material was run by electrophoresis on a gel and the developed bands were gel-purified using the QIAquick® Gel Extraction Kit (Qiagen) according to the manufacturer's instructions. ARG2 cDNA was amplified by PCR using the Phusion® High-Fidelity DNA Polymerase (New England Biolabs), the Arg2_*BamH*I_Fwd forward primer and the Arg2_*Xho*I_HAtag_Rev reverse primer **(Table 2-5)**. The PCR cDNA product was then digested with *BamH*I and *Xho*I restrictions enzymes (New England Biolabs) for 1.5hr at 37ºC, the digested genetic was run by electrophoresis on a gel and the developed bands were gel-purified using the QIAquick® Gel Extraction Kit (Qiagen) according to the manufacturer's instructions. Finally, both the digested pHR-SIN-IRES-

GFP vector and the digested ARG2 gene insert were ligated using T4 DNA ligase (New England Biolabs) overnight at 14°C. All primers for cloning and sequencing were designed in our lab, purchased from MWG Eurofins and used at a working final concentration of 5μM **(Table 2-5)**.

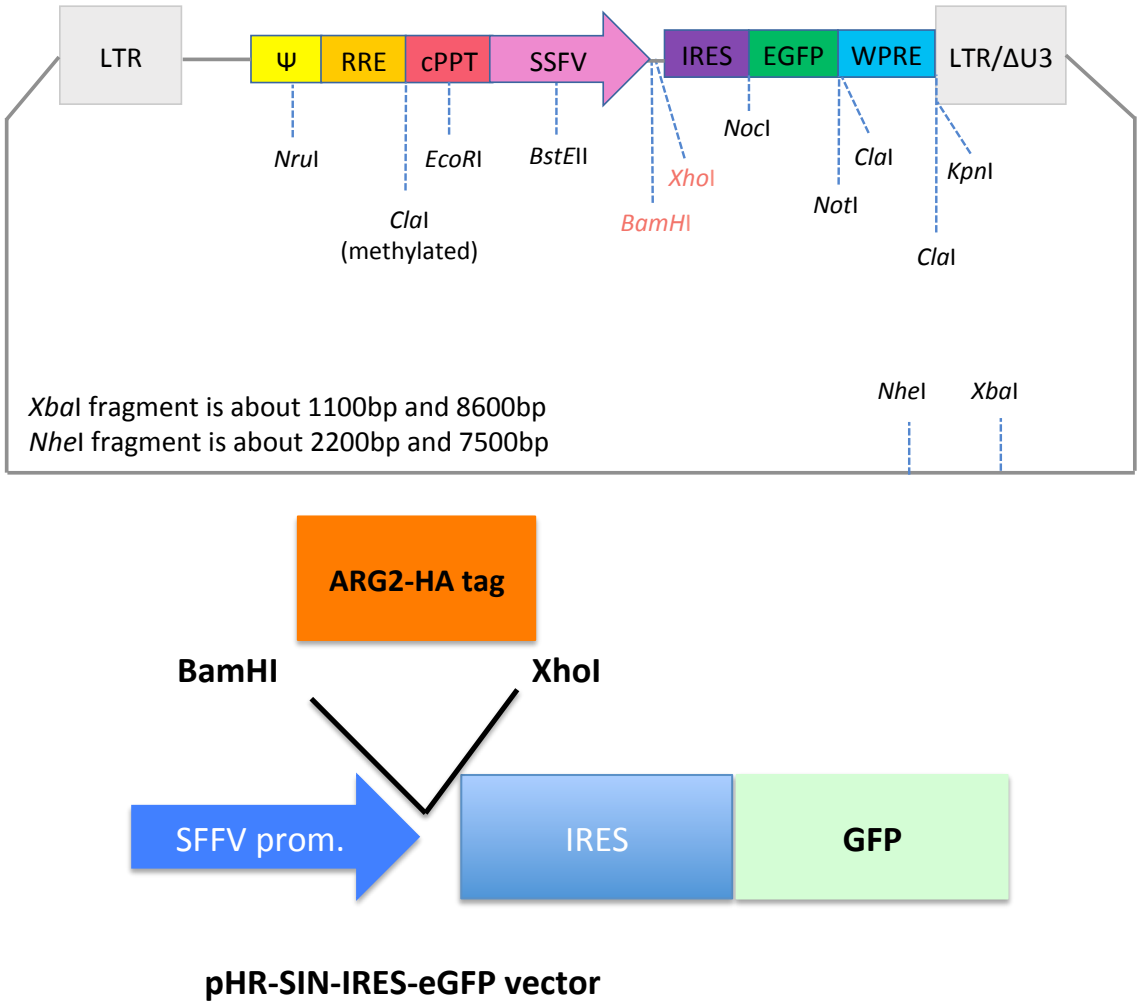



**Figure 2 - 1. Cloning of *ARG2*-HA into the pHR-SIN-IRES-GFP expression vector**
Upper panel depicts the map of pHR-SIN-IRES-GFP expression vector. Lower panel depicts the cloning of the ARG2-HA insert downstream of the SFFV promoter using the restriction enzymes *BamH*I and *Xho*I. LTR; Long terminal repeat, Ψ; Packaging signal sequence, RRE; Rev-responsive element, cPPT; Central polypurine tract, SFFV; Spleen focus-forming virus promoter, IRES; Internal ribosome entry site, EGFP; Enhanced green fluorescent protein, WPRE; Woodchuck provirus response element, LTR/ΔU3; Transcriptional activator of HIV.

| **Primer Name** | **Primer Sequence** |
|---|---|
| **Cloning Primers** | |
| *ARG2 overexpressing THP1 cells* | |
| Arg2_*BamH*I_Fwd | 5'-GGCGGATCC**ACC**ATGTCCCTAAGGGGCAGC**CT**-3' |
| Arg2_*Xho*I_HAtag_Rev | 5'-GGCCTCGAGCTAAGCGTAATCTGGAACATCGTATGGGTAAATTCTCACACGTGCTTG-3' |
| *Free soluble rhARG2 enzyme* | |
| rhArg2_*Nde*I_Fwd | 5'-GGACATATGGTCCACTCCGTGGCTGTGATAG-3' |
| rhArg2_*Xho*I_Rev | 5'-TGGCTCGAGAATTCTCACACGTGCTTG-3' |
| **Sequencing Primers** | |
| *ARG2 overexpressing THP1 cells* | |
| SFFV_Fwd | 5'-TGCTTCTCGCTTCTGTTCG-3' |
| IRES_Rev | 5'-ACATATAGACAAACGCACACCG-3' |
| *Free soluble rhARG2 enzyme* | |
| T7_Fwd (pGMT7) | 5'- TAATACGACTCACTATAGGG-3' |
| rT7_Rev | 5'-GCTAGTTATTGCTCAGCGGTGGC-3' |

**Table 2 - 5. Primers used for cloning and sequencing for generation of ARG2 overexpressing THP1 cells and recombinant human ARG2 (rhARG2) enzyme.** The *BamH*I restriction enzyme recognition site is depicted in red, the *Xho*I restriction enzyme recognition site is depicted in orange, the *Nde*I restriction enzyme recognition site

is depicted in magenta and the sequence encoding the HA epitope is shown in blue. A kozak sequence (shown in bold) was used to enhance expression. *ARG2*-specific sequences are underlined. Fwd=Forward primer, Rev=Reverse primer.

### 2.6.2 Transformation of bacteria

To transform 50µl of competent DH5α *E. coli* cells with 10µl of the ligation mixture, the two suspensions were incubated on ice for 10min before being exposed at 42 °C for 45sec (to induce cellular heat-shock and allow uptake of the genetic material) followed by another incubation on ice for 2min. Transformed bacteria were then allowed to grow in 200µl Luria-Bertani (LB) broth for 1hr at 37°C on a horizontal shaker. Under sterile conditions, bacteria were then plated on plates of LB agar containing 100µg/ml ampicillin and incubated overnight at 37°C. Ampicillin-resistant single colonies were selected the following day and screened by PCR gel electrophoresis to check for the insertion of the correct amplicon. The PCR product for screening was obtained using primers from the original PCR amplification of cDNA and the MangoTaq DNA polymerase kit (Bioline). Colonies that had successfully incorporated the required amplicon were carefully picked and expanded overnight in tubes of 5ml of LB broth with 100µg/ml ampicillin, placed in a 37°C incubator, shaking at 200rpm. The QIAprep® Spin Miniprep kit (Qiagen) was used according to the manufacturer's instructions to purify plasmids from each independent bacterial culture. Each plasmid had its sequence verified by in-house Sanger sequencing using the SFFV-FW and IRES-RV primers that recognize sequences within the pHR-SIN-IRES-GFP parental vector. Plasmids with the correct insert were purified using a Plasmid Midi kit (Qiagen) using starting material from the appropriate bacterial cultures.

### 2.6.3 Transfection and Lentiviral Transduction

To generate lentiviral particles for transduction, human embryonic kidney (HEK293T)

cells were co-transfected with the appropriate lentiviral transfer plasmid vectors carrying the ARG2 gene (obtained in 2.6.2) and envelope/packaging plasmids encoding for VSV-G protein and Gag-pol proteins, using the X-tremeGENE 9 transfection solution (Roche) according to the manufacturer's instructions. Following HEK293T cell growth for 72hr, the culture supernatant was collected and utilized fresh to directly transduce wild-type (WT) THP1 cells. Transduction efficiency was evaluated by measuring GFP fluorescence levels within cells under the microscope using Floid Cell Imaging station (ThermoFisher Scientific). Successfully transduced cells were FACS sorted based on the levels of GFP intensity. Selection and isolation of cells was also assisted by use of the HA tag. Western blotting, Arginase activity assay and Arginase-2 ELISA were used to confirm ARG2 expression.

## 2.7 Generation of recombinant human Arginase-2 (rhARG2)

In order to synthesize a free and soluble recombinant human Arginase-2 enzyme, we had to generate a lentiviral vector that would encode for the human ARG2 protein without that being bound to mitochondria but instead being free in the cytoplasm. As such, we could not use the same primers used for *ARG2* overexpression in THP1 cells. We had to ensure that the human *ARG2* that would be introduced in the vector lacked the mitochondrial signal peptide at the N-terminus (66 base pairs encoding for 22 amino acids). Thus, we designed our new primers, rhArg2_*Nde*I_Fwd and primer and the rhArg2_*Xho*I_Rev, in such a way so that both the N-terminus mitochondrial signal peptide and the C-terminus TAG stop codon were bypassed **(Table 2-5)**. In order to generate the rhARG2 lentivector, the parental vector pET-21a+ (a gift from SeWon Suh, #12652, Addgene) [352] was initially digested with *Nde*I and *Xho*I restriction enzymes and gel-purified in the same process as described earlier in section 2.6.1. cDNA originating from THP1 cells was then

PCR amplified using the Phusion® High-Fidelity DNA Polymerase (New England Biolabs), the rhArg2_*NdeI*_Fwd forward primer and the rhArg2_*XhoI*_Rev reverse primer **(Table 2-5)**. The PCR product was subsequently digested with the *Nde*I and *Xho*I restriction enzymes and gel-purified before finally being ligated to the *Nde*I- and *Xho*I-flanked pET-21a(+) vector in the same way as previously described in section 2.6.1. Following bacterial transformation with the vector (described earlier in 2.6.2) plasmids had their sequence verified by in-house Sanger sequencing using the T7 forward primer and rT7 reverse primer that recognize sequences within the pET-21a(+) parental vector. The extraction, purification, testing and further use of the rhARG2 enzyme are described in results Chapter 3.

## 2.8 Overexpression of ASS1 gene in primary human T-cells

CD8 T-cells were genetically engineered by lentiviral particle transduction to express *ASS1* in collaboration with Dr Uzi Gileadi. On day 0, CD8+ T-cells were purified from mononuclear cells from a healthy donor blood sample using the CD8 Microbeads kit (Miltenyi Biotec) and MACS separation columns (Miltenyi Biotec). They were then labelled with 5μM of cell tracker violet (CTV; Invitrogen/ThermoFisher Scientific) to monitor proliferation and transduced with lentiviral particles containing the vector encoding the human ASS1 gene and GFP. 24 hours later, CD8+ T-cells were stimulated using anti-CD3/anti-CD28 beads (Dynabeads®; ThermoFisher Scientific) at a ratio of 1:1. 24 hours post-stimulation, the T-cells were washed twice in PBS and cultured in selective medium (R10, R10 without arginine and R10 without arginine with added 0.4mM of citrulline). Medium was replenished again 48 hours later to ensure T-cells were not starved of any nutrients except arginine in the appropriate cultures. Finally, another 48 hours later, now day 6 of the experiment, the cells were harvested, and analysed by flow cytometry by

gating on single, live CTV+ CD8+ T-cells. Cells that had been successfully transduced with lentiviral particles expressed both ASS1 and GFP (ASS1+GFP+ CD8 T-cells). Cells that failed to be transduced acted as a natural control for the experiment as they did not express ASS1 or GFP. ASS1 expression was confirmed by flow cytometry in addition to the proliferation assay.

## 2.9 CRISPR-Cas9-mediated gene silencing

CRISPR-Cas9 technology was used to silence LAT1 (SLC7A5) in HeLa cells as described in the literature (a gift from Dr Hemza Ghadbane and Dr Elina Timosenko) [301]. Briefly, unique sequences in the coding region of the LAT1 gene (exon 1) were used to generate targeted chimeric guide RNAs. A px330 construct was used to transfect WT HeLa cells with Cas9 and the LAT1-specific CRISPR guide sequences. Gene-specific RNA guides were designed using crispr.mit.edu server [353]. qRT-PCR and Western blotting were used to confirm the knockout efficiency. CRISPR-Cas9 technology was used in the same way to delete the ATF4-biding motif at the ASS1 intronic enhancer in THP1 cells in collaboration with Dr Nicholas Crump. In this case, the pSpCas9-GFP plasmid and a plasmid containing two unique guide RNAs specifically flanking the ATF4 binding motif was used to co-transfect THP1 cells by electroporation. GFP-positive cells were identified and selected by FACS sorting after 24hrs of incubation and further plated in medium to generate clones. Clones were screened by PCR of the targeted region, and deletions confirmed by in-house Sanger sequencing.

## 2.10 shRNA-mediated gene knockdown

MISSION® short hairpin RNA (shRNA) lentiviral particles were purchased from Sigma-Aldrich for silencing of the ASS1 and ATF4 genes **(Table 2-6)**. Transduction of cell lines

with lentiviral particles was carried out as described earlier. Selection of transduced cells was achieved by treatment with puromycin (1μg/ml). This is because of the pLKO.1 plasmid in which both the shRNA and puromycin resistance genes are expressed under the control of the U6 promoter (Sigma Aldrich website). As a control vector, we used the Sigma Aldrich-recommended MISSION® pLKO.1-puro non-mammalian shRNA vector (Sigma Aldrich) that targets no known mammalian gene.

| **Target gene shRNA ID** | **shRNA sequence** |
|---|---|
| **ASS1** | |
| TRCN0000436210 | CCGGATGAACGTGCAGGGTGATTATCTCGA GATAATCACCCTGCACGTTCATTTTTTG |
| **ATF4** | |
| TRCN0000013573 | CCGGGCCTAGGTCTCTTAGATGATTCTCGAG AATCATCTAAGAGACCTAGGCTTTTT |

**Table 2 - 6. Sequences of shRNA used for gene knockdown and silencing.**

## 2.11 Arginase activity assay

Arginase activity in various samples was measured using a colorimetric Arginase activity assay as per the manufacturer's instructions (MAK-112; Sigma Aldrich). The assay measures the amount of urea synthesized as a result of Arginase activity by using the principle that Arginase converts arginine to ornithine and urea.

For cell culture supernatant, mouse serum and human plasma, sample types that contain naturally formed urea, 10 kDa Molecular Weight Cut-off Filters (Z677108; Sigma Aldrich) were used. This filter size maintains Arginase but allows urea to pass through and be depleted from the samples so that it does not interfere with the results. Following 2-3

rounds of centrifugation (30 min each), urea is finally filtered out and the sample is concentrated to 40µL. For cell lysates, 1 x $10^6$ cells are harvested and washed in PBS before being subjected for 10 minutes to 100µL of lysis buffer containing protease inhibitors (10mM Tris-HCl (pH 7.4), 1 µM pepstatin A, 1 µM leupeptin and 0.4% Triton X-100). Once the sample is prepared, 40 uL are added to each of two wells of a 96-well plate; one for the sample well and one for the sample blank well. As a control, we used 50 µL of prepared 1 mM urea standard working solution in one well (control well) and 50 µL of water in another well (control blank well). 10 µL of substrate buffer (8µL arginine buffer, 2µL manganese solution) is then added to each of the sample wells only but none of the control or sample blank wells. The wells are mixed, covered with aluminium foil and incubated for 2 hours at 37°C. After this step, 200µL of Urea reagent is added to all wells to stop the Arginase reaction. Once the reaction is inhibited, 10 µL of substrate buffer can be added to the sample blank wells so that all wells have the same volume. The plate is incubated for 60 minutes at room temperature and then absorbance (optical density) is measured using at 450 nm using spectrophotometer. The Arginase activity of each sample is calculated in Units per Litre (Units/L) using the following formula:

$$\textbf{Activity} = (\text{Sample}^{A450} - \text{Blank}^{A450}) / (\text{Standard}^{A450} - \text{Water}^{A450}) \times [\text{urea standard}] \times 50 \times 10^3) / (V \times T)$$

T= Reaction time in minutes (normally 120)

V= Sample volume added to well in µL (usually 40µL but can be as low as 1µL)

Urea Standard concentration = 1mM

50 = Reaction volume in µL

$10^3$ = mM to µM conversion factor

One Unit of Arginase activity as calculated in this method is equivalent to the amount of enzyme that will convert 1μmole of arginine to ornithine and urea per minute at pH 9.5 and temperature 37°C.

## 2.12 ELISA (Enzyme-linked immunosorbent assay)

### 2.12.1 Arginase-1 and Arginase-2 measurements

Human and mouse Arginase-1 and Arginase-2 serum or plasma levels were measured using commercially available sandwich ELISA kits as per manufacturer's instructions (all from Antibodies online, murine ARG1; ABIN810912, human ARG1; ABIN810911, murine ARG2; ABIN426879, human ARG2; ABIN1568500). Briefly, samples and standards were applied to microplates pre-coated with immobilized antibody against the desired target protein and incubated for a fixed time. Unwanted impurities and unbound substances were removed with multiple rounds of washing and a target-specific biotin-conjugated antibody was added. Following a fixed period of incubation, microplates were washed again and avidin-conjugated Horseradish Peroxidase (HRP) was added to react with biotin in the wells. Following another round of washing to remove unbound avidin-HRP, substrate solution was added leading to the generation of colour with intensity proportional to the amount of target protein bound in the first incubation step. Once the reaction was stopped the colour intensity was measured at a detection wavelength of 450nm using a spectrophotometer.

### 2.12.2 Interferon-gamma (IFN-γ) measurements

Interferon-gamma (IFN-γ) levels in human CD4+ T-cell culture supernatants were measured using a sandwich ELISA assay developed in-house and based on the same principle described above using the monoclonal anti-IFN-γ capture antibody R4-6A2 (No. 16-7312-81; ThermoFisher Scientific/eBiosciences) and the monoclonal anti-IFN-γ

biotinylated detection antibody XMG1.2 (No. 16-7311-81; ThermoFisher Scientific/eBiosciences). IFN-γ standards were obtained from Peprotech. Briefly, the anti-IFN-γ capture (primary) antibody was diluted in coating buffer ($NaHCO_3$ [pH 7.9] 100mM solution) to give a concentration of 2μg/mL. 25μL of this capture antibody solution were used to coat each well of a 96-well enhanced binding ELISA plate (Greiner). The plate was covered and incubated at 4ºC overnight. The following day, the plate wells were washed 6 times with washing buffer (PBS with 0.5% Tween-20) and blocked using blocking buffer (PBS with 10% FCS) at 200μL per well. The plate was kept in blocking buffer and covered for 120 min at room temperature before two further washes with washing buffer. IFN-γ standards were added in appropriate wells at 4ng/mL with serial double dilutions using blocking buffer to allow the generation of a standard curve. Samples (diluted in blocking buffer or undiluted) were added in the appropriate wells at a volume of 50μL. The plate was covered and incubated at 4ºC overnight. Plates were washed 6 times and 25μL of biotinylated anti-IFN-γ detection (secondary) antibody added in each well (1μg/mL working concentration by dilution in blocking buffer). The plates were covered and incubated for 60 min and were then washed 8 times in washing buffer. 25μL of avidin-peroxidase (3151; Sigma Aldrich), pre-diluted in blocking buffer 1:400 to give working concentration of 2.5μg/mL, was added in each well and plate covered and incubated at room temperature for 40 min. The plate was washed 8 times with washing buffer before the ABTS substrate and $H_2O_2$ mixture was added. The reaction was allowed to develop for 10-80 min based on the intensity of colour changes before eventually being stopped with 2M $H_2SO_4$. Absorbance was read at 405nM using a spectrophotometer (BMG SPECTROstar plate reader). A 4-parameter standard curve was made using the MARS data analysis software (BMG) and used to infer the concentration of cytokine in each sample well.

### 2.12.3 Arginine measurements

Human plasma and mouse serum L-arginine measurements were performed using a commercially available competitive inhibition enzyme immunoassay kit (CEB938Ge; Cloud-Clone) as per manufacturer's instructions. The principle of the assay is the same as described above for the Arginase sandwich ELISA with a pre-coated arginine-specific monoclonal antibody immobilized in each well of the microplate but with the exception that a competitive inhibition reaction is set up between biotin-labelled arginine and non-labelled arginine. In this way the amount of bound HRP conjugate is in fact inversely proportional to the concentration of arginine in the sample or standard. Hence the same inverse correlation holds true after addition of substrate for the spectrophotometer optical density reading, measured at 450nm, and arginine concentration for each sample, standard or control. Arginine levels were determined following the generation of a standard curve with log [Arginine] on the y-axis and optical density (absorbance) on the x-axis. Standards were plotted to generate a straight line of best fit, extrapolated using regression analysis. Graphpad Prism 6.0 was used to calculate the values.

### 2.12.4 Citrulline measurements

Human plasma citrulline was quantified using a commercially available detection kit (K6600; Immunodiagnostik). In brief, samples were pre-treated with appropriate reagents to eliminate any interference from irrelevant compounds before mixed with development solution to generate a red colour. The absorbance of each well was measured at 540nm using a spectrophotometer and the concentration of each sample determined based on a standard curve using standards and controls provided in the kit. Each sample was accompanied by a sample blank. The absorbance of the latter was subtracted from the sample absorbance value to eradicate the effect of sample matrix on absorption readings. In all the aforementioned ELISA assays, samples, standards and controls, including sample

blanks were tested in triplicate.

## 2.13 Protein expression analysis

### 2.13.1 Cell lysis

Cells were removed from culture and washed three times with ice-cold PBS to completely remove any medium before the cell pellet was dissolved in ice-cold lysis buffer (Lysis Buffer A: 10mM Tris-HCl [pH 7.4], 100mM NaCl, 1mM EDTA, 1mM EGTA, 1% Triton X-100, 10% glycerol, 0.1% SDS, 0.5% sodium deoxycholate or Lysis Buffer B: 50mM Tris-HCl [pH 8.0, 1% NP-40, 150mM NaCl, 0.1% SDS, 0.5% sodium deoxycholate) with cOmplete™ protease inhibitors (Roche) and incubated on ice for 30 min with regular vortexing every 5 min to facilitate cell lysis. At the end of the incubation period the mixture was centrifuged at 13,000 rpm for 30 min at 4°C and supernatant collected to eliminate nuclei and cell debris. 50µL of lysis buffer was used for every 1 x $10^6$ cells.

### 2.13.2 Quantification of protein concentration

The supernatants obtained from the lysis reaction were evaluated for total protein concentration using the bicinchoninic acid assay (BCA; Pierce™) as per manufacturer's instructions. Each sample lysate was then diluted in PBS to a concentration of 25µg and mixed with NuPAGE™ 4X LDS Sample Loading Buffer (NP0007; ThermoFisher Scientific) and NuPAGE™ 10X Sample Reducing Agent (NP0004; ThermoFisher Scientific) in a 4:1 and 10:1 ratio respectively. Mixtures were boiled for 4 min at 95°C and placed on ice before being centrifuged at 4°C for 1 min at 13,000 rpm.

### 2.13.3 Western blotting

20 µL of each prepared sample, as described above, was loaded onto separate wells of a NuPAGE™ Novex 4-12% Bis-Tris gel (NP0321; ThermoFisher Scientific) mounted into a protein gel electrophoresis chamber prefilled with Novex™ 10X Tris-Glycine SDS

Running Buffer (LC2675; ThermoFisher Scientific) diluted in a 1:10 ratio with double distilled water. Resolution was achieved at a voltage of 120V for 90 min. Proteins that had separated on the gel were then transferred onto a polyvinylidene difluoride (PVDF) membrane and incubated in BSA blocking buffer (5% BSA [Sigma Aldrich] and 0.5% Tween-20 dissolved in PBS) for 60 min at room temperature. The membrane was then incubated on a slow rocker with the appropriate primary antibody for 60 min at room temperature. The membrane was then washed for 15 min three times using washing buffer (0.1% Tween-20 dissolved in PBS) and incubated with the appropriate secondary antibody on a slow rocker overnight at 4$^{o}$C. The secondary antibody was either HRP-conjugated or fluorophore-conjugated as described previously. The membrane was washed for 20 min three times and dried. In the case of an HRP-conjugated secondary, ECL Plus Western Blotting Substrate (Pierce) was added according to the manufacturer's instructions and chemoluminescence was detected using the ChemiDoc platform (BioRad) and the Image lab software (BioRad). In the majority of experiments, where fluorophore-conjugated secondary antibodies were used, the membrane was dried for 60 min directly after the three 20 min washes and visualised using a near-IR fluorescence scanner linked to the Odyssey® Imaging System (LI-COR®) on which band analysis was carried out and band intensity measured. Band intensity of target proteins was normalised to that of loading controls on the same membrane, such as GAPDH and β-tubulin, using Microsoft Excel and the intensity measurements from the Odyssey® Imaging System. As a result of multi-colour analysis of fluorophore-conjugated secondary antibodies on the Odyssey® Imaging System, we were able to simultaneously detect two proteins on the same blot; one at 680nm (red bands) and one at 790nm (green bands).

## 2.14 Flow Cytometry

### 2.14.1 Live-Dead staining

Cells were first collected in a 96-well microplate and washed three times with PBS. In order to assess cell viability, they were stained with LIVE-DEAD® Fixable Aqua Dead Cell Stain (L34957; ThermoFisher Scientific) and incubated in the dark at 4ºC for 20 min. LIVE/DEAD dye was made to stock using DMSO as per manufacturer's instructions and then diluted in PBS (1:250) before mixed with the cell suspension at the final dilution shown in **Table 2-2**.

### 2.14.2 CFSE and CTV staining

In order to follow cellular proliferation, cells were labelled with either CellTrace$^{TM}$ CFSE (C34554; ThermoFisher Scientific) or CellTrace$^{TM}$ Violet (CTV; C34557; ThermoFisher Scientific) dyes whose intensity reduces every time a cell divides as the amount of dye splits between the two daughter cells during each division. Cells were first washed twice in cold PBS before being gently re-suspended in diluted CFSE or CTV at a concentration of 10 x$10^6$/ml for 8 min, at room temperature and protected from light. The reaction was then stopped by addition of excess RPMI medium with 5% FCS. Cells were centrifuged and washed twice in R10 medium before stimulation (described in section 2.3.1). Initial stocks of CFSE and CTV were made in DMSO as per manufacturer's instructions. This was followed by a 1:1000 dilution in the PBS cell suspension to give a final working concentration of 5μM.

### 2.14.3 Cell surface marker staining

For cell surface staining, cells were first stained for cell viability as described in the previous section. Still in the 96-well microplate, cells were then washed three times with FACS buffer (PBS with 1% fetal bovine serum [FBS]) and then stained for 30 min at 4ºC with the appropriate panel of fluorophore-conjugated antibodies at the dilutions designated

earlier. After another two rounds of washing with FACS buffer cells were resuspended in FACS buffer and transferred to FACS tubes for analysis.

### 2.14.4 Intracellular (cytoplasmic) staining

For targets present in the cell cytoplasm, such as ASS1, cells were first stained for LIVE/DEAD and surface antigens as described earlier, before being fixed for 20 min at room temperature using 100µL of eBioscience™ Intracellular Fixation Buffer (88-8824-00; ThermoFisher Scientific) to cross-link proteins. Cells were then washed in eBioscience™ 1X Permeabilisation Buffer (88-8824-00; ThermoFisher Scientific) to create pores in the cell membrane and allow intracellular staining antibodies to effectively reach the cytoplasm. Cells were then incubated in blocking buffer (1X Permeabilisation Buffer with 5% FBS, 5% human serum, 5% goat serum, 1% human Fc block and 1% BSA) for 30 min at room temperature. Cells were then incubated for 30 min at room temperature with antibodies targeting the intracellular proteins of interest, diluted to the concentrations designated in section 2X using 1X Permeabilisation Buffer. Cells were washed twice in 1X Permeabilisation Buffer before being washed and resuspended in FACS buffer and transferred to FACS tubes for analysis. Where appropriate another round of staining incubation and washing was performed to accommodate for unconjugated primary antibodies requiring detection by fluorophore-conjugated secondary antibodies as in the case of the ASS1 protein.

### 2.14.5 Running of samples

Fluorescence activated cell sorter (FACS) analysis was performed using a LSR Fortessa flow cytometer (BD) or a Cyan ADP flow cytometer (Dakocytomation). FACS sorting was performed using the Aria III SORP machine (BD). Appropriate gates for live, singlet cells and any other characteristics were set whilst samples were run. Where appropriate, single

stain and fluorescence minus one (FMO) controls were set up using cells or compensation beads (01-1111-42; ThermoFisher Scientific) for gating and compensation purposes.

## 2.15 IncuCyte Killing Assay

In order to evaluate the effect of Arginase-2 within human AML plasma on the killing ability of cytotoxic CD8+ T-cells we set up a killing assay, in collaboration with Dr Ji-Li Chen, using the IncuCyte® Live Cell Analysis platform (Essen BioScience, Sartorius, USA) which permits automated real-time measurements of cell viability and cell death. The NY-ESO-1-specific $CD8^+$ T cell clone (4D8) was kindly provided by Dr Ji-Li Chen and used as previously described in our lab [354-356]. Briefly, the killing ability of cytotoxic CD8+ T-cells was evaluated by their ability to kill target cells (THP1) by antigen-specific recognition using the NY-ESO9V peptide and the T-cell clone, 4D8, recognising this antigen. Effector 4D8 T-cells are expected to kill target cells presenting the NY-ESO9V peptide causing the release of intracellular fluorescent dye that had been previously incorporated by the target THP1 cells. Fluorescence release in the culture medium was measured automatically over 8 hours in various test conditions such as presence or absence of human AML plasma and presence or absence of Arginase-specific inhibitors. Control conditions included absence of fluorescent dye as background and absence of NY-ES9V peptide or absence of effector 4D8 CD8+ T-cells as negative controls.

## 2.16 Bioenergetic profiling to evaluate cancer cell glycolysis and oxidative phosphorylation

### 2.16.1 Sample preparation and overview of metabolic experiments

For cellular metabolism experiments we used the XFe96 Extracellular Flux Analyser (Seahorse Bioscience, now Agilent Technologies, USA) to measure extracellular acidification rate (ECAR) as a surrogate for glycolysis and oxygen consumption rate (OCR) representing oxidative phosphorylation and mitochondrial function. Both the ECAR/glycolysis stress test (103020-100; Agilent Technologies) and OCR/mitochondrial stress test (103015-100; Agilent Technologies) assays were performed according to the manufacturer's instructions. Briefly, THP1 cells were cultured for 72 hr in either complete R10 medium, arginine-free R10 medium with or without citrulline supplementation, or complete R10 medium with rhARG2 and with or without citrulline supplementation. On the morning of the 4$^{th}$ day, THP1 cells were washed twice in PBS and the appropriate Seahorse assay medium, counted by an automated haemocytometer (Countess$^{TM}$; ThermoFisher Scientific) using Trypan blue staining, suspended in the appropriate, pre-warmed Seahorse assay medium and seeded at a cell density of 50,000 per well (40µL/well) into Seahorse XF96 polystyrene cell culture plates (Seahorse Bioscience, Agilent Technologies). Each condition was seeded in 11 or 12 replicate wells. Plates had been previously coated with poly-D-lysine (30µl/well) dissolved in double distilled water to a concentration of 50µg/mL, and left at 4$^{o}$C overnight. Plates were then centrifuged briefly for 2 min at 1500rpm and checked under the microscope to ensure a monolayer of cells had formed. Wells were topped up to a volume of 180µl with the appropriate Seahorse medium for each assay. The plates were incubated in a 37$^{o}$C, $CO_2$-free incubator for 30 min whilst the Agilent Seahorse XFe96 sensor cartridges were calibrated on the machine. 4 wells in each plate (at positions A1, A12, H1, H12) contained no cells and

acted as calibration negative controls. Drugs appropriate for each assay were added to the injection chambers of each sensor cartridge and once the Seahorse plate was connected to the Seahorse sensor cartridge, the apparatus was inserted in the machine and the experiment was run. All experiments were run at temperature 37$^{o}$C, pH 7.4. Each experiment consisted of 12 8-min measurement cycles each composed of a mixing step (3 min), a waiting step (2 min) and finally a data acquisition step (3 min). In all experiments, the first 3 cycles gave baseline measurements whereas another 3 cycles took place after the addition of each of the 3 serially injected drugs (glycolysis stress test: glucose, oligomycin, 2-DG; mito stress test: oligomycin, FCCP, rotenone/antimycin A) to give treatment response measurements. ECAR and OCR were reported as absolute rates without normalisation to the number of cells (as the latter remained constant throughout experiments). ECAR was reported in mpH per min whereas OCR was reported in pmoles per min.

Seahorse OCR medium was made by dissolving glucose (to a final concentration of 10mM), sodium pyruvate (final concentration 1mM) and L-glutamine (final concentration 2mM) in Agilent Seahorse XF Base medium (102353; Agilent Technologies) and adjusting pH to 7.40. To make Seahorse ECAR medium L-glutamine was added in Agilent Seahorse XF Base medium to a final concentration of 2mM and pH adjusted to 7.35. Each condition was done in 11 or 12 replicates in the same experiment and each experiment was done in duplicate. Ideal conditions, including seeding cell density in each well and drug concentrations, were determined prior to the actual experiments by preliminary optimization experiments as per the manufacturer's instructions. THP1 cells were used at a density of 50,000 cells per well.

**2.16.2 Glycolysis stress test analysis**

For the glycolysis stress test, glucose was injected to give a final concentration of 10mM,

whereas final working concentrations were 1μM for oligomycin and 50mM for 2-DG. All drugs were obtained from Seahorse Bioscience. In the glycolysis stress test, addition of saturating amounts of glucose occurs first and leads to an increase in the ECAR that represents the basal rate of glycolysis, the conversion of glucose to pyruvate **(Figure 2-2)**. Subsequently, addition of oligomycin causes inhibition of ATP synthase shifting the production of energy (in the form of ATP) from mitochondrial respiration (oxidative phosphorylation) to glycolysis. The increase in ECAR as a result of this shift gives the maximum glycolytic capacity of the cell. 2-deoxy-glucose (2-DG), a glucose analogue is added last to competitively inhibit glucose hexokinase and shut down glycolysis. The accompanied drop in ECAR confirms that acidification generated in the experiment is truly due to glycolysis. The difference between maximal and basal glycolysis is known as the glycolytic reserve and denotes the ability of the cell to react to demands in energy using glycolysis.

### 2.16.3 Mitochondrial respiration stress test analysis

For the mitochondrial stress test, final working concentrations following injection into wells were 1μM for oligomycin, 0.5μM for FCCP and 0.5μM for rotenone/antimycin A. All drugs were obtained from Seahorse Bioscience. In the mitochondrial stress test, the experiment begins with basal respiration rate **(Figure 2-3)**. Oligomycin, added first, inhibits ATP synthase (complex V in the mitochondrial electron transport chain) decreasing OCR. This decrease in OCR corresponds to ATP production associated with mitochondrial respiration. FCCP is then added to uncouple the proton gradient in the mitochondria leading to disruption of the mitochondrial membrane potential. This allows electrons to move freely and oxygen consumption (OCR) is maximized. The peak of OCR following FCCP injection is used to calculate the maximal possible respiration rate of the cell. Finally, the third injection delivers a mix of rotenone and antimycin A, which inhibits

complex I and complex III respectively, of the mitochondrial electron transport chain and thus reduces OCR. The two drugs combined, completely abolish mitochondrial respiration enabling estimation of non-mitochondrial respiration. Spare respiratory capacity indicates the difference between maximal and basal respiration. It is a crucial measurement as it shows the ability of cells to react to enhanced energy demand; an indicator of cell fitness.

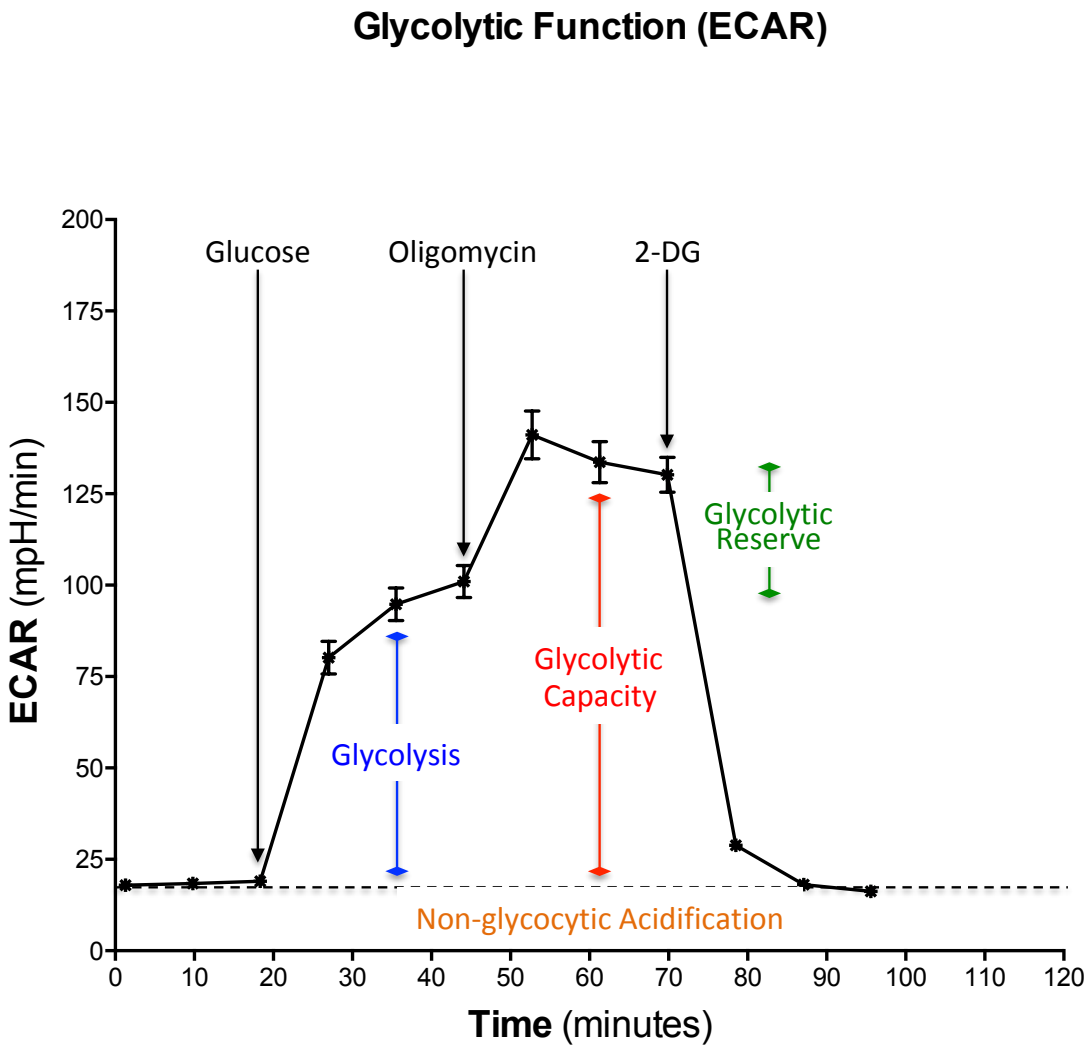



**Figure 2 - 2. Representative Glycolysis Stress Test profile of the key parameters of glycolytic function.**
Cellular glycolytic function is evaluated by directly measuring extracellular acidification rate (ECAR). Sequential injections of glucose, oligomycin and 2-DG allow measurement of glycolysis and glycolytic capacity, and calculation of glycolytic reserve and non-glycolytic acidification. Bars represent mean and standard deviation. Each data point is the mean of eleven replicate measurements at a specific timepoint.

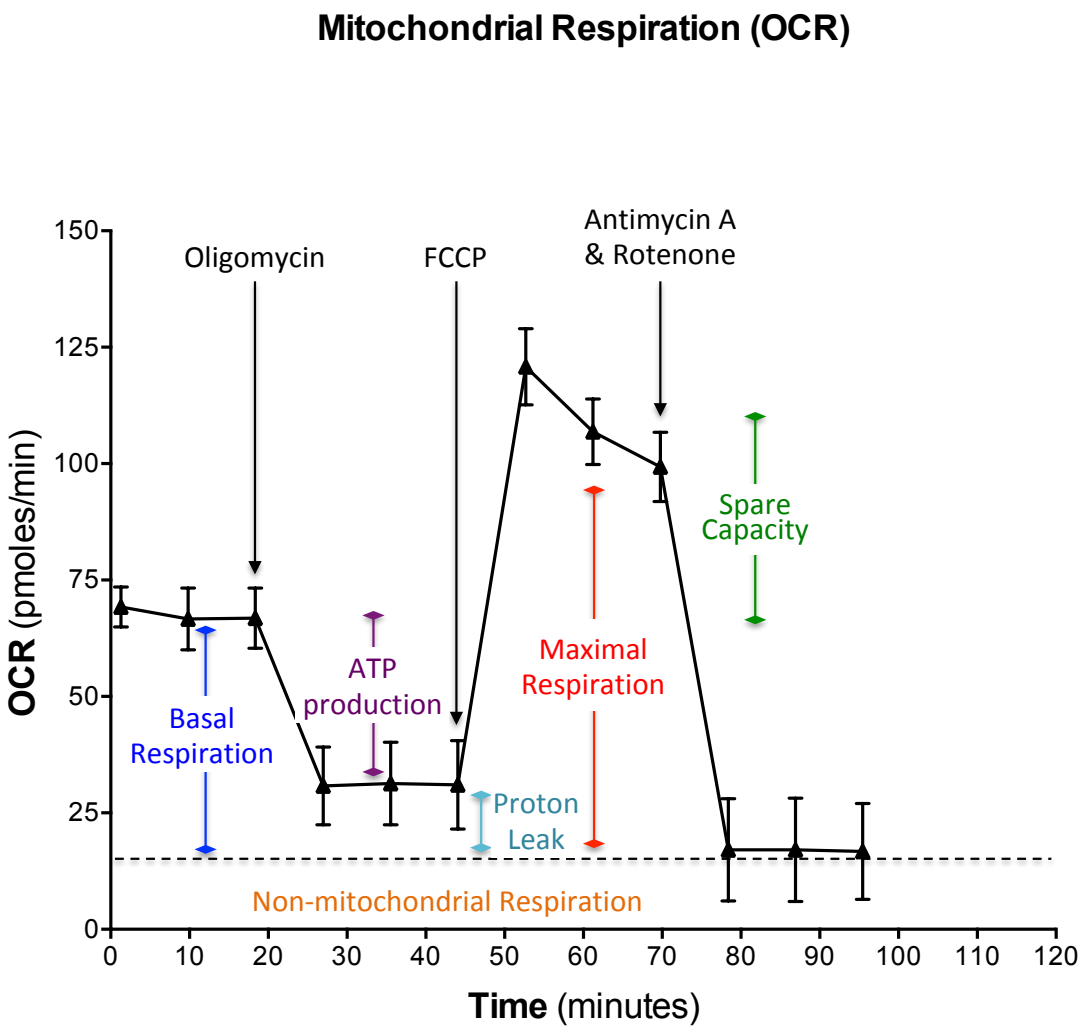



**Figure 2 - 3. Representative Stress Test profile of the key parameters of mitochondrial respiration.**
Key parameters of mitochondrial function are evaluated by measuring the cellular oxygen consumption rate (OCR). Basal respiration is initially measured and subsequently, sequential injections of oligomycin, FCCP and antimycin-A/Rotenone allow measurement of ATP production, maximal respiration and non-mitochondrial respiration, and calculation of proton leak and spare respiratory capacity. Bars represent mean and standard deviation. Each data point is the mean of eleven replicate measurements at a specific timepoint.

## 2.17 Metabolomic analysis

### 2.17.1 Intracellular amino acid measurements by liquid-chromatography mass-spectrometry (LC-MS)

Static and influx measurements of intracellular amino acid concentrations were carried out

in collaboration with Dr Zhanru Yu and Prof Benedikt Kessler. Briefly, WT THP1 cells were first cultured in differential medium (Complete R10 medium, arginine-depleted R10 medium and arginine-depleted, citrulline-supplemented R10 medium) for 72 hr. Cells were washed in PBS twice and counted to give a pellet composed of 25 x $10^6$ cells for each of the three conditions. Each cell pellet was kept in an eppendorf tube on ice before 400 µl of 80% cold (kept at -80 °C) aqueous methanol was added. The suspension was mixed by gentle vortex for 30 min at room temperature. Following an incubation for 60 min at –80 °C, the cells were centrifuged at 14,000 x g for 10 min at 4°C to remove cell debris. The supernatant, containing the intracellular metabolites of interest was transferred to a new eppendorf tube. 400 µl of ice-cold 80% aqueous methanol was added to the old tube containing the cell debris pellet. This suspension was mixed by gentle vortex for 5 min at room temperature and centrifuged at 14,000 x g for 10 min at 4°C. The resulting supernatant was transferred to the eppendorf tube containing the remaining supernatant obtained previously. The combined supernatant for each condition was concentrated and dried using a low-pressure vaccum evaporator (Speed-Vac) without the use of heat to remove solvent with minimum stress on the solute, which contains the metabolites of interest. This process left us with a dry, solid sample of our metabolites (plus any salts present in supernatant solution) which were stored at -80°C. On the day of the liquid chromatography-mass spectrometry (LC-MS) analysis, the dried samples were re-constituted in 100µL of ice-cold water with 0.1% formic acid. The mixtures were centrifuged at 1200rpm for 30 min and then 2000 x g for 2 min. The top solution following centrifugation was directly injected into the LC-MS system. A quality control (QC) was tested first using 5µL of each sample. Analysis of intracellular arginine and intracellular citrulline was performed using ultra high-performance liquid chromatography quadruple-time of flight mass spectrometry (HPLC–QTOF-MS). For the analysis, a 1290 Infinity

Ultra HPLC system (Agilent Technologies) was fitted with an Acquity Ultra HPLC Glycoprotein Amide Column, (300Å, 1.7 µm, 2.1 mm × 150 mm; cat. No. 176003702; Waters) and coupled to a 6560 Ion mobility QTOF-LC mass spectrometer (Agilent Technologies) equipped with an Agilent Jet Stream ESI-AJS electrospray ionization source (AJS-ESI; Agilent Technologies). Data were acquired in QTOF mode using positive electrospray ionisation (ESI+). Two reference ions; m/z 121.0508 and m/z 922.0097 were used as internal standards. The Dual AJS ESI settings were as follows: gas temperature at 300°C, drying gas flow rate at 8L/min, nebulizer pressure 35MPa, sheath gas temperature at 350°C, sheath gas flow rate at 11L/min, capillary voltage (Vcap) 3500V and nozzle voltage at 1000V. The fragmentor of the QTOF mass spectrometer was set to 400V. The starting ion gradient was composed of 20% buffer A (water with 0.1% formic acid) and 80% buffer B (acetonitrile with 0.1% formic acid) with a flow rate of 0.3mL and a total run time of 9 min as follows: 0-8 min, linear increase of buffer A from 20% to 35%; 8-9 min, linear decrease of buffer A from 35% to 20%. Each run of the gradient was followed by a 3-min re-equilibration/post-time to re-equilibrate the column. Raw mass spectrometry data files were analysed using the MassHunter Qual Software package (Agilent Technologies, version B8.0), along with a combination of mass and retention time used for the characterization of each metabolite. For the identification of compounds, raw mass spectrometry data were processed using the molecular feature extraction function in the MassHunter software. Acetonitrile, methanol and water were all of LC-MS grade and obtained from Merck.

**2.17.2 Heavy-labelled amino acid influx measurements for amino acid cellular uptake**

In order to dynamically measure the uptake of citrulline into THP1 cells we used the same methodology as described in section 2.17.1 above with the exception that supplementation of the arginine-depleted R10 medium was carried out using heavy isotope-labelled

citrulline ($^{13}$C5-$^{2}$H4-L-citrulline; Cat. No. CDLM-7139-MPT-PK; Cambridge Isotope laboratories) rather than unlabelled citrulline as described in the previous experiment. This allowed us to track citrulline influx into THP1 cells in real-time and confirm its conversion to arginine by following the heavy isotope-labelled atoms that were indeed transferred from citrulline molecules to arginine molecules. 35 x $10^6$ cells were used for the complete R10 medium and arginine-free R10 medium conditions and 60 x $10^6$ cells for the arginine-free, heavy isotope-labelled citrulline-supplemented R10 medium condition, with reagent volumes adjust to number of cells.

## 2.18 Chromatin Immunoprecipitation (ChIP)

We performed ChIP-sequencing (ChIP-seq) and ChIP-qPCR in collaboration with Dr Nicholas Crump and Prof Tom Milne, as previously described in the literature [357, 358], to assess the ability of transcription factors such as ATF4, c-myc, and CEBPβ to bind to target genes of interest. In short, cells were removed from culture (72-96 hr in differential medium) and were washed twice in ice-cold PBS before being fixed. For the first fixation step cells were suspended for 30 min in 2mM disuccinimidyl glutarate (Sigma-Aldrich; 80424) and for the second step they were suspended for 30 min in 1% formaldehyde. Cells were subsequently lysed for 10 min on ice in lysis buffer comprising of 50mM Tris (pH 8.1), 1% SDS and 10mM EDTA supplemented with protease inhibitors (Sigma-Aldrich; P8340). Fixed samples of up to $10^8$ cells were sonicated on a Covaris (Woburn, MA) according to the manufacturer's protocol to end up with fragments of approximately 200-500bps. Prior to incubation with the relevant antibody, a 50µL aliquot of the fragmented, diluted chromatin lysate was removed to be used as total input where the signal from the input samples represents 5% of the total chromatin used in each ChIP. The remaining chromatin was incubated overnight with the appropriate antibody at 4$^{o}$C (e.g in the case of

ATF4 ChIP-seq, anti-ATF4; Cell Signalling Technology 11815). For transcription factor ChIP, antibody:chromatin complexes were isolated by 1:1 incubation with a mixture of Protein A and Protein G dynabeads (ThermoFisher Scientific) for 3-5 hr, and then gathered with a magnet. For histone ChIP, antibody:chromatin complexes were isolated using a mixture of Protein A and Protein G agarose beads (ThermoFisher Scientific) and collected by centrifugation. Chromatin-bound beads were washed three times with a solution of 50 mM HEPES-KOH, pH 7.6, 500 mM LiCl, 1 mM EDTA, 1 % NP40, 0.7 % Na-deoxycholate supplemented with protease inhibitors. Samples were then washed in Tris-EDTA solution (10mM Tris-HCl [pH 8.0], 1mM EDTA) before eluted in a solution of 50mM Tris-HCl [pH 8.0], 10mM EDTA and 1% SDS. Following elution, samples were digested with RNase A (ThermoFisher Scientific) and proteinase K (ThermoFisher Scientific) and then purified using a PCR cleanup kit (Qiagen). ChIP samples were quantified relative to input DNA [357, 358]. Briefly, 'the amount of genomic DNA co-precipitated with antibody was calculated as a percentage of total input using the formula $\Delta C_T = C_T$(input) - $C_T$ (ChIP), % total = $2^{\Delta CT}$ x 5.0%' [357]. ChIP-seq samples were prepared for sequencing using NEBNext Multiplex Oligos for Illumina and analysed as discussed later in section 2.19.1. For ChIP-qPCR, gene-specific primers were designed based on ChIP-seq results of transcription factor binding sites and on previously reported binding sites. Antibodies used for ChIP included anti-ATF4 (D4B8, #11815, Cell Signalling Technology), anti-CEBPβ (A302-738A, Bethyl Laboratories), anti-c-myc (#9402S, Cell Signalling Technology), anti-H3K27me3 (#07-440, Millipore), anti-H3K4me3 (#39159, Active Motif), anti-H3K9me2 (ab1220, Abcam) and anti-H3K9me3 (ab8898, Abcam). PCR Primers used for ChIP were designed in-house and purchased from MWG **(Table 2-7)**.

### 2.18.1 DeepBind analysis to identify transcription factor binding sites

ChIP-based experiments for transcription factor binding at the *ASS1* promoter, enhancer and other regions were complemented with computational analysis using a machine learning technique 'DeepBind' in collaboration with Dr Hashem Koohy and according to the literature [359]. Briefly, the *ASS1* promoter, enhancer and random sequences within the *ASS1* locus were scanned by 'DeepBind' using a sequence length of 20bp and step size of 1bp to identify specific motifs for transcription factor binding. At each position, binding specificity scores were calculated and compared to thousands of background scores to estimate the significance level.

| **Primer Name** | **Primer Sequence** |
|---|---|
| Negative control - Fwd | 5'-GGCTCCTGTAACCAACCACTACC-3' |
| Negative control - Rev | 5'-CCTCTGGGCTGGCTTCATTC-3' |
| ASS1 promoter - Fwd | 5'-ATCTGCAGGTGGCTGTGAA-3' |
| ASS1 promoter - Rev | 5'-GCAGAGCAGGACTGGCA-3' |
| ASS1 intron - Fwd | 5'-ATCTGCCCAGCTCATTTCTC-3' |
| ASS1 intron - Rev | 5'-TGCATGTGTGTGATGTGTTTG-3' |
| SLC7A5 - Fwd | 5'-GAGGGTGGCACTTGCCTAAA-3' |
| SLC7A5 - Rev | 5'-CCCCACAGGCTGGGAATATC-3' |
| SLC7A1 - Fwd | 5'-CACGCTTACTCACTCGGTGT-3' |
| SLC7A1 - Rev | 5'-GCCTCCACGGAGTCCATTTT-3' |
| SLC1A5 - Fwd | 5'-GCCTTGGCCTTAGCTACTATT-3' |
| SLC1A5 - Rev | 5'-AAAGGGACGGCTTCATATCTC-3' |
| ASNS - Fwd | 5'-AGGAGCCAGGTCGGTATAA-3' |
| ASNS - Rev | 5'-GTAAGCAGGTCAGGGTGATG-3' |
| HoxC8 - Fwd | 5'-CAGAAGGGTAGATAGGAGCCTGC-3' |
| HoxC8 - Rev | 5'-TCAAACAGCGAAGGAGAGGAAG-3' |

**Table 2 - 7. PCR primers used in ChIP experiments.**

## 2.19 Evaluation of DNA accessibility using Assay for Transposase-Accessible Chromatin with high throughput sequencing (ATAC-seq)

ATAC was conducted in collaboration with Dr Nicholas Crump and Prof Tom Milne, as previously described in the literature [360, 361] on 50,000 THP1 cells or T-cells using the Tn5 transposase (Illumina). Briefly, 50,000 cells were harvested from the culture they had been kept for 72 hr and span down at 500 x g for 5 min at 4$^{o}$C. They were then washed twice with cold PBS and the final pellet was resuspended in 50µL of the transposition reaction mix (22.5µL of nuclease free water, 25µL TD 2X reaction buffer [FC-121-1030; Illumina] and 2.5µL TDE1 Nextera Tn5 Transposase [FC-121-1031; Illumina]) and incubated at 37$^{o}$C for 30 min. Nextera indices were incorporated using NEBNext High-Fidelity 2X PCR mastermix (M0541; New England Biolabs) with 12 cycles to PCR amplify the transposed DNA fragments. The optimal number of cycles to reduce artefacts was determined empirically by quick screening using the TapeStation 2200 system (Agilent Techonologies) to analyse the quantity, quality, integrity and size of PCR products. Samples were purified with a MinElute PCR purification kit (#28004, Qiagen). The purified samples were eluted in 20µL of Elution Buffer (10mM Tris-HCl, pH 8).

### 2.19.1 Sequencing process for ChIP and ATAC analysis

Prior to sequencing, ChIP and ATAC samples were analysed in collaboration with Dr Nicholas Crump for size distribution using a 2200 TapeStation system with D1000 ScreenTape (Agilent Technologies), then quantified using a KAPA Library Quantification Kit (Kapa Biosystems). Samples were sequenced in-house using an Illumina® NextSeq 500 machine (Illumina; 75 cycles, paired-end), following the manufacturer's instructions. Quality control of FASTQ reads, alignment, PCR duplicate filtering, blacklisted region filtering and UCSC data hub generation was performed using NGSeqBasic, an in-house pipeline developed by Jelena Telenius

(http://userweb.molbiol.ox.ac.uk/public/telenius/PipeSite.html). Briefly, FASTQ files were filtered using fastQC (0.11.4) and mapped against the human genome assembly hg19 (NCBI build 37). Unmapped reads were trimmed using trim_galore (0.3.1), options --length --qualFilter 20, then mapped again. Finally, short unmapped reads from this step were combined using flash (1.2.8), options –m 9 –x 0.125, and mapped again. PCR duplicates were removed with samtools rmdup (0.1.19), and any reads mapping to Duke blacklisted regions (UCSC) were removed with bedtools (2.17.0). The bam files were used to generate directories of sequencing reads (tags) using the homer (4.7) command makeTagDirectory (http://homer.salk.edu/homer/), normalising the number of reads to counts per $10^7$ total reads. The makeUCSCfile command was used to generate bigwig files from the tag directories, which were visualised in UCSC.

Motif analysis was conducted using the FIMO function of MEME Suite [362], using transcription factor binding profiles from JASPAR [363-365].

## 2.20 Assessment of DNA methylation by bisulfite sequencing

Bisulfite sequencing to assess DNA methylation status was performed in collaboration with Dr Nicholas Crump and Prof Tom Milne. Genomic DNA was purified from cells using a DNeasy Blood & Tissue Kit (Qiagen). 500 ng of DNA was bisulfite-treated using the EZ DNA Methylation-Lightning Kit (Zymo Research) according to the manufacturer's instructions. Bisulfite-treated DNA was then amplified with bisulfite-specific primers using ZymoTaq DNA polymerase (Zymo Research). PCR products were cloned into the pCR2.1 TA cloning vector (ThermoFisher Scientific) and used to transform Stellar Competent Cells (Clontech Laboratories, Inc.). Cells were grown on LB-agar plates containing 5-bromo-4-chloro-3-indlyl-β-D-galactopyranoside (X-gal), a chromogenic substrate of the β-galactosidase enzyme used in blue-white screening to identify plasmid

insertions. Normally, in non-recombinant bacteria, β-galactosidase hydrolyses X-gal in the agar plate to 5-bromo-4-chloro-indoxyl which upon dimerization gives rise to a blue insoluble pigment (5,5'-dibromo-4,4'-dichloro-indigo). However, when bacteria take up the plasmid vector containing the foreign DNA of interest (recombinant bacteria), the host β-galactosidase production is inhibited, X-gal is not hydrolysed and the solution in the agar plate remains white. At least 12 distinct white colonies were identified sent for sequencing (Eurofins), with results aligned against the unmodified sequence to identify methylation events. PCR primers used bisulfite sequencing are shown in **Table 2-8**.

| **Primer Name** | **Primer Sequence** |
|---|---|
| ASS1 promoter – Fwd | 5'- GTTTTGTGTTTATAATTTGGGATGG -3' |
| ASS1 promoter – Rev | 5'- CCCCAAAAAAACTAAACTCCTAATT -3' |
| ASS1 intron – Fwd | 5'- TTTTTGTTTCGGGTTGTAAATGTAGTTTAG -3' |
| ASS1 intron – Rev | 5'- ATAACTAAACAAATATAAACTCTAAAACCTTCAACC -3' |

**Table 2 - 8. PCR primers used in bisulfite sequencing experiments.**

## 2.21 Statistical analysis

Statistical analysis was performed using the Graphpad Prism software (Version 6.0, Graphpad, San Diego, CA). Statistical significance was determined using unpaired or paired, two-tailed student's t-test or where appropriate, one-way ANOVA. Findings were considered statistically significant if p-value was $< 0.05$ where * means $p<0.05$, ** means $p<0.01$, and *** means $p<0.001$.

# Chapter 3: Arginase-mediated arginine degradation in AML: Effects on T-cells and therapeutic targets for cancer immunotherapy

## 3.1 Introduction

AML is a haematological malignancy that is recognized to cause general immunosuppression. Pancytopenia as a result of bone marrow (BM) suppression cannot account on its own for the global immune dysfunction observed in the disease. In this chapter we aim to understand the biological mechanisms of AML-mediated suppression of T-cells, the key players in anti-tumour immune responses. Furthermore, we aim to investigate whether our previous findings of increased systemic Arginase levels in human AML patients are also applicable to AML animal models. Finally, in this chapter we aim to de novo generate recombinant human Arginase proteins in order to investigate the effects of Arginase-mediated arginine depletion of T-cell effector function and proliferation and to test the first Arginase-specific small molecule inhibitors for potential therapeutic use.

## 3.2 Arginase-2 protein levels and enzymatic activity are high in AML patient plasma

Firstly, in order to expand on our previous findings [130], we tested Arginase activity by colorimetric test and Arginase-2 levels by ELISA in plasma collected from 23 AML patients and 10 healthy controls. We demonstrated that Arginase activity was significantly higher in plasma from AML patients (n=15) compared healthy controls (mean 84.61 vs

2.73 Units/L; p<0.001) **(Figure 3-1).** This was in line with significantly higher Arginase-2 protein concentrations measured in AML patient plasma compared to healthy controls (mean 79.9 vs 1.69 ng/mL; p<0.001) **(Figure 3-2).** Arginase-1 protein remained undetectable in all samples.

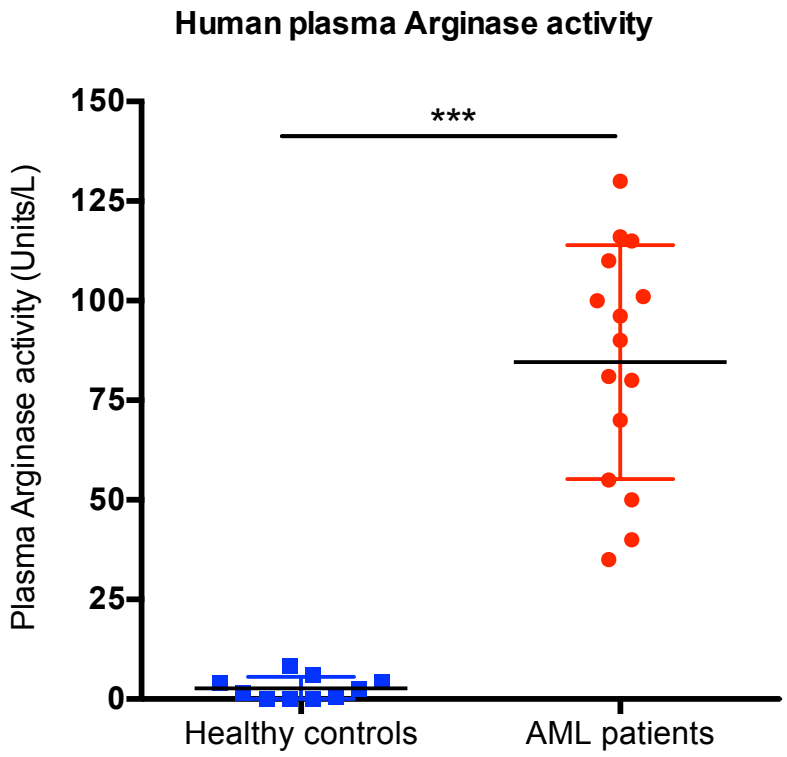



**Figure 3 - 1. Plasma Arginase activity is significantly higher in AML patients compared to healthy controls.**
Plasma was obtained from blood drawn from healthy volunteers (n=10) and AML patients (n=15). Arginase activity was measured for each sample based on the conversion of arginine to urea by means of a colorimetric assay. Bars represent mean and standard deviation. *** p< 0.001. Each data point is the mean of triplicate measurements for that specific sample.

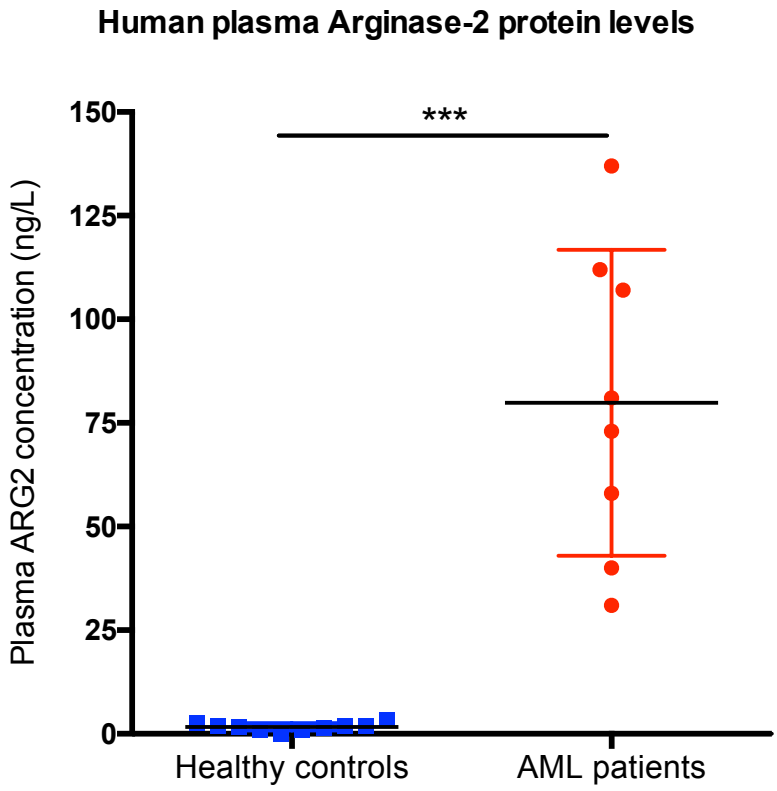



**Figure 3 - 2. Plasma levels of Arginase-2 (ARG2) protein are significantly higher in AML patients compared to healthy controls.**
Plasma was obtained from blood drawn from healthy volunteers (n=10) and AML patients (n=8). Arginase-2 concentration was measured by means of ELISA for each sample. Bars represent mean and standard deviation. *** $p < 0.001$. Each data point is the mean of triplicate measurements for that specific sample.

## 3.3 Arginase-2 protein levels and enzymatic activity are also high in AML mouse models leading to systemic arginine depletion

### 3.3.1 A spontaneous AML mouse model shows higher Arginase activity and lower serum arginine levels than healthy control mice

In order to investigate whether we can extend our findings in humans to animal models, we made use of three distinct mouse models; two of AML and one of myeloproliferative disease. Firstly, we tested a spontaneous AML mouse model based on Rag-based knockout

of the *EZH2* and *RUNX1* genes and constitutive expression of *FLT3* through internal tandem duplication. Serum Arginase activity, as measured by the conversion of arginine to urea using a calorimetric assay, was significantly higher in EZH2$^{-/-}$ RUNX1$^{-/-}$ Rag FLT3-ITD AML mice compared to wild-type (WT)/littermate C57BL/6 controls (mean 213.50 vs 5.66 units/L; p=0.0002 **(Figure 3-3).** In line with this finding, serum arginine levels, as measured by ELISA, were significantly lower in AML mice, when compared to littermate/WT controls (mean 19.44 vs 101.00 μM; p=0.0004, to a concentration below the 50 μM threshold of healthy immune function **(Figure 3-4)**.

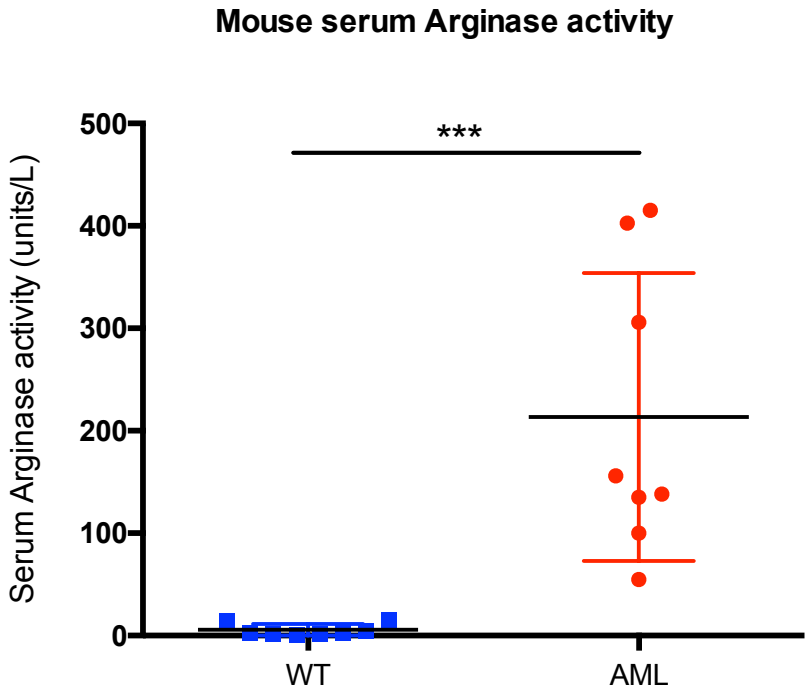



**Figure 3 - 3. Serum Arginase activity is significantly higher in mice with AML compared to healthy control mice.**
Serum was obtained from blood obtained by cardiac puncture of culled mice. Mice with AML (based on genetic testing, clinical features and biochemical metrics; n=) and healthy littermate/WT control mice (n=8) had been exposed to the same conditions for the same amount of time prior to sacrifice. Arginase activity was measured for each sample based on the conversion of arginine to urea by means of a colorimetric assay. Bars represent mean and standard deviation. *** p< 0.001. Each data point is the mean of triplicate measurements for that specific sample.

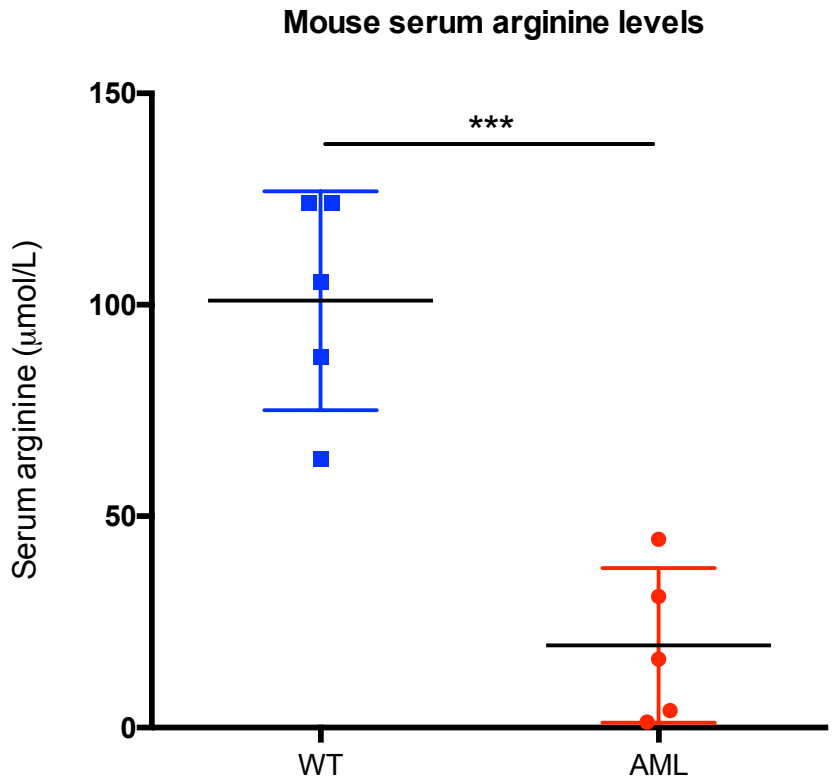



**Figure 3 - 4. Serum arginine levels are significantly lower in AML mice compared to healthy control mice.**
Serum was obtained from blood obtained by cardiac puncture of culled mice. Mice with AML (n=5) and healthy littermate/WT control mice (n=5), exposed to the same conditions for the same amount of time prior to sacrifice, had their serum arginine levels measured by means of competitive inhibition enzyme immunoassay. Bars represent mean and standard deviation. *** $p < 0.001$. Each data point is the mean of triplicate measurements for that specific sample.

### 3.3.2 High Arginase activity in the spontaneous AML mouse model is purely due to the presence of high serum concentration of Arginase-2 with no contribution from Arginase-1

The enhanced Arginase activity measured in AML corresponded almost exclusively to significantly higher serum levels of the Arginase-2 isoenzyme in AML compared to control mice (mean 147.60 vs 1.73 ng/mL; p=0.005) **(Figure 3-5)**. In contrast, Arginase-1 was essentially absent in serum of both sets of mice thus, not contributing to the measured Arginase activity **(Figure 3-6)**. Serum Arginase activity showed a robust positive

correlation with serum ARG2 protein levels (R=0.90; p=0.002) and a significant negative correlation with serum arginine levels in serum (R=-0.99; p=0.0004) strongly suggesting that, in the context of AML, the reduction in systemic arginine is a direct effect of amino acid breakdown by the Arginase-2 enzyme **(Figure 3-7; top and bottom panels)**.

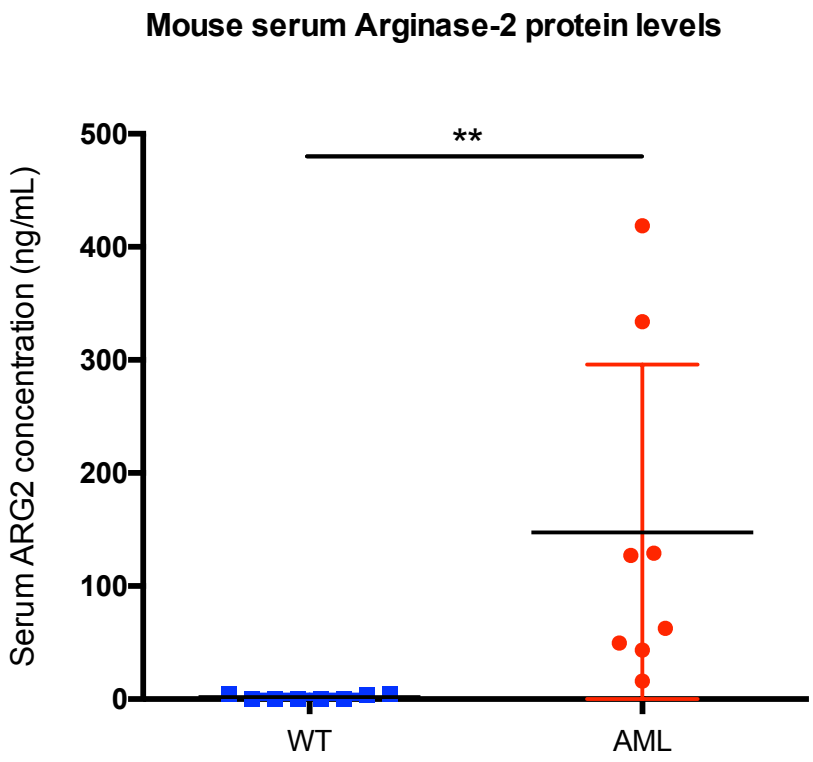



**Figure 3 - 5. Serum levels of Arginase-2 (ARG2) protein are significantly higher in AML mice compared to healthy control mice.**
Serum was obtained from blood obtained by cardiac puncture of culled mice. Mice with AML (n=8) and healthy littermate/WT control mice (n=8) had their serum Arginase-2 protein levels measured by means of ELISA. Bars represent mean and standard deviation. *** p< 0.001. Each data point is the mean of triplicate measurements for that specific sample.

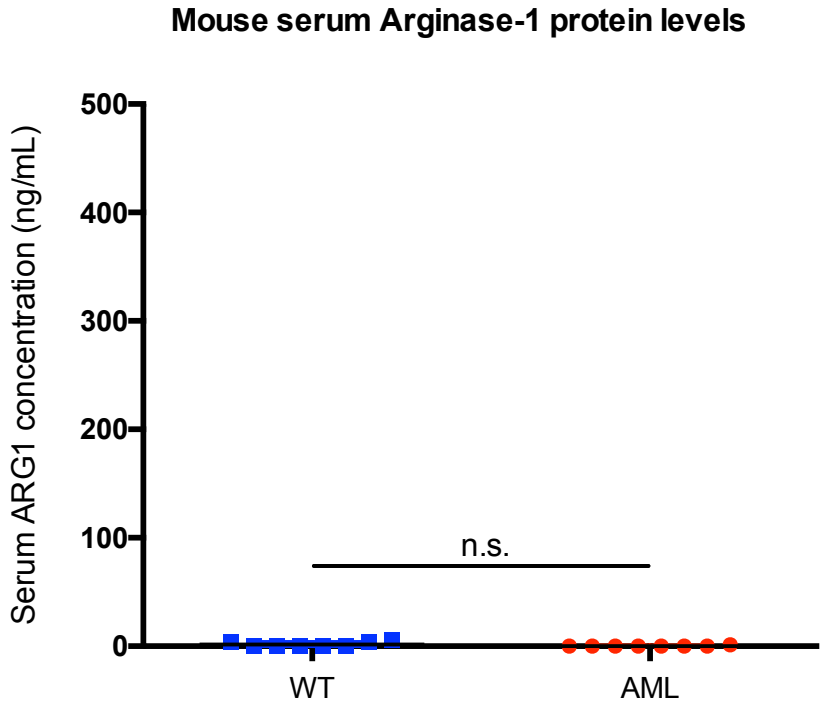



**Figure 3 - 6. Arginase-1 (ARG1) protein is not detected in the serum of AML mice or healthy control mice and so cannot be the source of Arginase activity in the AML context.**
Serum was obtained from blood obtained by cardiac puncture of culled mice. Mice with AML (n=8) and healthy littermate/WT control mice (n=8) had their serum Arginase-1 protein levels measured by means of ELISA. Arginase-1 levels were consistently non-detectable in both populations suggesting the lack of the Arginase-1 isoenzyme in the serum of these mice. n.s means non-significant $p>0.05$. Each data point is the mean of triplicate measurements for that specific sample.

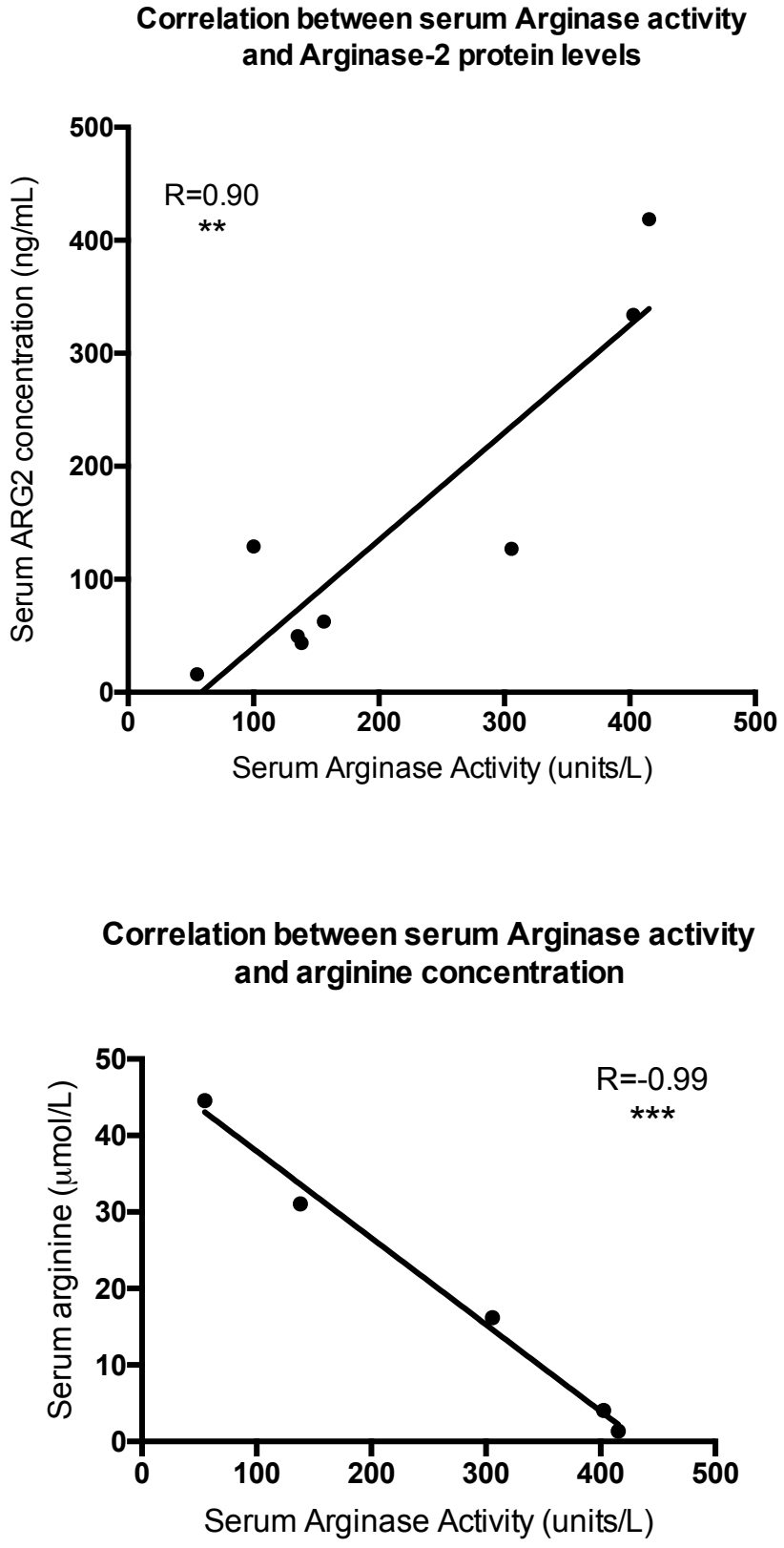
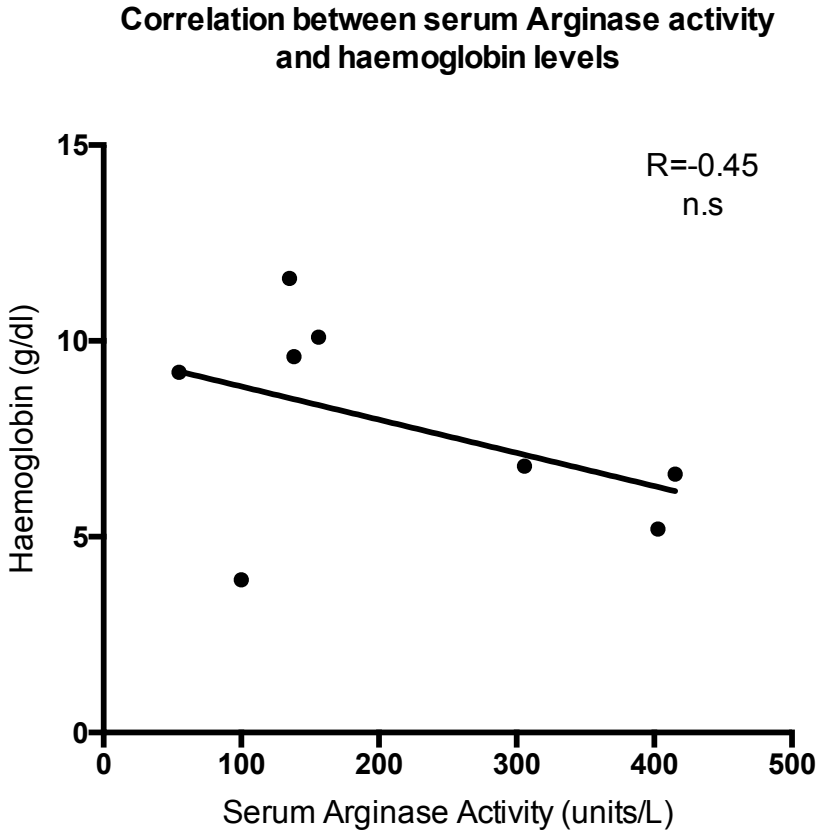



**Figure 3 - 7. Arginase-2 specific activity is most likely responsible for depletion of arginine levels in the serum of AML mice.**
Arginase activity in the serum of AML mice shows a strong positive correlation with serum Arginase-2 concentration (r=0.90; top panel) and a strong negative correlation with

serum arginine concentration (R=-0.99; bottom panel). *** p< 0.001, ** p< 0.01. Each data point is the mean of triplicate measurements for that specific sample.

### 3.3.3 Serum Arginase activity in the spontaneous AML mouse model is closely linked to clinical indices of disease

Additionally, serum Arginase activity correlated with clinical markers of disease burden in AML. There was a negative correlation trend (that did not reach statistical significance) with haemoglobin concentration (R=-0.45; p>0.05) and a significant strong positive correlation with white cell count (R=0.87; p=0.002) **(Figure 3-8 top and bottom panels)**.



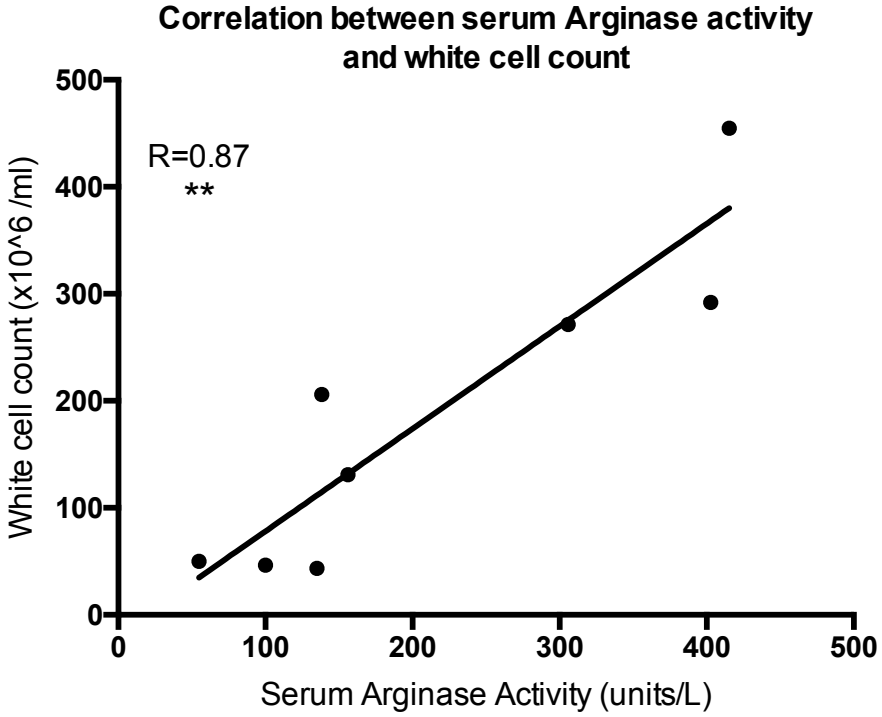



**Figure 3 - 8. Arginase activity is associated with clinical indices of AML disease severity.**
Arginase activity in the serum of AML mice shows a negative correlation with blood haemoglobin levels (R=-0.45; top panel) and a strong positive correlation with blood white cell counts (R=0.87; bottom panel). ** $p< 0.01$, n.s means non-significant $p>0.05$. Each data point is the mean of triplicate measurements for that specific sample.

### 3.3.4 An inducible AML mouse model also shows high serum Arginase activity that increases over time with enhanced disease burden

In order to confirm these findings we tested an inducible AML mouse model in which disease develops with complete penetrance after injecting WT C57BL/6 mice with primary AML blasts that carry mutations in either the 'K' or the 'L' allele of the C/EBPα gene. Our findings in this inducible AML model with regards to Arginase activity were similar to, albeit much less pronounced than, the spontaneous AML model. Serum Arginase activity was significantly higher in AML when compared to control mice (mean 12.53 vs 1.60 units/L; p=0.003) **(Figure 3-9)**. Furthermore, we took advantage of the ability to induce the disease in this model to study the kinetics of serum Arginase activity. We observed that

mean Arginase activity rises with time with significant differences between baseline (2.12 units/L), 3 weeks (6.51 units/L; p=0.02 vs WT) and 4-5 weeks (16.53 units/L; p=0.0009 vs WT, p=0.007 vs week 3) post induction (one-way ANOVA: $R^2$=0.90, p=0.0003) **(Figure 3-10)**.

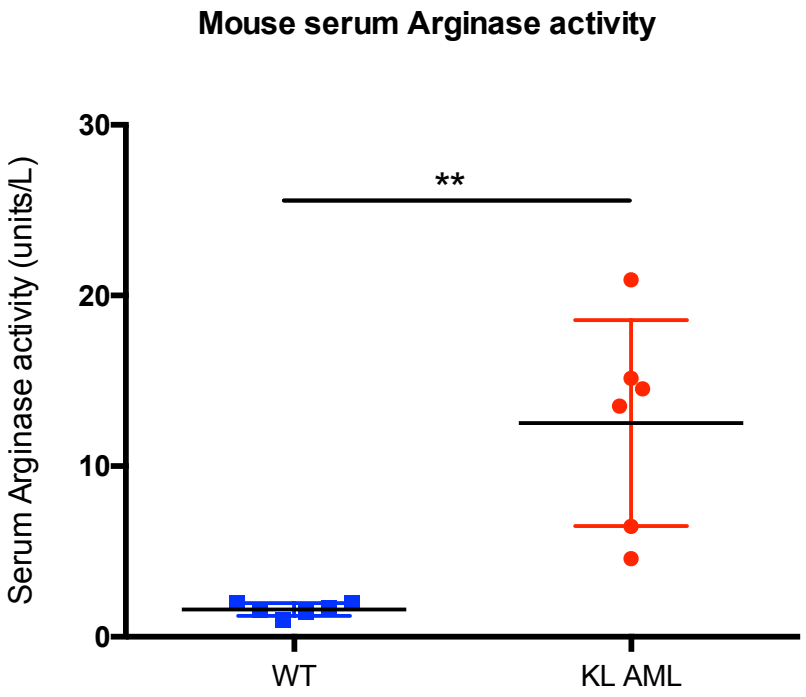



**Figure 3 - 9. Serum Arginase activity is significantly higher in our 'inducible' AML mouse model compared to healthy control mice.**
Serum was obtained from blood obtained by cardiac puncture of culled mice. Mice with inducible AML (n=6) and healthy WT control mice (n=6) had been exposed to the same conditions for the same amount of time prior to sacrifice. Arginase activity was measured for each sample based on the conversion of arginine to urea by means of a colorimetric assay. Bars represent mean and standard deviation. ** p< 0.01. Each data point is the mean of triplicate measurements for that specific sample.

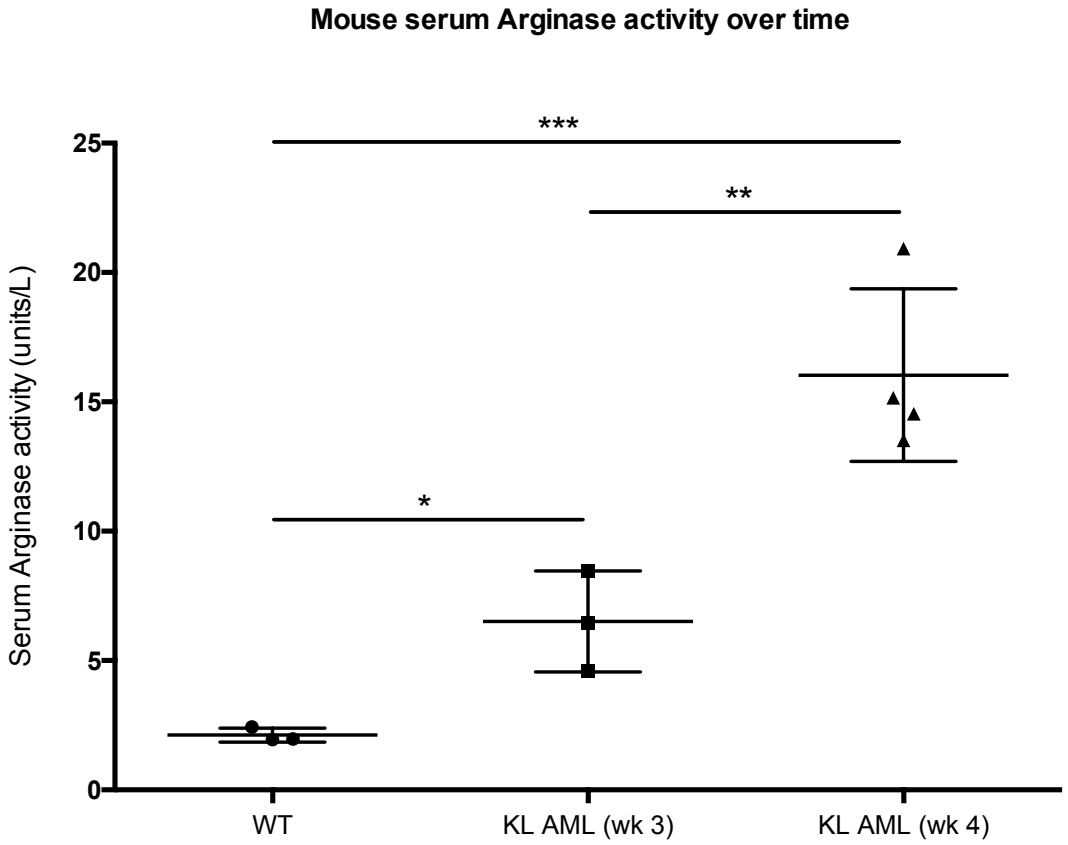


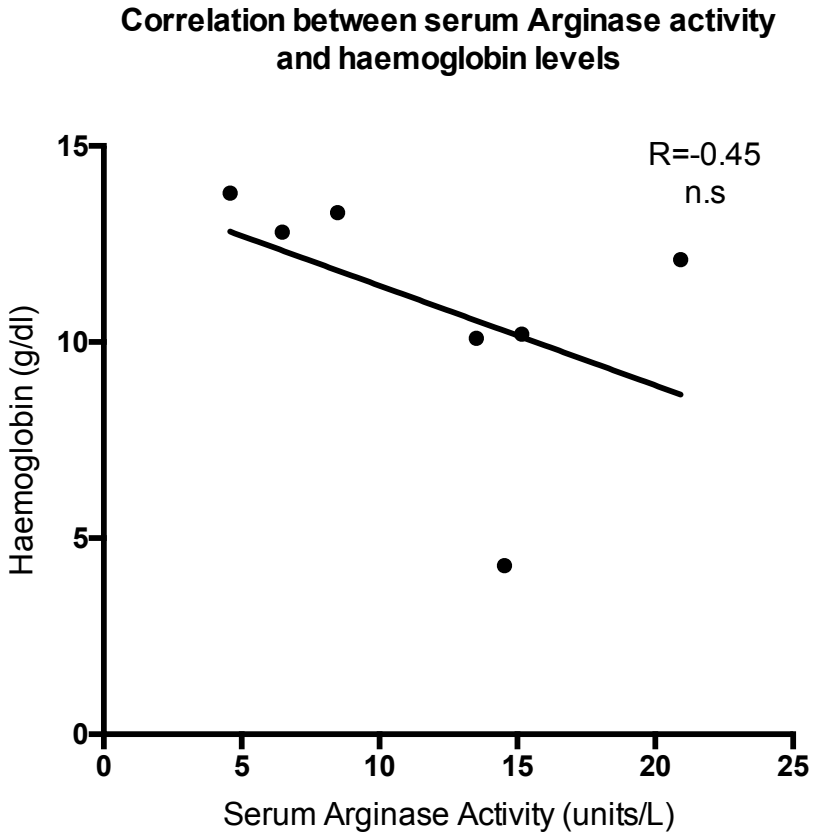

**Figure 3 - 10. Serum Arginase activity correlates with disease progression over time.** Serum Arginase activity was measured for and compared between three different mice groups; healthy WT at either baseline, week 3 or week 4 (n=3), KL AML at week 3 post-induction (n=3) and KL AML at week 4 post-induction (n=4). Arginase activity for each sample was measured based on the conversion of arginine to urea by means of a colorimetric assay. Bars represent mean and standard deviation. *** $p< 0.001$, ** $p< 0.01$, * $p< 0.05$. Each data point is the mean of triplicate measurements for that specific sample.

### 3.3.5 Serum Arginase activity is closely linked to clinical indices of disease in the inducible AML mouse model too

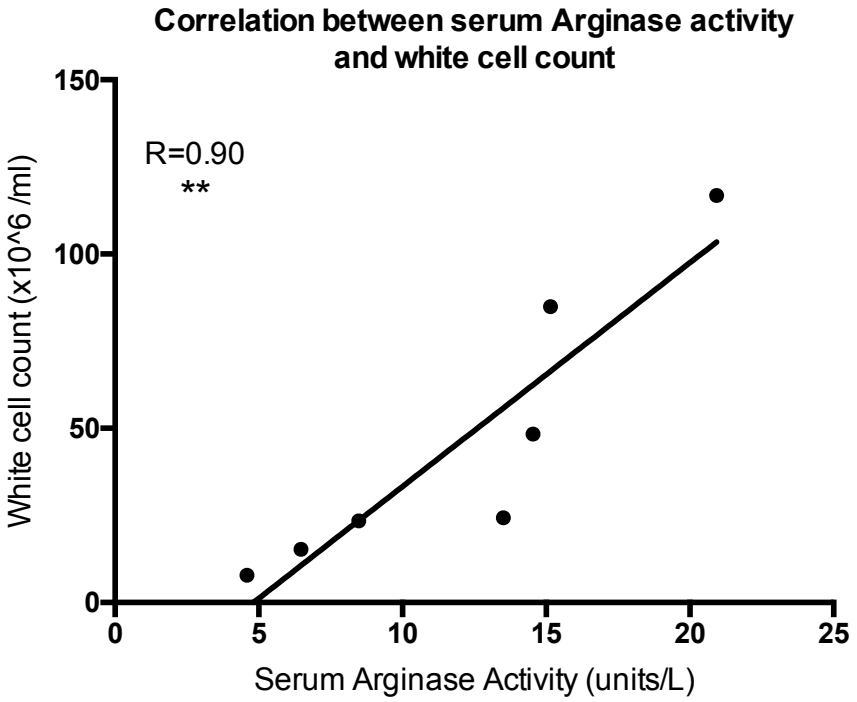
In similar fashion to the spontaneous AML model, the inducible AML model displayed correlations between serum Arginase activity and biomarkers of disease severity. Serum Arginase activity showed positive correlation with white cell count ($R=0.90$; $p=0.005$) and bone marrow leukaemic blasts ($R=0.93$; $p=0.008$) **(Figure 3-11; panels B and D)**. Haemoglobin count ($R=-0.45$; $p>0.05$) and platelet count ($R=-0.83$; $p=0.02$) showed

negative correlation with serum Arginase activity **(Figure 3-11; panels A and C)**. These findings support the notion and our previous findings that Arginase is released from the expanding leukaemic blasts that make up the majority of the peripheral white cell count as disease progresses [130].

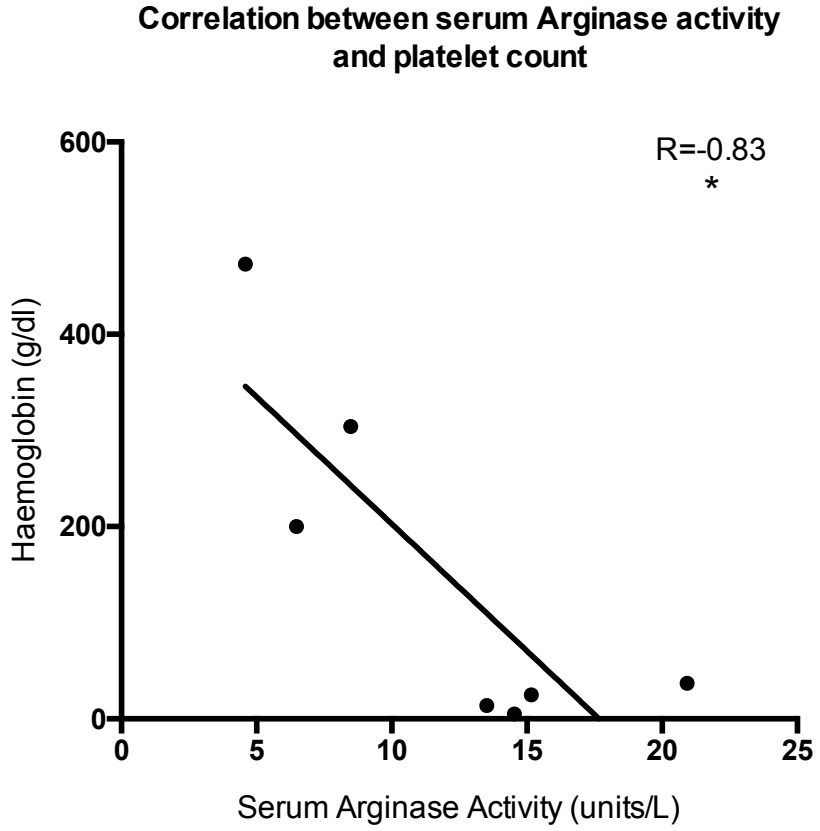
**A**



**B**


Correlation between serum Arginase activity and white cell count
R=0.90
**
White cell count (x10^6 /ml)
150
100
50
0
0
5
10
15
20
25
Serum Arginase Activity (units/L)

**C**


Correlation between serum Arginase activity and platelet count
R=-0.83
*
Haemoglobin (g/dl)
600
400
200
0
0
5
10
15
20
25
Serum Arginase Activity (units/L)

**D**

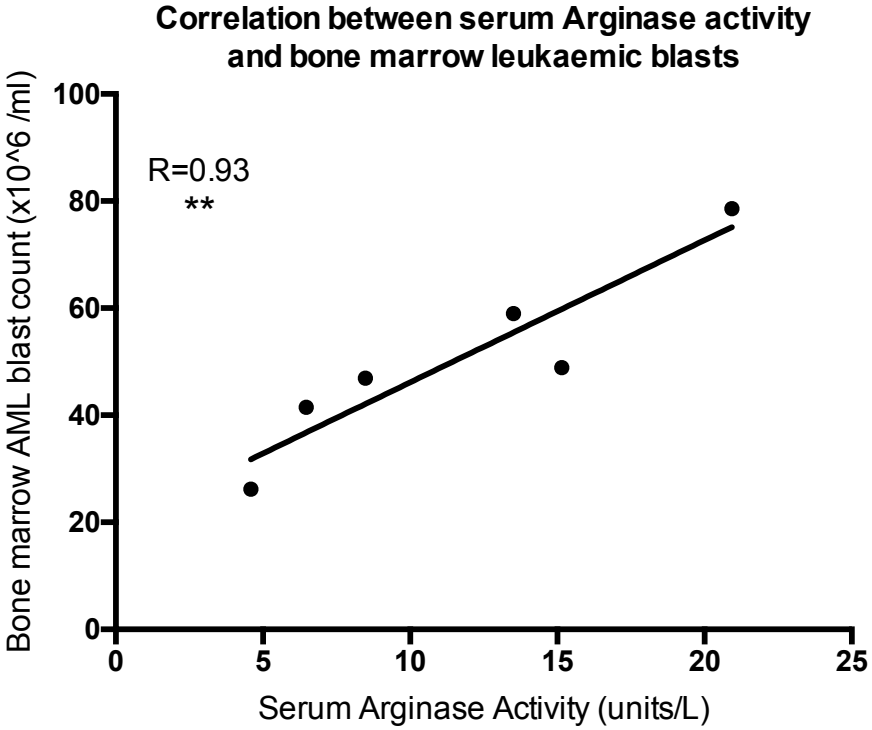



**Figure 3 - 11. Arginase activity is associated with clinical indices of AML disease severity in an inducible AML mouse model.**
Arginase activity in the serum of mice with inducible AML shows a negative correlation with (A) blood haemoglobin levels (R=-0.45, n.s) and (C) blood platelet count (R=-0.83, *). In contrast, serum Arginase activity in mice with inducible AML displays a strong positive correlation with (B) blood white cell counts (R=0.90; **) and (D) bone marrow leukaemic blast cell counts (R=0.93; **). ** $p< 0.01$, * $p< 0.05$, n.s means non-significant $p>0.05$. Each data point is the mean of triplicate measurements for that specific sample.

### 3.3.6 A mouse model of myeloproliferative disease also shows high serum Arginase activity because of high serum levels of the Arginase-2 enzyme

Finally, we tested a mouse model of myeloproliferative disease driven by induced deficiency in the autophagy pathway in haematopoietic stem cells (HSC) following *Atg7* knockout. We also detected enhanced Arginase activity in the serum of these mice compared to control mice (mean 114.00 vs 15.20 units/L; p=0.004) **(Figure 3-12)**. Furthermore, we showed that serum ARG2 protein levels were significantly higher in mice

with myeloproliferative disease (*Atg7* KO) compared to control mice (mean 105.70 vs 2.08 ng/mL; p=0.006) **(Figure 3-13)**. As in our AML models, ARG1 protein levels were virtually undetectable in the serum of these mice **(Figure 3-14)**. Serum Arginase activity was entirely due to the presence of ARG2 protein in the serum of these mice. The positive correlation between these two measurements was significantly strong (R=0.96; p<0.0001) **(Figure 3-15)**.

Overall, we established that a phenotype similar to that seen in human AML plasma could be observed in the serum of mouse models of AML and myeloproliferative disease. This means that our mouse models can now be used to understand the biology behind this clinical observation and to test drugs for therapeutic potential. A potential mechanism is the release of mitochondrial components, including the mitochondrial ARG2 enzyme, as a result of cellular deregulation in these disease states.

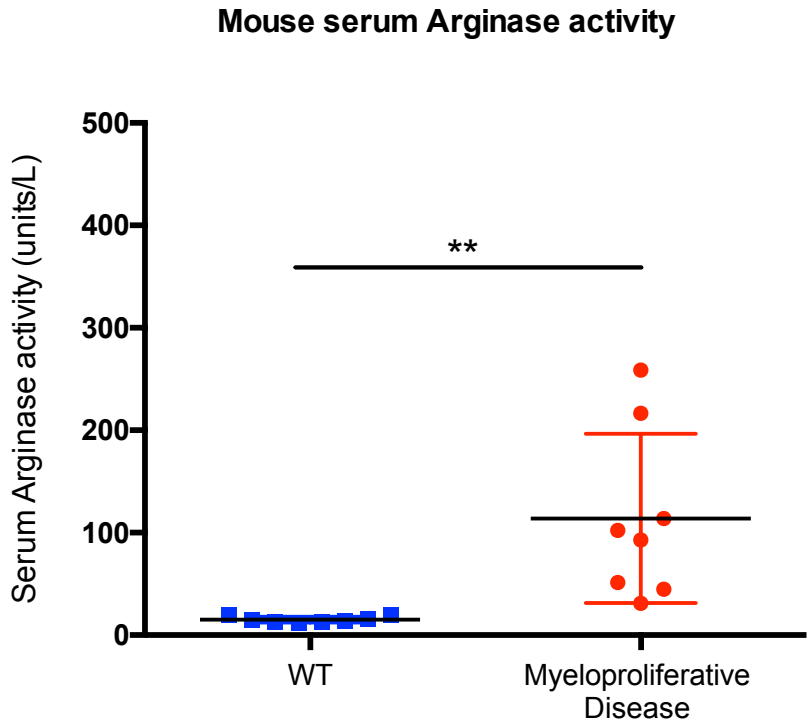



**Figure 3 - 12. Serum Arginase activity is significantly higher in autophagy-deficient mice with myeloproliferative disease compared to healthy control mice.**

Serum was obtained from blood obtained by cardiac puncture of culled mice. Mice with myeloproliferative disease (n=8) and healthy WT/littermate control mice (n=8) had been exposed to the same conditions for the same amount of time prior to sacrifice. Arginase activity was measured for each sample based on the conversion of arginine to urea by means of a colorimetric assay. Bars represent mean and standard deviation. ** $p < 0.01$. Each data point is the mean of triplicate measurements for that specific sample.

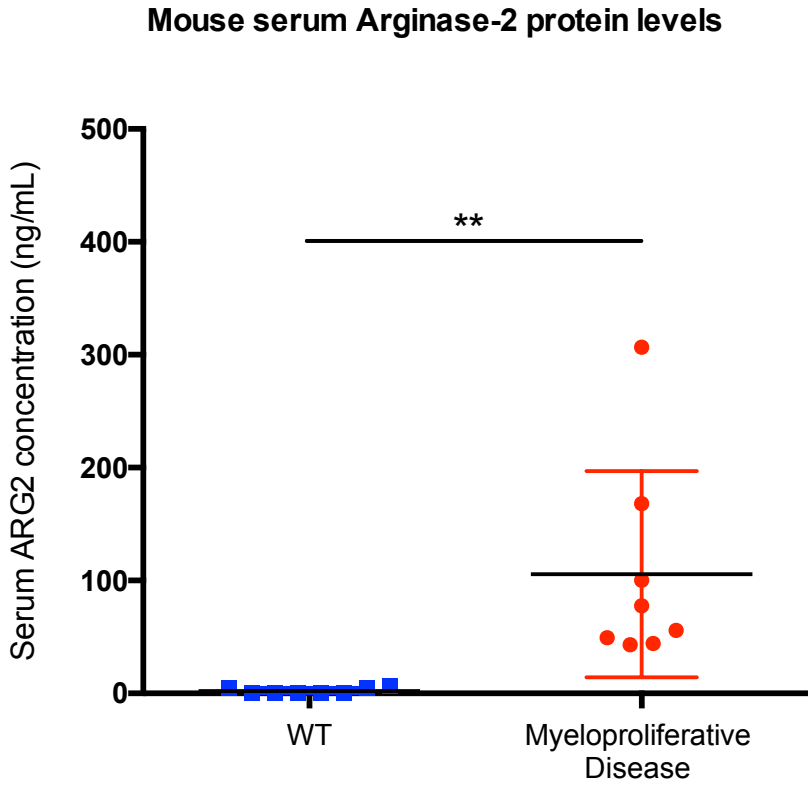



**Figure 3 - 13. Serum levels of Arginase-2 protein are significantly higher in autophagy-deficient mice with myeloproliferative disease compared to healthy control mice.**
Serum was obtained from blood obtained by cardiac puncture of culled mice. Mice with myeloproliferative disease (n=8) and healthy littermate/WT control mice (n=8) had their serum Arginase-2 protein levels measured by means of ELISA. Bars represent mean and standard deviation. *** $p < 0.001$. Each data point is the mean of triplicate measurements for that specific sample.

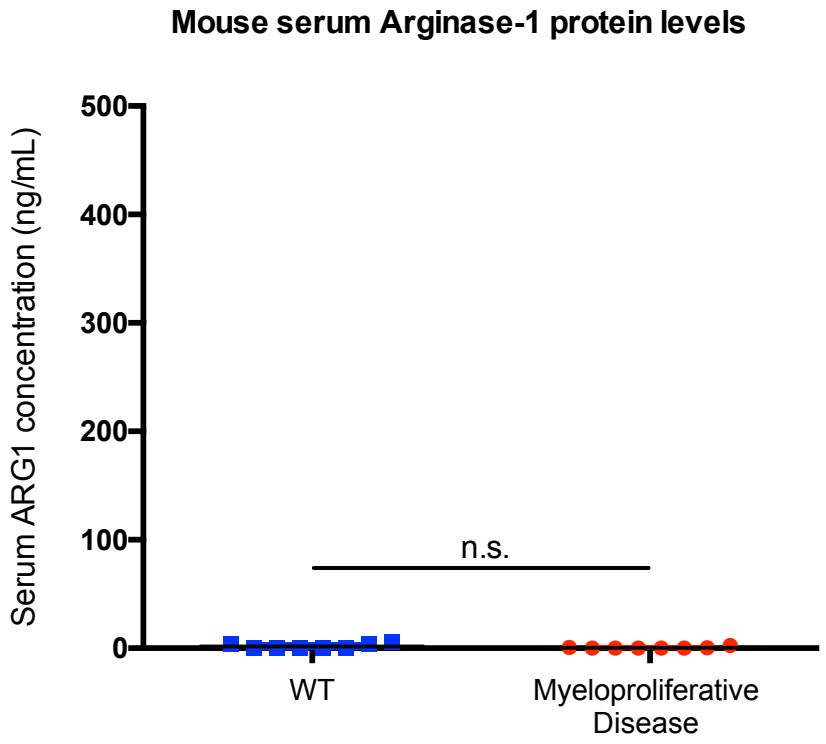



**Figure 3 - 14. Arginase activity in the serum of mice with myeloproliferative disease does not source from Arginase-1, which has undetectable levels in both diseased and healthy control mice.**
Serum was obtained from blood obtained by cardiac puncture of culled mice. Mice with myeloproliferative disease (n=8) and healthy littermate/WT control mice (n=8) had their serum Arginase-1 protein levels measured by means of ELISA. Arginase-1 levels were consistently non-detectable in both populations signifying the lack of the Arginase-1 isoenzyme in the serum of these mice. n.s means non-significant $p>0.05$. Each data point is the mean of triplicate measurements for that specific sample.

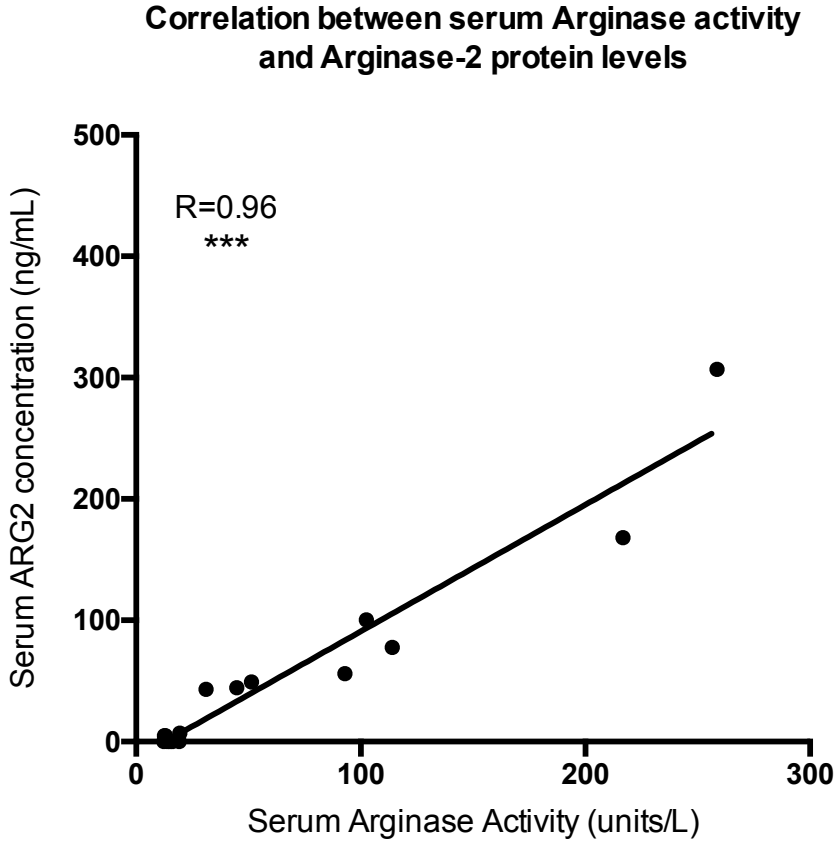



**Figure 3 - 15. Arginase activity seems to be purely due to the presence of Arginase-2 protein in the serum of mice with myeloproliferative disease.**
Arginase activity in the serum of AML mice shows a strong positive correlation with serum Arginase-2 concentration (R=0.96). *** $p < 0.001$. Each data point is the mean of triplicate measurements for that specific sample.

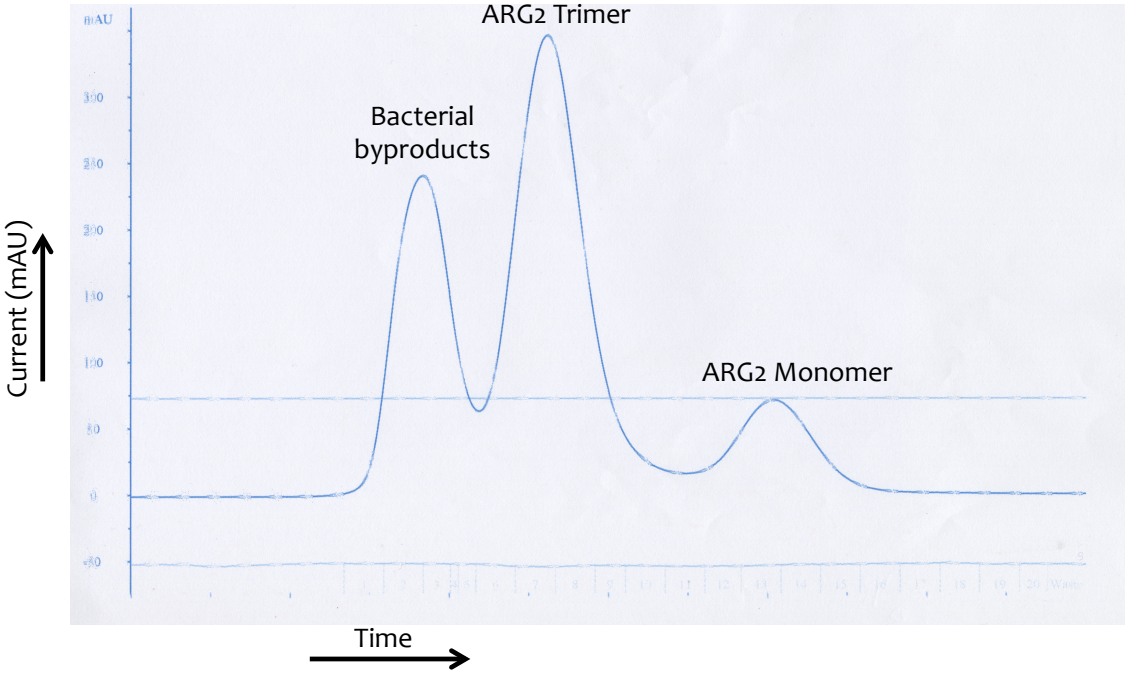
## 3.4 Generation of Recombinant human Arginase-2 protein

In comparison to Arginase-1, very little is known about the effects of Arginase-2 on the immune system. Thus, we decided to generate recombinant human Arginase-2 protein (rhARG2) in order to investigate its effects on T-cells and to test potential therapeutic drugs targeting the inhibition of ARG2 enzymatic activity.

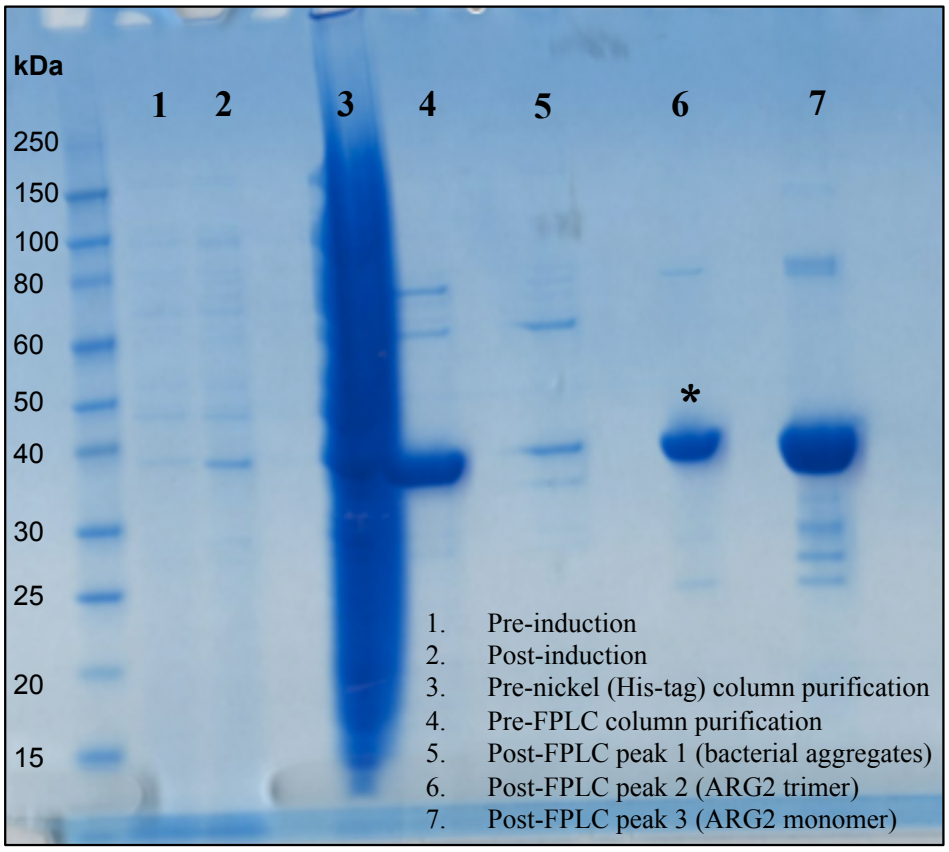
As described in Chapter 2, RNA was extracted from LNCaP (prostate cancer) and THP-1 (AML) cells lines and converted to cDNA. The *ARG2* cDNA sequence, excluding the part encoding for the mitochondrial signal peptide, was amplified by PCR using the primers

shown in **Table 2-5**. Amplified cDNA was cloned into the pET-21a(+) plasmid with a His-tag sequence at the C-terminus **(Figure 2-2)** as described in section 2.6.1. This was used as a vector to transform bacteria as described in section 2.6.2. DNA from colonies was tested for the correct sequence and plasmid minipreps made to transform competent E.coli bacteria (PRare). Bacteria were induced to synthesize proteins using IPTG. Bacterial proteins were purified through a His-binding nickel column before being subjected through High-performance liquid chromatography (HPLC). Arginase-2 trimeric and monomeric forms were separated from each other and from other unwanted bacterial products **(Figure 3-16A)**. A high purity (>95%) for the trimer was established on sodium dodecyl sulfate polyacrylamide gel electrophoresis (SDS-PAGE) **(Figure 3-16B)**. The identity and purity of the proteins was further confirmed using automated immunoblot imaging (Peggy Sue™) as per the manufacturer's instructions (Proteinsimple Ltd) **(Figure 3-16C)**. Enzymatic activity was confirmed and quantified for both the trimer (mean activity, 25.06 units/mg) and monomer (mean activity, 8.585 units/mg) using the calorimetric Arginase activity assay described in Materials and methods **(Figure 3-16D)**. As expected, the enzymatic activity of the rhARG2 trimer was approximately three times that of the monomer. Protein concentration was measured using the BCA as described in Materials and methods (section 2.13.2).

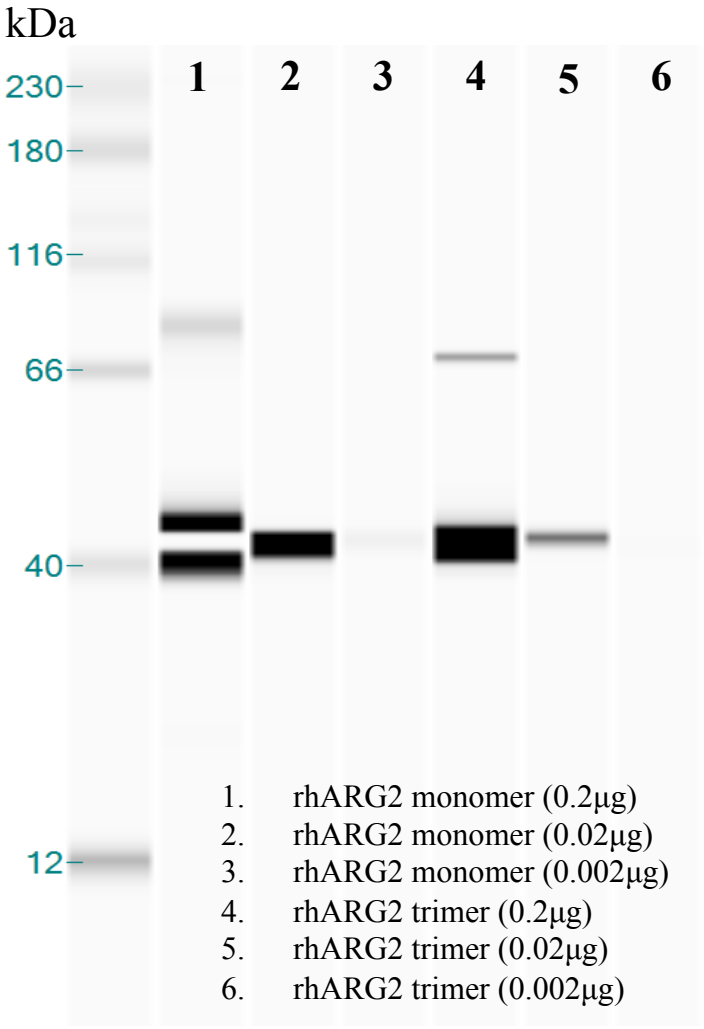
**A**


ARG2 Trimer
Bacterial byproducts
ARG2 Monomer
Current (mAU)
Time

**B**


kDa
1 2 3 4 5 6 7
250
150
100
80
60
50
40
30
25
20
15
*
1. Pre-induction
2. Post-induction
3. Pre-nickel (His-tag) column purification
4. Pre-FPLC column purification
5. Post-FPLC peak 1 (bacterial aggregates)
6. Post-FPLC peak 2 (ARG2 trimer)
7. Post-FPLC peak 3 (ARG2 monomer)

**C**




1. rhARG2 monomer (0.2μg)
2. rhARG2 monomer (0.02μg)
3. rhARG2 monomer (0.002μg)
4. rhARG2 trimer (0.2μg)
5. rhARG2 trimer (0.02μg)
6. rhARG2 trimer (0.002μg)

**D**

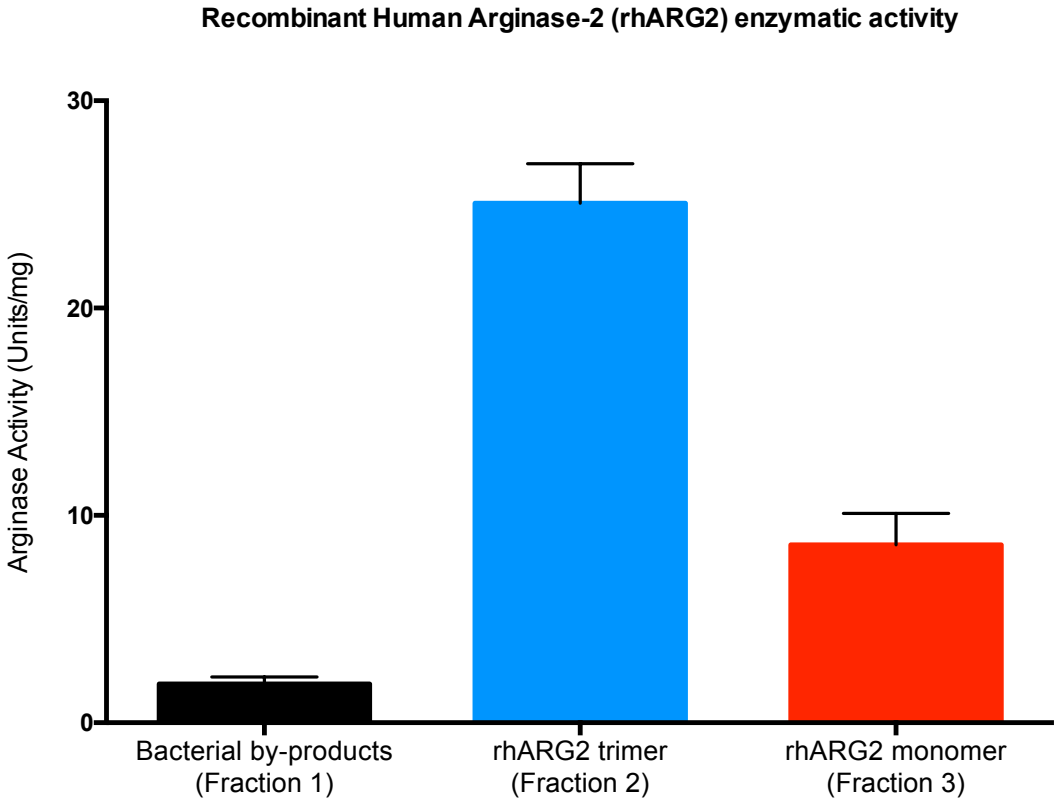



**Figure 3 - 16. De novo generation of a highly purified and active recombinant human Arginase-2 (rhARG2) protein.**
(A) Peaks following HPLC isolation and purification were used to distinguish between bacterial secretion by-products and the trimeric and monomeric forms of purified rhARG2 protein. Peaks coincided with expected calculated molecular weights of the rhARG2 trimer and monomer. (B) SDS-PAGE was used to confirm the high degree of purity of the trimeric form of rhARG2 (lane 6; starred band) compared to pre-induction (lane 1), post-induction (lane 2), pre-His-tag column purification (lane 3) and pre-HPLC purification (lane 4) samples. The purity of the rhARG2 monomer is also displayed in lane 7. According to our calculations, both rhARG2 trimer and monomer samples were more than 95% pure. (C) Capillary electrophoresis automated immunoblot was used to confirm the identity of the rhARG2 protein subunit originating from different concentrations of either the trimer or monomer HPLC peak. (D) Arginase activity assay confirms that both the rhARG2 trimer (blue) and monomer (red) are enzymatically active. Arginase activity levels were normalized to the amount of protein to display the amount of activity per mg of protein made and to confirm that the trimer has almost 3-fold higher enzymatic activity than the monomer. Bars represent mean with standard deviation derived from measurements done in triplicate.

## 3.5 Evaluation of novel Arginase inhibitors to block Arginase-2 activity

### 3.5.1 Novel small molecule Arginase inhibitors can effectively block the enzymatic activity of the synthetic rhARG2

Making use of our own recombinant human Arginase-2 (rhARG2) protein we tested the novel, membrane-permeable Arginase-specific inhibitors, OAT081 and OAT090 (a gift from OncoArendi Therapeutics), for their ability to block the enzymatic activity that converts arginine to urea and ornithine **(Figure 3-17)**. These novel small molecular inhibitors were designed de novo as part of collaboration with industrial partners, so that their structure had similar physical and chemical properties to arginine in order to act competitively at the active site of the Arginase enzyme. Unfortunately, the structure of the two inhibitors cannot be revealed in this work for confidentiality purposes. Using a calorimetric Arginase activity assay we evaluated their pharmacokinetic properties to show that these small molecule inhibitors are very effective at blocking Arginase activity **(Figure 3-18)**. The IC50 values were 1375nM for OAT081 and 77.8nM OAT090 respectively (Figure 3-19; top and bottom panels respectively). These IC50 values are arguably significantly low suggesting that our inhibitors are indeed very efficacious and as such, promising for future therapeutic use. We confirmed the inhibitory ability and IC50 value of OAT081 at different concentrations of rhARG2 in PBS, where the enzymatic activity was consistently reduced by approximately 50% in the presence of the small molecule inhibitor **(Figure 3-19)**.

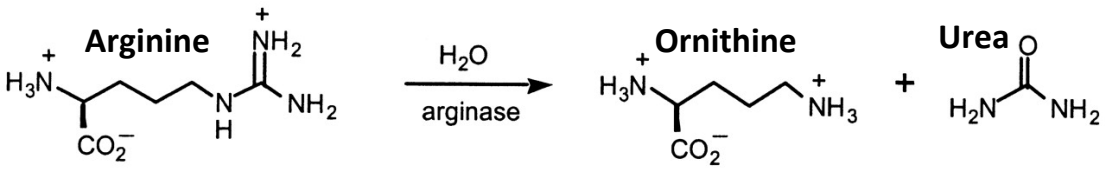



**Figure 3 - 17. The hydrolytic reaction of arginine breakdown.**
Arginine is broken down to ornithine and urea by the action of Arginase in a hydrolytic reaction.

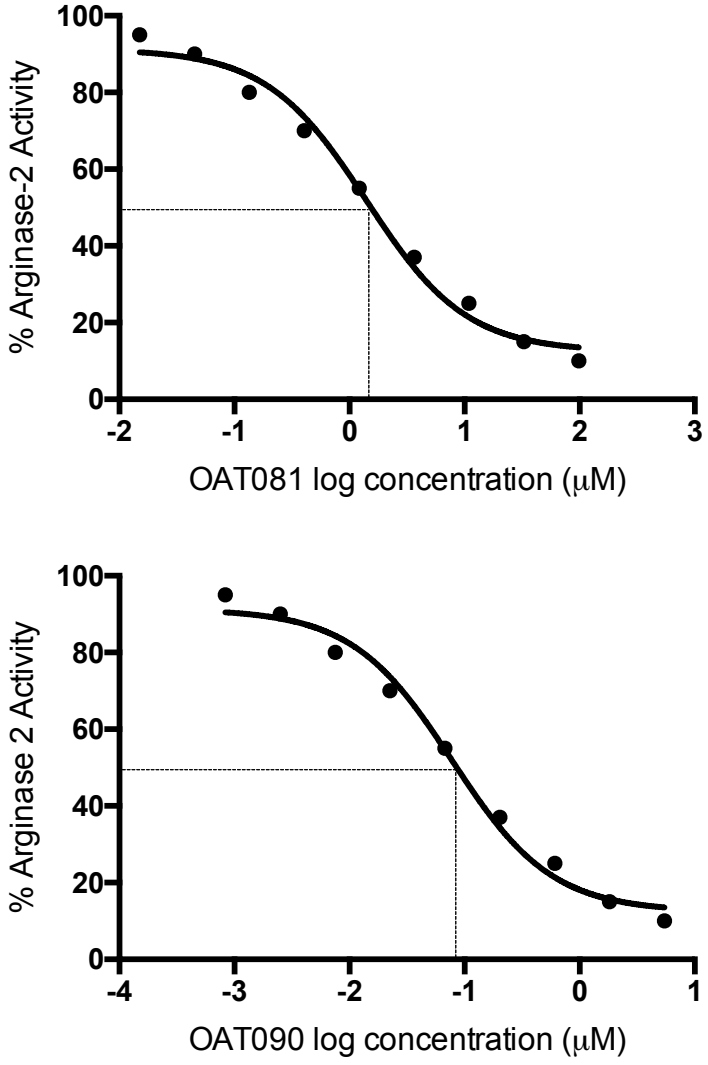



**Figure 3 - 18. Small molecule inhibitors OAT081 and OAT090 can inhibit rhARG2.**
We used our synthetic rhARG2 protein to prove that the small molecule inhibitors OAT081 (top panel) and OAT090 (bottom panel) have the ability to inhibit the enzymatic activity of Arginase. We calculated the IC50 of each inhibitor by measuring the % of rhARG2 activity at different inhibitor concentrations and identifying the concentration at which the rhARG2 was 50% of baseline (no inhibitor). The IC50 was 1375nM for OAT081 and 77.8nM for OAT090. Results are representative of experiments performed in triplicate.

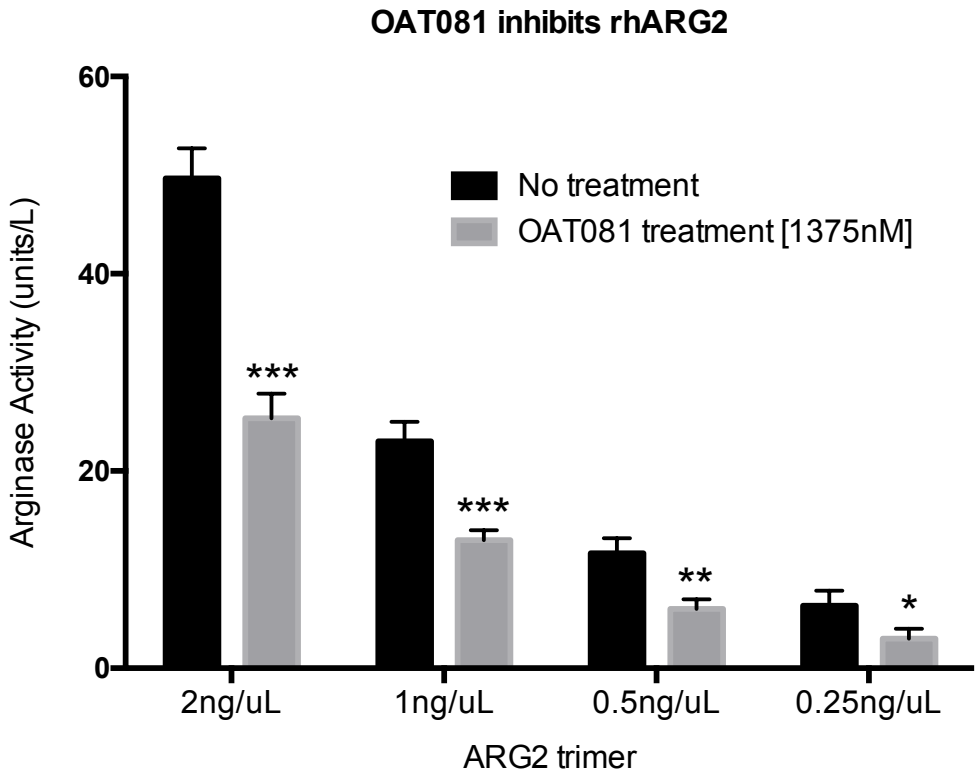



**Figure 3 - 19. Small molecule inhibitor OAT081 can inhibit rhARG2 at various concentrations.**
We used our small molecule inhibitors OAT081 at the IC50 concentration (1375nM) calculated in earlier experiments to prove that it is significantly efficacious at inhibiting rhARG2 activity by approximately 50% at various concentrations of the enzyme. Experiments were performed in PBS. *** $p< 0.001$, ** $p< 0.01$, * $p< 0.05$. Bars represent mean with standard deviation derived from measurements done in triplicate.

### 3.5.2 Novel small molecule Arginase inhibitors can effectively block the enzymatic activity of Arginase-2 from the mitochondria of human cancer cells in culture

To extent our results, we also tested the ability of the novel Arginase-specific inhibitor OAT081 to block biologically active Arginase-2 originating from human cells and more specifically human mitochondria. Firstly, we proved that whole cell lysate (WCL), mitochondrial lysate (mito lysate) and intact mitochondria (intact mito) from the ARG2-overexpressing THP1 cells (ARG2-THP1) we had generated, all had significant measured Arginase enzymatic activity when compared to wild-type (WT) THP1 cells **(Figure 3-20)**.

Using the Arginase-2 ELISA kit, we confirmed that this Arginase activity in ARG2-THP1 cells was the result of the presence of Arginase-2 **(Figure 3-21**). Furthermore, by incubating intact mitochondria from ARG2-THP1 cells in full R10 medium, we confirmed that the Arginase-2 activity within these intact mitochondria was sufficient to breakdown arginine and deplete its levels to below 50μM over 48 hrs, a concentration previously shown to be non-compatible with adequate T-cells proliferation in vitro **(Figure 3-22)**. Finally, we showed that a 72-hr incubation with OAT081 in culture completely abolished Arginase-2 activity from the ARG2-THP1 mitochondria **(Figure 3-23)**. The statistically significant inhibition in the enzymatic activity suggests that our novel Arginase-specific inhibitor OAT081 was effective, not only against the human recombinant Arginase-2 protein (as shown earlier), but also against Arginase-2 originating from a more realistic a biological system such as intact mitochondria or whole cell lysate. Given this, it is possible that OAT081 can have profound effects on Arginase-mediated inhibition of T-cell proliferation.

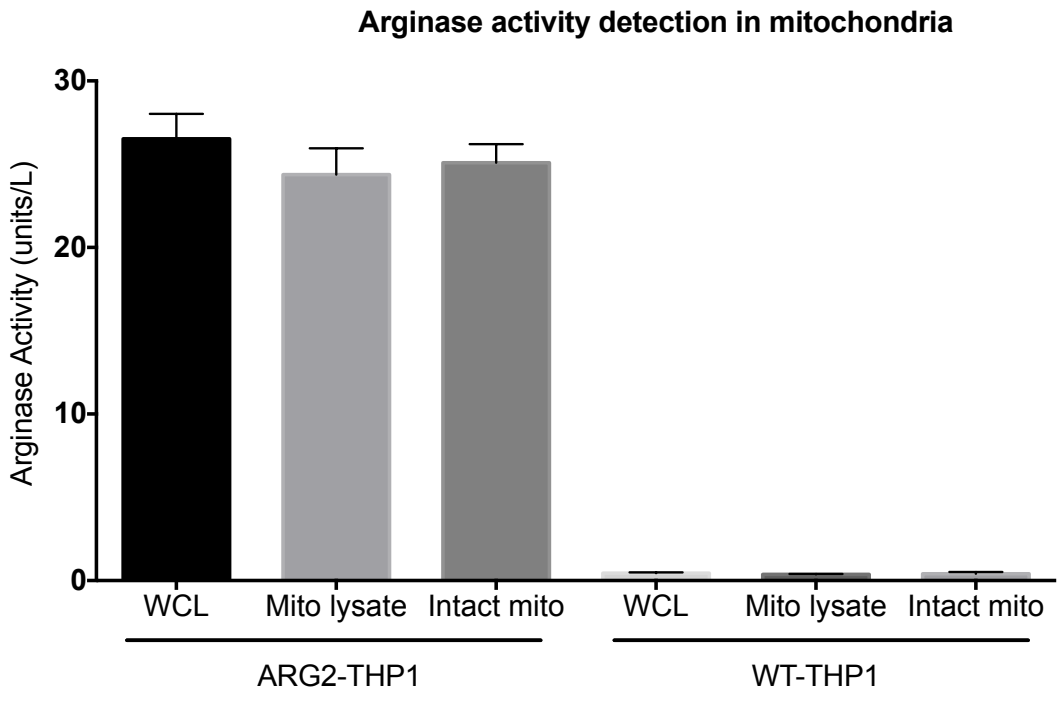


**Figure 3 - 20. ARG2-overexpressing THP1 cells have significant Arginase activity that originates in the mitochondria.**
Arginase activity was measured for each sample (40μL) based on the conversion of arginine to urea by means of a colorimetric assay. Whole cell lysate (WCL) from ARG2-overexpressing THP1 (ARG2-THP1) cells had similar activity to intact (intact mito) or lysed mitochondria (lysed mito) from ARG2-THP1 cells. Arginase activity was significantly higher (*** $p<0.0001$) in ARG2-THP1 compared to WT-THP1 cells for all three types of samples. Mitochondria were purified using magnetic-based separation and anti-TOM22 MACS beads as described in Materials and methods. Bars represent mean with standard deviation derived from measurements done in triplicate.

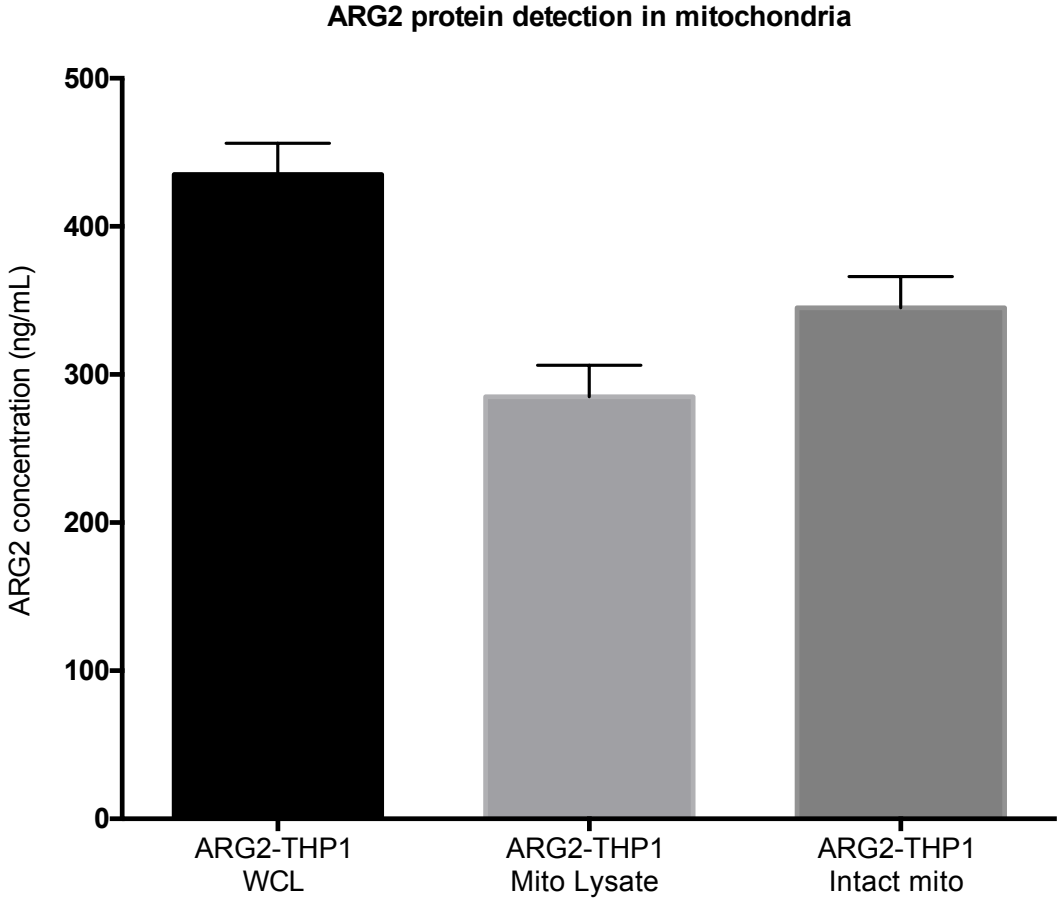



**Figure 3 - 21. ARG2-overexpressing THP1 cells express significant amounts of Arginase-2 protein that originates in the mitochondria.**
Arginase-2 protein concentration was measured for each sample (50μL) by ELISA. Whole cell lysate (WCL) from ARG2-overexpressing THP1 (ARG2-THP1) cells had similar activity to intact (intact mito) or lysed mitochondria (lysed mito) isolated and purified from ARG2-THP1 cells. Bars represent mean with standard deviation derived from measurements done in triplicate.

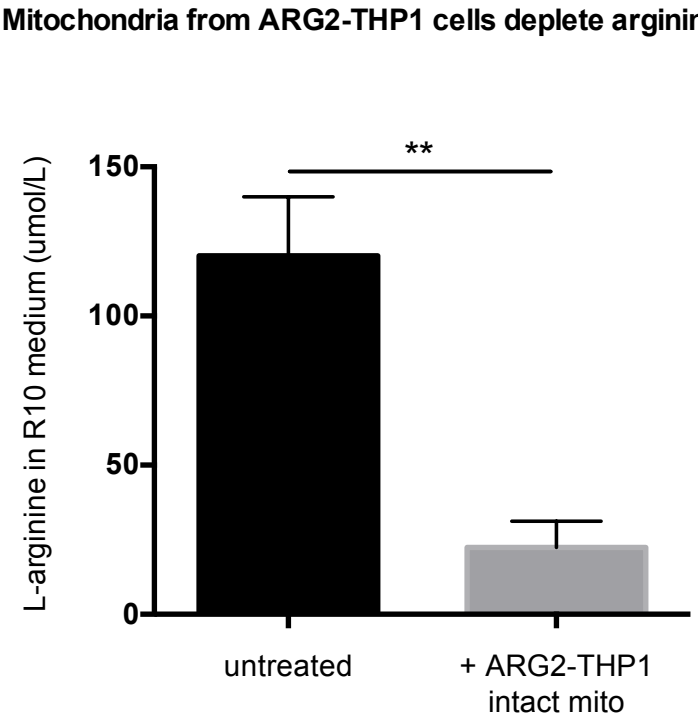



**Figure 3 - 22. Intact mitochondria from ARG2-overexpressing THP1 cells can break down and thus deplete arginine in culture medium.**
Intact mitochondria purified from 5 x $10^6$ ARG2-THP1 cells and with confirmed Arginase activity, were incubated in R10 culture medium for 48hrs. Arginine concentration, measured by ELISA, was shown to be significantly lower in medium with mitochondria compared to untreated culture medium. ** $p<0.001$. Bars represent mean with standard deviation derived from measurements done in triplicate.

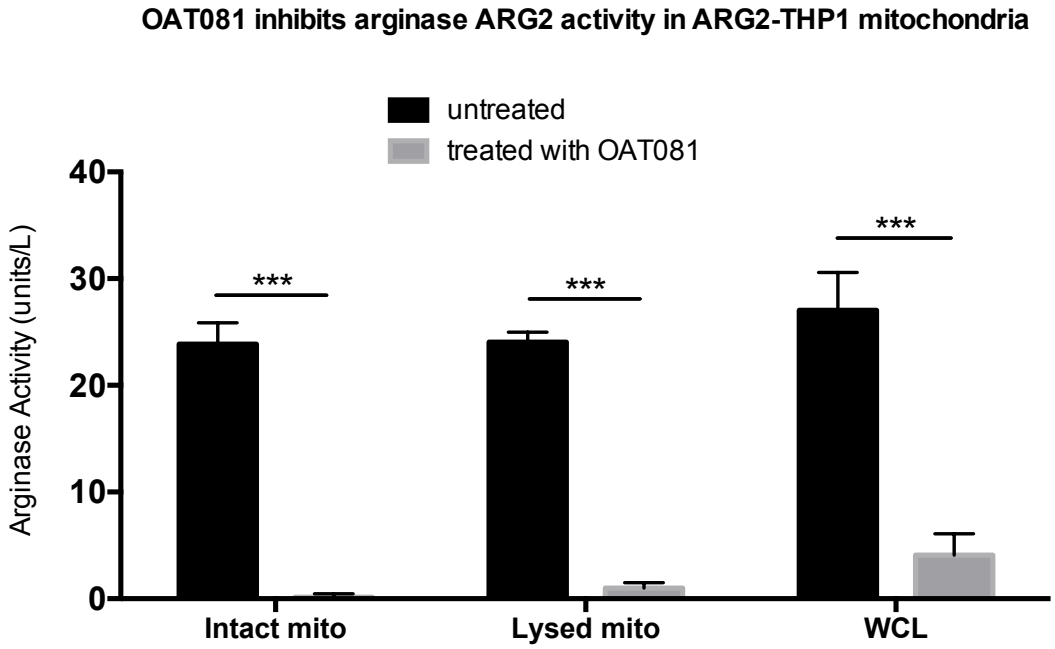



**Figure 3 - 23. Novel Arginase-specific small molecule inhibitors can block Arginase-2 present in mitochondria from ARG2-THP1 cells.**
Arginase activity was measured for each sample (40μL) based on the conversion of arginine to urea by means of a colorimetric assay. Arginase activity from whole cell lysate (WCL) and intact or lysed mitochondria from ARG2-overexpressing THP1 (ARG2-THP1) cells was almost completely abolished when samples were treated in culture for 72hr with the Arginase-specific small molecule inhibitor OAT081 (10μM). *** $p<0.0001$. Bars represent mean with standard deviation derived from measurements done in triplicate.

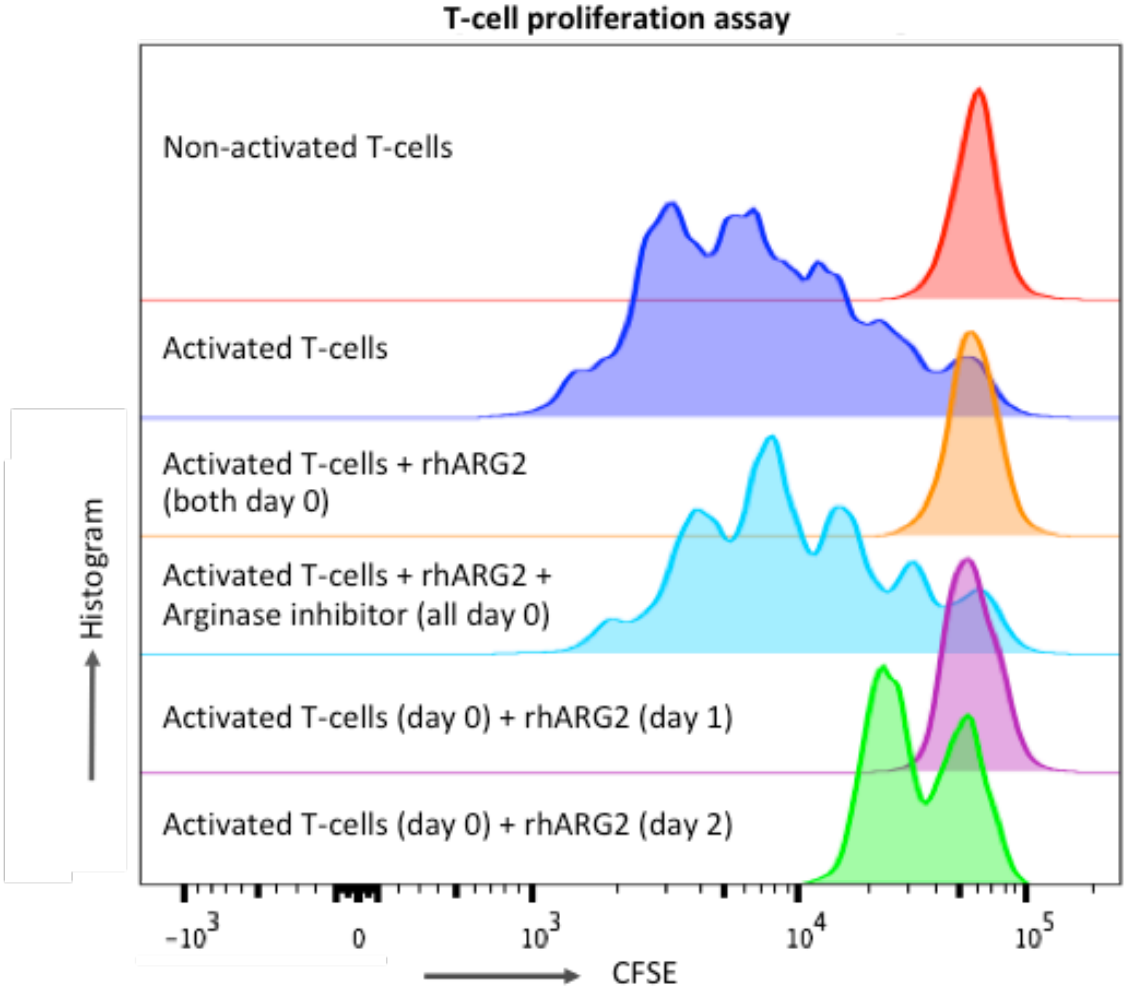
## 3.6 Arginase-2 inhibits proliferation of stimulated T-cells, an effect that is reversible with use of novel small molecule Arginase inhibitors

### 3.6.1 The novel small molecule Arginase inhibitor, OAT-081, can rescue T-cell proliferation in the presence of recombinant human Arginase-2 (rhARG2)

In order to investigate whether rhARG2 can dampen the immune response, we tested its ability to inhibit T-cell proliferation *in vitro*. CD4+ and CD8+ T cells were labeled with CFSE (to allow tracking of cell division) before stimulation with anti-CD3/CD28 beads (1:1 ratio) and culture in RPMI medium for 96 hours. The addition of rhARG2 (at a final concentration of 5μg/ml) in the culture, either at the same time as stimulation or 24 hours

later, completely abolished T-cell proliferation **(Figure 3-24A and B)**. Interestingly, the addition of rhARG2 48 hours post-stimulation, at which point T-cells had already undergone one cycle of proliferation, was still able to block further expansion **(Figure 3-24A; bottom panel)**. Furthermore, addition of our Arginase-specific inhibitor, OAT081 (10μM), at the same time as stimulation and in the presence of rhARG2 prevented any anti-proliferative effects allowing T-cell expansion to the same degree as baseline activation with anti-CD3/CD28 beads without rhARG2 **(Figure 3-24A and B)**.

**A**



**B**

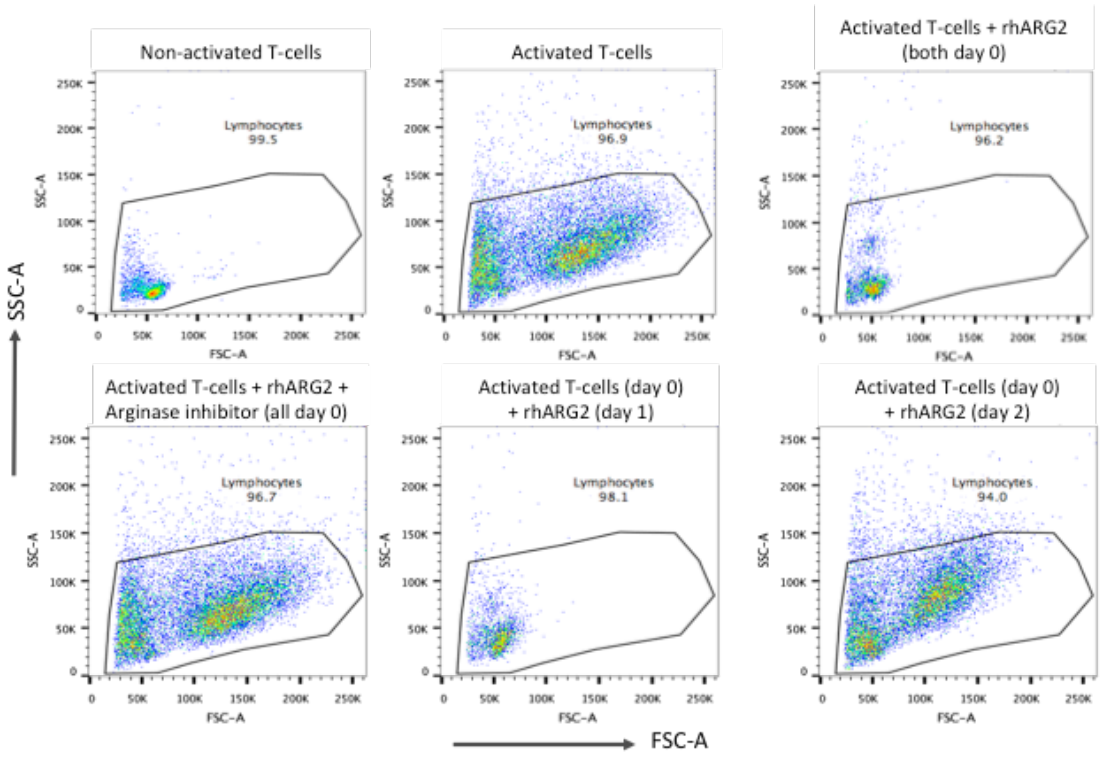



**Figure 3 - 24. rhARG2 can inhibit proliferation of stimulated T-cells, an effect that can be abrogated by Arginase inhibitors.**
(A) Histogram displaying CFSE dilution of T-cells upon stimulation with anti-CD3/CD28 beads (used in a 1:1 ratio). Each peak represents one cycle of proliferation. (B) FACS plots showing the changes in physical parameters; SSC-A (vertical axis) and FSC-A (horizontal axis) of T-cells upon stimulation. Proliferation of non-activated T-cells (A - red panel, B - top left panel) was compared to activated T-cells alone (A - blue panel, B - top middle panel) or with the addition of rhARG2 at same time as stimulation (day 0; A - orange panel, B - top right panel), 1 day post-stimulation (A - purple panel, B - bottom middle panel) or 2 days post-stimulation (A - green panel, B – bottom right panel). T-cell proliferation in the presence of rhARG2 could be rescued by the addition of Arginase-specific small molecule inhibitors (OAT081) at the time of stimulation (A - blue panel, B - bottom left panel).

### 3.6.2 The novel small molecule Arginase inhibitor, OAT-081, can rescue T-cell proliferation in the presence of human mitochondria expressing Arginase-2

To reinforce our findings, we confirmed the results above using mitochondria from THP1 cells overexpressing Arginase-2. In this way, we investigated whether the enzyme is still active when it is part of free-circulating intact mitochondria and also whether its

detrimental effects on human T-cells are also observed in their murine counterparts. Mitochondria from 5 x$10^6$ Arginase-2 overexpressing THP1 cells were initially purified using a commercially available human mitochondria isolation kit according to the manufacturer's instructions (Cat. No. 130-094-532; Miltenyi Biotec). The purification was based on magnetic beads binding to TOM22, an outer mitochondrial membrane protein, and MACS distillation using MACS separation columns (Miltenyi Biotec). Purified mitochondria were incubated with splenocytes (5 x$10^5$) from OT-1 mice that were labelled with CFSE as previously described and stimulated with the ovalbumin (OVA) peptide and IL-2 to induce proliferation. Proliferation of CD8+ T-cells, the main immune cell population expected to expand under these conditions, was evaluated by flow cytometry as previously described following a gating strategy as shown in **Figure 3-25**. In the presence of mitochondria, activated CD8+ T-cells failed to proliferate compared to baseline conditions, an effect that was abolished by the simultaneous addition of the Arginase-specific small molecule inhibitor, OAT081 to the culture of mitochondria and splenocytes **(Figure 3.26A and B)**. This suggests that similar to human T-cells, murine T-cells also have their proliferation suppressed by Arginase-2. Finally, the findings of this experiment prove that Arginase-2 still possesses significant enzymatic activity that can suppress T-cells even when bound to intact mitochondria that are free in culture. This is not surprising given that mitochondria have their own arginine transporters (members of the SLC25 family) and can thus, take up arginine from the culture medium and break it down by the action of the intact mitochondrial enzyme Arginase-2. This possibility is extremely relevant in the context of AML as previously discussed. It also reinforces the intriguing hypothesis that mitochondria, often secreted from tumour and host cells, are key active players in cancer-associated metabolic and immunological effects.

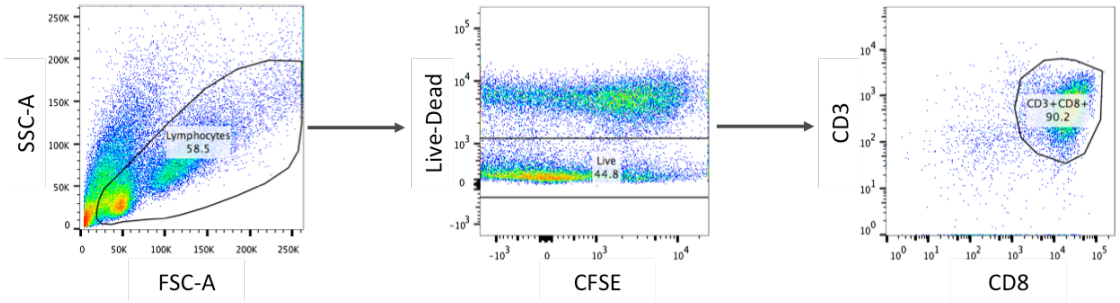
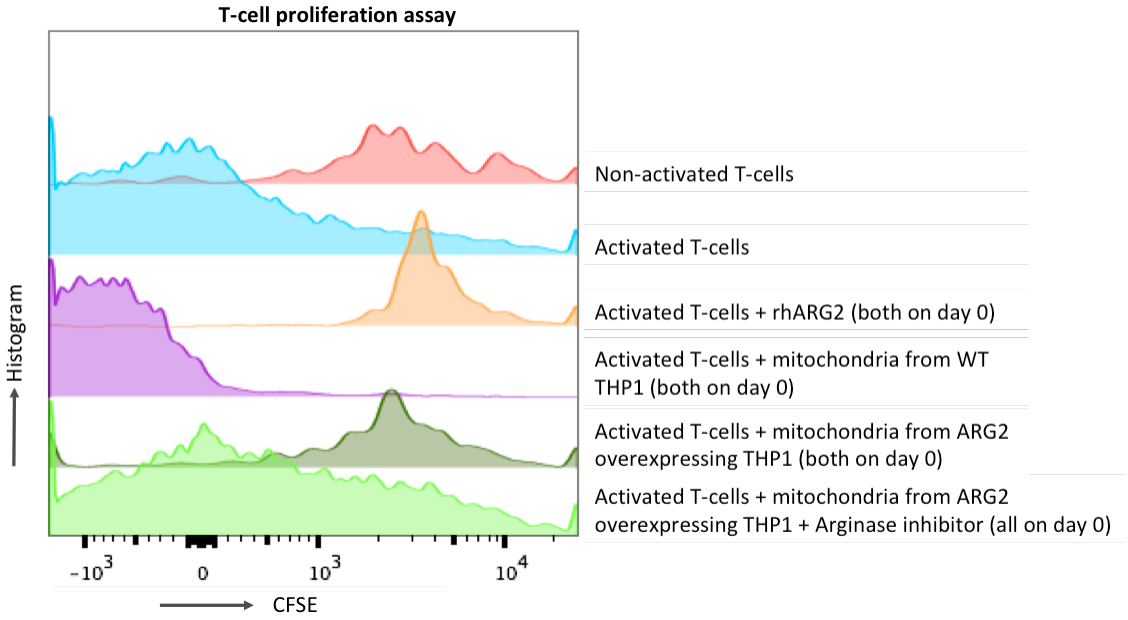



**Figure 3 - 25. Gating strategy used to select and analyse live CD8+ T-cells.** Lymphocytes were first gated based on physical parameters FSC and SSC followed by gating on live cells only before cells positive for surface markers CD3 and CD8 were isolated.

**A**



**B**

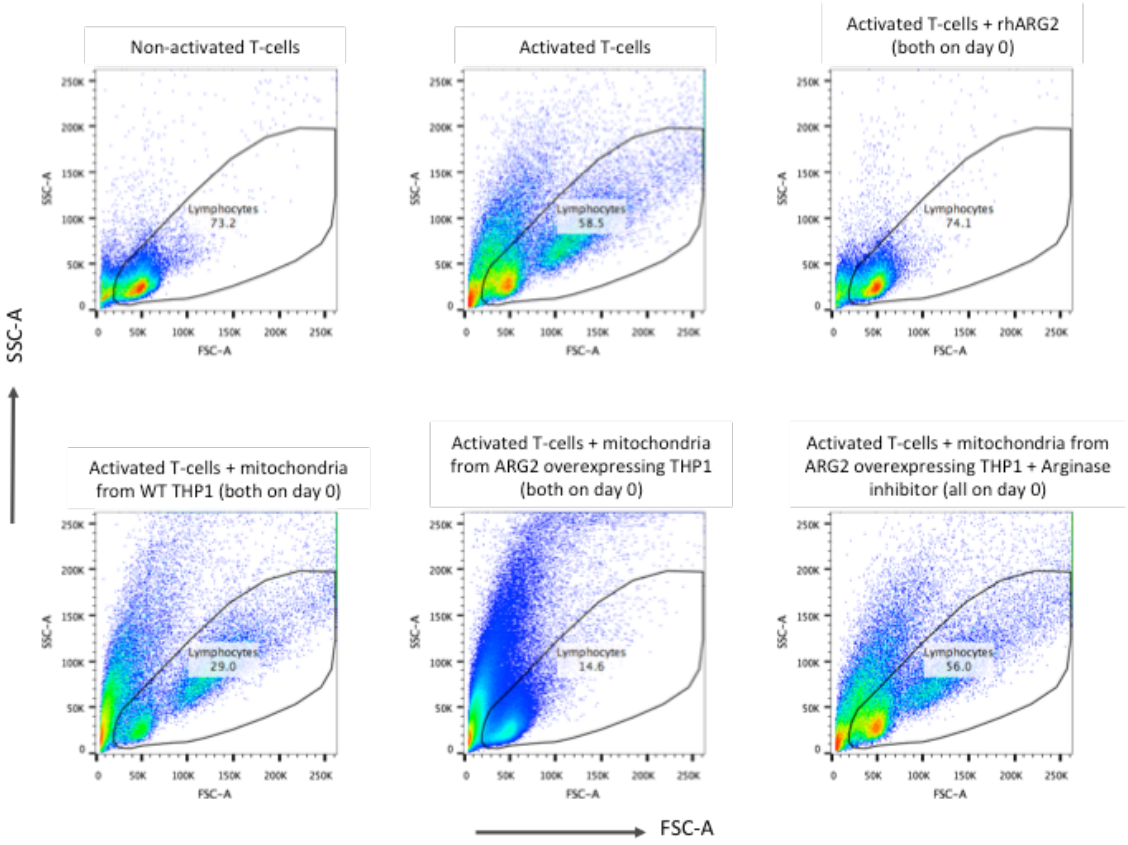



**Figure 3 - 26. Free intact mitochondria from THP1 overexpressing Arginase-2 can inhibit proliferation of stimulated murine T-cells, an effect that can be abrogated by Arginase inhibitors.**
(A) Histogram displaying CFSE dilution (a surrogate marker of proliferation) of murine CD8+ T-cells upon stimulation with OVA. (B) FACS plots showing the changes in physical parameters; SSC-A (vertical axis) and FSC-A (horizontal axis) of murine CD8+ T-cells following stimulation. Proliferation of non-activated T-cells (B - red panel, C - top left panel) was compared to activated T-cells alone (B - blue panel, C - top middle panel) or with the addition of rhARG2 at same time as stimulation (day 0; B - orange panel, C - top right panel). The addition of mitochondria from WT THP1 cells (B - purple panel, C - bottom middle panel) did not suppress proliferation. In contrast, the addition of mitochondria from ARG2 overexpressing THP1 cells (B – dark green panel, C – bottom right panel) inhibited T-cell proliferation to the same extent as treatment with rhARG2. T-cell proliferation in the presence of Arginase-2 overexpressing mitochondria could be rescued by the addition of Arginase-specific small molecule inhibitors (OAT081) at the time of stimulation (B – light green panel, C - bottom left panel).

## 3.7 Recombinant human Arginase-2 (rhARG2) and arginine starvation cause downregulation of surface CD3 in stimulated T-cells

In addition to suppression of proliferation, treatment of stimulated human T-cells with rhARG2 caused significant downregulation of the T-cell co-receptor CD3, an effect that was again abolished in the presence of the Arginase-specific small molecule inhibitor OAT081 **(Figure 3-27)**. Culture of stimulated T-cells in arginine-depleted RPMI medium had a similar influence on CD3 cell surface expression as treatment with rhARG2, suggesting that this outcome is the result of the intrinsic activity of the Arginase enzyme to hydrolyse arginine rather than some other extrinsic factor unrelated to the protein's enzymatic function.

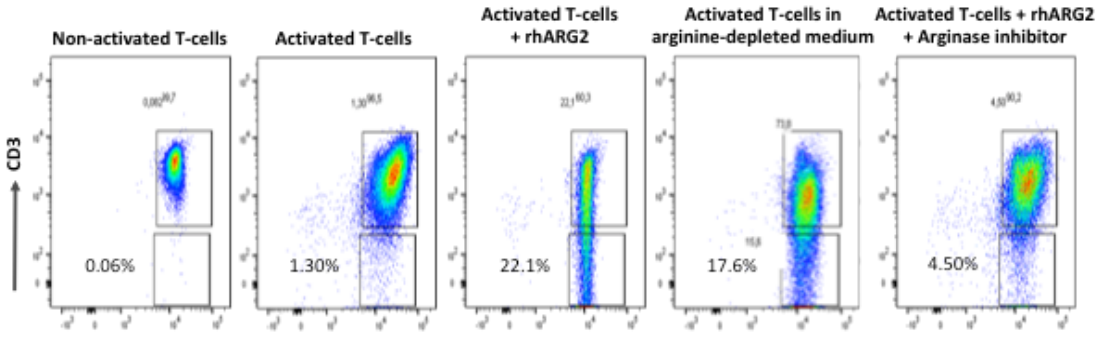



**Figure 3 - 27. rhARG2 treatment and arginine starvation inhibit lead to downregulation of the CD3 co-receptor in stimulated T-cells, an effect that can be prevented by Arginase inhibitors.**
FACS plots showing surface expression of CD3 (y-axis) on human T-cells upon activation. In contrast to non-stimulated T-cells (1st panel), activated T-cells (2nd panel) begin to show slight downregulation of CD3 (1-2%). Upon stimulation in the presence of rhARG2 (3rd panel) or under conditions of arginine starvation (4th panel), the proportion of T-cells downregulating CD3 cell surface expression enhances significantly (22.1% and 17.6% respectively). CD3 expression in the presence of both rhARG2 and small molecule Arginase inhibitors (5th panel) is restored to similar levels as observed in untreated stimulated T-cells.

## 3.8 Recombinant human Arginase-2 (rhARG2) and arginine starvation inhibit the mTOR pathway in stimulated T-cells

In order to understand the underlying molecular changes governing the Arginase-2-mediated suppression of T-cell proliferation, we investigated the function of the mTOR pathway, often influenced by the absence of amino acids [256]. More specifically, activation of mTOR pathway by proliferation stimuli such as growth factors and cytokines, leads to initiation of translation, protein synthesis, cell growth and cell division [256]. Using phosphorylation of the ribosomal protein S6 (pS6), a downstream target of p70 S6 kinase, itself a substrate of mTOR, as a surrogate marker of the functionality and activation of the mTOR pathway, we investigated the effects of Arginase-2 and arginine depletion. Using flow cytometry, we showed that anti-CD3/CD28 bead-based stimulation induces phosphorylation of S6 (pS6), suggesting that it enhances the activity of mTOR pathway in T-cells **(Figure 3-28)**. However, both treatment with rhARG2 and culture in arginine-depleted medium decreased this phosphorylation in stimulated T-cells, to an extent even more pronounced than treatment with rapamycin, the archetypal inhibitor of mTOR **(Figure 3-28)**. This suggests that, by depleting arginine in the microenvironment, Arginase-2 inhibits the activation and function of the mTOR pathway, an effect that might, at least partly, explain the ability of Arginase-2 to suppress activated T-cell proliferation.

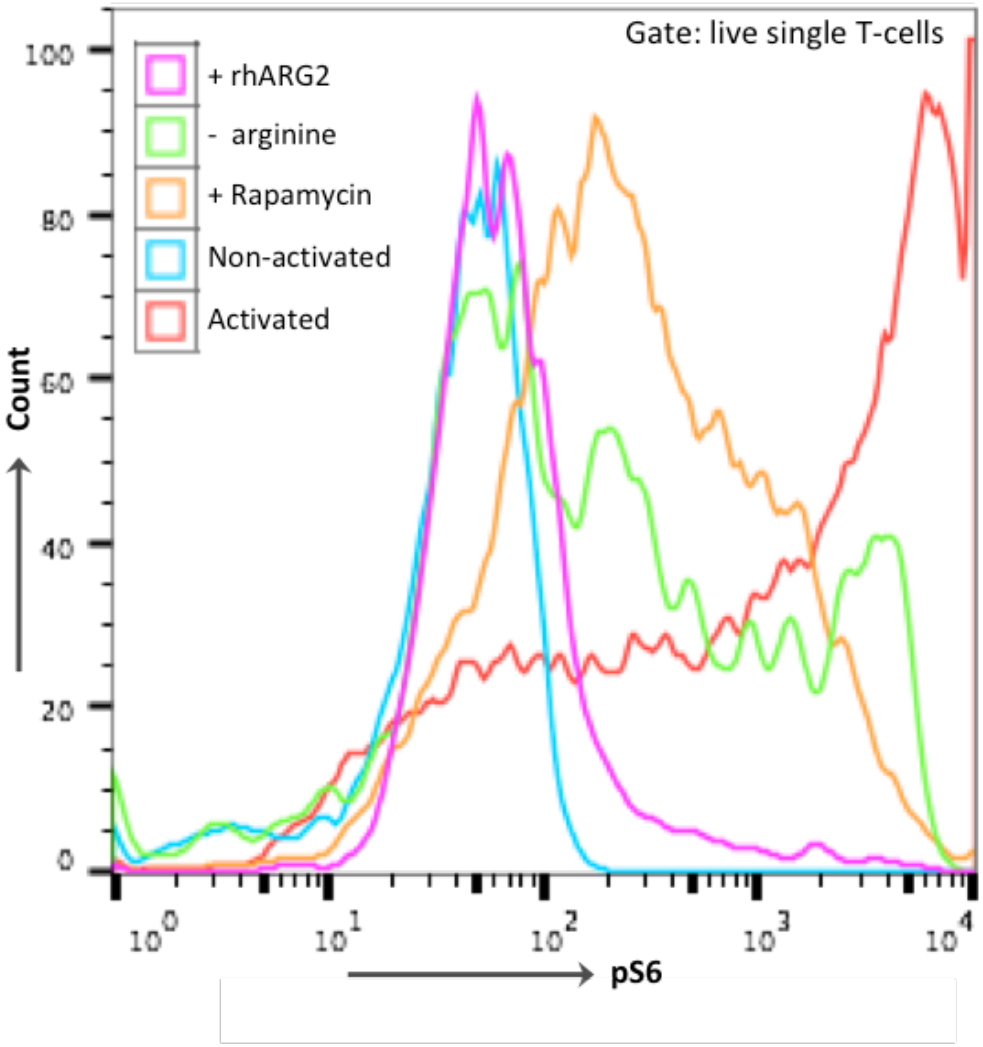



**Figure 3 - 28. Treatment of stimulated T-cells with rhARG2 or arginine-depleted culture medium abolishes the phosphorylation of S6, a surrogate marker of the mTOR pathway activation involved in cell proliferation.**
FACS histogram showing intracellular expression of pS6 (x-axis) on human T-cells after 72hrs in culture. pS6 expression in T-cells significantly increases upon anti-CD3/CD28 stimulation (red) compared to non-activated T-cells (blue). This is abolished in the presence of rhARG2 (magenta) or when T-cells are stimulated in arginine-free culture medium (green). Suppression of pS6 expression in stimulated T-cells by rhARG2 treatment or arginine starvation is stronger than the suppression induced by rapamycin, the archetypal mTOR pathway inhibitor (orange). This highlights how detrimental the effect of Arginase-mediated arginine depletion is on T-cells.

## 3.9 Recombinant human rhARG2 inhibits T-cell effector function by suppressing production of interferon gamma (IFN-γ)

CD4+ T-cell activation is generally linked to the production and secretion of interferon gamma (IFN-γ), one of the characteristic cytokines that confer effector function status. Using our rhARG2 protein, we investigated the effect of Arginase-2 on the ability of CD4+ T-cells to generate IFN-γ over 72 hrs. We showed that CD4+ T-cells were able to release IFN-γ only upon stimulation with anti-CD3/CD28 dynabeads (mean IFN-γ, 1.40ng/ml vs 0.03ng/ml for unstimulated, $p<0.0001$) **(Figure 3-29)**. However, upon treatment with rhARG2, the release of IFN-γ was significantly reduced in stimulated cells to similar levels seen in non-stimulated CD4+ T-cells (mean IFN-γ, 0.12ng/ml vs 0.03ng/ml for unstimulated, $p>0.05$) **(Figure 3-29)**. Furthermore, this effect was abolished with the use of the Arginase-specific inhibitor OAT081 (mean IFN-γ, 1.24ng/ml vs 0.03ng/ml for unstimulated, $p<0.0001$), in the presence of rhARG2, suggesting that blockade of the enzymatic activity of Arginase relieved the suppression on CD4+ T-cells restoring their ability to generate IFN-γ **(Figure 3-29)**.

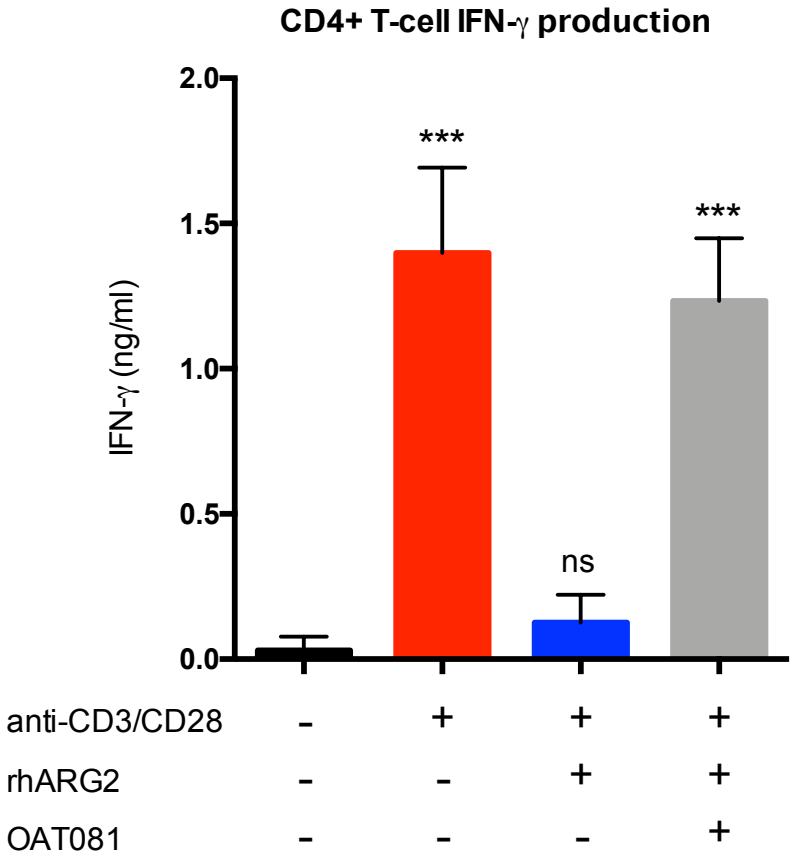



**Figure 3 - 29. rhARG2 suppresses interferon gamma (IFN-γ) release suppressing CD4+ T-cell effector function.**
CD4+ T-cells were cultured for 96hr with or without anti-CD3/CD28 stimulation beads, with or without rhARG2 and with or without OAT081. IFN-γ was measured by ELISA at the end of the incubation period. CD4+ T-cell stimulation (red) induced significant IFN-γ release, which was completely abolished by the treatment with rhARG2 (blue), an effect that was abrogated by the simultaneous presence of the Arginase-specific small molecule inhibitor OAT081 (grey). All comparisons were made against non-stimulated CD4+ T-cells (black); *** $p < 0.001$, ns non-significant. Bars represent mean with standard deviation derived from measurements done in triplicate.

## 3.10 AML plasma-derived Arginase-2 suppresses the cancer killing ability of effector CD8+ T-cells

Finally, we looked at the effect of Arginase-2 activity in human AML plasma on the ability of effector CD8+ T-cells to kill target cells by antigen-specific recognition using the NY-ESO9V peptide and the T-cell clone, 4D8, recognising this antigen as previously described

in our lab [354-356]. We set up a killing assay using the IncuCyte live cell analysis system whereby effector 4D8 T-cells could kill target THP1 cells carrying and presenting the NY-ESO9V peptide causing the release of intracellular fluorescent dye that had been previously incorporated by the target THP1 cells. By measuring fluorescence in real-time over 8 hours, we were able to show that effector T-cells could kill target THP1 cells only in the present of antigenic peptide **(Figure 3-30)**. Interestingly, the addition of human AML plasma significantly reduced the killing ability of effector T-cells an effect that could be, at least partially, reversed by the Arginase inhibitor OAT081 **(Figure 3-30)**. This suggests that, in addition to inhibiting the function of CD4+ T-cells by suppressing IFN-γ release, Arginase in human AML plasma can also suppress the effector function of CD8+ T-cells in terms of their cancer killing ability.

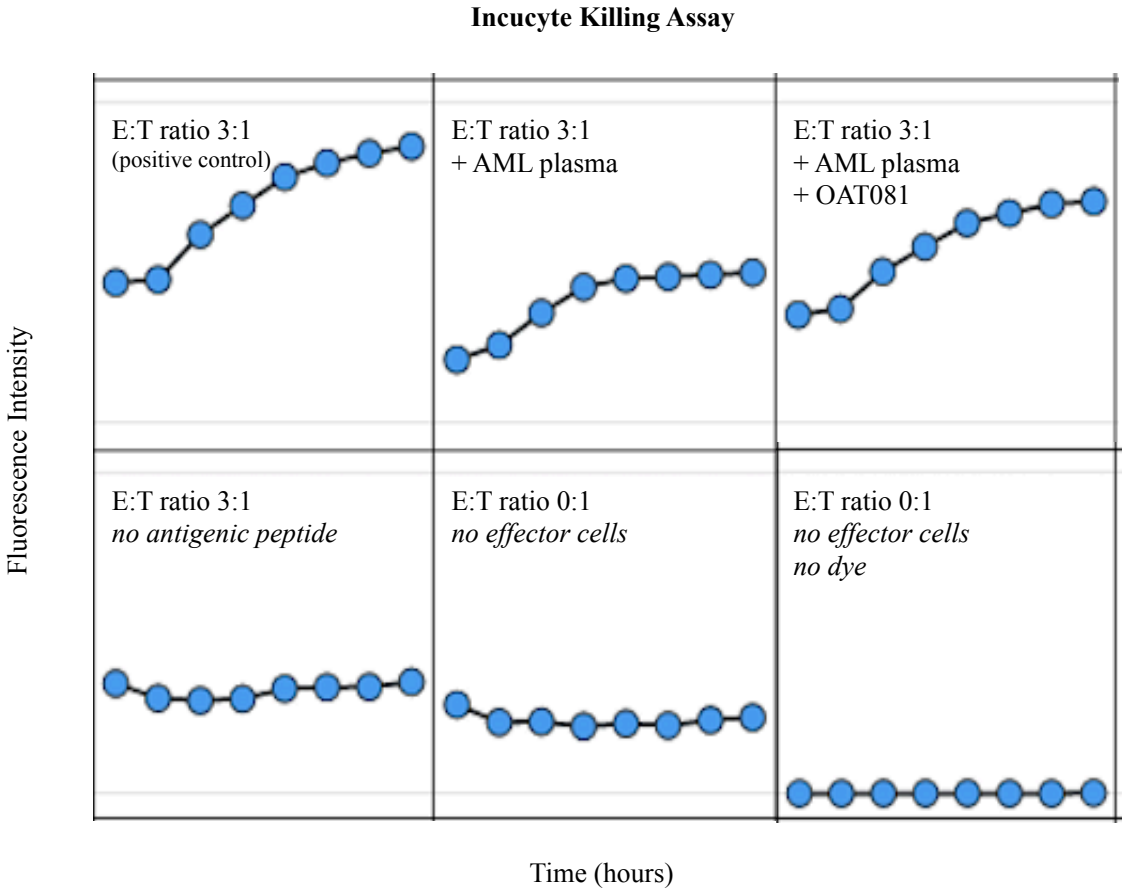



**Figure 3 - 30. Arginase in AML plasma suppresses the cancer killing ability of effector CD8+ T-cells.**
The Incucyte killing assay was used to measure cell death of target cancer (THP1) cells (T) induced by effector CD8+ T-cells (E) by measuring the release of intracellular fluorescent dye from the latter against background signal in the absence of any dye (bottom right panel) over 72hr. No cell death occurred in the absence of antigenic peptide (THP1 not carrying NY-ESO9V; bottom left panel), or in the absence of effector CD8+ T-cells (bottom middle panel). In contrast, significant cancer cell death occurred at an E:T ratio of 3:1 (top left panel). The ability of effector CD8+ T-cells to kill cancer cells was abolished in the presence of plasma derived from AML patients. The killing ability of effector CD8+ T-cells was rescued even in the presence of AML plasma by the simultaneous treatment of cells with the Arginase-specific small molecule inhibitor OAT081, suggesting that the AML-related inhibition of immune-mediated is due to the presence of Arginase in AML plasma. The data points shown are representative of experiments done in triplicate.

## 3.11 Discussion

It is now well established that cancers often evade the immune system by generation of nutritional stress that is detrimental to tumour-infiltrating T-cells. One way of achieving

this is by hijacking amino acid metabolism as in the case of the arginine pathway through expression or secretion of Arginase isoenzymes by cancer cells or cancer-associated cells, mainly MDSC, to break down the semi-essential amino acid arginine. Arginine has been shown to be crucial not only for the physiological function of the immune system but also the capacity of T-cells to survive and drive anti-tumour immune responses [366]. Hence the deprivation of arginine can lead to cancer immune escape. Having recently observed that Arginase is released in the bloodstream of AML patients to potentially cause immunosuppression, our aim was to confirm, understand and extend these findings to identify potential targets for cancer immunotherapy.

Firstly, we showed that Arginase activity is higher in plasma from AML patients compared to healthy controls and demonstrated that this Arginase activity is exclusively due to the presence of the mitochondrial Arginase-2 (ARG2) isoenzyme. We extended these findings to two distinct AML mouse models with raised Arginase-2-specific activity and systemic arginine depletion and also revealed a correlation between Arginase-2 levels and Arginase activity with peripheral haemoglobin, peripheral platelet counts, white cell count and bone marrow AML blast count, all clinical indices often used in AML patients to establish the burden of the disease. As expected, the correlation of Arginase-2 activity was positive in relation to white cell count and bone marrow AML blasts and negative in relation to haemoglobin and platelets.

In an effort to understand the original source of Arginase-2, we also studied a mouse model of myeloproliferation in which autophagy, and thus mitophagy, was impaired in haematopoietic stem cells. Interestingly, this autophagy/mitophagy-deficient model of myeloproliferative disease also showed raised Arginase-2 activity compared to wild type controls. Given that Arginase-2 is a mitochondrial enzyme, this finding could possibly be explained by a hypothesis that suggests dying or stressed AML blasts in peripheral blood

actively secrete or passively release mitochondrial components that incorporate and protect Arginase-2 thus allowing for enhanced stability and longer half-life than expected in the organism's bloodstream. Using a THP1-ARG2 overexpressing cell line we confirmed that Arginase-2 is localized in the mitochondria and also demonstrated that mitochondria purified from these genetically engineered cells have intact Arginase-2 activity. RNA-seq data from primary human AML blasts demonstrated that ARG2 was not overexpressed in leukaemic cells from AML patients compared to myeloid cell subpopulations from healthy controls suggesting that the increased plasma Arginase-2 levels observed are not the result of increased transcription but perhaps a post-transcriptional modification, translational events or perhaps simply due to a simple quantitative effect of having a huge number of AML blasts circulating in patient bloodstream. Our results shed some light as to the source of Arginase-2 but further experiments need to be performed in order to definitively identify the mechanism of this phenomenon.

As our main focus was on potential therapeutic interventions, we generated a recombinant human Arginase-2 (rhARG2) protein and confirmed its enzymatic activity, both as trimer and monomer. Then, we tested novel Arginase-specific small molecule inhibitors and showed that they can block Arginase activity at significantly lower concentrations in comparison to the current best commercially available Arginase inhibitors (such as nor-NOHA), which are not very selective. To our knowledge, these are the most effective verified Arginase-specific small molecule inhibitors currently available.

Using combinations of human AML plasma, mitochondria from our ARG2-overexpressing THP1 cells, our rhARG2 and the novel Arginase-specific small molecular inhibitor (OAT081) we investigated the effects of Arginase-mediated arginine depletion on the function of T-cells. We demonstrated that both mitochondria from ARG2-overexpressing THP1 cells and the rhARG2 were able to deplete arginine in the culture medium and

inhibit T-cell proliferation (both antigen-driven and CD3/CD28 global stimulation-driven), an effect prevented in both contexts by the use of Arginase-specific small molecule inhibitors. Furthermore, we showed that Arginase treatment and arginine starvation of activated CD4+ or CD8+ T-cells inhibit the expression of the TCR co-stimulatory partner molecule CD3 and deactivate the mTOR pathway, effects that might explain the inability of T-cells to proliferate. Moreover, we showed that the effector function of T-cells is also compromised. Treatment with Arginase or culture in arginine-free medium suppressed IFN-γ production in CD4+ T-cells whilst the addition of Arginase-2-containing AML human plasma to CD8+ cytotoxic T-cells impeded their killing capacity in vitro against antigen-specific tumour cells. Both of these effects were prevented or reversed by our novel Arginase-specific small molecular inhibitors.

Despite the efficacy of our Arginase inhibitors in blocking the enzyme's activity and rescuing T-cells from the effects of arginine deprivation, there is still a potential issue to address. The substantial homology between the Arginase-1 and Arginase-2 isoenzymes with essentially identical active sites means that our inhibitors cannot differentiate between the two isoenzymes and their use could potentially cause side effects such as hepatotoxicity, by disrupting the hepatic urea-ammonia cycle. Further work will be needed to identify better inhibitors that are selective for Arginase-2.

All in all, in this chapter we revealed the release of active Arginase-2 in the blood of AML patients and mouse models and investigated the effects of Arginase-2 on T-cells. We showed that inhibition of Arginase-2 and prevention of arginine depletion, using small molecule inhibitors, can relief the detrimental Arginase-mediated suppression on T-cell proliferation and effector function. Our results suggest that Arginase inhibition might be relevant in the context of AML and potentially other cancers characterized by high Arginase activity in the tumour microenvironment where it can have significant therapeutic

implications by boosting anti-tumour immunity. Further work in vivo will be required to prove this possibility and its impact on disease progression. Finally, our results have highlighted a question that still remains unanswered; how do cancer cells such as AML blasts, and cancer-associated immunosuppressive host cells such as MDSCs, manage to survive and thrive in an environment depleted of arginine as a result of high Arginase activity? We attempt to answer this intriguing question in the following chapter.

# Chapter 4: The effect of (Arginase-dependent) arginine starvation on the expression profile of genes involved in amino acid metabolism and transport in cancer cells and T-cells

## 4.1 Introduction

The mechanisms by which cancer cells, and more specifically AML blasts, are able to adapt to amino acid depletion in the tumour microenvironment are poorly understood and remain to be elucidated. In the introduction we discussed how various solid tumours appear to break down arginine and other amino acids, such as tryptophan, in the tumour microenvironment to suppress tumour-specific lymphocytes. In the previous chapter, we showed that in AML, Arginase-2 is released in plasma to cause systemic depletion of arginine and consequently suppression of T-cell proliferation. In this chapter, we aim to identify and understand the adaptation mechanisms that allow cancer cells, including leukaemic blasts, but not T-cells, to survive and continue to proliferate in the absence of arginine. Given the detrimental effects of Arginase-dependent arginine depletion on the proliferation of T-cells, we hypothesized that cancer cells might perhaps possess an inducible adaptation mechanism that permits them to survive and continue to grow in such conditions giving them a competitive advantage against the host immune system.

## 4.2 The signatures of differential gene expression in cancer cells and T-cells upon arginine deprivation show both similarities and differences

In contrast to T-cells, which suffer proliferative arrest and effector dysfunction as a result of Arginase-dependent arginine starvation, cancer cells remain resistant to the detrimental effects of an arginine-depleted environment. Using THP1 cells as a model of human monocytic AML, we investigated the effect of arginine starvation on the transcriptomic profile of tumour cells and T-cells. T-cells were sorted with MACS beads to select the CD4 population following PBMC isolation from blood of distinct healthy donors for each experiment before being subsequently activated using anti-CD3/CD28 stimulation beads. In a reductionist approach, THP1 cells and primary activated human CD4 T-cells were separately exposed and cultured in either complete R10 medium (+ Arg) or medium lacking the amino acid arginine (arginine-depleted medium; - Arg) for 72 hrs in triplicate biological experiments then RNA levels were analysed by Illumina microarray (in collaboration with Dr Steve Taylor and Dr Lars Ronn Olsen) to compare the transcriptomic response to arginine deprivation **(Figure 4-1)**. We identified six distinct signatures of differentially expressed genes in the absence of arginine: up-regulated in both T-cells and THP1 cells (I, n=495), down-regulated in both T-cells and THP1 cells (II, n=380), up-regulated in THP1 cells only (III, n=312), down-regulated in THP1 cells only (IV, n=440), up-regulated in T-cells only (V, n=1510), and down-regulated in T-cells only (VI, n=2192), indicating that the cell types have unique and common responses to arginine starvation **(Figures 4-1 and 4-2)**. An interesting finding was that when looking purely at genes changing their expression (either down- or up-regulation), there was a much higher number affected in T-cells only (n=5443) compared to THP1 only (n=1091), suggesting that the former population is much more plastic and responsive to metabolic stress **(Figures 4-2A and B)**.

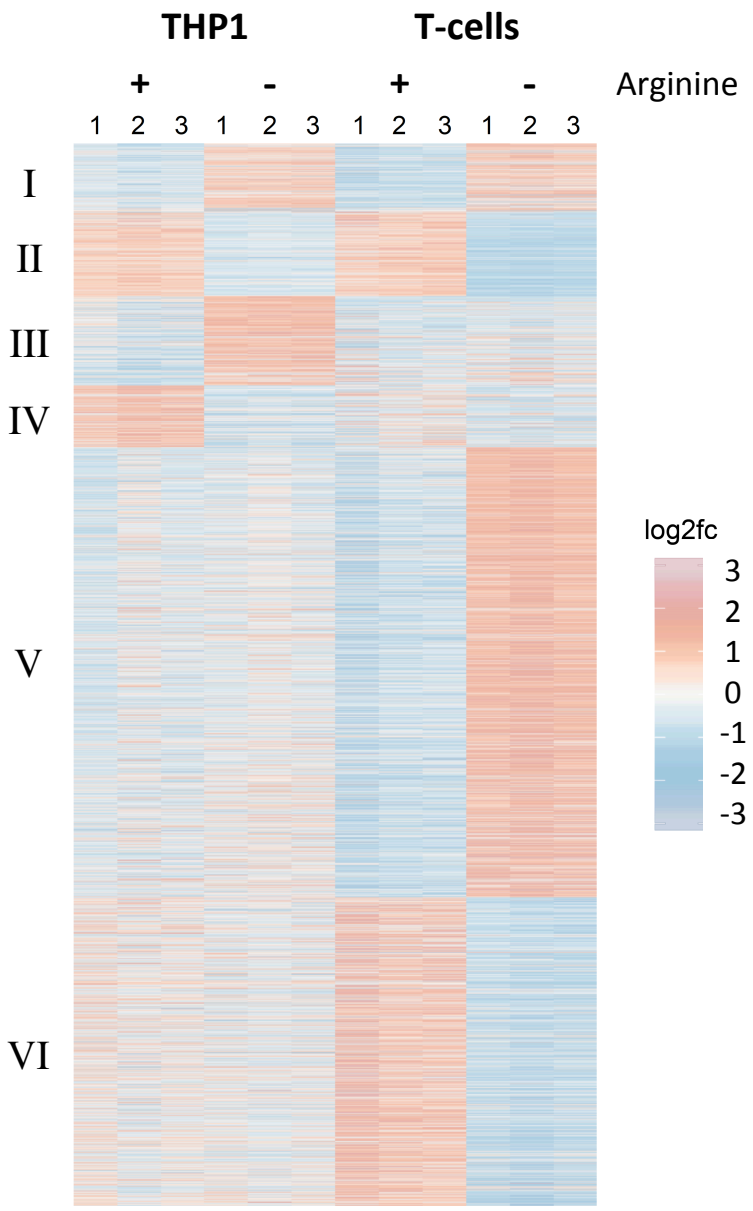
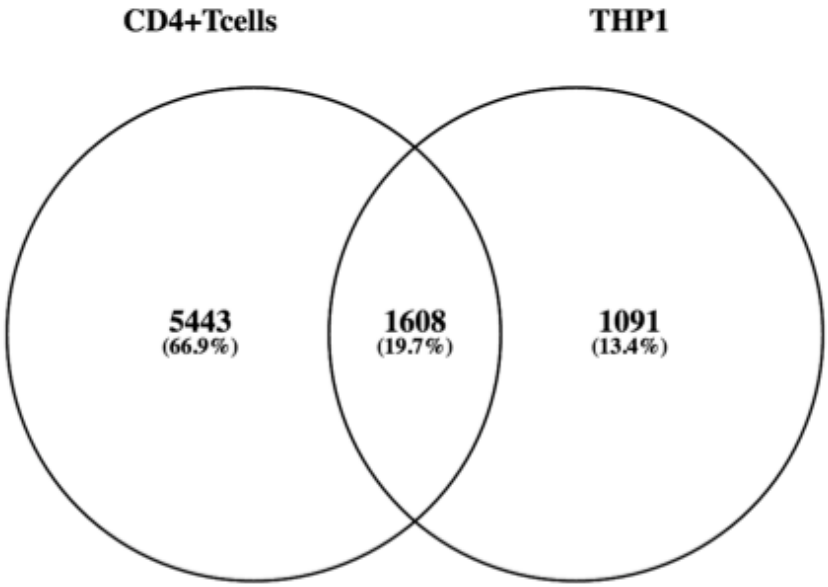



**Figure 4 - 1. The signature of differential gene expression upon arginine starvation differs between cancer cells and T-cells.**
Heat map representing the differential gene expression in THP1 cancer cells and stimulated T-cells induced after a 72hr incubation to arginine starvation in culture. Genes upregulated in response to arginine deprivation are shown in red whereas genes downregulated in response to arginine deprivation are shown in blue. Six distinct signatures are recognized; I - genes upregulated in both cell types, II – genes downregulated in both cell types, III – genes upregulated in cancer cells only, IV – genes downregulated in cancer cells only, V – genes upregulated in T-cells only and VI- genes downregulated in T-cells only. Data shown were analysed following an Illumina microarray and represent triplicate experiments for each condition (1-3).

**A**




**B**

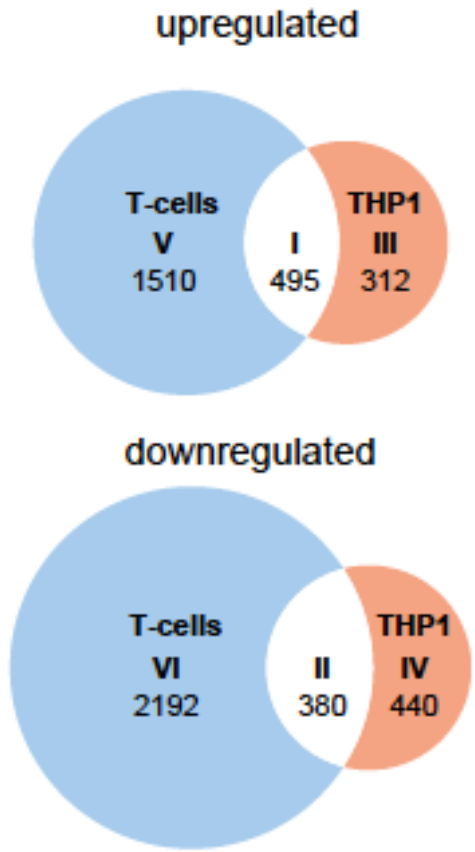



**Figure 4 - 2. Comparison of up- and down-regulated genes in THP1 and T-cells following arginine starvation.**
(A) Venn diagram showing the total number of genes that are differentially expressed in THP1 and T-cells upon arginine starvation. (B) Venn diagram showing the number of

genes up- or downregulated in THP1 and T-cells in response to arginine starvation. Stimulated T-cells undergo a significantly larger genetic reprogramming upon arginine deprivation as they both upregulate and downregulate more genes than THP1 cells.

## 4.3 Arginine starvation induces a genetic reprogramming in cancer cells but not T-cells that involves upregulation of proteins involved in arginine metabolism and might be driven by the ATF4 transcription factor

A KEGG pathway analysis identified significant differential expression of genes likely involved in a general response to nutrient starvation, including apoptosis, cell cycle, autophagy, inflammation, glucose/monosaccharide metabolism, glycolysis and tRNA amino-acylation. More interestingly, when we focused on genes only upregulated in THP1 cells upon arginine starvation **(class III; Figures 4-1 and 4-2)** we found that arginine biosynthesis and amino acid biosynthesis were amongst the top 5 pathways of differentially expressed genes **(Figure 4-3, left panel)**. This suggested that THP1 cells might be better suited at responding to the stress induced by deprivation of an amino acid such as arginine. Further analysis, confirmed that there was indeed significant upregulation of a number of genes in THP1 cells which were more likely to permit a specific response to arginine deprivation, including those involved in amino acid metabolism and amino acid transporters **(Figure 4-4)**.

Furthermore, the transcription factor ATF4, master regulator of the cellular integrated stress response (including nutritional stress), was moderately upregulated in our microarray at the RNA level in both cancer cells and T-cells following arginine starvation **(Figure 4-4)**. Consistent with this, genes containing an ATF4-binding motif formed one of the most prominent classes of genes upregulated only in cancer cells **(Class III genes; Fig 4-3 right panel)**, although surprisingly this motif was not enriched in up-regulated genes in T-cells.

This suggested that the huge transcriptome reprogramming (in the form of gene upregulation) occurring in THP1 cells only but not T-cells might be driven by the ATF4 transcription factor that governs responses to metabolic stress.

In addition, although the ARG2 gene was significantly upregulated in T-cells upon stimulation ($p<0.0001$), both our microarray and qRT-PCR proved that it was in fact downregulated in activated T-cells exposed to arginine starvation for 72hr ($p<0.001$), consistent with a need to conserve arginine levels under starvation conditions **(Figures 4-4 and 4-5)**. In contrast, ARG2 expression was not affected by arginine starvation in non-activated T-cells nor THP1 cells, consistent with the high levels of Arginase-2 in the serum of AML patients (described in Chapter 3). ARG1 remained stable in both cell types without a response to the lack of arginine **(Figure 4-4)**.

A number of transporters were upregulated upon arginine depletion in both THP1 and T-cells, including the cationic amino acid transporter of arginine SLC7A1 (CAT1), suggesting that a common response to arginine depletion is to facilitate import of the amino acid from the extracellular space **(Figure 4-4)**. However, other multifunctional amino acid transporters such as SLC1A5 and SLC7A5 (LAT1) showed more significant upregulation in cancer cells than in T-cells, suggesting that enhanced amino acid uptake is important and may confer a survival advantage on the cancer cells **(Figure 4-4)**.

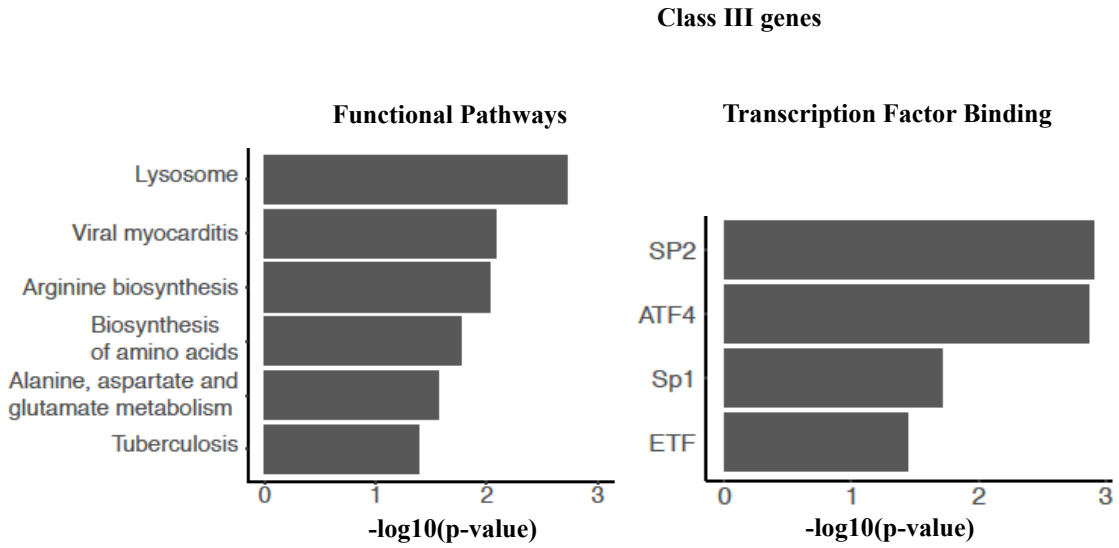



**Figure 4 - 3. A significant number of genes upregulated upon arginine starvation in THP1 cells but not T-cells belong to the arginine biosynthesis pathway and contain binding motifs for the transcription factor ATF4.**
A KEGG database pathway and genomic analysis was carried out to identify the biological pathways and transcription factor binding motifs enriched in the genes upregulated in THP1 cells but not T-cells upon arginine starvation. Three of the top six biological pathways identified are part of amino acid metabolism namely; arginine biosynthesis (3$^{rd}$), amino acid biosynthesis (4$^{th}$) and alanine/aspartate/glutamate metabolism (5$^{th}$). Binding motifs for the transcription factor (TF) ATF4, the master regulator of the cellular response to metabolic stress, were also significantly enriched (2$^{nd}$ top hit amongst TF binding motifs) in genes upregulated in THP1 cells only.

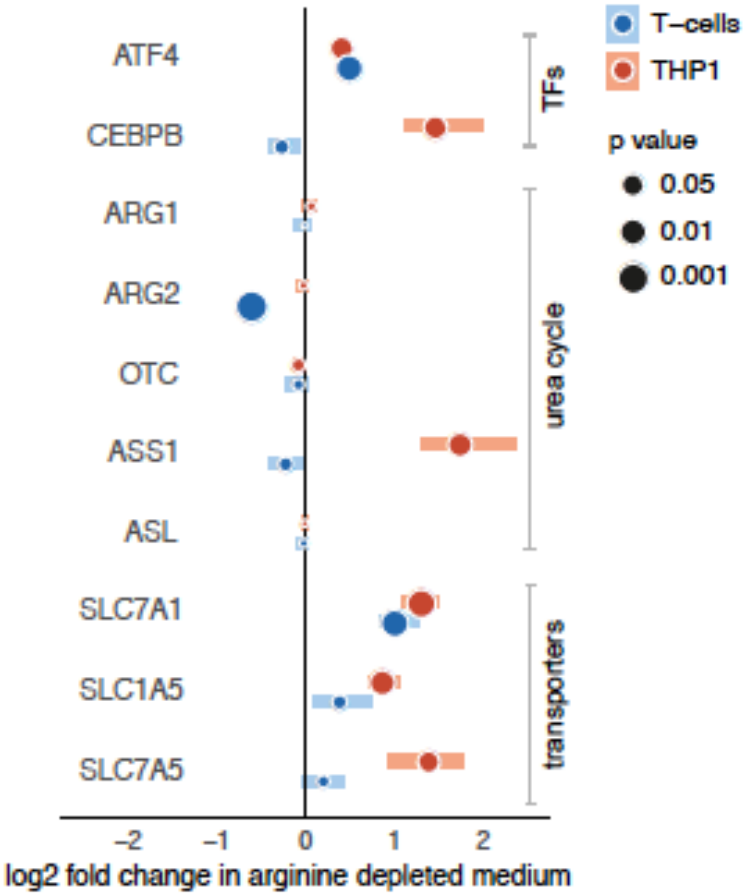



**Figure 4 - 4. Forest plot showing changes of expression of key genes involved in arginine uptake and metabolism.**
In terms of transcription factors, ATF4 is upregulated to a similar extent in THP1 cells (red) and T-cells (blue) whereas its binding partner CEBPβ is significantly upregulated in THP1 cells but not T-cells. Arginase-1 (ARG1), Arginase-2 (ARG2), ornithine transcarbamylase (OTC) and argininosuccinate lyase (ASL), genes involved in the urea-ammonia cycle (which forms part of arginine de novo synthesis and metabolism) are not upregulated in either of the two cell types in response to arginine starvation. Argininosuccinate synthase (ASS1) was the only gene involved in the ammonia-urea cycle that was upregulated in response to arginine starvation and this was only in THP1 cells but not T-cells. ASS1 is the enzyme controlling the rate-limiting step in the ammonia-urea cycle where citrulline is eventually converted to arginine. Amino acid transporters SLC7A1 (CAT1), SLC1A5 (ASCT2) and SLC7A5 (LAT1) were upregulated in both cell types although the upregulation of the latter two was significantly higher in THP1 cells than T-cells. Data points represent mean log2-fold change in gene expression with 95% confidence interval and associated p-values to denote statistical significance of results with experiments done in triplicate.

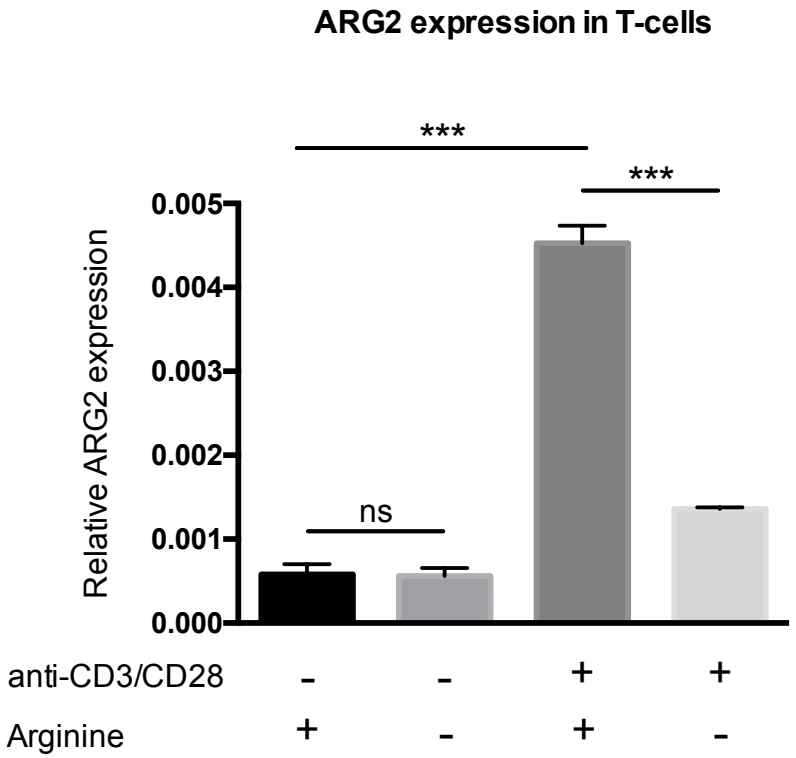



**Figure 4 - 5. Stimulated T-cells downregulate the expression of ARG2 in response to arginine to starvation.**
qRT-PCR shows that non-activated T-cells do not alter their ARG2 gene expression when deprived of arginine. However, stimulated T-cells significantly downregulate ARG2 expression in response to arginine starvation. Additionally, in environments of normal arginine levels, activation of T-cells induces significant ARG2 upregulation. *** $p<0.001$, ns means non-significant. Bars represent mean with standard deviation derived from measurements done in triplicate.

## 4.4 ASS1 is upregulated in response to arginine starvation in cancer cells but not T-cells although an ATF4-based response is mounted in both cell types

Amongst the enzymes involved in the urea cycle and arginine biosynthesis, ASS1 was amongst the most significantly upregulated in cancer cells but not T-cells upon arginine deprivation **(Figure 4-4)**. Given that ASS1 catalyses one of the rate-limiting steps in the urea cycle, converting ornithine/citrulline to arginine, its upregulation may permit cancer

cells to synthesize arginine de novo, conferring a survival advantage over immune cells in arginine-starved microenvironments **(Figure 4-6)**. We did not detect statistically significant changes in the expression of ornithine transcarbamoylase (OTC) or argininosuccinate lyase (ASL) in either cell type **(Figure 4-4)**, suggesting that ASS1 might indeed be the limiting factor for de novo arginine synthesis.

In line with our microarray findings, we observed upregulation of ASS1 at RNA and protein levels in response to arginine deprivation by qRT-PCR and fluorescent western blotting, respectively ($p<0.0001$ for both) **(Figures 4-7A, 4-8, 4-9)**. This upregulation was limited to THP1 cancer cells, as levels of ASS1 RNA and protein remained significantly lower and unchanged in T-cells ($p>0.05$ for both) **(Figures 4-7A, 4-8)**. Crucially, this was not due to the inability of T-cells to respond to arginine depletion, as ATF4, the key transcription factor in the response to amino acid starvation, was upregulated to similar levels in THP1 and T-cells confirming our microarray findings ($p<0.001$ for both THP1 and T-cells at both RNA and protein levels) **(Figures 4-3, 4-7B, 4-8)**.

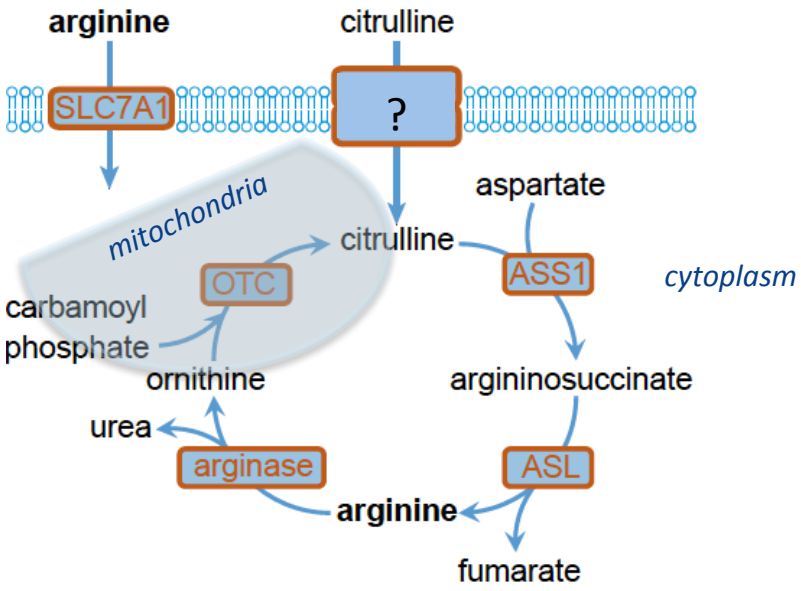



**Figure 4 - 6. Schematic diagram showing the roles of key genes in arginine uptake and metabolism.**

Arginine can be taken up by cells from the extracellular space through arginine transmembrane transporters such as SLC7A1. It can also be synthesized *de novo* within cells as part of the ammonia-urea cycle where citrulline is converted to arginine by the sequential action of ASS1 and ASL. Arginine itself can then be recycled to citrulline via the ornithine intermediate by the sequential actions of Arginase and OTC enzymes. Ornithine enters the mitochondria to be converted by OTC to citrulline, which then exits into the cytoplasm to re-join the urea cycle. There is also speculation that citrulline can be taken up into cells from the extracellular space by means of citrulline-selective transmembrane transporters, a hypothesis that we address later in this work.

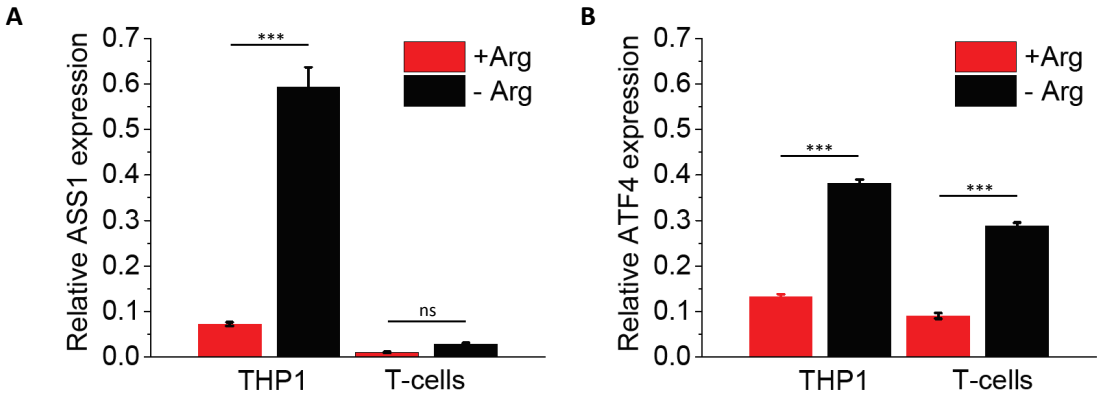



**Figure 4 - 7. Arginine starvation induces upregulation of ASS1 RNA only in THP1 cells but upregulation of ATF4 RNA in both THP1 and T-cells.**
qRT-PCR analysis in the presence (red) and absence (black) of arginine (over 72hr) shows that (A) ASS1 gene expression is significantly upregulated in THP1 cells but not T-cells. In contrast, (B) ATF4 gene expression is upregulated significantly in both cell types. Interestingly baseline levels of ASS1 are also higher in THP1 than T-cells. *** $p<0.001$, ns means non-significant. Bars represent mean with standard deviation derived from triplicate measurements relative to expression of the housekeeping gene GAPDH.

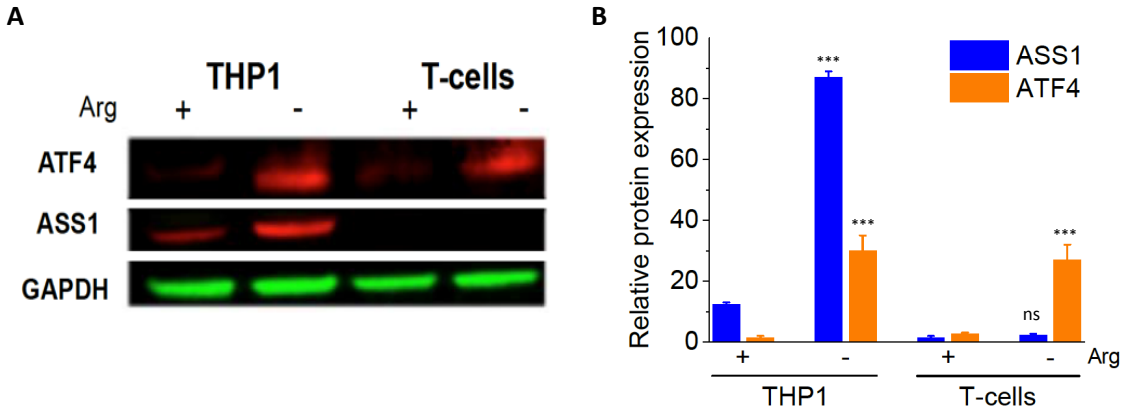



**Figure 4 - 8. Arginine starvation induces upregulation of ASS1 protein only in THP1 cells but upregulation of ATF4 protein in both THP1 and T-cells.**
(A) Fluorescent western blotting (WB) confirms that, similar to RNA levels, ASS1 protein levels increase upon arginine starvation in THP1 cells but not T-cells. This is not due to lack of sensing the lack of arginine since ATF4 protein levels are upregulated in both THP1 and T-cells. (B) Protein levels obtained from fluorescent WB were normalized against the housekeeping protein GAPDH and plotted to confirm that the upregulation of ASS1 (blue) and ATF4 (yellow) in THP1 cells in response to arginine starvation is significant. In T-cells, only ATF4 protein levels were upregulated significantly whereas ASS1 protein levels showed no change. *** $p<0.001$, ns means non-significant. Bars represent mean with standard deviation derived from measurements done in triplicate.

## 4.5 ASS1 is required for citrulline metabolism to promote cancer cell growth in the absence of arginine

In order to test the functional implications of this discrepancy in ASS1 upregulation, we measured cell proliferation under conditions of arginine starvation. Whilst neither THP1 nor T-cells were able to grow in the absence of arginine, supplementing arginine-depleted medium with exogenous citrulline (0.2mM) restored a normal growth rate for THP1 cells ($p<0.0001$ vs control; Figure 4-9A). In contrast, the growth arrest of T-cells induced by arginine depletion was unaffected by the addition of citrulline ($p>0.05$ vs control; Figure 4-9B). This suggests that THP1 cells may exploit ASS1 upregulation in response to arginine depletion to recycle extracellular citrulline and use it as a substrate for *de novo* synthesis of arginine, a phenomenon that does not occur in T-cells.

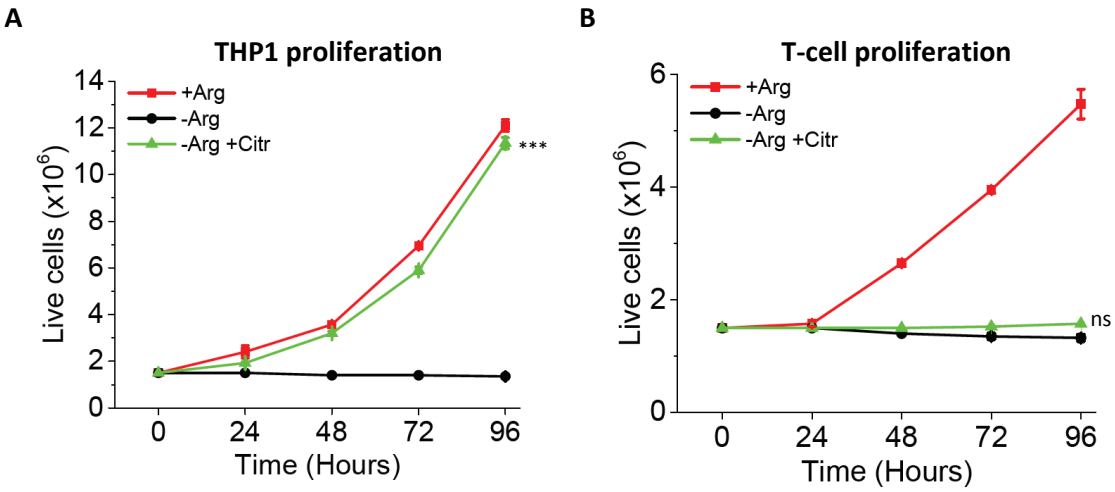



**Figure 4 - 9. THP1 cells can use citrulline as an alternative arginine source and can thus proliferate in arginine-free conditions whereas T-cells fail to do so.**
In vitro growth curves show that neither (A) THP1 cancer cells nor (B) T-cells can proliferate in the absence of arginine (black) whereas normal proliferation occurs when the cells are cultured in full R10 medium for 96hr (red). Interestingly, medium supplementation with exogenous citrulline allowed THP1 cancer cells, but not T-cells, to proliferate to levels similar to baseline despite the lack of arginine in the medium (green). This suggests that cancer cells can utilize citrulline to synthesize arginine de novo, an ability not shared by T-cells, perhaps due to the lack of ASS1 upregulation. Statistical comparisons were made between conditions of -Arg +Citr vs conditions of -Arg; *** $p<0.001$, ns means non-significant. Data points represent mean with standard deviation derived from measurements done in triplicate.

## 4.6 Arginine starvation does not induce ASS1 upregulation in monocytes suggesting that ASS1 upregulation in THP1 cells is a cancer-specific rather than a lineage-specific effect

In order to identify the origins of this discrepancy and decide whether this is a lineage effect (monocytic vs lymphocytic) or a cancer-related effect (transformed cancerous vs healthy) we tested primary monocytes/macrophages from healthy donors (with help from Dr Mashiko Setshedi). By MACS-enriching for CD14+ cells in PBMC from healthy controls and culturing these cells with M-CSF in full or arginine-depleted medium, we

showed that unlike THP1 cancer cells, healthy monocytes (differentiating towards macrophages) were significantly less able to upregulate ASS1 upon arginine starvation but more importantly, they already had much lower baseline levels of ASS1 compared to THP1 cells, thus mimicking the behaviour of healthy T-cells **(Figure 4-10)**. This finding argues against a lineage effect and in favour of the discrepancy being the result of cancer cells gaining an advantageous ability to adapt to their environment following their transformation.

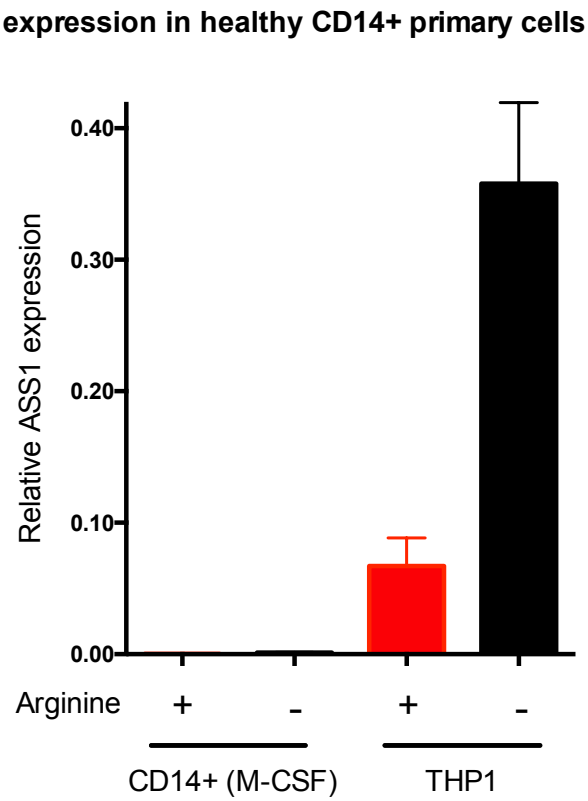



**Figure 4 - 10. Arginine starvation does not induce upregulation of ASS1 RNA in CD14+ monocytes unlike THP1 cells suggesting this is a cancer-specific rather than a lineage-specific effect.**
qRT-PCR analysis in the presence (red) and absence (black) of arginine (over 48hr) shows that ASS1 gene expression is significantly upregulated in THP1 cells ($p<0.0001$) but not primary CD14+ monocytes ($p>0.05$). Interestingly baseline levels of ASS1 are also higher in THP1 than CD14+ monocytes/macrophages. Bars represent mean with standard deviation derived from triplicate measurements relative to expression of the housekeeping gene GAPDH.

## 4.7 Analysis of the ASS1 upregulation kinetics

We evaluated the kinetics of ASS1 upregulation to show that the protein levels increase continuously to reach a maximum level between 72-96hrs **(Figure 4-11A)**. We also showed that the addition of exogenous citrulline even in the presence of arginine, can partially enhance ASS1 upregulation to a certain extent **(Figure 4-11B)**. This suggests that there is a substrate-induction and a product-inhibition effect by citrulline and arginine respectively, that regulates the levels of ASS1 in cancer cells.

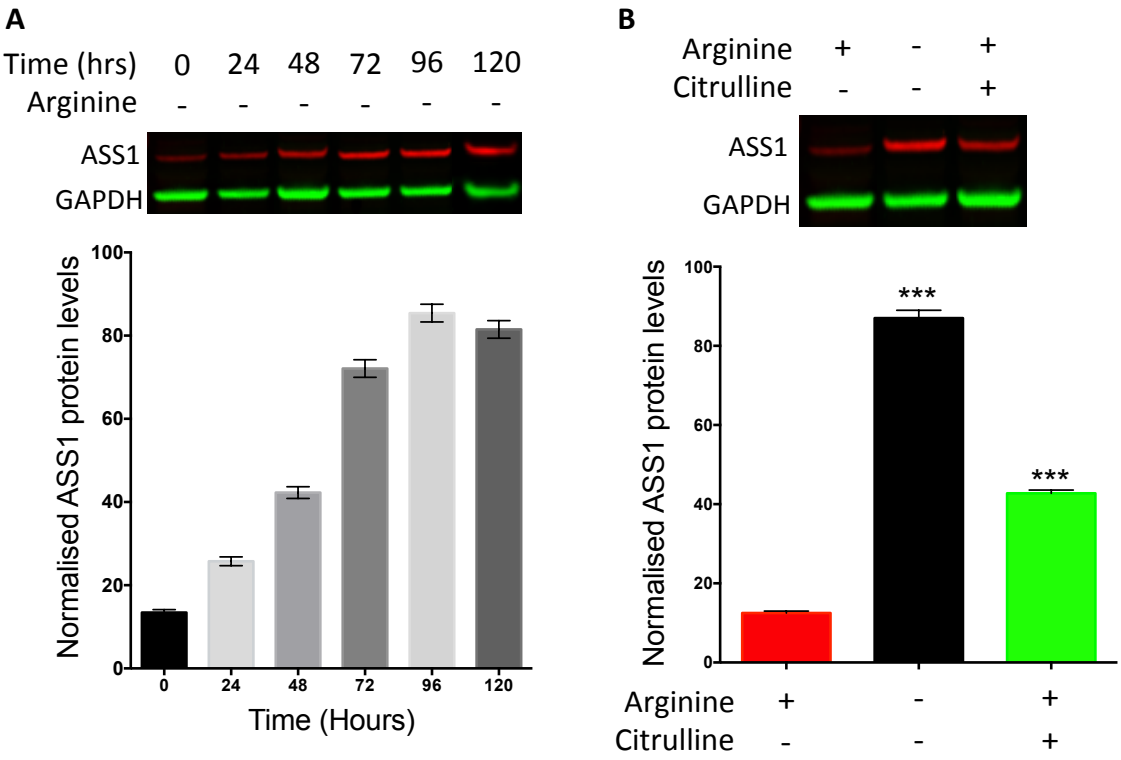



**Figure 4 - 11. ASS1 protein levels in THP1 cells increase with time to a maximum at 96hr after exposure to arginine starvation whereas the presence of citrulline can partially drive ASS1 expression even in sufficient arginine levels.**
(A) Fluorescent western blotting (WB) shows that ASS1 protein levels increase upon arginine starvation in THP1 cells to reach a maximum amount at 96hr post induction, a result confirmed by plotting normalized protein levels at different time points. (B) Fluorescent WB and normalized protein level plotting shows that, in THP1 cells, ASS1 protein is upregulated by the absence of arginine, an indirect ASS1 product (black). It also seems that ASS1 expression is also partially driven by its substrate citrulline, as even when

arginine is sufficient, the levels of ASS1 do not go down to baseline (red) when citrulline is also present (green). This suggests that the enzyme is tightly regulated to ensure a specific range of arginine maintained to avoid both deficit and excess. Protein levels obtained from fluorescent WB were normalized against the housekeeping protein GAPDH. Statistical comparisons were made against the condition of sufficient arginine without citrulline; *** $p<0.001$. Bars represent mean with standard deviation derived from measurements done in triplicate.

## 4.8 Treatment with Arginase-2 has similar transcriptional and translational effects in THP1 cancer cells as their exposure to arginine starvation

In order to link our latest findings to the clinical observations made in Chapter 3, we cultured THP1 cells in complete medium and treated them with rhARG2 for 72 hrs. The key transcriptional changes upon arginine deprivation, observed in THP1 cells were recapitulated by culturing cells in the presence of rhARG2, including the upregulation of SLC7A1 (CAT1), SLC7A5 (LAT1), ASS1 and ATF4 **(Figure 4-12)**.

Importantly, citrulline was still also able to rescue the growth arrest of THP1 cells induced by the addition of rhARG2 to the medium, confirming that the effects we observed following arginine depletion were representative of those produced by physiological loss of arginine **(Figure 4-13A)**. We confirmed by western blotting that ASS1 was upregulated at the protein level by rhARG2 treatment, allowing THP1 cells to utilize exogenous citrulline **(Figure 4-13B)**.

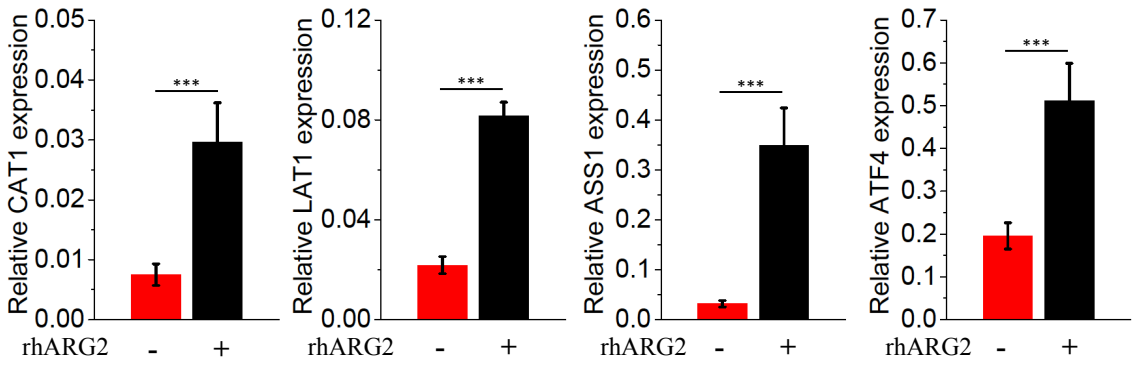



**Figure 4 - 12. Arginine-starvation-induced upregulation of ASS1, ATF4, SLC7A1 and SLC7A5 in THP1 cells is recapitulated by incubation of cells with recombinant human Arginase-2 (rhARG2).**
qRT-PCR analysis in the presence (black) and absence (red) of rhARG2 (after 72hr) shows that, similar to arginine starvation conditions, *ASS1, ATF4, CAT1* and *LAT1* gene expression is significantly upregulated in THP1 cells (*** $p<0.0001$). This suggests that 72hr treatment with rhARG2 causes sufficient arginine depletion to induce the genetic reprogramming in cancer cells. Bars represent mean with standard deviation derived from triplicate measurements relative to expression of the housekeeping gene *GAPDH*.

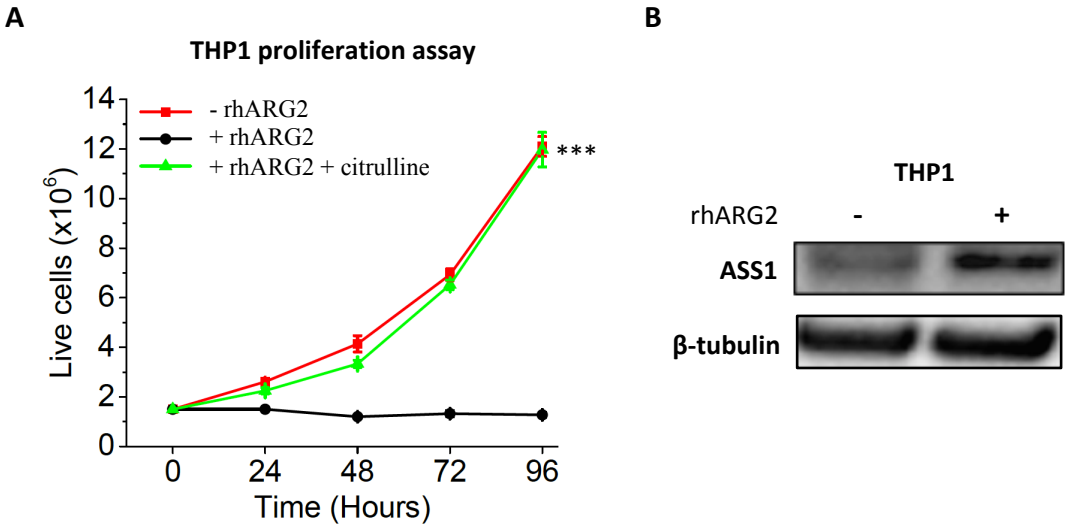



**Figure 4 - 13. THP1 cells display elevated ASS1 protein levels upon incubation of with rhARG2 and can thus utilize exogenous citrulline and proliferate despite rhARG2-induced arginine depletion in culture.**
(A) *In vitro* growth curves show that neither THP1 cancer cells cannot proliferate in the presence of rhARG2 (black) whereas normal proliferation occurs when the cells are cultured in full R10 medium without rhARG2 for 96hr (red). Medium supplementation with exogenous citrulline allowed THP1 cancer cells to proliferate to levels similar to baseline despite the presence of rhARG2 in the medium (green). Western blotting shows that treatment with rhARG2 induces significant ASS1 protein upregulation (relative to housekeeping protein β-tubulin). These results suggest that the effects of rhARG2-induced arginine depletion on cancer cells can be overcome by ASS1-mediated utilization of

exogenous citrulline to synthesize arginine *de novo*. For growth curves, data points represent mean with standard deviation derived from measurements done in triplicate and statistical comparisons were made between conditions of -Arg +Citr vs conditions of –Arg where *** denotes $p<0.001$.

## 4.9 ASS1 upregulation in response to arginine starvation is an effect that occurs globally in multiple cancer cell lines

In addition to THP1 cells, we observed a similar (albeit variable) arginine starvation-induced upregulation of ASS1 in other cell lines representative of multiple liquid and solid cancers, including HeLa (cervical cancer; **Figure 4-14A**), LNCaP (prostate cancer; **Figure 4-14B**), RT112 (bladder cancer; **Figure 4-15**), OCI-AML (AML; **Figure 4-16A**), MOLM-13 (AML; **Figure 4-16B**), HL-60 (APML; **Figure 4-16C**) and NB-4 cells (APML; **Figure 4-17**), demonstrating that this is not a THP1- or AML-specific response and may in fact form a more global mechanism for cancer immune evasion. ASS1 upregulation was statistically significant in all cases ($p<0.001$) and consequently all aforementioned cell lines were able to recycle citrulline to arginine and thus proliferate in arginine-depleted medium ($p<0.001$ vs no arginine control in all cases).

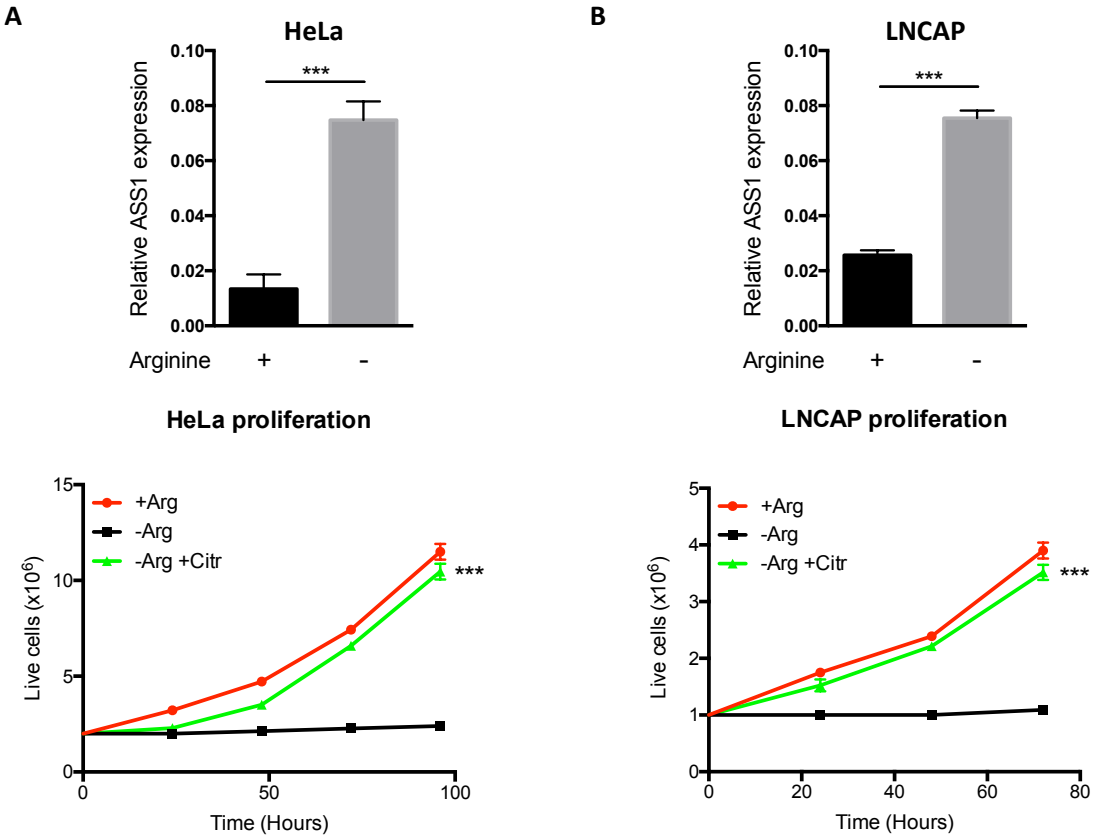



**Figure 4 - 14. ASS1 upregulation upon arginine depletion is also observed in human solid tumour cell lines, such as HeLa (cervical cancer) and LNCAP (prostate cancer), where it allows cancer cells to utilise citrulline and proliferate in the absence of arginine.**

qRT-PCR analysis (top panels) in the presence (black) and absence (grey) of arginine (after 72hr) shows that *ASS1* gene expression is significantly upregulated in (A) HeLa (cervical) and (B) LNCAP (prostate) cancer cells. *In vitro* growth curves (bottom panels) show that similar to THP1 cancer cells, both (A) HeLa and (B) LNCAP cells fail to proliferate in the absence of arginine (black) but can utilize exogenous citrulline to proliferate despite the lack of arginine in the culture medium (green) achieving similar growth levels as in the presence of arginine (red). For qRT-PCR data, bars represent mean with standard deviation derived from triplicate measurements relative to expression of the housekeeping gene *GAPDH*. For growth curves, data points represent mean with standard deviation derived from measurements done in triplicate and statistical comparisons were made between conditions of -Arg +Citr vs conditions of –Arg. *** denotes $p<0.001$.

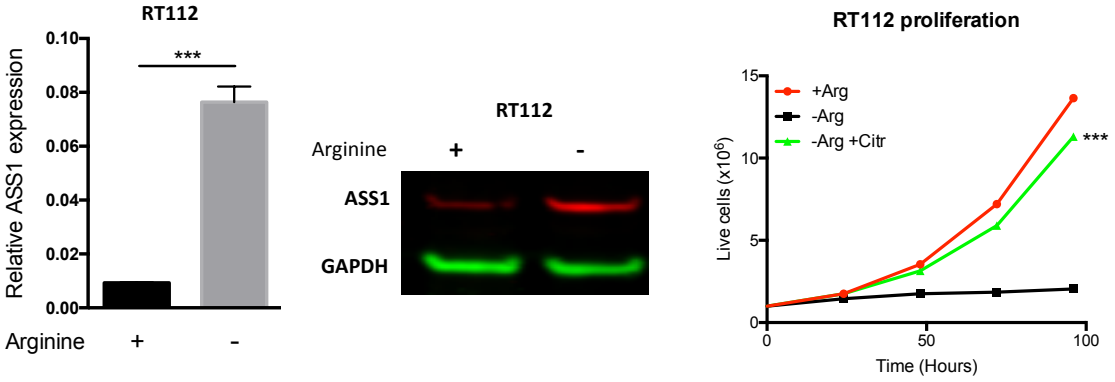



**Figure 4 - 15. ASS1 upregulation, at gene and protein level, upon arginine depletion is also observed in the human bladder cancer cell line RT112, where it allows cancer cells to utilise citrulline and proliferate in the absence of arginine.**
qRT-PCR analysis (left panel) and fluorescent western blotting (middle panel) show that ASS1 is significantly upregulated both at RNA and protein level in RT112 (bladder) cancer cells in response to arginine starvation for 72hr. *In vitro* growth curves (right panel) show that RT112 cells fail to proliferate in the absence of arginine (black) but can utilize exogenous citrulline to proliferate despite the lack of arginine in the culture medium (green) achieving similar growth levels as in the presence of arginine (red). For qRT-PCR data, bars represent mean with standard deviation derived from triplicate measurements relative to expression of the housekeeping gene *GAPDH*. For growth curves, data points represent mean with standard deviation derived from measurements done in triplicate and statistical comparisons were made between conditions of -Arg +Citr vs conditions of –Arg. *** denotes $p<0.001$.

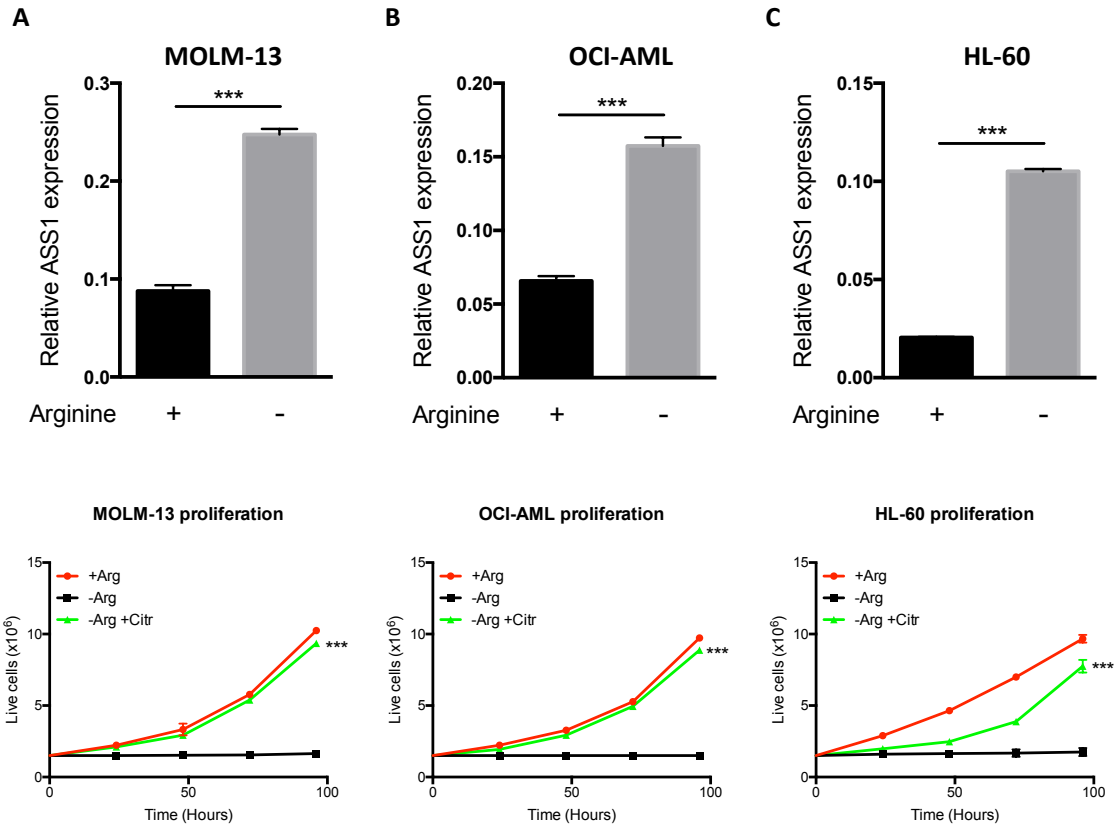



**Figure 4 - 16. ASS1 upregulation upon arginine depletion is also observed in various human leukaemic cell lines, such as MOLM-13 (AML), OCI-AML (AML) and HL-60 (APML) where it allows cancer cells to utilise citrulline and proliferate in the absence of arginine.**

qRT-PCR analysis (top panels) in the presence (black) and absence (grey) of arginine (after 72hr) shows that *ASS1* gene expression is significantly upregulated in (A) MOLM-13 (AML), (B) OCI-AML (AML) and (C) HL-60 (APML) cancer cells. *In vitro* growth curves (bottom panels) show that similar to THP1 cancer cells, both (A) MOLM-13 (AML), (B) OCI-AML (AML) and (C) HL-60 (APML) fail to proliferate in the absence of arginine (black) but can utilize exogenous citrulline to proliferate despite the lack of arginine in the culture medium (green) achieving similar growth levels as in the presence of arginine (red). For qRT-PCR data, bars represent mean with standard deviation derived from triplicate measurements relative to expression of the housekeeping gene *GAPDH*. For growth curves, data points represent mean with standard deviation derived from measurements done in triplicate and statistical comparisons were made between conditions of -Arg +Citr vs conditions of –Arg. *** denotes $p<0.001$.

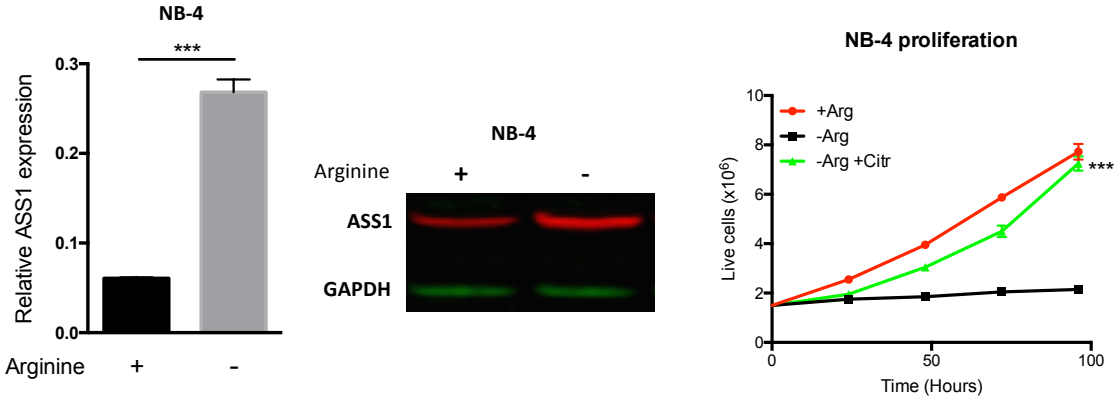



**Figure 4 - 17. ASS1 upregulation, at gene and protein level, upon arginine depletion is also observed in the human acute promyelocytic leukaemia (APML) cell line NB-4, where it allows cancer cells to utilise citrulline and proliferate in the absence of arginine.**
qRT-PCR analysis (left panel) and fluorescent western blotting (middle panel) show that ASS1 is significantly upregulated both at RNA and protein level in NB-4 (APML) cancer cells in response to arginine starvation for 72hr. *In vitro* growth curves (right panel) show that NB-4 cells fail to proliferate in the absence of arginine (black) but can utilize exogenous citrulline to proliferate despite the lack of arginine in the culture medium (green) achieving similar growth levels as in the presence of arginine (red). For qRT-PCR data, bars represent mean with standard deviation derived from triplicate measurements relative to expression of the housekeeping gene *GAPDH*. For growth curves, data points represent mean with standard deviation derived from measurements done in triplicate and statistical comparisons were made between conditions of -Arg +Citr vs conditions of –Arg. *** denotes $p<0.001$.

## 4.10 Citrulline uptake in THP1 cancer cells is dependent on the SLC7A5 (LAT1) and SLC1A5 amino acid transporters

In our initial microarray, expression of several transporter proteins was observed to be upregulated upon arginine depletion in both THP1 and T-cells, including the cationic amino acid transporter SLC7A1 (CAT1; the major arginine importer), suggesting that a common response to arginine depletion is to enhance the import of arginine from the extracellular environment. Additionally, SLC7A5 (LAT1) and SLC1A5 showed much stronger upregulation in THP1 than in T-cells **(Figure 4-4)**. This discrepancy, combined with the fact that SLC7A5 and SLC1A5 preferentially facilitate movement of neutral

amino acids, prompted us to consider the possibility that these transporters may be required for import of citrulline. We therefore firstly confirmed the significant upregulation of SLC7A5 (LAT1) ($p<0.0001$) and SLC1A5 ($p<0.0001$) in THP1 cells upon arginine depletion by qRT-PCR **(Figure 4-18A)**. We subsequently used specific small molecule inhibitors of these transporters to test their role in cell proliferation of cancer cells in the absence of arginine **(Figure 4-18B)**. Treatment with BCH, a competitive inhibitor of SLC7A5 (LAT1), showed a moderate reduction in THP1 growth in citrulline-supplemented arginine-depleted medium, as did treatment with the SLC1A5 inhibitor GPNA **(Figure 4-18B top right & bottom left panels)**. Notably, co-treatment with BCH and GPNA resulted in a stronger, but not complete, growth inhibition, suggesting that both transporters are important in citrulline uptake and thus promote cell growth in the absence of arginine **(Figure 4-18B, bottom right panel)**. However, inhibition of these transporters did not have such a strong effect on growth in the presence of arginine, suggesting that they are not required for import of arginine itself, and that the detrimental effect observed was at least partially attributable to lack of citrulline import.

We confirmed these results in WT HeLa cells, where we showed that SLC7A5 (LAT1) was upregulated upon arginine depletion **(Figure 4-19A)** and its knockout reduced citrulline-dependent proliferation in the absence of arginine **(Figure 4-19B)**. The SL7A5/LAT1 KO HeLa cells used in these experiments were a gift from Dr Hemza Ghadbane and Dr Elina Timosenko who had previously generated this cell line in our lab as described in the literature [301].

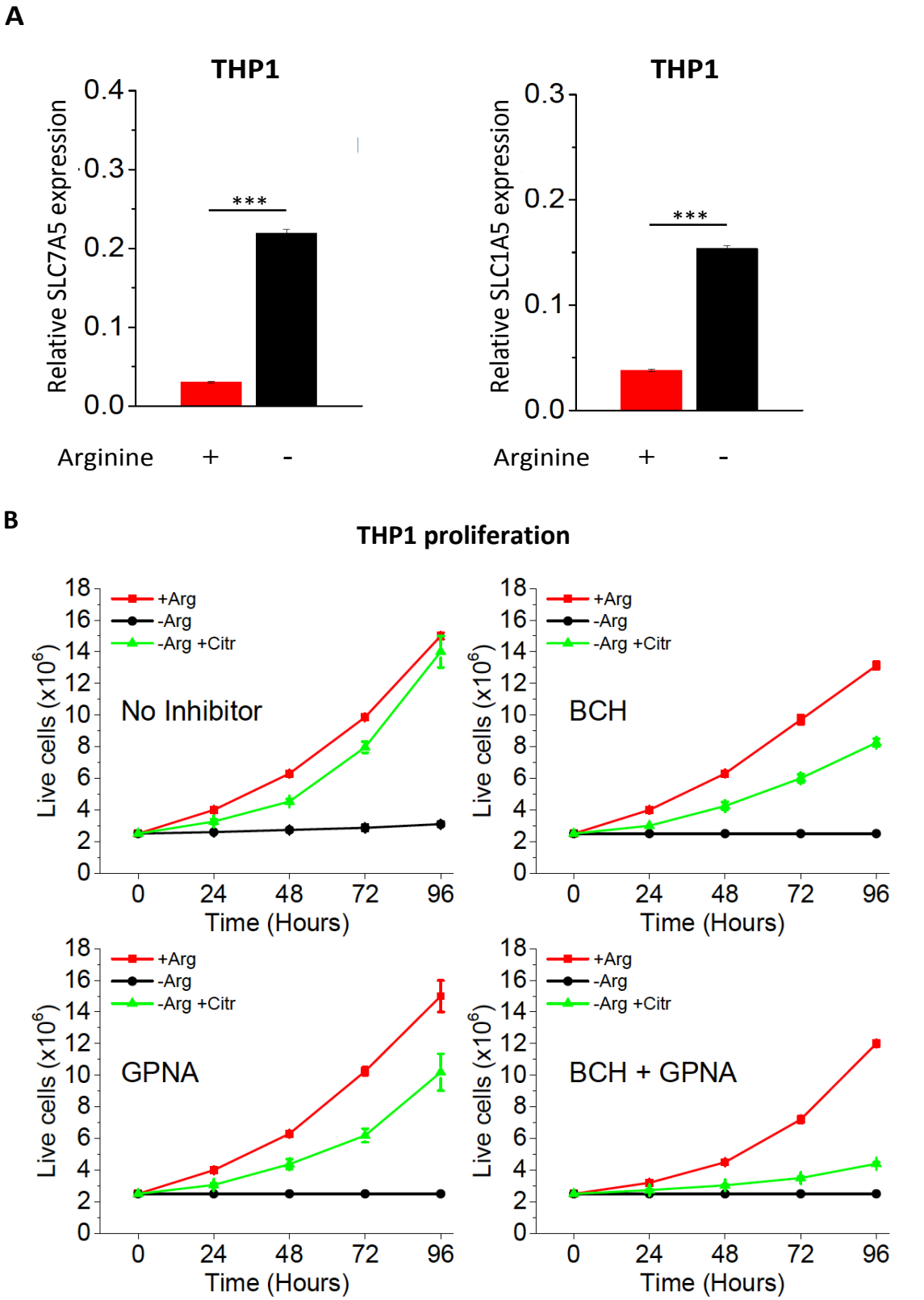



**Figure 4 - 18. Extracellular citrulline is imported into THP1 cancer cells through the transmembrane amino acid transporters SLC7A5 and SLC1A5, which are upregulated in response to arginine starvation.**
(A) qRT-PCR analysis shows that *SLC7A5* (left) and *SLC1A5* (right) are significantly upregulated at RNA level in THP1 cancer cells in response to arginine starvation. (B) *In*

*vitro* growth curves show that treatment of THP1 cells with the transporter inhibitors BCH (targeting SLC7A5; top right panel) or GPNA (targeting SLC1A5; bottom left panel) partially abrogates the ability of cancer cells for citrulline-dependent growth in arginine-free conditions (top left panel). Combining the two inhibitors together (bottom right panel) has a synergistic effect that almost completely abrogates the citrulline-dependent growth of THP1 cells. For qRT-PCR data, bars represent mean with standard deviation derived from triplicate measurements relative to expression of the housekeeping gene *GAPDH*. For growth curves, data points represent mean with standard deviation derived from measurements done in triplicate. *** denotes $p<0.001$.

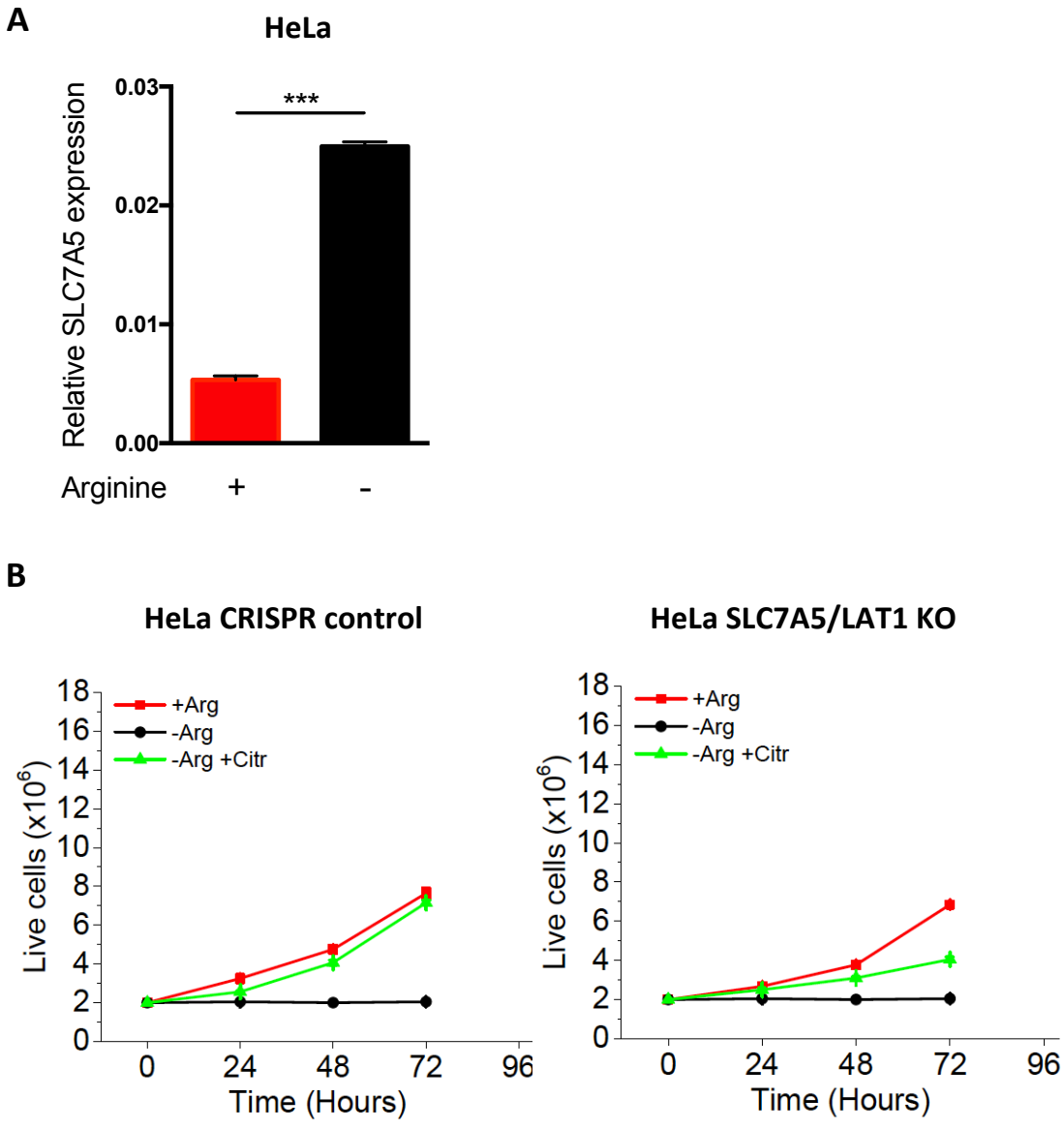



**Figure 4 - 19. Deletion of the SLC7A5 gene, which is upregulated in response to arginine starvation in HeLa cells, reduces the rate of citrulline-dependent cancer cell growth.**
(A) qRT-PCR analysis shows that *SLC7A5* is significantly upregulated at RNA level in HeLa cancer cells in response to arginine starvation (left panel). (B) *In vitro* growth curves

show that CRISPR *SLC7A5* KO in HeLa cells (right panel) partially abrogates the ability of cancer cells for citrulline-dependent growth in arginine-free conditions compared to CRISPR control cells (left panel). For qRT-PCR data, bars represent mean with standard deviation derived from triplicate measurements relative to expression of the housekeeping gene *GAPDH*. For growth curves, data points are representative of measurements done in triplicate. *** denotes $p<0.001$.

## 4.11 Uptake of extracellular citrulline is necessary for de novo arginine synthesis intracellularly by THP1 cancer cells

To demonstrate that exogenous citrulline was in fact imported by cancer cells and converted to arginine, we analysed intracellular arginine and citrulline levels in THP1 cells by liquid chromatography mass spectrometry (LC-MS) in collaboration with Dr Zhanru Yu and Prof Benedikt Kessler **(Figure 4-20)**. Depletion of arginine in the culture medium abolished the intracellular arginine peak observed by LC-MS from cells grown in complete medium, but this peak was restored in the presence of citrulline, despite the lack of arginine in the medium **(Figure 4-20, left panel)**. Intracellular citrulline was only detected in conditions of exogenous citrulline supplementation, indicating that the source of citrulline was the extracellular medium **(Figure 4-20, right panel)**.

In addition, we tried to follow the uptake and conversion of citrulline into arginine. Cells were treated in culture with exogenous heavy-labeled citrulline (L-[5-$^{13}$C; 99%, 4, 4, 5, 5, $^{2}H_2$; 95%] citrulline). We were able to detect a heavy-labelled citrulline signal in the intracellular fraction of these cells, followed by the appearance of a strong intracellular peak of heavy-labeled arginine ($^{13}$C, $^{2}H_2$-arginine) suggesting that citrulline was taken up and converted to arginine **(Figure 4-21, red)**. No such peak was observed in the absence of extracellular heavy-labelled citrulline **(Figure 4-21, green)**. This confirmed that in the

absence of arginine, THP1 cells are able to import citrulline for use in the de novo synthesis of arginine.

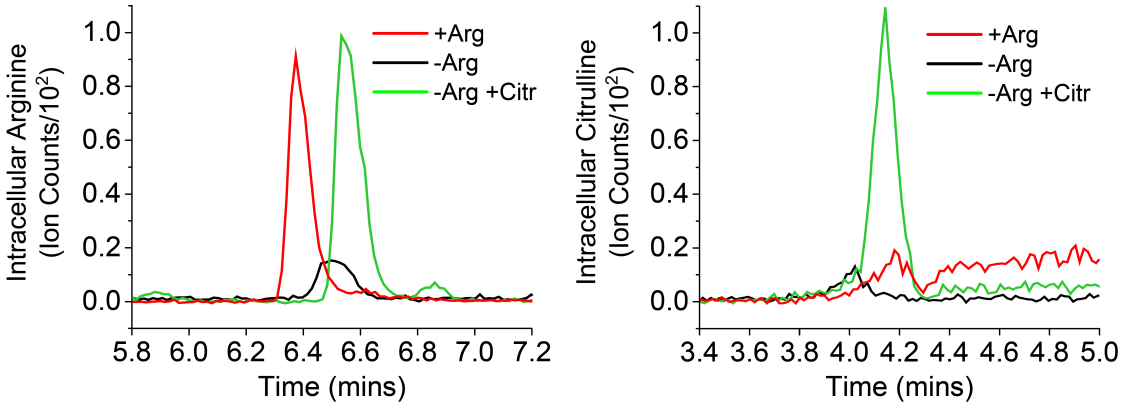



**Figure 4 - 20. Citrulline is taken up by THP1 cancer cells and in its presence, newly-formed arginine is detected intracellularly.**
Liquid chromatography-mass spectrometry (LC-MS) was used to measure the concentration of intracellular arginine (left panel) and intracellular citrulline (right panel) in THP1 cells cultured in arginine-sufficient medium (red), arginine-deficient medium (black) or arginine-deficient medium supplemented with 0.2mM of exogenous citrulline (green). Intracellular citrulline is only detected in the condition of arginine-deficient medium supplemented with exogenous citrulline whereas intracellular arginine is only detected in THP1 cells cultured in arginine-sufficient medium or arginine-deficient medium supplemented with exogenous citrulline. These results suggest that extracellular citrulline can be imported in THP1 cancer cells and, in response to arginine starvation, can be used intracellulary for *de novo* arginine synthesis. Data points are representative of measurements done in triplicate.

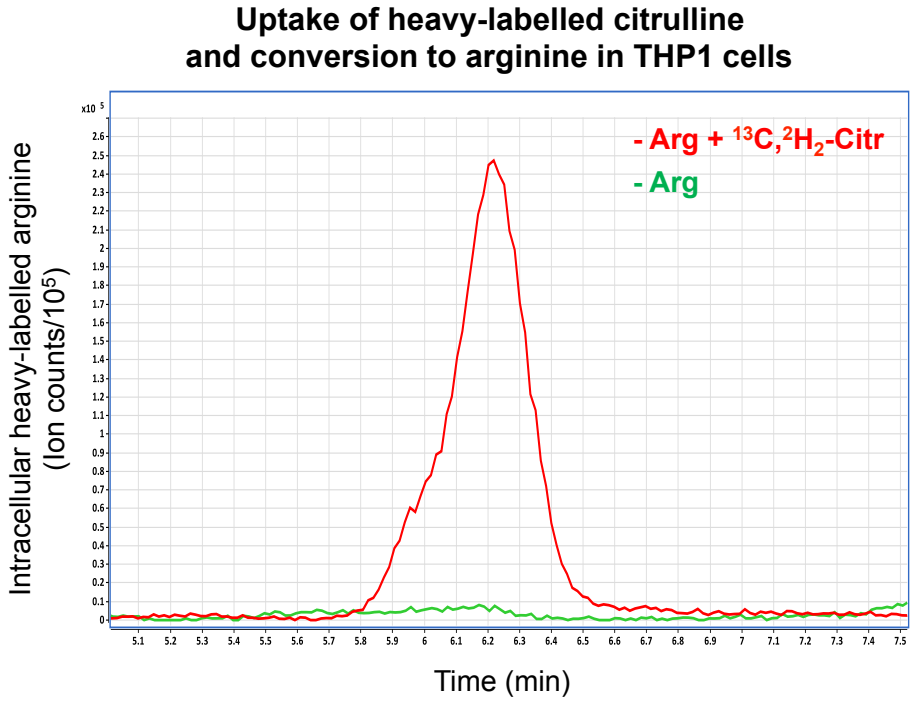



**Figure 4 - 21. In response to arginine starvation, citrulline is taken up by THP1 cancer cells and converted to *de novo* arginine intracellularly.**
Liquid chromatography-mass spectrometry (LC-MS) was used to detect the presence of any heavy-labelled $^{13}C$, $^{2}H_2$-arginine intracellularly in THP1 cells. Heavy-labelled arginine intracellulary was only detected, and in significant amounts, when arginine-deficient medium was supplemented with heavy-labelled $^{13}C$, $^{2}H_2$-citrulline (red) but not in the absence of citrulline supplementation (green). The 'transfer' of the heavy label from extracellular citrullien to intracellular arginine confirms our hypothesis that exogenous citrulline is imported into THP1 cells from the extracellular space and is then converted to arginine intracellularly, likely via the action of ASS1. Data points are representative of measurements done in triplicate.

## 4.12 Arginine deprivation also affects glucose metabolism in cancer cells by reversing the Warburg effect

Whilst arginine is clearly required for protein synthesis, we observed that arginine depletion also has a striking effect on cellular glucose metabolism. Incubation of THP1 cells in arginine-free medium seems to inhibit the Warburg effect, as it strongly reduces the rate of glycolytic activity (as measured by extracellular acidification rate; ECAR, $p<0.001$) and partially enhances the overall rate of mitochondrial respiration (as measured

by oxygen consumption rate; OCR) and specifically spare respiratory capacity, the difference between maximum and baseline OCR which denotes the potential bioenergetic reserve a cell can utilize at times of stress ($p<0.01$) **(Figures 4-22A and 4-23A)**. These effects were mirrored by inclusion of recombinant human Arginase-2 (rhARG2) in full medium **(Figures 4-22B and 4-23B)**. More importantly, the effects were reversed by the addition of exogenous citrulline ($p<0.001$ vs no arginine, $p>0.05$ vs full medium for glycolysis and $p<0.01$ vs no arginine, $p>0.05$ vs full medium for mitochondrial respiration/spare respiratory capacity), indicating that the metabolic changes are a direct result of low intracellular arginine levels. Overall, this argues that the advantageous effects of recycling citrulline to arginine in cancer cells may extend beyond protein synthesis by restoring normal tumour metabolism and facilitating cancer cells to utilise glycolysis rather than mitochondrial oxidative phosphorylation.

The reduction in glycolysis can be explained by the fact that key enzymes involved in this process were downregulated at the transcription level by arginine starvation (as observed in our differential gene expression microarray analysis), a common finding in THP1 and T-cells although much more prominent in the latter **(Figure 4-24)**. Key glycolysis genes that were downregulated under conditions of arginine depletion are the three regulatory enzymes that control rate-limiting steps in the sequence; Hexokinase (HK) that catalyses the first glycolysis step converting glucose to glucose-6-phosphate (GP), Phosphofructose kinase (PFK) and Pyruvate kinase (PK) that catalyses the last step. Other enzymes downregulated at the gene level (to various extents) include GP isomerase (PGI), Aldolase (ALDO), Triose-phosphate isomerase (TPI), glyceraldehyde 3-phosphate dehydrogenease (GAPDH), Phosphoglycerate kinase (PGK), Phosphoglycerate mutase (PGAM) and Enolase (ENO).

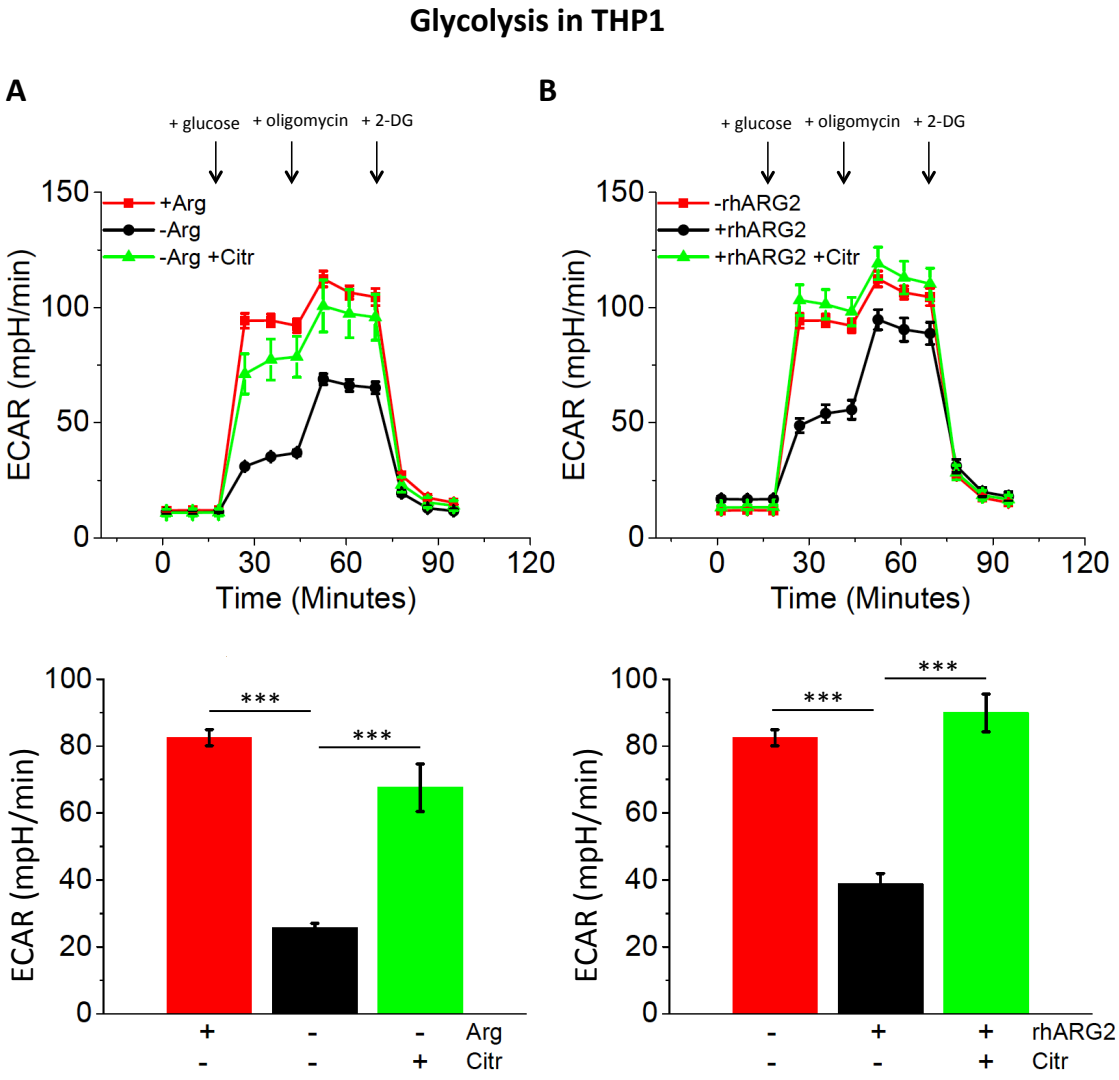



**Figure 4 - 22. Arginine starvation inhibits the glycolytic activity of cancer cells an effect that is reversed by citrulline supplementation.**
Seahorse experiments following a 72hr cell culture demonstrate the metabolic changes in glycolysis that occur in THP1 cancer cells under (A) arginine starvation or (B) incubation with rhARG2. (A) Metabolic profiling of extracellular acidification rate (ECAR; y-axis) over time (x-axis) and following sequential treatment with glucose (glycolysis fuel), oligomycin (ATP synthase inhibitor) and 2-deoxyglucose (2-DG; glycolysis inhibitor) shows that ECAR (a measure of glycolytic activity) is reduced in the absence of arginine (left panel; black line) or the presence of rhARG2 (right panel; black line) and can be restored to baseline levels (red line) by exogenous supplementation of medium with citrulline over 72hrs of cell culture. (B) Statistical analysis and plotting of data confirm that the absence of arginine (left panel; black bar) or the presence of rhARG2 (right panel; black bar) causes significant decrease in ECAR compared to baseline (presence of arginine and absence of rhARG2; red bar) an effect that is reversed by the presence of citrulline in the medium (green bar). Bars represent mean with standard deviation derived from a total of 30 biological replicates from three distinct experiments. *** denotes $p<0.001$.

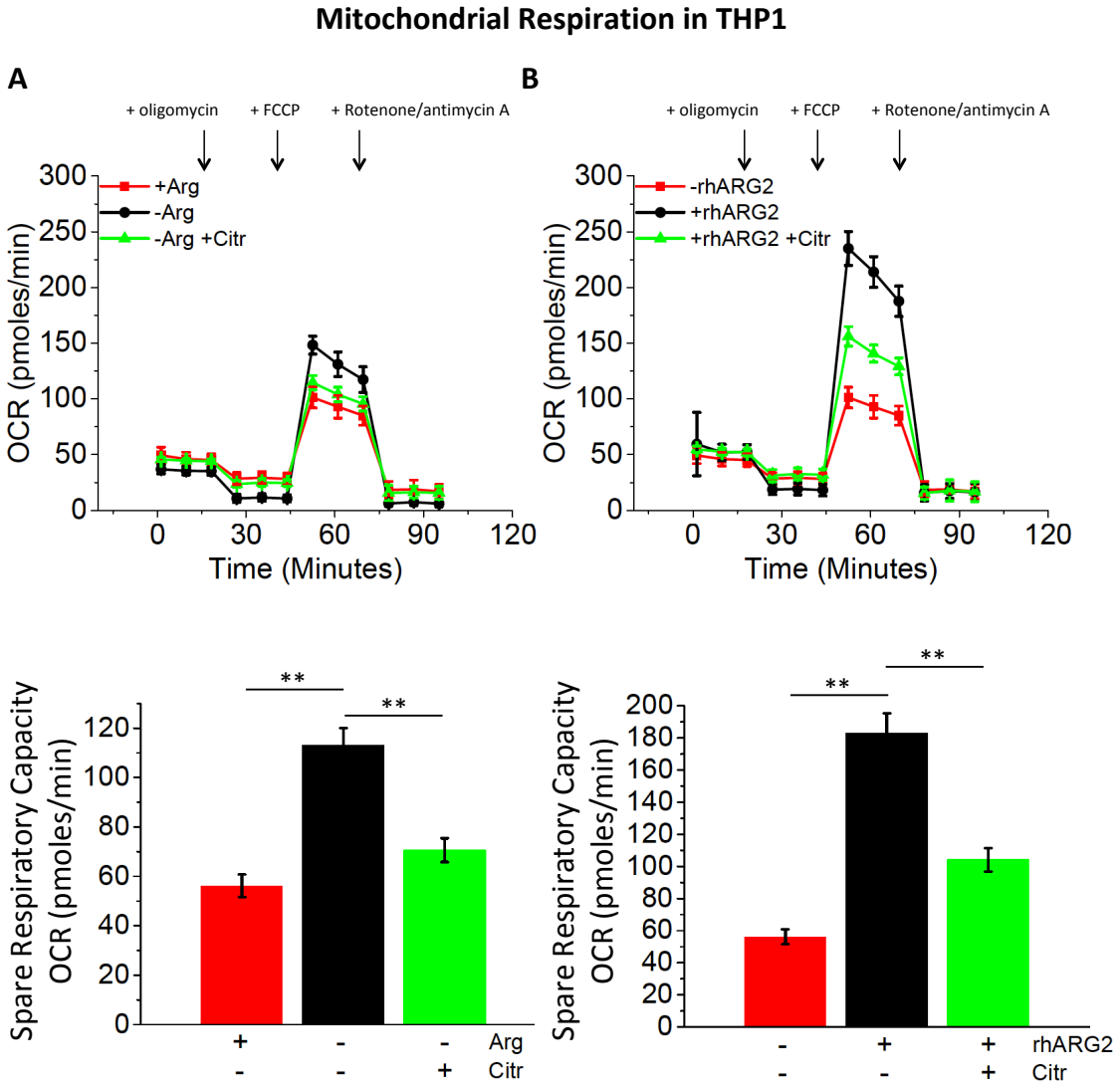



**Figure 4 - 23. Arginine starvation promotes mitochondrial respiration in cancer cells an effect that is reversed by citrulline supplementation.**
Seahorse experiments following a 72hr cell culture demonstrate the metabolic changes in mitochondrial function that occur in THP1 cancer cells under (A) arginine starvation or (B) incubation with rhARG2. (A) Metabolic profiling of oxygen consumption rate (OCR; y-axis) over time (x-axis) and following sequential treatment with oligomycin (ATP synthase inhibitor), FCCP (uncouples proton gradients) and rotenone/antimycinA (electron transport inhibitors) shows that OCR (a measure of mitochondrial respiration) is slightly enhanced in the absence of arginine (left panel; black line) or the presence of rhARG2 (right panel; black line) and can be, at least partially, restored to baseline levels (red line) by exogenous supplementation of medium with citrulline over 72hrs of cell culture. (B) Statistical analysis and plotting of data confirm that the absence of arginine (left panel; black bar) or the presence of rhARG2 (right panel; black bar) causes significant increase in OCR compared to baseline (presence of arginine and absence of rhARG2; red bar) an effect that is, at least partially, reversed by the presence of citrulline in the medium (green bar). Bars represent mean with standard deviation derived from a total of 30 biological replicates from three distinct experiments. ** denotes $p<0.01$.

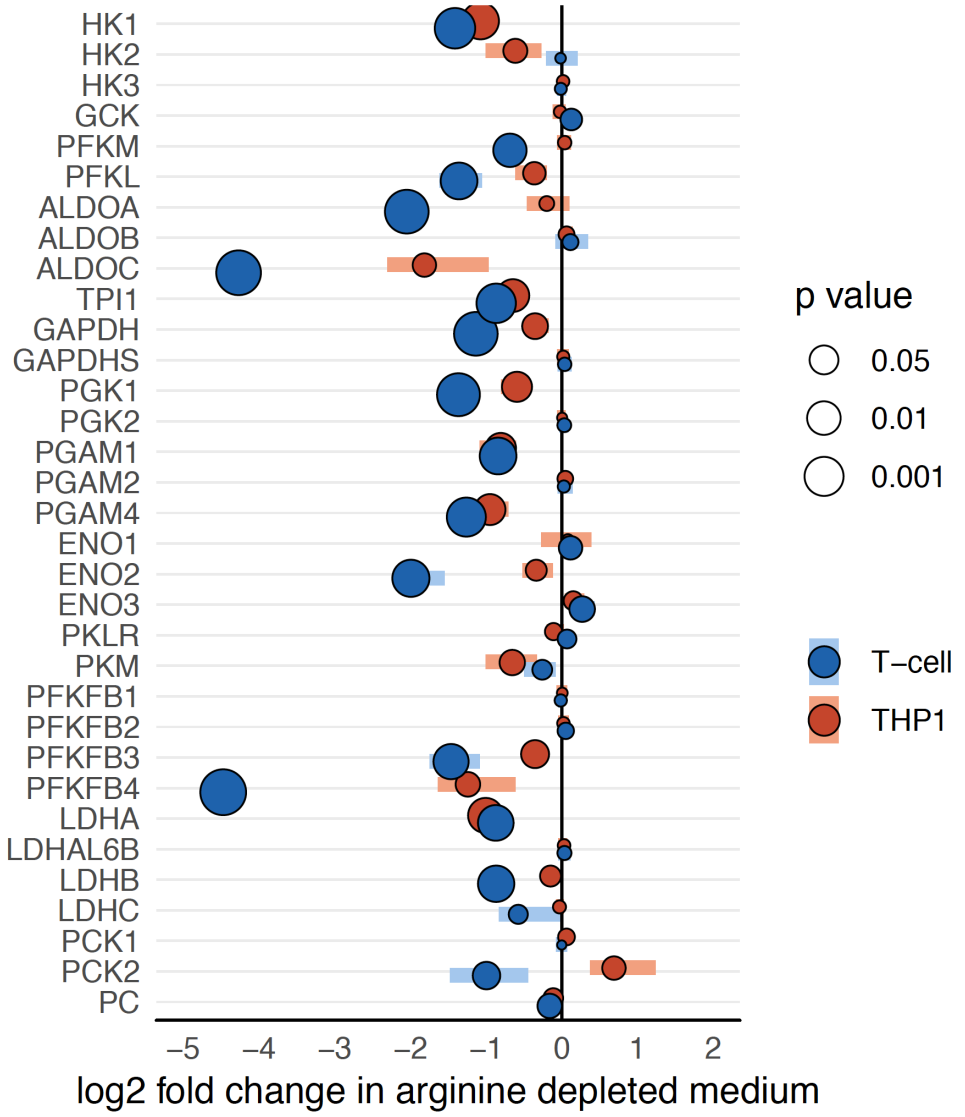



**Figure 4 - 24. Forest plot showing arginine starvation leads to downregulation in expression of key genes involved in the glycolysis and gluconeogenesis pathway in THP1 and T-cells.**
Although to different extents, the vast majority of key genes of the glycolysis pathway are downregulated in both THP1 (red) and T-cells (blue) at the RNA level in response to arginine starvation. Data points represent mean log2-fold change in gene expression with 95% confidence interval for experiments done in triplicate.

## 4.13 Upregulation of ATF4 and ASS1 to utilize extracellular citrulline is clinically relevant in the context of AML

### 4.13.1 ASS1 and ATF4 show higher expression in AML blasts compared to healthy myeloid cells

Having identified a role for ASS1 and ATF4 in the growth of cancer cells in arginine-depleted medium, we analysed their expression in primary AML blasts from patients using RNA-seq (in collaboration with Dr Lynn Quek), to demonstrate physiological and clinical relevance. We found both ATF4 and ASS1 to be significantly upregulated in AML blasts when compared to healthy controls **(Figure 4-25)**, consistent with the lower arginine levels in patient serum previously reported in our lab [367].

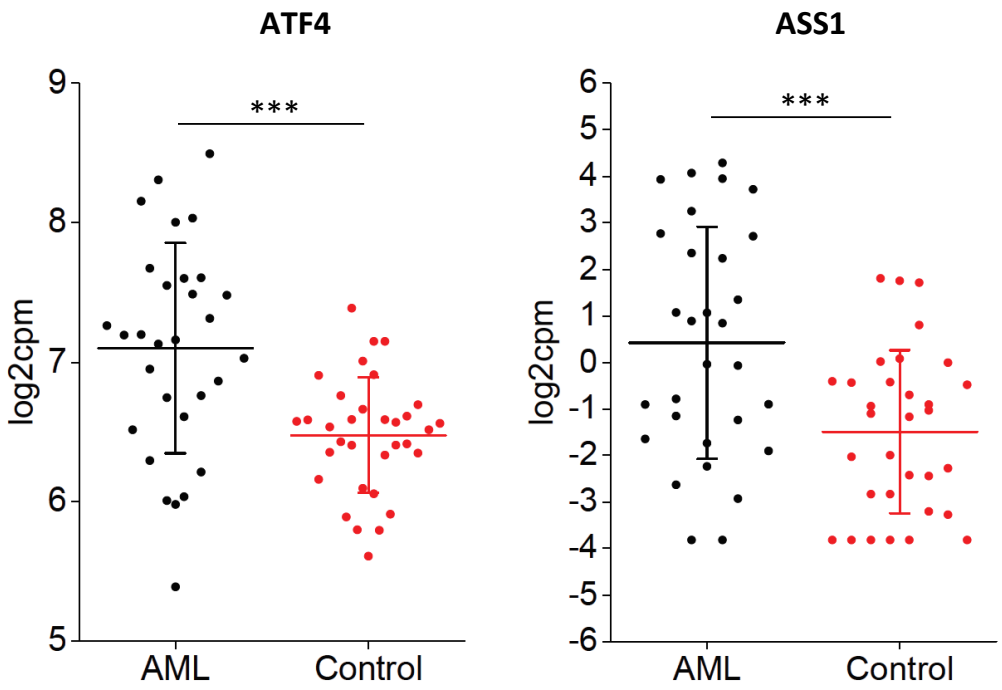



**Figure 4 - 25. ATF4 and ASS1 are overexpressed in AML blasts from patients compared to myeloid cell populations from healthy controls.**
RNA-seq analysis shows that both *ATF4* (left panel) and *ASS1* (right panel) are expressed at significantly higher levels in AML patient blasts (black) compared to myeloid cells from healthy individuals (red). Bars represent mean and standard deviation. *** $p < 0.001$.

### 4.13.2 Plasma citrulline levels are higher in AML patients compared to healthy controls

Strikingly, we found plasma citrulline levels to be significantly elevated in AML patients, from about 25 μM in healthy donors to 100-150 μM **(Figure 4-26A)**, a level, which we have shown to be permissive and sufficient for proliferation of THP1, cells in the absence of arginine **(Figure 4-26B)**. These findings suggest that ASS1 upregulation is a plausible mechanism to facilitate cancer cell growth in these patients as the citrulline present in the plasma of AML patients could be the source for the substrate of ASS1 and thus, de novo generation of arginine by the cancer cells. Additionally, our earlier finding that citrulline can still induce partial ASS1 expression even in the presence of sufficient arginine levels **(Figure 4-11B)** suggests that the increased plasma citrulline levels in AML patients can work in synergy with arginine starvation to drive ASS1 upregulation in AML blasts even further.

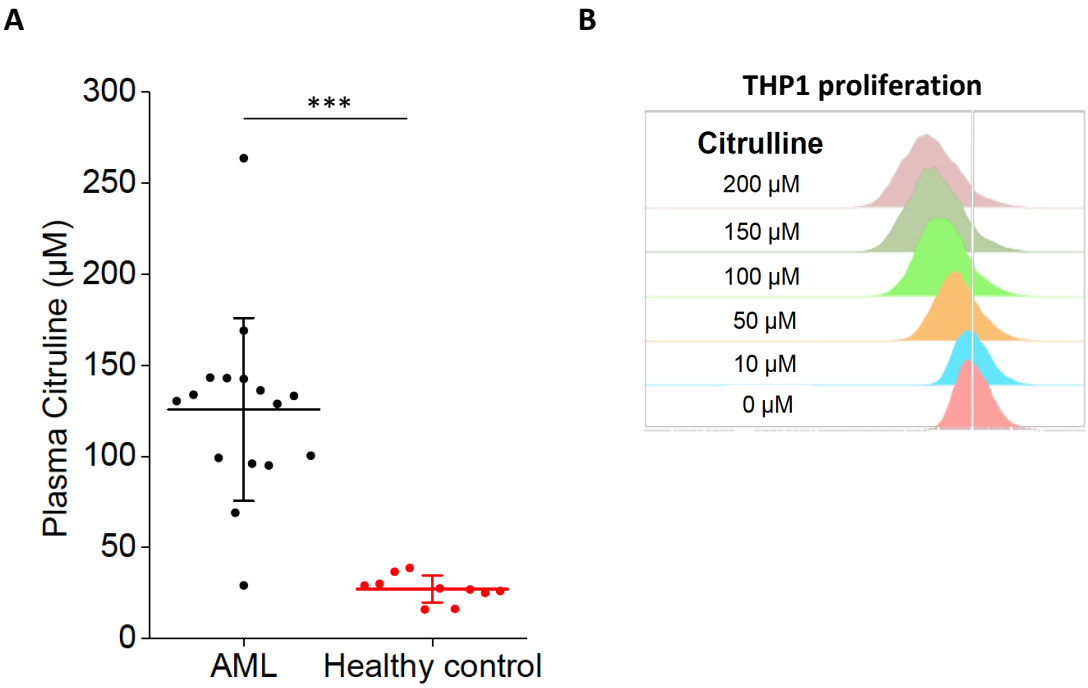



**Figure 4 - 26. Citrulline levels are higher in plasma from AML patients compared to healthy controls and are sufficient to support THP1 cell proliferation in the absence of arginine.**
(A) Citrulline levels, measured by ELISA, are higher in the plasma of AML patients compared to healthy controls. (B) THP1 cells are able to proliferate in arginine-depleted medium over a range of exogenous citrulline concentrations (as low as 50μM) that fits with the citrulline levels measured in the plasma of AML patients. Bars represent mean and standard deviation. *** $p < 0.001$. Each data point is the mean of triplicate measurements for that specific sample.

### 4.13.3 Mouse AML blasts behave similar to human ones in that they can utilize citrulline to grow in arginine-depleted conditions

Finally, we showed that primary murine leukaemic AML blasts displaying CEBPa overexpression from the aforementioned inducible AML mouse model (a gift from Dr Amit Grover and Prof Claus Nerlov) responded to citrulline supplementation in arginine-depleted medium similarly to THP1 cells, further suggesting that this is a clinically relevant and global aspect of cancer cells **(Figure 4-27)**.

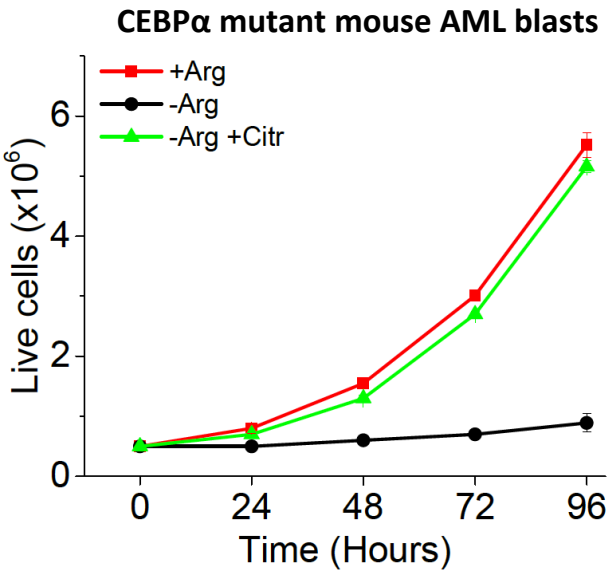



**Figure 4 - 27. Similar to THP1 cancer cells, primary AML blasts from our CEBPα mouse model can also use citrulline as an alternative arginine source to proliferate in arginine-free conditions.**
*In vitro* growth curves show that primary AML blasts obtained from culled mice carrying the CEBPα mutation cannot proliferate in the absence of arginine (black) whereas normal proliferation occurs when the blasts are cultured in full arginine –sufficient R10 medium for 72hr (red). Interestingly, medium supplementation with exogenous citrulline allowed murine AML blasts, to proliferate to levels similar to baseline despite the lack of arginine in the medium (green). Comparisons were made between conditions of -Arg +Citr vs conditions of –Arg to show strong statistical significance ($p<0.001$). Data points represent mean with standard deviation derived from measurements done in triplicate.

## 4.14 Discussion

Having shown the detrimental but reversible effects of Arginase-2-mediated arginine depletion on T-cell proliferation and effector function in the previous chapter, we then wanted to understand how cancer cells themselves, and more specifically AML blasts, are able to withstand the effects of arginine deprivation in the tumour microenvironment and continue to proliferate and function. We hypothesized that cancer cells possess an adaptation mechanism, not shared with host T-cells, that allows them to resist the nutritional stress generated by starvation of arginine, and perhaps other amino acids or nutrients too. In order to test this hypothesis, we took a reductionist, in vitro approach by

exposing THP1 cells, a cell line modelling AML, and primary human activated T-cells in complete R10 medium or arginine-free R10 medium for 72 hr. This system gave us the opportunity to evaluate the impact of arginine starvation on the reprogramming of the transcriptomic profile of cancer cells and compare it to that observed in T-cells using an Illumina differential gene expression microarray. Firstly, our results convincingly established that there are six distinct transcriptomic signatures exhibited in response to arginine starvation; genes downregulated only in THP1 cancer cells, genes upregulated only in THP1 cancer cells, genes downregulated only in T-cells, genes upregulated only in T-cells, genes downregulated in both cancer and T-cells and finally genes upregulated in both cancer and T-cells. It was also clear that T-cells showed differential expression in a larger number of genes compared to cancer cells, suggesting a more extensive remodelling of the transcriptome. However, more important to us, was to evaluate more closely the genes that were upregulated in cancer cells but not T-cells. Identification of key genes in this category could explain the adaptation mechanism permitting cancer cells to withstand arginine deprivation in the tumour microenvironment and giving them a competitive advantage over host immune cells.

Our results clearly demonstrated that a significant proportion of genes upregulated in response to arginine starvation only in cancer cells, were involved in cellular metabolism, including amino acid biosynthesis, amino acid transport, glutamine metabolism, glucose metabolism/glycolysis and autophagy. Of significance, we observed significant upregulation of *ASS1*, the enzyme catalysing the rate-limiting step in the hepatic urea cycle, participating in the recycling of arginine by mediating the conversion of the precursor citrulline to arginine. Furthermore, we identified the transcription factors most strongly linked with genes only upregulated in cancer cells, but not T-cells in response to arginine starvation, one of which was ATF4, the master regulator of the cellular response

to metabolic stress.

Interestingly, unlike *ASS1*, *ASL* and *OTC*, enzymes also forming part of the urea cycle, were not upregulated in any cell type. On the other hand, a variety of amino acid transporters, including the main arginine transporter SLC7A1 and other genes related to amino acid metabolism such as ASNS were upregulated in both cancer cells and T-cells. However, *SLC1A5* and *SLC7A5*, both neutral amino acid transporters previously reported to assist tumour growth when overexpressed [368], were also significantly upregulated in cancer cells but either not at all or to a much lower extent in T-cells. In line with recent reports suggesting that ARG2 is the main isoenzyme involved in arginine metabolism in effector T-cells [366], we showed that *ARG1* was undetectable and not upregulated in any of the two cell types whereas *ARG2*, although upregulated upon T-cell stimulation, it was in fact downregulated in activated T-cells upon arginine starvation but remained unchanged in cancer cells.

Although not our top hit, *ASS1* did display one of the most significant upregulation shifts in response to arginine starvation in cancer cells. That, along with the biological plausibility of ASS1 being a key enzyme in explaining the discrepancy observed between cancer cells and T-cells in resisting arginine-free conditions led us to look at the *ASS1* gene in more detail. We confirmed the upregulation of ASS1 mRNA and protein in THP1 cells but not T-cells in response to arginine starvation by qRT-PCR and fluorescent western blotting and studied the kinetics of the upregulation. To our knowledge, this is the first time dynamic upregulation of ASS1 has been shown in cancer in response to arginine deprivation. We showed that the discrepancy between cancer cells and activated T-cells is not the result of lack of sensing the absence of arginine as both cell types were able to upregulate ATF4 both at the genetic and the proteomic level in response to arginine starvation.

We then extended our findings by demonstrating a potential role of ASS1 in the competitive advantage of cancer cells to proliferate in arginine-free conditions. THP1 cancer cells were able to continue growing in the absence of arginine when medium was supplemented with citrulline, an arginine precursor. In contrast, T-cells were unable to utilize the exogenous citrulline and failed to proliferate in arginine-depleted medium even when citrulline was present in the extracellular environment. Additionally, we showed that this effect is not THP1-specific but rather globally applicable in a cancer context. We demonstrated the upregulation of *ASS1* in arginine-depleted culture medium in various human cancer cell lines, both solid (prostate, cervical, bladder) and liquid (AML and PML), and showed that this finding correlated with the ability of cancer cells to utilize exogenous citrulline and proliferate in the absence of extracellular arginine. This observation of starvation-induced *ASS1* upregulation in cell lines representative of a number of solid and liquid tumours supports reports of ASS1 overexpression in a number of cancers [240-243], and contrasts reports identifying ASS1 as a tumour suppressor gene often silenced by tumour-specific mechanisms [225-233]. This suggests that further work is necessary to untangle the exact role of ASS1 in cancer biology and also highlights the importance of precision and personalised medicine when making decisions about potential therapeutic avenues.

Moreover, using LC-MS with heavy-labelled amino acids, we revealed that citrulline is indeed taken up from extracellular space into cancer cells and is converted to arginine. This result is important as it makes a strong case of ASS1 being the key enzyme driving the compensatory mechanism employed by THP1 cells to resist arginine starvation, explaining the discrepancy observed between cancer cells and T-cells. Importantly, we showed for the first time that SLC7A5 and SLC1A5 are likely to act as the main citrulline transporters in cancer as their inhibition by specific small molecule inhibitors (BCH and

GPNA respectively) suppressed THP1 proliferation in arginine-free, citrulline-supplemented R10 medium. Given that these two transporters are often upregulated in cancer, an effect that we also observed for THP1 and HeLa cells in response to arginine starvation (microarray and qRT-PCR), makes this result particularly important as it highlights the dependence of arginine-deprived cancer cells on citrulline and moreover, paves additional avenues for cancer therapies by manipulating amino acid transport. Reinforcing our results, at the time of this work, another research group suggested that at times of arginine starvation, along with SLC7A1 (CAT1), the major arginine transporter, T-cells can also upregulate SLC3A2 (4F2hc) and SLC7A5 (LAT1) to facilitate uptake of citrulline [284, 369]. Although in our experiments we see only minimal upregulation of SLC7A5 in CD4+ T-cells when compared to THP1 cells, the role of SCL7A5 in citrulline transport seems to be important in principle. Furthermore, we also show an additional role for SLC1A5 (ASTC2; known mainly as a glutamine transporter) as a citrulline transporter, suggesting that unlike T-cells, THP1 cells upregulate more than one transmembrane transporters to import citrulline and they do it at much higher levels than immune cells. Importantly, we showed that the mechanism we propose is of clinical relevance since RNA-seq experiments showed that the expression of both ASS1 and ATF4 was higher in primary AML blasts from patients compared to the non-transformed monocytic and myelocytic cellular components obtained from healthy volunteers. We identified the source of extracellular citrulline as the plasma of AML patients, where levels of this metabolite are significantly higher compared to plasma from healthy controls. Interestingly, AML plasma citrulline levels match the range of citrulline concentrations at which arginine-starved THP1 cells are able to utilize citrulline synthesize arginine de novo and continue proliferating. The original mechanism of citrulline generation/release into the bloodstream in the context of AML remains to be elucidated but our hypothesis is that ornithine is

converted to citrulline by ornithine transcarbamylase (OTC), a mitochondrial enzyme just like Arginase-2. Based on our hypothesis, the two enzymes are perhaps found circulating in plasma attached to mitochondrial membrane components released from dying or leaky AML blasts. The proximity of the two enzymes means that they would be able to sequentially metabolise arginine to ornithine and then ornithine to citrulline, allowing circulating AML blasts to take in the latter and recycle it back to arginine intracellularly. We hope to address this hypothesis in the future, as it would also shed light as to the origins of Arginase-2 in the context of AML, a question that still remains unanswered.

In this chapter, we also studied the kinetics of the ASS1 upregulation to show that it peaks at 96hr and can be suppressed by the presence of arginine or induced by presence of citrulline. We demonstrated that rhARG2 treatment mimics the upregulation of ASS1, ATF4 and amino acid transporters seen in response to arginine depletion arguing that this mechanism might have physiological relevance in solid tumours with high Arginase activity or prevalent MDSC as well as in AML where Arginase-2 is released in patient serum to suppress T-cell function.

Finally, we studied the effects of arginine starvation on the Warburg effect that often characterises cancer cells. We demonstrated that the lack of arginine, either by rhARG2 treatment or by using arginine-depleted medium, abolished the Warburg effect by driving THP1 cells away from glycolysis and partially enhancing their respiratory capacity i.e. the ability for oxidative phosphorylation. Citrulline supplementation of the arginine-free medium restored the glycolytic profile of THP1 cells suggesting that arginine has multiple metabolic functions in cancer cells and perhaps explaining, along with the mTOR pathway, the impact of arginine on cell proliferation. Interestingly, genes encoding for glycolytic enzymes were globally downregulated in both THP1 and T-cells in response to arginine starvation explaining this result. Our findings support and complement suggestions that

arginine deprivation can inhibit the Warburg effect in ASS1-deficient cancer thus, highlighting the potential of modulating arginine metabolism in the context of cancer immunotherapy [370].

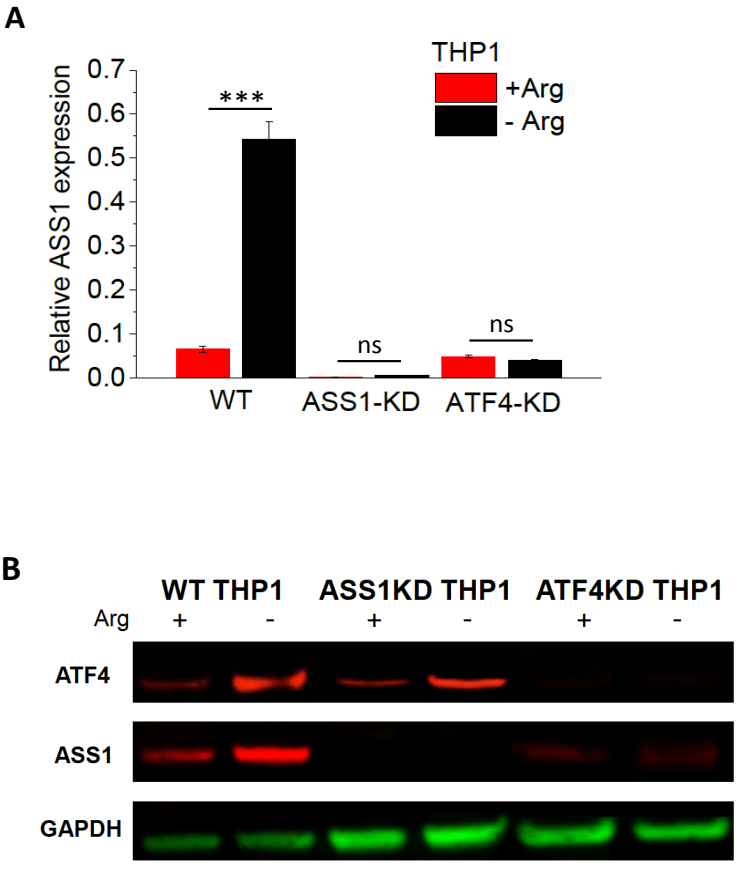
Together, our findings reveal that although both cancer cells and T-cells are able to sense and respond to arginine starvation e.g. by upregulating ATF4, only cancer cells can utilize exogenous citrulline in order to proliferate in the absence of arginine. This discrepancy is most likely the result of the ability of cancer cells to upregulate ASS1, a urea cycle enzyme that mediates the conversion of citrulline to arginine. Citrulline is higher in plasma of AML patients than healthy controls and requires intact SLC7A5 and SLC1A5 transporters in order to be taken up by cancer cells. All in all, we show that ASS1 upregulation and the uptake and conversion of citrulline to arginine are the features leading to a competitive advantage for cancer cells over T-cells to adjust to the arginine-depleted tumour microenvironment often seen in solid and tumours and leukaemias like AML. In the next chapter we attempt to explain how this discrepancy comes about by investigating the regulatory networks that facilitate ASS1 upregulation in cancer cells but not T-cells.

# Chapter 5: The discrepancy between cancer cells and T-cells in adapting to arginine starvation can be explained by differences in epigenetic regulation of ASS1 expression

## 5.1 ATF4-dependent ASS1 expression is required for citrulline utilisation to promote THP1 growth in arginine-deprived conditions

Having identified the importance of citrulline in restoring tumour cell growth, we wanted to demonstrate the importance of ASS1 in arginine synthesis and cancer cell proliferation in arginine-depleted conditions. In order to do so, we evaluated the proliferative potential of THP1 cells following ASS1 knockdown. Indeed, knocking down ASS1 in THP1 (ASS1 KD THP1) abrogated their ability to utilise citrulline to proliferate in arginine-depleted medium **(Figures 5-1A, B, C and 5-2A)**. In contrast to non-transfected or GFP control-transfected THP1, ASS1 KD THP1 cells were unable to grow without arginine, even in the presence of citrulline. In order to understand the transcriptional induction of ASS1, we asked whether ATF4 is required for ASS1 expression. We tested ATF4 as it is a key transcription factor activated upon amino acid starvation and was also one of the top hits in our initial microarray amongst transcription factors binding to genes upregulated by THP1 cells but not T-cells in response to arginine deprivation **(Figure 4-4)**. Indeed, knockdown of ATF4 in THP1 cells almost completely abolished upregulation of ASS1 upon arginine depletion **(Fig 5-1A, B, C)**. Furthermore, THP1 cells in which ATF4 had been knocked down (ATF4 KD THP1) were unable to proliferate without arginine even in the presence

of citrulline, thus recapitulating the functional effect observed in ASS1 knockdown cells (ASS1 KD THP1) **(Figure 5-2B)**. These findings suggest that ATF4 regulates ASS1 at the level of transcription and thus both ATF4 and ASS1 are required for citrulline-dependent proliferation of THP1 cells in environments lacking arginine.



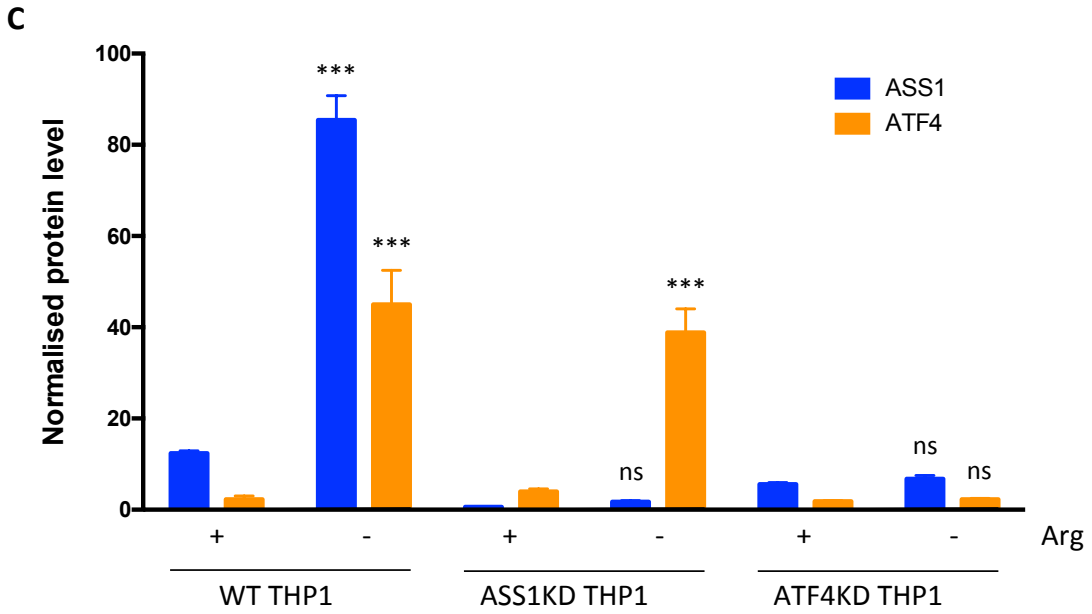



**Figure 5 - 1. ASS1 upregulation in response to arginine starvation is dependent on the transcription factor ATF4.**
(A) qRT-PCR data relative to housekeeping gene *GAPDH* show that shRNA-based knockdown of the transcription factor ATF4 in THP1 cancer cells abrogated their ability to upregulate *ASS1* at the RNA level in response to arginine starvation. (B) Fluorescent western blot confirms that induction of ASS1 at the protein level upon arginine starvation also fails upon ATF4 knockdown in THP1 cells. (C) Protein levels obtained from fluorescent WB were normalized against the housekeeping protein GAPDH and plotted to confirm that the upregulation of ASS1 in response to arginine starvation (blue) is completely abolished by ATF4 knockdown (yellow) in THP1 cells. *** $p<0.001$, ns means non-significant. Bars represent mean with standard deviation derived from triplicate measurements.

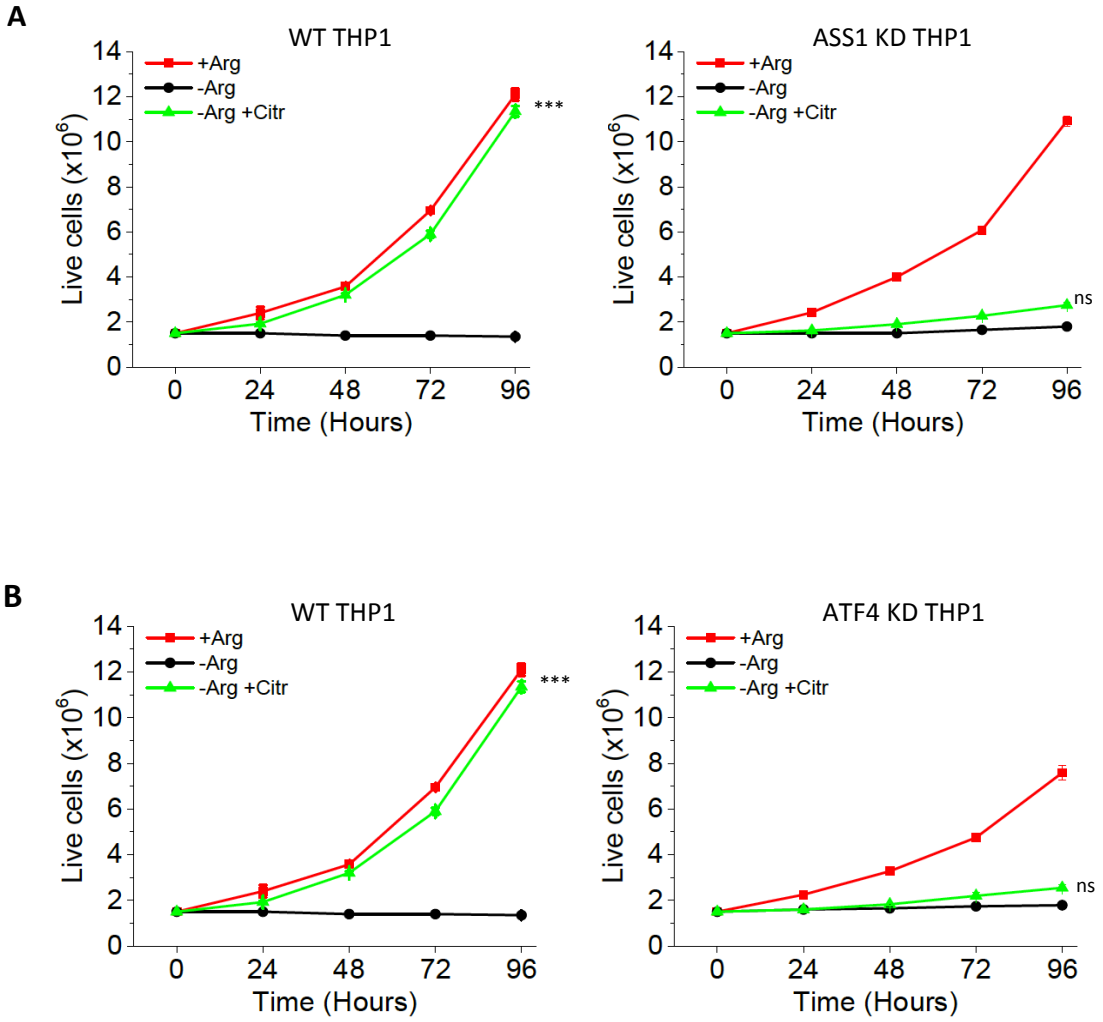
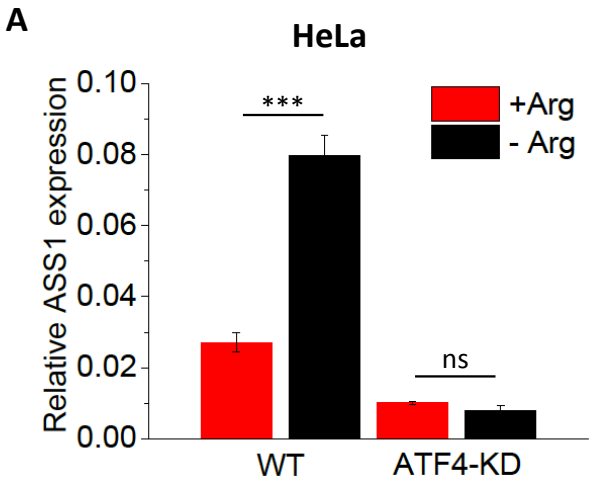



**Figure 5 - 2. Citrulline-dependent growth of THP1 cells under arginine starvation is dependent on both ASS1 and ATF4.**
*In vitro* growth curves (over 96hr of cell culture) show that unlike their wild-type (WT) counterparts (left panels), THP1 cells in which the (A) *ASS1* or (b) *ATF4* gene has been silenced by shRNA knockdown (ASS1 KD THP1 and ATF4 KD THP1; right panels) are unable to utilize extracellular citrulline and thus, fail to proliferate in arginine-deficient conditions (green line). Similar to WT THP1, ASS1 KD THP1 and ATF4 KD THP1 cells were still able to proliferate in arginine-sufficient medium (red line) and unable to do so in the absence of arginine without citrulline supplementation (black line). Statistical comparisons were made between conditions of -Arg +Citr vs conditions of –Arg. *** denotes $p<0.001$, ns denotes not significant. Data points represent mean with standard deviation derived from measurements done in triplicate.

## 5.2 ATF4-dependent ASS1 expression is required for the growth of solid tumour HeLa cells in the absence of arginine suggesting it is a phenomenon applicable to a variety of cancers

To extend this analysis to other tumour cells, we also looked at the response of HeLa cells to arginine deprivation. HeLa cells showed the same ATF4-dependent upregulation of ASS1 upon arginine depletion **(Figure 5-3A, B, C)**, and, strikingly, demonstrated the same dependence on citrulline for arginine-depleted growth **(Figure 5-4)**. Thus, in HeLa as in THP1 cells, ATF4-dependent ASS1 upregulation provides a mechanism for cell growth in the absence of arginine, suggesting that this is a common mechanism in cancer cells from both solid and liquid tumours.



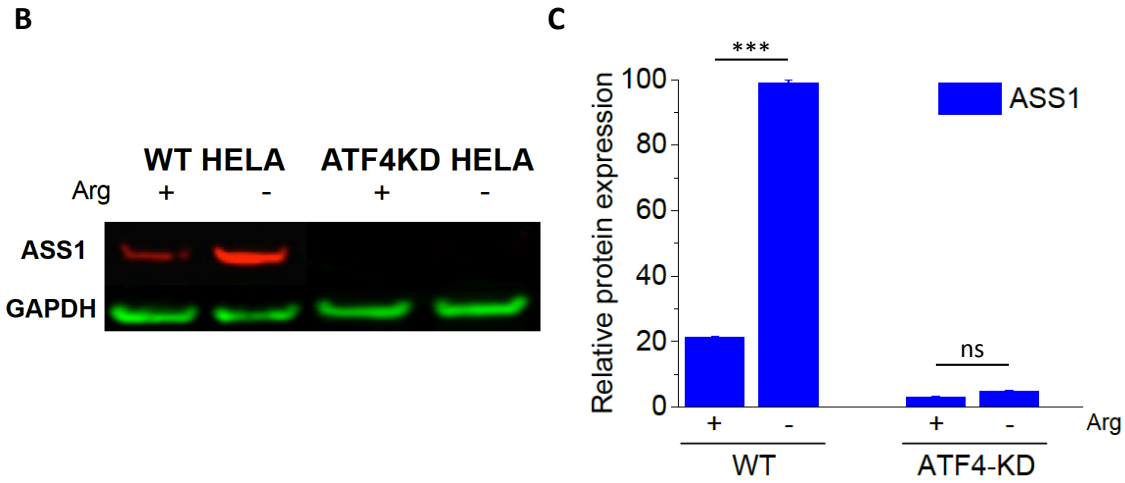



**Figure 5 - 3. ASS1 upregulation in HeLa cells is also abrogated by ATF4 knockdown.** (A) qRT-PCR data relative to housekeeping gene *GAPDH* show that shRNA-based knockdown of the transcription factor ATF4 in HeLa cervical cancer cells abrogated their ability to upregulate *ASS1* at the RNA level in response to arginine starvation. (B) Fluorescent western blot confirms that induction of ASS1 at the protein level upon arginine starvation also fails upon ATF4 knockdown in HeLa cancer cells. (C) Protein levels obtained from fluorescent WB were normalized against the housekeeping protein GAPDH and plotted to confirm that the upregulation of ASS1 in response to arginine starvation (blue) is completely abolished by ATF4 knockdown in HeLa cells. *** denotes $p<0.001$, ns means non-significant. Bars represent mean with standard deviation derived from triplicate measurements.

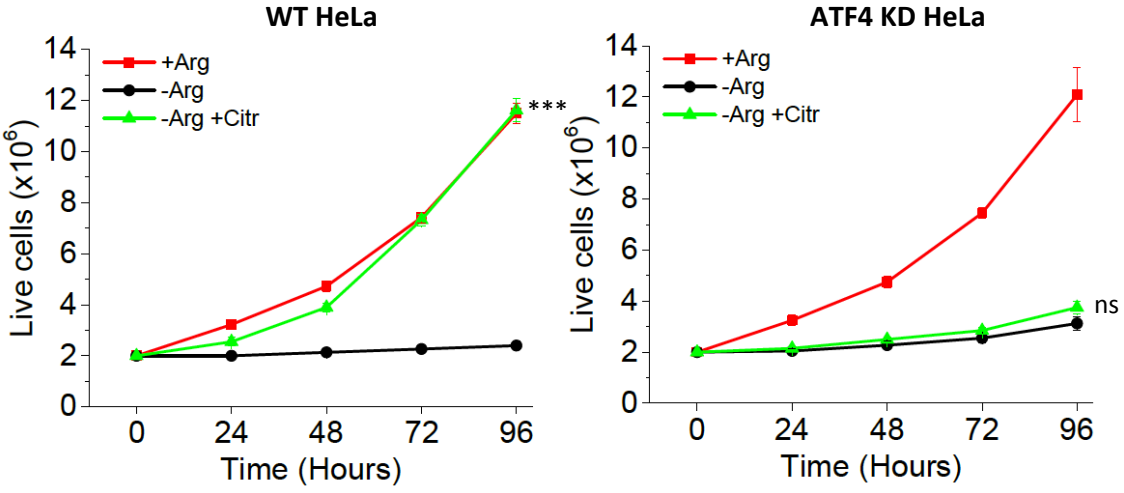


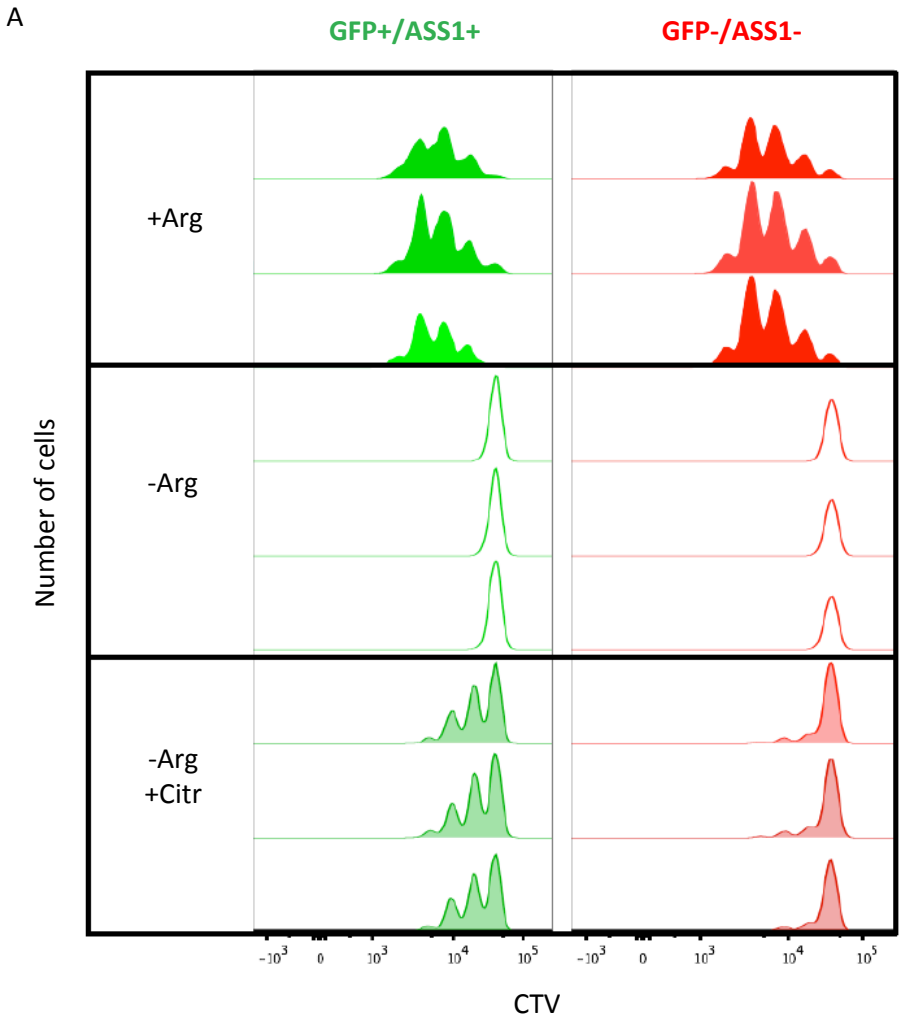

**Figure 5 - 4. Citrulline-dependent growth of HeLa cells under arginine starvation is dependent on ATF4.**
*In vitro* growth curves (over 96hr of cell culture) show that unlike their wild-type (WT) counterparts (left panel), HeLa cancer cells in which the *ATF4* gene has been silenced by shRNA knockdown (ATF4 KD HeLa; right panel) are unable to utilize extracellular

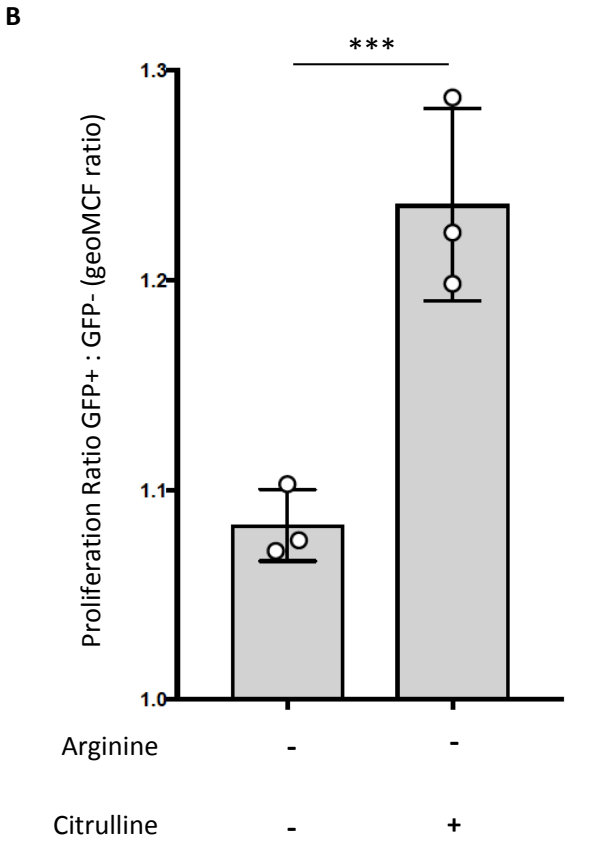
citrulline and thus, fail to proliferate in arginine-deficient conditions (green line). Similar to WT HeLa, ATF4 KD HeLa cells were still able to proliferate in arginine-sufficient medium (red line) and unable to do so in the absence of arginine without citrulline supplementation (black line). Statistical comparisons were made between conditions of -Arg +Citr vs conditions of –Arg. *** denotes $p<0.001$, ns denotes not significant. Data points represent mean with standard deviation derived from measurements done in triplicate.

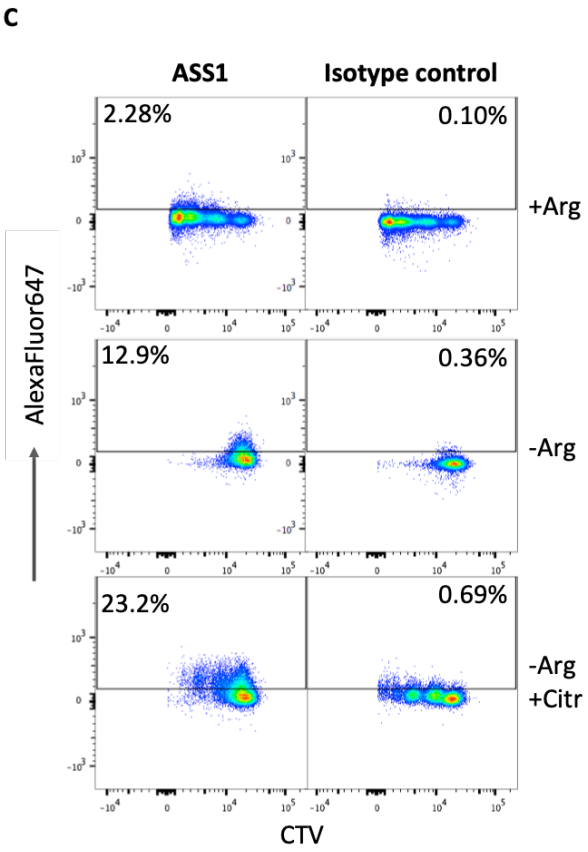
## 5.3 Gain-of-function studies show that ASS1 expression is sufficient to permit T-cell proliferation in the absence of arginine and presence of citrulline

In addition to proving that loss of ASS1 abolishes the functional advantage of cancer cells, we further showed that gain of ASS1 is sufficient for cell growth in the absence of arginine, by genetically modifying T-cells to overexpress ASS1 (in collaboration with Dr Uzi Gileadi). In a gain of function experiment, stimulated CD8+ T-cells were transfected with a plasmid for co-expression of ASS1 and GFP, and then labelled with Cell Trace Violet (CTV) to monitor proliferation before being cultured for 96h in different media (full medium [+Arg], arginine-depleted medium [-Arg] or arginine-depleted medium supplemented with citrulline [-Arg +Citr]). Non-transfected T-cells in the same culture acted as negative control and were compared to transfected T-cells in their ability to proliferate in arginine-free environments by utilising exogenous citrulline. Whilst growth in arginine-depleted medium was minimal for both T-cell populations, in the presence of citrulline, GFP+ cells divided more frequently than GFP- cells **(Figure 5-5A)**, indicating that ASS1 expression facilitated cell growth and expansion under these conditions. ASS1-expressing GFP+ T-cells were better able to compete with non-transfected (ASS-/GFP-) cells in arginine-depleted medium supplemented with citrulline **(Figure 5-5B)**, and proliferated more to form a larger proportion of the total T-cell population in culture

**(Figure 5-5C, D)**. This proliferative advantage in arginine-depleted, citrulline-supplemented medium was true both when we approached our analysis by looking at ASS1+ cells by intracellular ASS1 staining **(Figure 5-5C)** and when we looked at GFP+ cells **(Figure 5-5D)**. These findings demonstrate that upregulation of this single gene truly provides a strong competitive advantage to cancer or other cells growing in arginine-depleted environments, suggesting ASS1 as a potential target for genetic modification of T-cells before adaptive transfer into patients in the appropriate context. Intriguingly, there was some proliferation of GFP- cells as well, perhaps as a result of the presence small amounts of endogenous ASS1 expression in T-cells.




B
***
Proliferation Ratio GFP+ : GFP- (geoMCF ratio)
1.3
1.2
1.1
1.0
Arginine - -
Citrulline - +


C
ASS1
Isotype control
2.28%
0.10%
+Arg
12.9%
0.36%
-Arg
23.2%
0.69%
-Arg
+Citr
AlexaFluor647
CTV

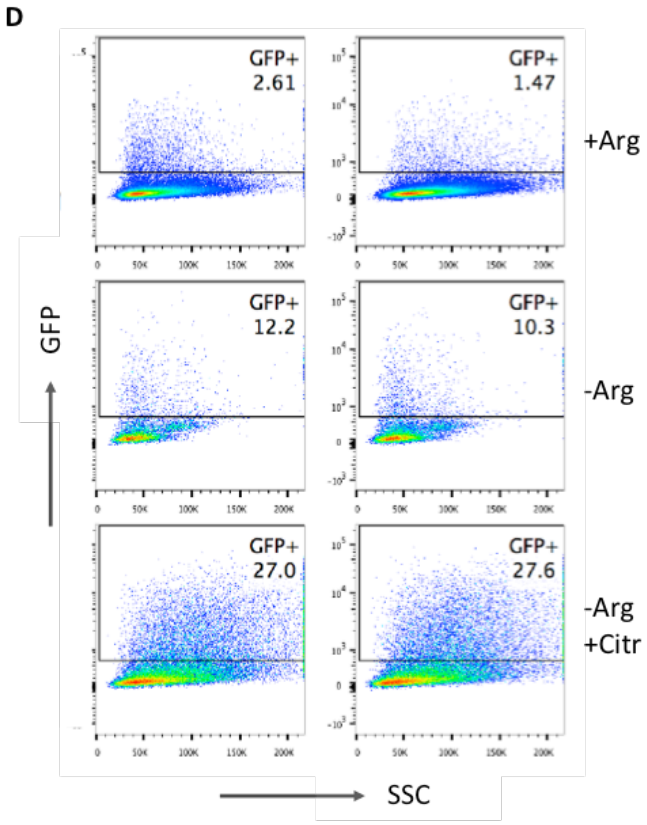



**Figure 5 - 5. Genetic modification of T-cells to achieve exogenous expression of ASS1 enables citrulline-dependent growth under arginine starvation.**
Stimulated CD8+ T-cells were transfected with a GFP+/ASS1+ expressing vector, labeled with cell trace violet (CTV) dye to monitor proliferation and then cultured for 96hr. Successfully transfected T-cells were shown to express both GFP and ASS1 whereas non-transfected T-cells expressed none of the two markers. The two populations were allowed to compete with each other in culture. (A) FACS analysis shows that, under arginine starvation conditions in the presence of extracellular citrulline (bottom panel), only GFP+ASS1+ T-cells (green) are able to grow whereas GFP-ASS1- T-cells fail to do so (red). Both cell populations were able to grow to the same extent in arginine-sufficient medium (top panel) and none of the two grew in arginine-deficient conditions without citrulline supplementation (middle panel). This suggests that ASS1 expression is necessary and sufficient for cells to utilize citrulline and grow in arginine-free environments. Each peak represents one proliferation cycle (CTV on x-axis). Triplicate experiments are displayed for each condition. (B) The proliferation ratio of GFP+:GFP- T-cells was plotted to show that the two cell populations proliferate equally in arginine-deficient medium but upon supplementation of this medium with citrulline the GFP+ ASS1-expressing T-cells are able to compete with and significantly outgrow the wild-type GFP-/ASS1- T-cells. Data points represent mean with standard deviation derived from measurements done in triplicate where *** denotes $p<0.001$. (C) FACS plots to display the raw data that confirm that T-cell proliferation in arginine-free conditions depends on ASS1 expression (represented by AlexaFluor647 fluorescence intensity) and the presence of extracellular citrulline. (D) FACS plots to display the raw data that confirm that ASS1-expressing GFP+ T-cells have a significant proliferation advantage in arginine-deficient citrulline-

supplemented medium (-Arg +Citr) and are thus able to compete with GFP-/ASS1- T-cells. As such, they constitute a larger proportion of the total T-cell population in -Arg +Citr conditions (27.0-27.6%) than they do in arginine-sufficient (+Arg; 1.47-2.61%) or arginine-deficient (-Arg; 10.3-12.2%) conditions. For FACS plots, representative duplicate experiments are shown.

## 5.4 ASS1 expression is dependent on epigenetically regulated binding of ATF4 to an internal enhancer

Despite the fact that both cancer cells and T-cells were able to sense arginine deprivation and, in response, upregulate ATF4, only the cancer cells upregulated ASS1, a transcriptional target of ATF4. To investigate the mechanism behind this dichotomous transcriptional response to the same stimulus, in collaboration with Dr Nicholas Crump and Prof Tom Milne, we conducted ChIP-seq for ATF4 and its binding partner CEBPβ, in arginine-depleted THP1 and T-cells, to ask whether the transcription factors are bound to the same genomic loci. Surprisingly, whilst about 4,000 ATF4 peaks were observed in T-cells, more than 60,000 were detected in THP1 cells **(Figure 5-6A)**. Notably, about two-thirds of the T-cell ATF4 peaks were present in THP1 cells, including at the promoters of *SLC7A1* **(Figure 5-10, panels 1-2)** and *ASNS* **(Figure 5-11, panels 1-2)**, genes that are upregulated in both cell types upon arginine starvation. This suggests that, whilst ATF4 binding is less restricted and thus, stronger in the cancer cells, most of the T-cell targets are retained. Importantly, in both cell types, the majority of ATF4 binding sites were also occupied by CEBPβ **(Figure 5-6B)**, consistent with their ability to heterodimerise [371, 372].

In order to understand why ASS1 is specifically upregulated only in cancer cells and not T-cells, we analysed the ATF4 distribution across ASS1 in the absence of extracellular arginine (using the ATF4 ChIP-seq). Whilst ATF4 was not detected at the ASS1 promoter

in THP1 cells, a significant peak of binding was observed about 3.5 kb downstream of the promoter, within the first intron of the gene **(Figure 5-7, panel 1)**. The exact same distribution was true in the case of HeLa cells, a cervical cancer cell line, in the absence of extracellular tryptophan **(Figure 5-7, panel 2)**. This suggests that the observed phenomenon is perhaps globally applicable to multiple cancers and in response to a variety of nutritional stresses such as starvation of different amino acids in the microenvironment, highlighting the relevance of this response in therapies targeting the immunosuppressive tumour microenvironment. More importantly, in contrast to the cancer cells, ATF4 binding was negligible at ASS1 in T-cells, with only an extremely small peak observed at the intronic binding site **(Figure 5-7, panel 3)**, consistent with the inability of T-cells to transcriptionally upregulate ASS1. In line with the earlier finding of ATF4 and CEBPβ sharing multiple common bindings sites, we also detected significant CEBPβ binding at the ASS1 intronic site, consistent with the presence of an ATF4/CEBPβ binding motif here **(Figure 5-7, panel 4-5)**. This CEBPβ binding was also only present in THP1 cells but not T-cells, in the absence of arginine suggesting that this transcription factor might also have a role in the discrepancy observed between cancer cells and T-cells in upregulating ASS1 in response to nutritional stress (see more later). In contrast to the *ASS1* intronic enhancer, there was significant binding of ATF4 and CEBPβ at the promoter of the *SLC7A1* and *ASNS* genes in both THP1 and T-cells **(Figure 5-8A, B)**. This lack of discrepancy in transcription factor binding at these genes is in line with the fact that they are upregulated by both THP1 and T-cells in response to arginine starvation. This suggests that the discrepancy observed between these two cell types in terms of their ability to upregulate genes following ATF4/CEBPβ binding is unique and specific to certain target metabolic genes such as *ASS1*.

Having identified this region of interest in intron 1 of the *ASS1* gene by ATF4 ChIP-seq, we tried to characterize its properties. We showed that this ATF4 (and CEBPβ) binding site is flanked by peaks of H3K4me1 (Histone 3, lysine 4, monomethylation) and H3K27ac (Histone 3, lysine 27, acetylation) **(Fig 5-7, panels 7-8)**. These epigenetic features are characteristic of an active enhancer, suggesting this intronic region where ATF4 binds, may regulate *ASS1*. As is typical of promoter regions, the ASS1 promoter was rich in a different epigenetic mark, namely H3K4me3 (Histone 3, lysine 4, trimethylation) **(Figure 5-7, panel 6)**.

The binding of ATF4 in THP1 and T-cells at this potential intronic ASS1 enhancer was subsequently validated by ChIP-qPCR (performed in collaboration with Dr Nicholas Crump), also confirming its arginine starvation-dependent chromatin association **(Figure 5-9)**. Genes that were earlier shown (Chapter 4) to be upregulated in both cell types upon arginine depletion (including SLC7A1) showed a clear and significant increase in ATF4 binding ($p<0.01$) in both THP1 and T-cells when arginine was absent in the microenvironment, whereas ATF4 levels were consistently low at a negative control region irrespective of arginine levels ($p>0.05$). In contrast, ATF4 binding at the ASS1 intron was induced by arginine deprivation only in THP1 cells ($p<0.001$) but not T-cells where ATF4 binding remained unchanged at already low basal levels. Interestingly, in contrast to the ASS1 intronic region, there was consistently low ATF4 binding at the ASS1 promoter region in both THP1 and T-cells, an effect that did not significantly changed by arginine starvation ($p>0.05$).

Furthermore, in order to confirm that this site is a functional enhancer for *ASS1*, we generated a mutant THP1 line in which the ATF4 motif at this locus was deleted using CRISPR technology in collaboration with Dr Nicholas Crump **(Figure 5-10A)**. This mutation eliminated ATF4 binding at *ASS1*, but not at *SLC7A1* **(Figure 5-10B)**.

Consequently, the ATF4-binding motif deletion completely abrogated *ASS1* expression **(Figure 5-10D, E)** and citrulline-dependent growth **(Figure 5-10C)** in the absence of arginine. Given these results, we concluded that this locus acts as an enhancer for *ASS1* in THP1 cells, with ATF4 binding absolutely required for gene activation.

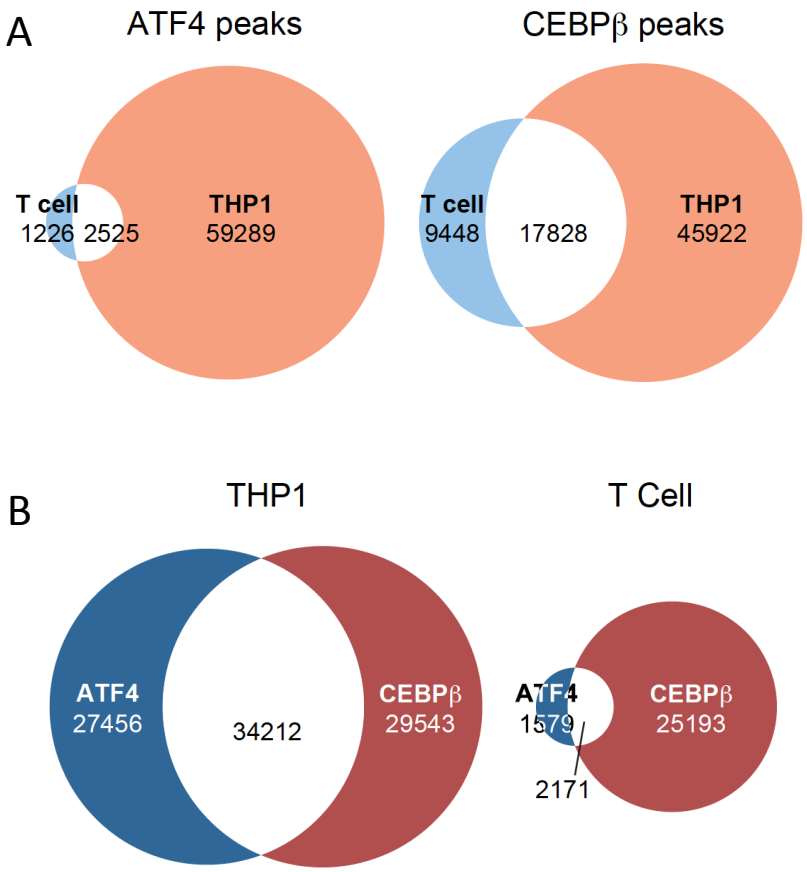



**Figure 5 - 6. ATF4 and CEBPβ have more binding sites in THP1 cells than T-cells and a large proportion of these sites are shared by the two transcription factors.**
(A) A subset of ATF4- and CEBPβ-bound sites are shared between the genome of THP1 and T-cells, but cell type-specific binding events are also observed. Interestingly, there are a significantly higher number of such sites across the genome of THP1 cells compared to that of T-cells.
(B) There is a strong overlap between ATF4- and CEBPβ-bound sites in both THP1 and T-cells suggesting potential binding partnerships between the two transcription factors.

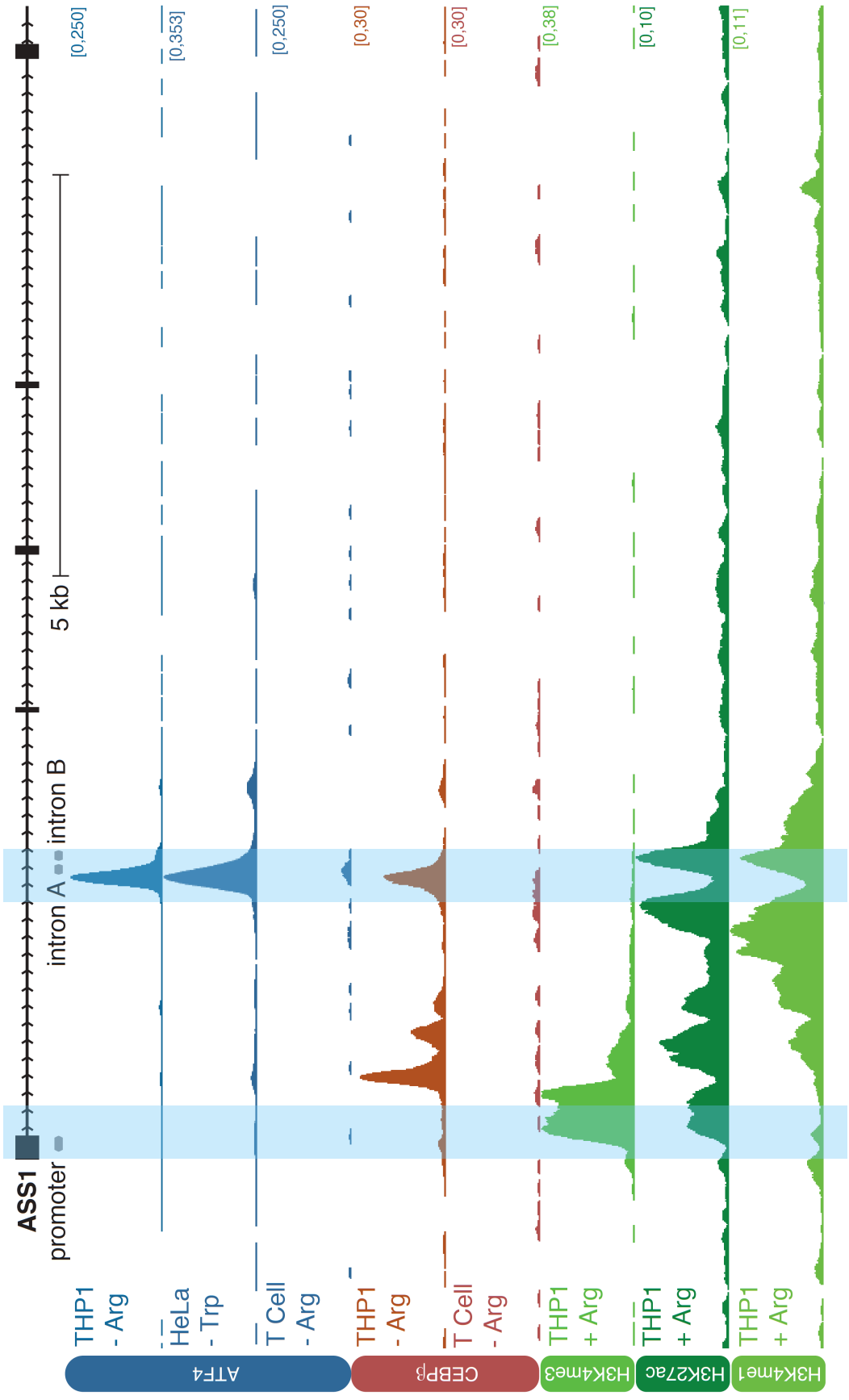

ASS1
promoter
intron A
intron B
5 kb
[0,250]
[0,353]
[0,250]
[0,30]
[0,30]
[0,38]
[0,10]
[0,11]
THP1 - Arg
HeLa - Trp
T Cell - Arg
THP1 - Arg
T Cell - Arg
THP1 + Arg
THP1 + Arg
THP1 + Arg
ATF4
CEBPβ
H3K4me3
H3K27ac
H3K4me1

**Figure 5 - 7. ATF4 and CEBPβ ChIP-seq in THP1, HeLa and T-cells reveals the presence of a tumour-preferred enhancer within the first intron of the ASS1 locus.** A ChIP-seq was performed for ATF4 and its potential binding partner CEBPβ in THP1 cancer cells, HeLa cancer cells and T-cells under conditions of arginine starvation (panels 1-5). This revealed the presence of a strong tumour-specific ATF4/CEBPβ binding site within the first intron of the ASS1 locus (highlighted region on the right), present only in THP1 and HeLa cancer cells (panels 1-2 and 4) but not T-cells (panels 3 and 5). This is in line with ASS1 upregulation in response to arginine starvation only in cancer cells but not T-cells. Furthermore, analysis of histone modifications shows that this binding region is flanked by peaks of Histone 3, lysine 4, monomethylation (H3K4me1) and Histone 3, lysine 27, acetylation (H3K27ac), epigenetic features characteristic of an active enhancer, suggesting that this intronic region, where ATF4/ CEBPβ bind, may regulate *ASS1* (panels 7 and 8; highlighted region on the right). Additionally, the *ASS1* promoter was rich in Histone 3, lysine 4, trimethylation (H3K4me3) an epigenetic mark typical of promoter regions (panel 6; highlighted region on the left).

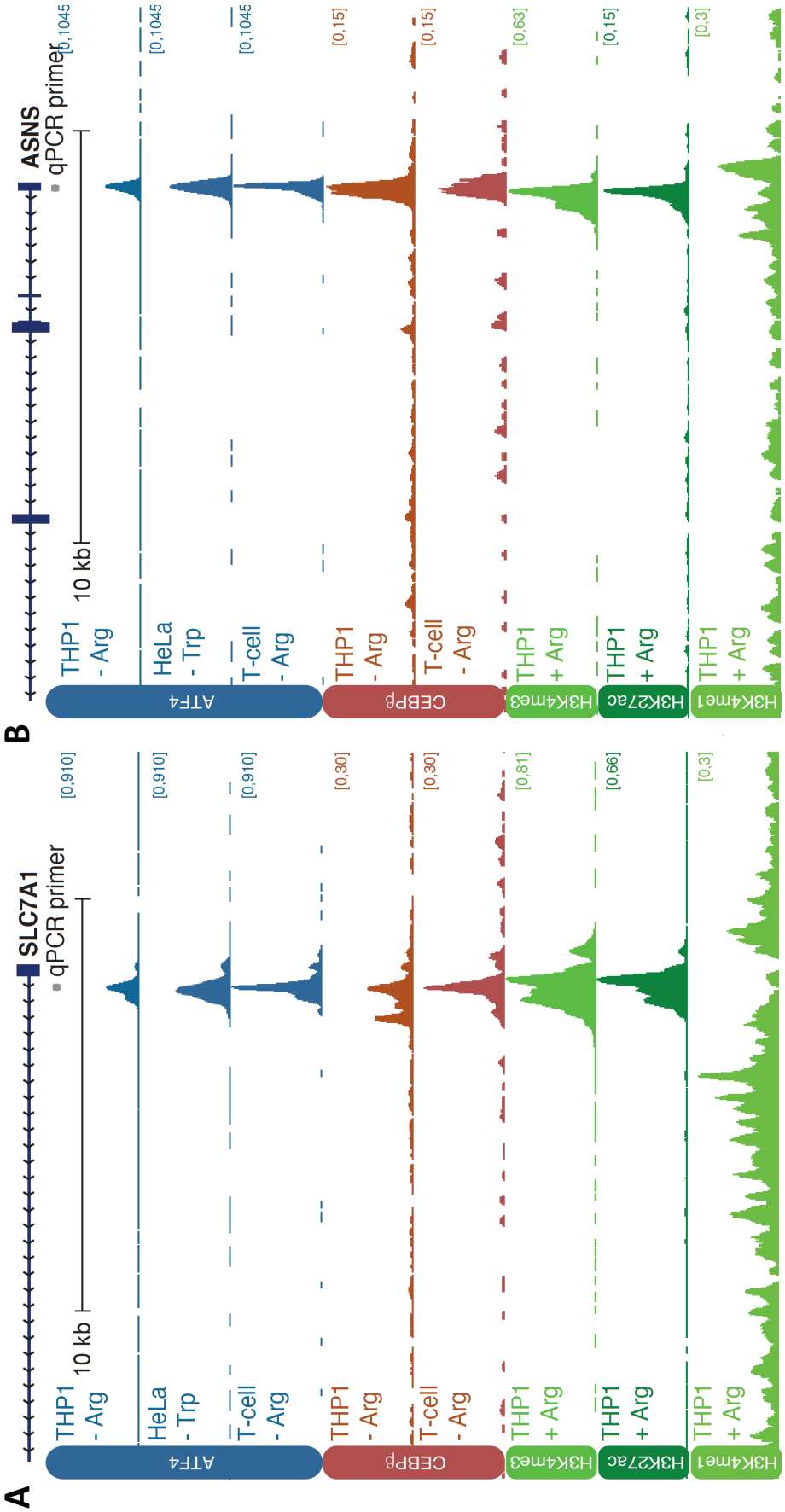

A
SLC7A1
qPCR primer
10 kb
THP1 - Arg
HeLa - Trp
T-cell - Arg
THP1 - Arg
T-cell - Arg
THP1 + Arg
THP1 + Arg
THP1 + Arg
ATF4
CEBPβ
H3K4me3
H3K27ac
H3K4me1
[0,910]
[0,910]
[0,910]
[0,30]
[0,30]
[0,81]
[0,66]
[0,3]
B
ASNS
qPCR primer
10 kb
THP1 - Arg
HeLa - Trp
T-cell - Arg
THP1 - Arg
T-cell - Arg
THP1 + Arg
THP1 + Arg
THP1 + Arg
ATF4
CEBPβ
H3K4me3
H3K27ac
H3K4me1
[0,1045]
[0,1045]
[0,1045]
[0,15]
[0,15]
[0,63]
[0,15]
[0,3]

**Figure 5 - 8. ATF4 and CEBPβ ChIP-seq in THP1, HeLa and T-cells reveals the presence of a global, non-tumour-specific enhancer near the promoter of the SLC7A1 and ASNS loci.**
A ChIP-seq was performed for ATF4 and its potential binding partner CEBPβ in THP1 cancer cells, HeLa cancer cells and T-cells under conditions of arginine starvation (panels 1-5). This revealed the presence of strong ATF4/CEBPβ binding sites near the promoters of (A) SLC7A1 and (B) ASNS loci, present not only in THP1 and HeLa cancer cells (panels 1-2 and 4) but also T-cells (panels 3 and 5) suggesting these are not tumour-specific. This is in line with SLC7A1 and ASNS upregulation in response to arginine starvation seen in both cancer cells and T-cells. Analysis of histone modifications shows both of these binding regions are flanked by peaks of Histone 3, lysine 4, monomethylation (H3K4me1) and Histone 3, lysine 27, acetylation (H3K27ac), epigenetic features characteristic of an active enhancer (panels 7 and 8). Additionally, both gene promoters were rich in Histone 3, lysine 4, trimethylation (H3K4me3) an epigenetic mark typical of promoter regions (panel 6).

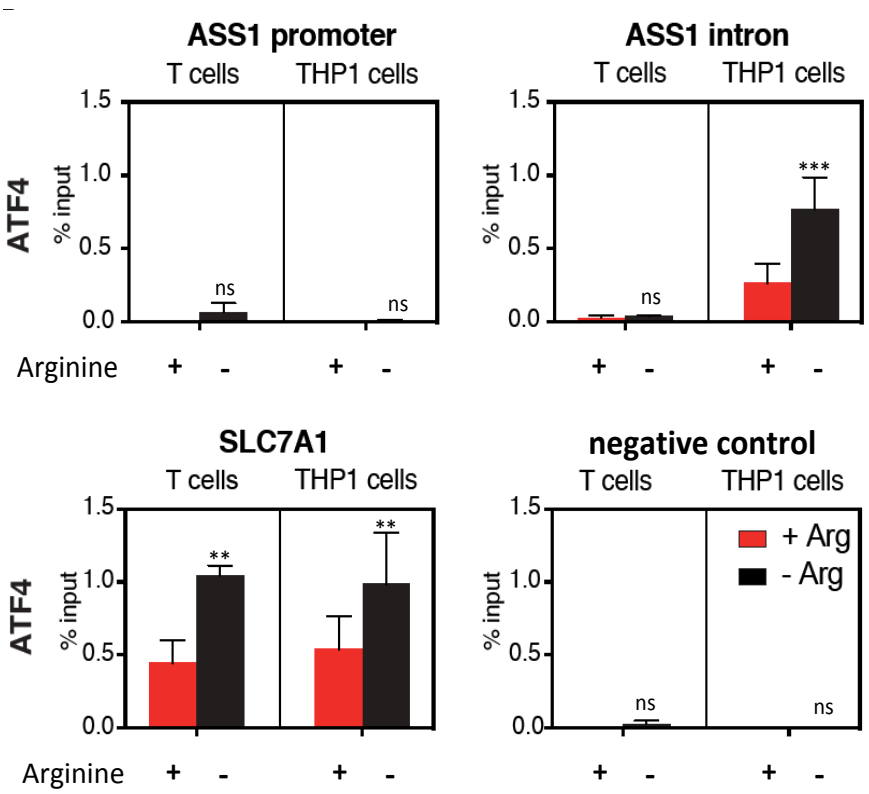



**Figure 5 - 9. ATF4 ChIP-qPCR shows that ATF4 binding at the ASS1 intronic enhancer only occurs in THP1 cells but not T-cells and is augmented in response to arginine starvation.**
ChIP-qPCR was performed for ATF4 binding at various regions of interest across the genome in THP1 and T-cells in sufficient arginine conditions (red) and following exposure to arginine deficiency (black). ATF4 binding at the ASS1 promoter is negligible in both cell types and not affected by the presence or absence of arginine (top left panel) reflecting a similar pattern to our negative control gene (HoxC8; bottom right panel). Significant

ATF4 binding is detected at the ATF4/CEBPβ binding site near the SLC7A1 promoter (our positive control) at baseline (bottom left panel). ATF4 binding is enhanced upon arginine starvation in both cell types, in line with our earlier observation that both THP1 and T-cells are able to upregulate SCL7A1 expression in response to arginine deprivation (bottom left panel). In contrast, ATF4 binding at the ASS1 intronic enhancer is only detected in THP1 cells in which it is significantly augmented upon arginine starvation (top right panel). T-cells display no ATF4 binding at the ASS1 enhancer at baseline and this is unaffected by arginine starvation. These findings are in line with our earlier results suggesting that THP1 cells express significant ASS1 and upregulate expression further in response to arginine starvation whereas T-cells fail to do so and remain with their negligible baseline ASS1 expression. For ChIP-PCR data, bars represent mean with standard deviation derived from triplicate measurements. *** denotes $p<0.001$, ** denotes $p<0.01$, ns denotes not significant ($p>0.05$).

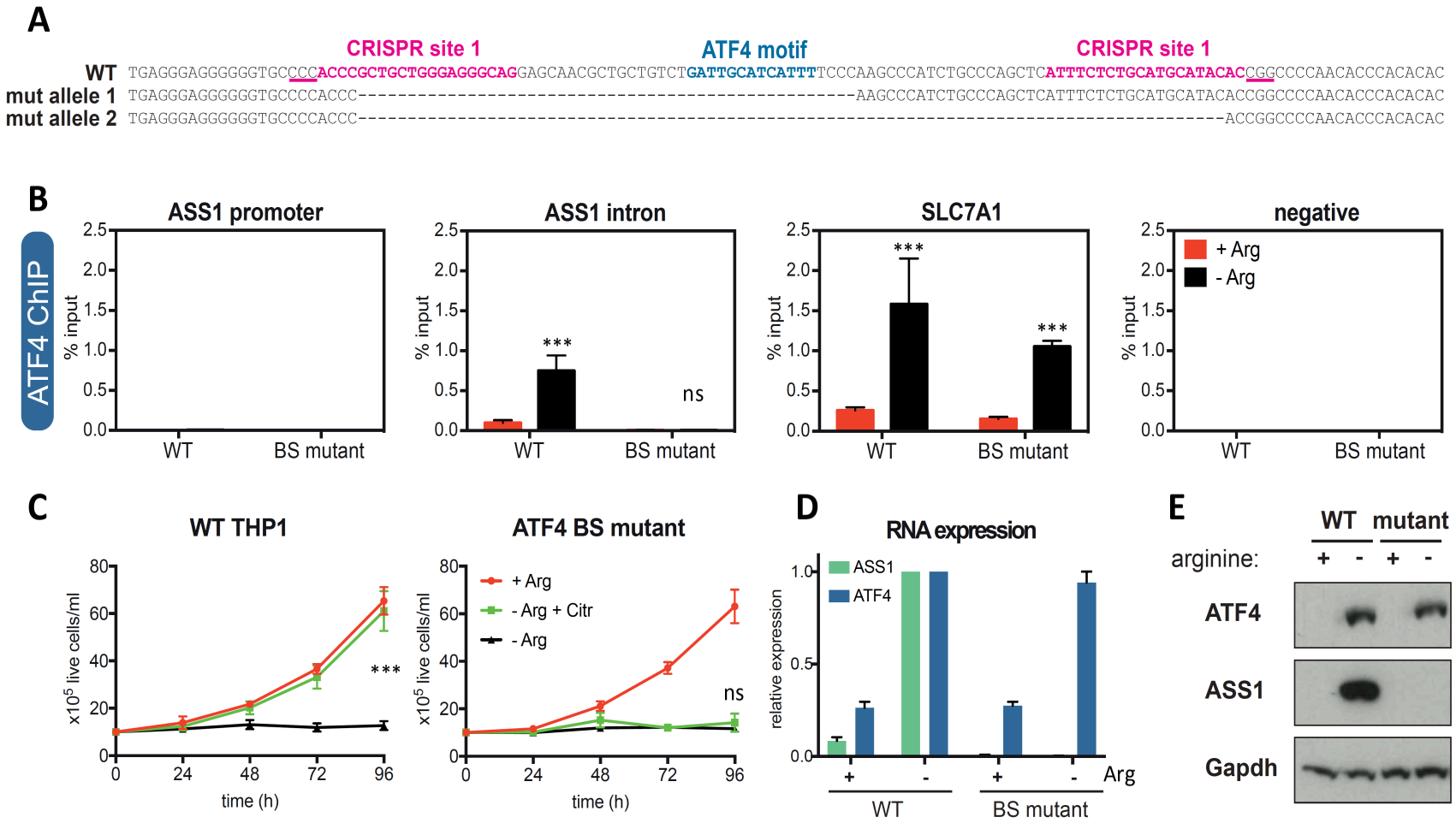

A
CRISPR site 1
ATF4 motif
CRISPR site 1
WT TGAGGGAGGGGGGTGCCCACCCGCTGCTGGGAGGGCAGGAGCAACGCTGCTGTCTGATTGCATCATTTTCCCAAGCCCATCTGCCCAGCTCATTTCTCTGCATGCATACACCGGCCCCAACACCCACACAC
mut allele 1 TGAGGGAGGGGGGTGCCCCACCC----------AAGCCCATCTGCCCAGCTCATTTCTCTGCATGCATACACCGGCCCCAACACCCACACAC
mut allele 2 TGAGGGAGGGGGGTGCCCCACCC----------ACCGGCCCCAACACCCACACAC
B
ATF4 ChIP
ASS1 promoter
ASS1 intron
SLC7A1
negative
% input
WT
BS mutant
***
ns
+ Arg
- Arg
C
WT THP1
ATF4 BS mutant
x10^5 live cells/ml
time (h)
+ Arg
- Arg + Citr
- Arg
D
RNA expression
ASS1
ATF4
relative expression
Arg
E
WT mutant
arginine:
ATF4
ASS1
Gapdh

**Figure 5 - 10. Deletion of the ATF4-binding motif sequence in the ASS1 intronic enhancer in THP1 abolishes ATF4 binding, ASS1 expression and citrulline utilization.**
(A) The ATF4-binding site (BS) motif within the ASS1intronic enhancer was deleted by CRISPR technology in THP1 cells so that wild-type (WT) and BS mutant cells could be compared. (B) ATF4 ChIP-qPCR was performed at various regions of interest across the genome in WT and BS mutant THP1 cells in conditions of arginine sufficiency (red) and arginine deficiency (black). As expected no ATF4 binding at the ASS1 promoter is detected in either cell type with no impact following exposure to arginine starvation (panel 1) reflecting a similar pattern to our negative control gene (HoxC8; panel 4). Significant ATF4 binding is measured at the ATF4/CEBPβ binding site near the SLC7A1 promoter (our positive control) at baseline in both WT and BS mutant THP1 cells (panel 3). ATF4 binding is enhanced upon arginine starvation in both cell types (panel 3). In contrast, ATF4 binding at the ASS1 intronic enhancer is only detected in WT THP1 cells in which it is significantly augmented upon arginine starvation (panel 2). ATF4 binding at the ASS1 enhancer is completely abolished in BS mutant THP1 cells compared to WT THP1 cells both at baseline and in conditions of arginine starvation (panel 2). (C) In contrast to their WT THP1 counterparts, BS mutant THP1 cells are lose the ability to utilize exogenous citrulline in order to proliferate in arginine-deficient conditions (green) to the same extent as arginine sufficient conditions (red). This functional difference is because of the inability of BS mutant THP1 cells to express ASS1in response to arginine starvation, both at the (D) RNA (by qRT-PCR) and (E) protein (by western blot) levels when compared to WT THP1 cells. This is despite ATF4 upregulation suggesting that the ability to sense and respond to arginine deprivation is still intact in BS mutants (D and E). Overall, these findings confirm that cancer cell ASS1 expression and citrulline utilization to adopt to arginine starvation conditions depends on ATF4/CEBPβ biding at the ASS1 intronic enhancer. For ChIP-qPCR and qRT-PCR data, bars represent mean with standard deviation derived from triplicate measurements. For qRT-PCR this is relative to expression of the housekeeping gene *GAPDH*. For growth curves, statistical comparisons were made between conditions of -Arg +Citr vs conditions of –Arg and data points represent mean with standard deviation derived from measurements done in triplicate. *** denotes $p<0.001$, ns denotes not significant ($p>0.05$).

## 5.5 Expression of ASS1 in THP1 and T-cells is regulated by changes in chromatin accessibility

In order to understand the differential binding of ATF4 in cancer and T-cells, we analysed the accessibility of chromatin at ASS1 using ATAC-seq in collaboration with Dr Nicholas Crump and Prof Tom Milne **(Figure 5-11, panels 7-11)**. In THP1 cells, peaks of accessibility were visible at the promoter, consistent with poised/active expression, and at the intronic ATF4 (and CEBPβ) binding site, consistent with transcription factor binding.

Notably, whilst accessibility increased at these loci upon arginine depletion, these regions were also accessible in the presence of arginine (i.e. in the absence of ASS1 transcription). Thus, the intronic locus is already found in an open state prior to ATF4 binding. In contrast, chromatin accessibility at ASS1 was much lower in T-cells, with a strongly reduced ATAC peak at the promoter and little or no signal detected at the intronic ATF4 binding site under either condition. The fact that this peak is absent in T-cells, both in the presence and absence of arginine, suggests that a lack of accessibility may prevent ATF4 binding to ASS1. In contrast, ATAC-seq at the ATF4-binding sites near the promoters of SLC7A1 and ASNS showed comparable chromatin accessibility between THP1 and T-cells irrespective **(Figure 5-12)**. This is in line with the ability of both THP1 and T-cells to express these genes and upregulate their expression in response to arginine. Taken together with the effects of ATF4 knockdown **(Figures 5-1 and 5-2)**, these data argue that ATF4 activates ASS1 in THP1 cells by directly binding to an intragenic enhancer within intron 1. In T-cells, ATF4 is less able to bind at this locus, perhaps because of a lack of chromatin accessibility, and so ASS1 is not induced upon arginine depletion.

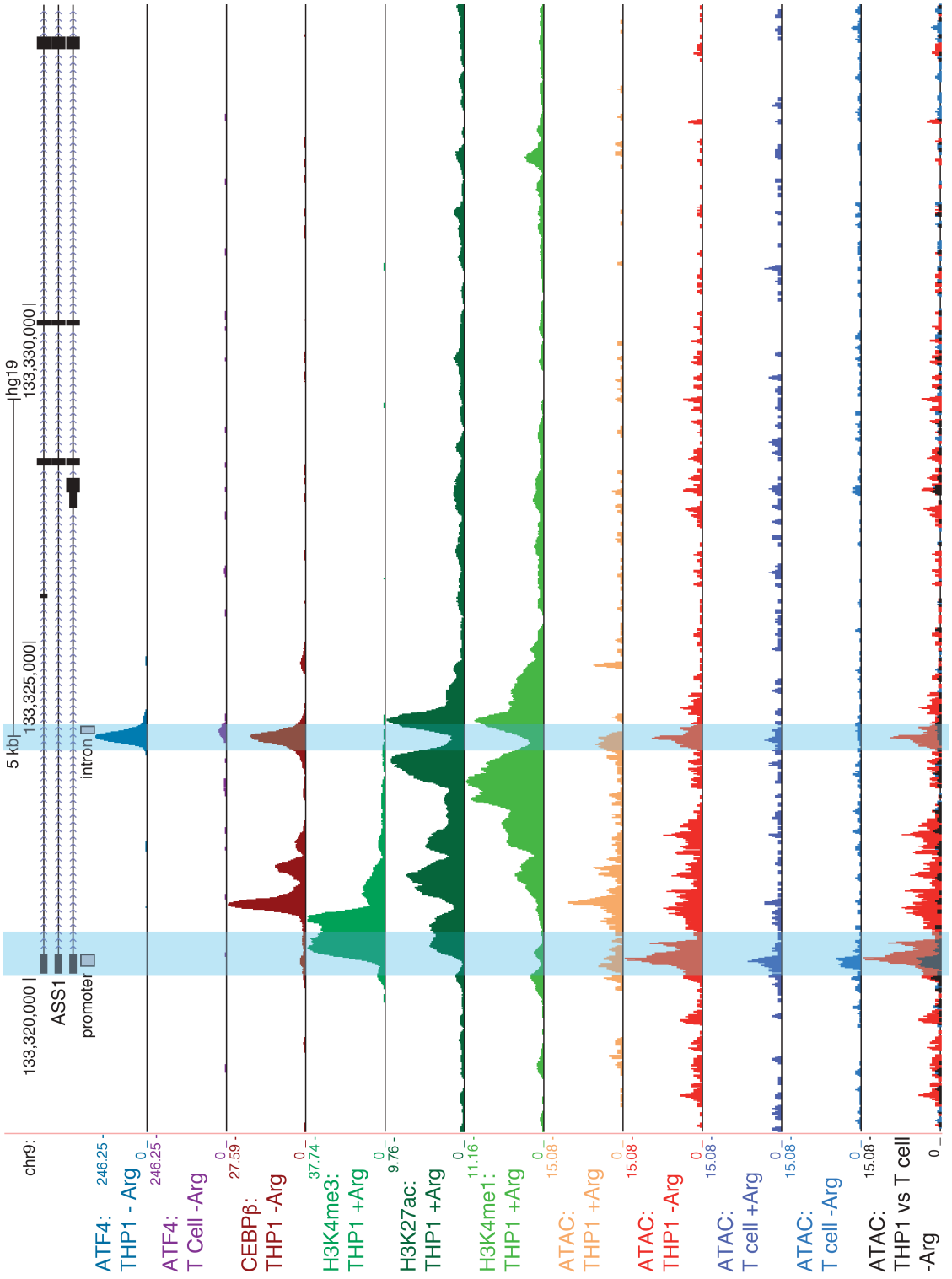

hg19
133,330,000
133,325,000
5 kb
133,320,000
ASS1
promoter
intron
chr9:
ATF4: THP1 - Arg
ATF4: T Cell -Arg
CEBPβ: THP1 -Arg
H3K4me3: THP1 +Arg
H3K27ac: THP1 +Arg
H3K4me1: THP1 +Arg
ATAC: THP1 +Arg
ATAC: THP1 -Arg
ATAC: T cell +Arg
ATAC: T cell -Arg
ATAC: THP1 vs T cell -Arg
246.25
27.59
37.74
9.76
11.16
15.08

**Figure 5 - 11. ATAC-Seq reveals decreased chromatin accessibility for ATF4/ CEBPβ transcription factors to bind at the ASS1 intronic enhancer in T-cells compared to THP1 cancer cells.**
Assay for Transposase-Accessible Chromatin using sequencing (ATAC-Seq) was performed at the ASS1 locus showing that chromatin accessibility is significantly lower in stimulated T-cells compared to THP1 cells both at the ASS1 promoter and the ASS1 intronic enhancer where the ATF4 and CEBPβ transcription factors bind (highlighted areas, panels 7-10). Furthermore, chromatin accessibility appears to enhance upon arginine starvation in THP1 cells (panel 7 vs 8), an effect not observed in T-cells (panel 9 vs 10). The difference in chromatin accessibility in arginine starvation conditions, at both promoter and intronic enhancer, between THP1 (red) and T-cells (blue) is clearly seen when the signals from the two cell types are superimposed on each other (panel 11). This could explain the lack of ATF4 (and CEBPβ) binding in T-cells contrary to THP1 cells (panels 1-3).

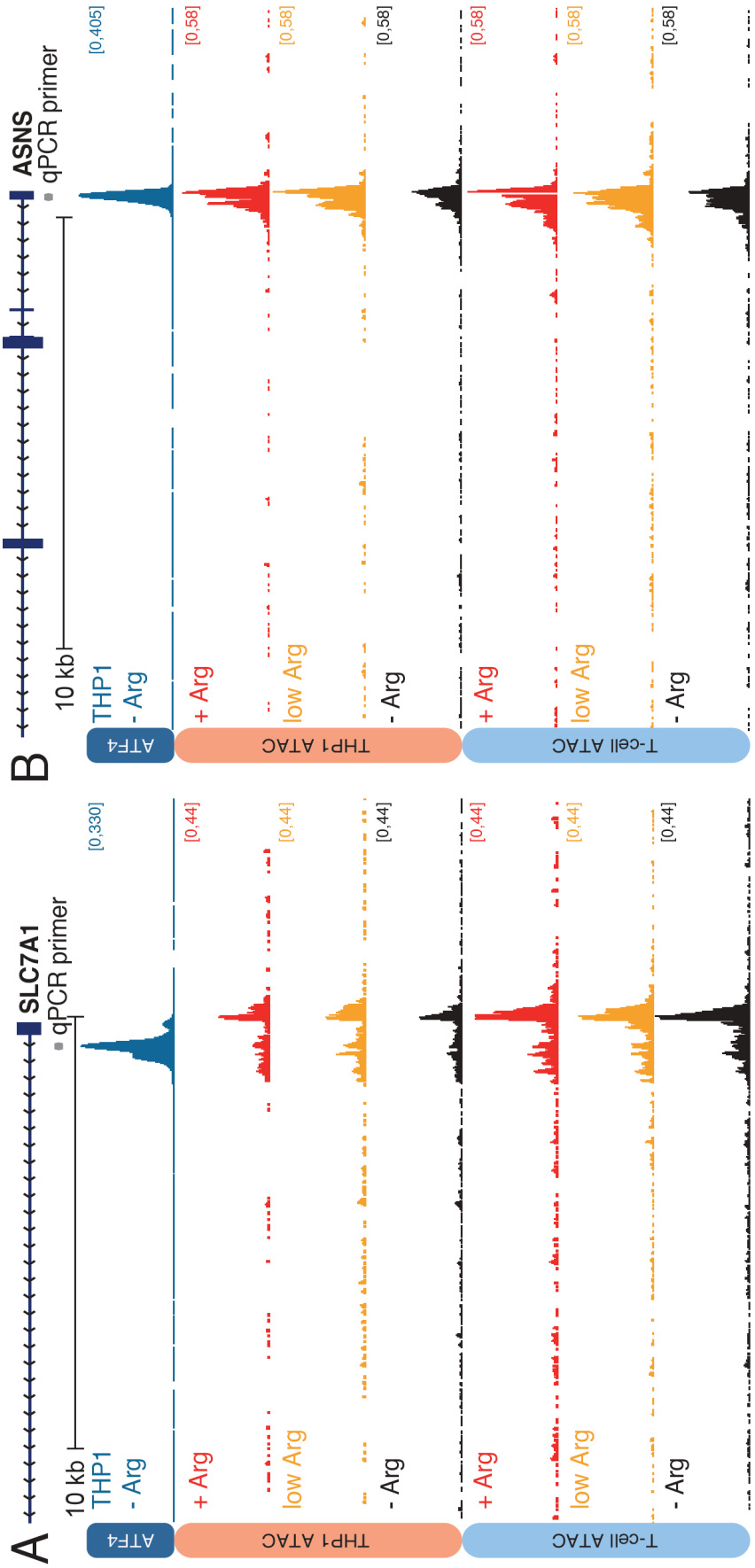

A
SLC7A1
qPCR primer
10 kb
THP1
- Arg
[0,330]
[0,44]
+ Arg
low Arg
- Arg
ATF4
THP1 ATAC
T-cell ATAC
B
ASNS
qPCR primer
10 kb
THP1
- Arg
[0,405]
[0,58]
+ Arg
low Arg
- Arg
ATF4
THP1 ATAC
T-cell ATAC

**Figure 5 - 12. ATAC-Seq reveals no differences between THP1 and T-cells in chromatin accessibility at the ATF4-binding sites in the promoter region of the SLC7A1 and ASNS genes.**
Assay for Transposase-Accessible Chromatin using sequencing (ATAC-Seq) was performed at the (A) SLC7A1 and (B) ASNS loci to show that chromatin accessibility at the ATF4 binding sites (panel 1; blue) is similar between stimulated T-cells (panels 5-7) and THP1 (panels 2-4) cells irrespective of whether the cells are in arginine-sufficient (red), arginine-low (yellow) or arginine-deficient (black) conditions.

## 5.6 The ASS1 internal enhancer is epigenetically repressed in T cells

To understand the mechanism that controls chromatin accessibility and consequently ATF4 binding at ASS1 intron 1 and explain the dichotomy between cancer cells and T-cells, we looked for the presence of epigenetic marks associated with silent or repressive chromatin. In collaboration with Dr Nicholas Crump, we showed that levels of the heterochromatic repressive histone marks H3K9me2 and H3K9me3 at the ASS1 intron were higher in T-cells than in THP1 cells, and comparable to levels at *HoxC8*, a gene which is developmentally silenced in hematopoietic cells **(Figure 5-13, top panel)**. An almost identical pattern to H3K9me2 and H3K9me3 was observed for H3K27me3, another histone modification associated with repressive chromatin states, whose levels were again much higher in T-cells compared to THP1 cells at the *ASS1* intronic enhancer site **(Figure 5-14)**. Notably, these repressive histone modifications were not confined to the ATF4 binding site in T-cells, but were also higher at the *ASS1* promoter, suggesting that the gene might be in a repressive chromatin state **(Figures 5-13, top panel and 5-14)**. Consistent with this, H3K4me3 at the promoter was strongly depleted in T-cells compared to THP1 cells **(Figure 5-13, bottom panel)**. In contrast, levels of H3K9me2, H3K9me3 and H3K27me3 at the ATF4-binding site in *SLC7A1*, a gene that transcriptionally responds to arginine deprivation comparably in THP1 and T-cells, were similarly low in the two cell types **(Figure 5-13)**.

More strikingly, in T-cells but not THP1 cells, arginine starvation produced a strong elevation in the levels of both H3K9me2/3 and H3K27me3 at all loci tested **(Figures 5-13, top panel and 5-14)**. This may indicate the presence of a protective large-scale gene shutdown program in response to significant nutritional stress, consistent with the downregulation of ~2500 genes **(Figure 4-2)**.

As H3K9 methylation is often found associated with DNA methylation [373] we analysed the ASS1 locus by bisulfite sequencing, concentrating on the promoter and intronic ATF4 binding site **(Figure 5-15)**. Unlike previous reports of ASS1 being silenced by promoter DNA methylation in a number of tumours, we found that the CpG-rich promoter of ASS1 is almost exclusively non-methylated in both THP1 and T-cells, indicating that this is not the mechanism for differential regulation **(Figure 5-15)**. In contrast, the intronic region was much less CpG-dense, and in general more heavily methylated in both cell types. However, the upstream portion, which interestingly incorporates the ATF4 consensus motif, shows a higher degree of cytosine methylation in T-cells compared to THP1, in particular at CpG +3601, with 80% methylation in T-cells and 0% methylation in THP1 **(Figure 5-15)**.

Taken together, these findings argue that *ASS1* expression is regulated by the ability of ATF4 to access its internal enhancer. In T-cells, the ASS1 enhancer exists in a more repressive chromatin environment, with higher levels of H3K9 and DNA methylation and reduced accessibility, which prevents ATF4 binding and so blocks gene induction. In THP1 cells, this repressive environment is absent, allowing an accessible chromatin structure to facilitate ATF4 binding and gene activation.

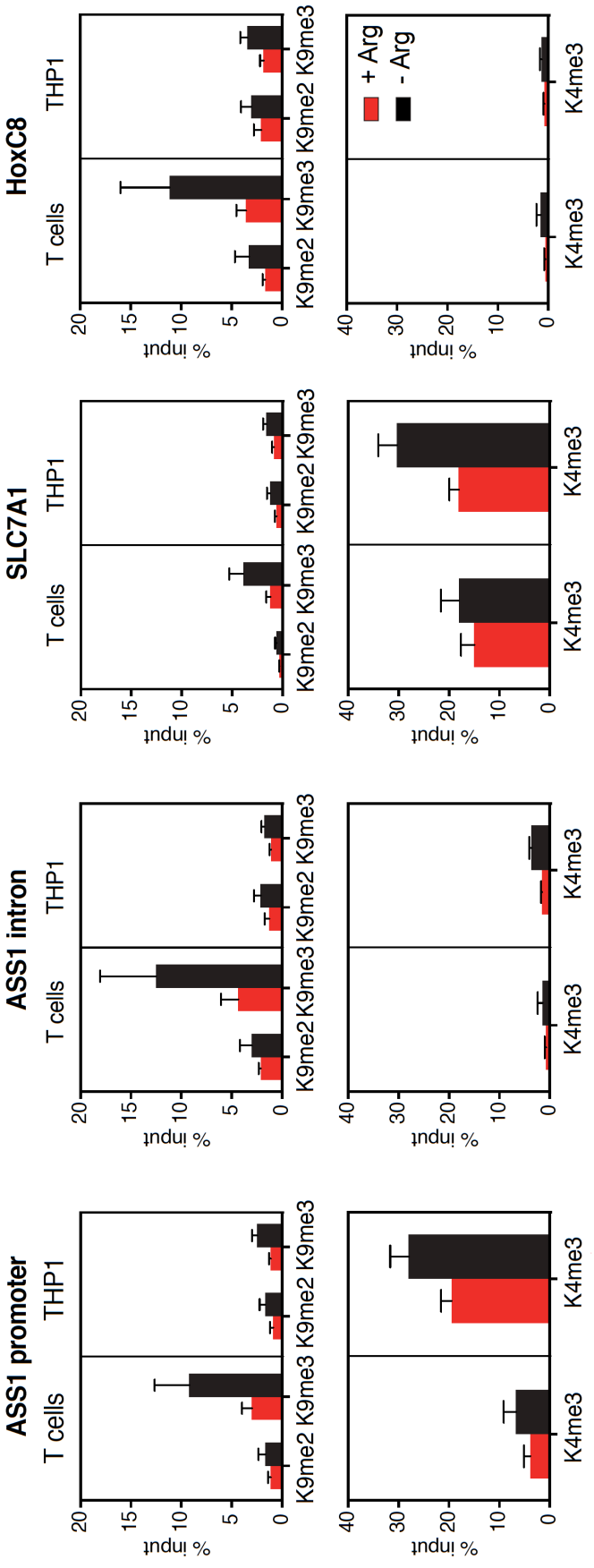

HoxC8
SLC7A1
ASS1 intron
ASS1 promoter
T cells
THP1
% input
K9me2
K9me3
K4me3
+ Arg
- Arg

**Figure 5 - 13. Lack of chromatin accessibility and ATF4 binding at the ASS1 intronic enhancer in T-cells is the result of conspicuous repressive heterochromatic histone modifications H3K9me2 and H3K9me3.**
Having identified restricted chromatin accessibility at the promoter and intronic enhancer of ASS1 in T-cells, but not THP1 cells, we performed a ChIP for various histone modifications. This ChIP reveals the existence of a repressive chromatin environment at the ASS1 locus in T-cells (but not THP1 cells) in the form of heterochromatic histone modifications H3K9me2 and H3K9me3. H3K9me2/3 is significantly higher ($p<0.001$) in T-cells compared to THP1 cells at both the ASS1 promoter and intronic enhancer (at normal arginine levels; red) and is further enhanced in the absence of arginine (black), an effect not seen in THP1 cells (panels 1 and 2; top row). At the same sites, the levels of the active H3K4me3 were also found to be lower in T-cells compared to THP1 cells (panels 1 and 2; bottom row). In contrast, low H3K9me2/3 and high H3K4me3 levels were detected in both cell types at the ATF4-binding region in SLC7A1, a gene that is expressed in both T-cells and THP1 cells (panel 3; top and bottom rows). HoxC8, a non-expressed gene in either cell type, was used as negative control (panel 4; top and bottom rows). Bars represent mean with standard deviation derived from triplicate measurements.

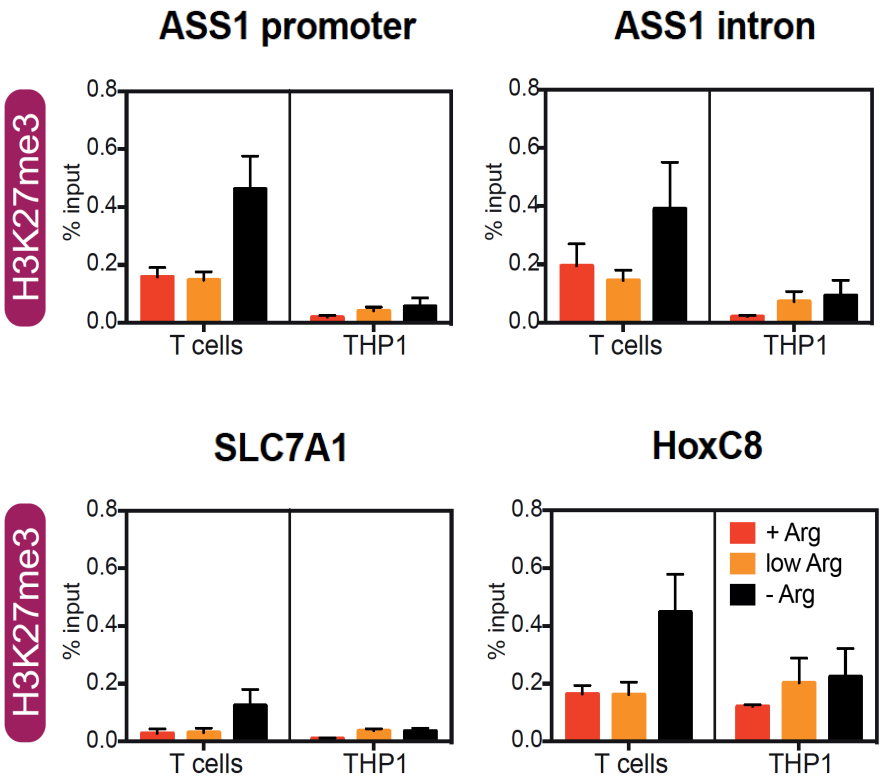



**Figure 5 - 14. High levels of the repressive heterochromatic histone modification H3K27me3 also lead to reduced chromatin accessibility and ATF4 binding at the ASS1 intronic enhancer in T-cells.**
ChIP reveals the existence of high levels of the repressive heterochromatic histone modification H3K27me3 at the ASS1 locus in T-cells but not THP1 cells with similar pattern to H3K9me2 and H3K9me3. H3K27me3 is significantly higher ($p<0.001$) in T-cells compared to THP1 cells at both the ASS1 promoter and intronic enhancer even at arginine-sufficient conditions (red) but is further enhanced in the absence of arginine

(black) but not in low arginine conditions (yellow), an effect less pronounced in THP1 cells (top panels). In contrast, low H3K27me3 levels were detected in both cell types at the ATF4-binding region in SLC7A1, a gene that is expressed in both T-cells and THP1 cells (bottom left panel). HoxC8, a non-expressed gene in either cell type, was used as negative control to show high H3K27me3 levels in both THP1 and T-cells (bottom right panel). Bars represent mean with standard deviation derived from triplicate measurements.

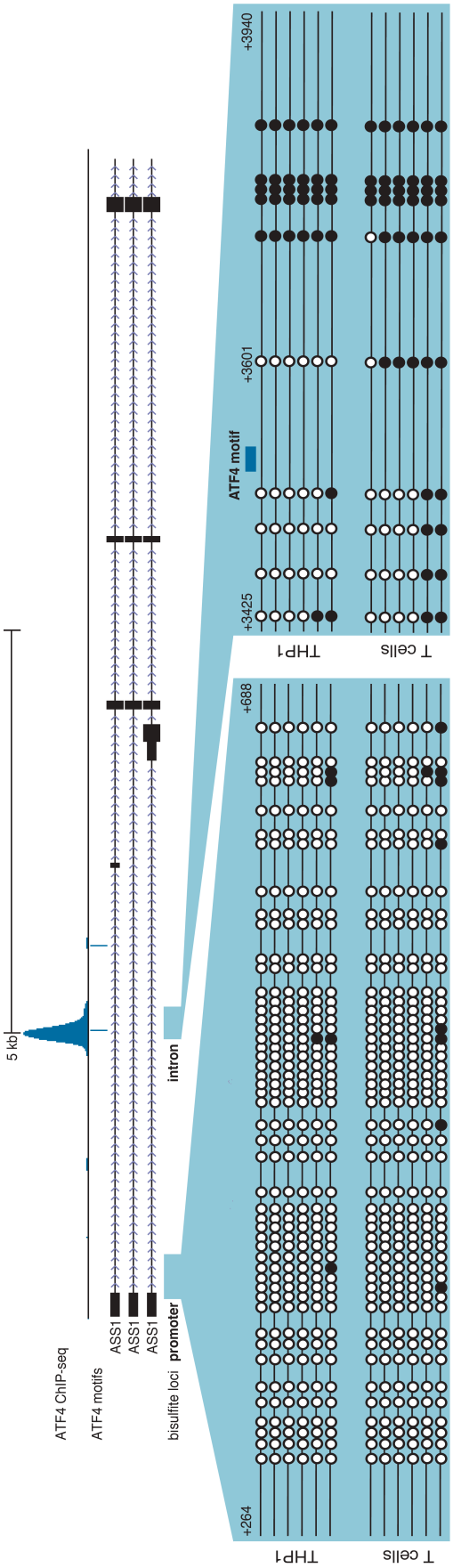

+3940
+3601
ATF4 motif
+3425
T cells
THP1
+688
+264
T cells
THP1
intron
promoter
5 kb
ATF4 ChIP-seq
ATF4 motifs
ASS1
ASS1
ASS1
bisulfite loci

**Figure 5 - 15. DNA methylation at the ASS1 intronic enhancer is more pronounced in T-cells than THP1 cells further restricting chromatin accessibility and ATF4/ CEBPβ binding.**
Bisulphite sequencing analysing DNA methylation status of CpG islands reveals a non-methylated ASS1 promoter (highlighted region on left) in both THP1 and T-cells and significantly higher levels of DNA methylation at the intronic enhancer (highlighted region on right).

## 5.7 The repressive H3K9me2/3 may be regulated by KDM4C

The histone H3K9 demethylase KDM4C has been suggested to be recruited to ATF4-target genes [374], which may explain the reduced H3K9 methylation at ASS1 observed in THP1 cells compared to T-cells. Indeed, our preliminary data show that treatment of THP1 cells with the KDM4C inhibitor SD70, enhanced H3K9me3 and thus abrogated ATF4 binding at the ASS1 enhancer **(Figure 5-16A, B)**. Consequently, SD70 treatment abolished induction of ASS1 expression upon arginine starvation in THP1 cells **(Figure 5-17)**. Furthermore, patient AML blasts showed higher transcript levels of *KDM4C* compared to healthy cells **(Figure 5-18)**. These findings are consistent with the hypothesis that reduction in H3K9 methylation in THP1 cells may provide a mechanism to facilitate induction of ASS1.

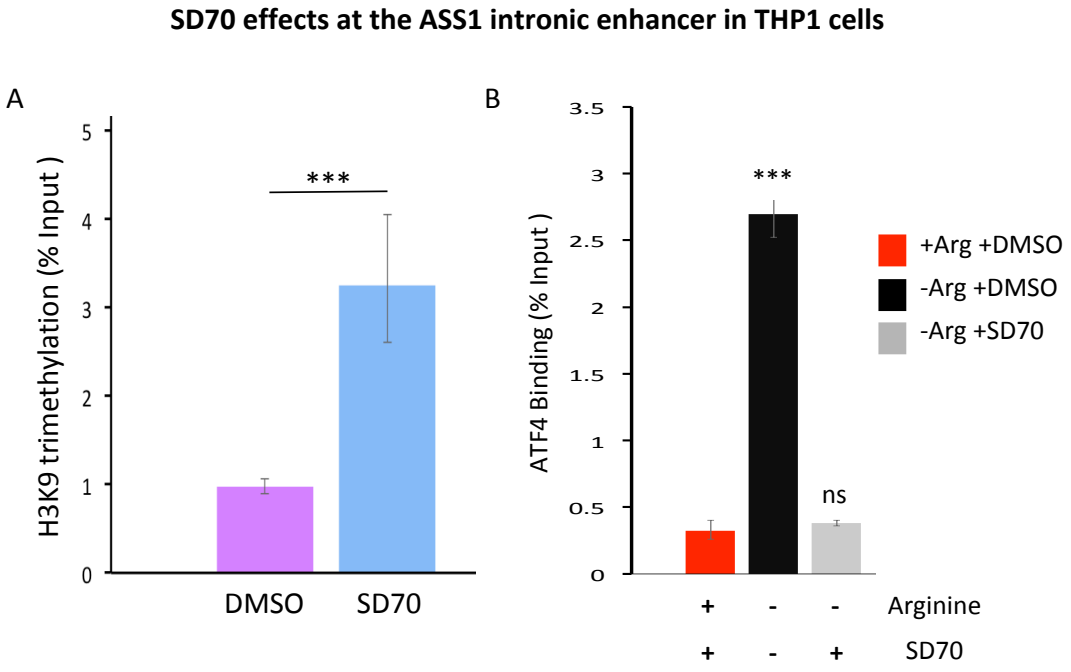



**Figure 5 - 16. SD70 inhibits KDM4C-mediated H3K9 demethylation abrogating ATF4 binding at the ASS1 intronic enhancer in cancer cells.**
THP1 cancer cells were cultured in differential R10 medium for 72 hrs and treated with SD70, a pharmacological inhibitor of KDM4C the enzyme that demethylates H3K9 or with DMSO. (A) ChIP for H3K9me3 shows that when compared to the negative control (DMSO treatment; pink), SD70 (blue) was able to prevent the reduction in the levels of the repressive H3K9me3 at the ASS1 intronic enhancer. (B) ATF4 ChIP shows that the augmentation of ATF4 binding at the ASS1 intronic enhancer observed in response to arginine starvation (black) from baseline (arginine-sufficient medium; red) is completely abolished in the presence of SD70 (grey). Bars represent mean with standard deviation derived from triplicate measurements. *** denotes $p<0.001$, ns denotes not significant ($p>0.05$). Comparisons were made against conditions of arginine-sufficiency with DMSO.

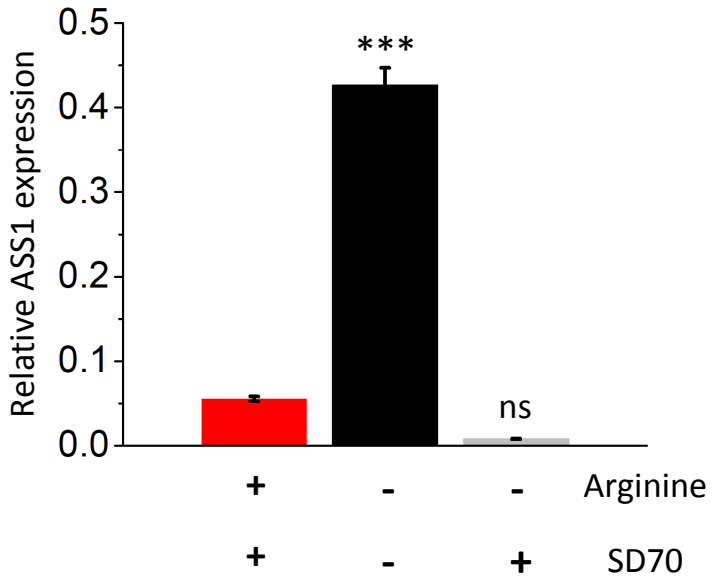



**Figure 5 - 17. SD70 inhibits ATF4-mediated ASS1 upregulation in response to arginine starvation in THP1 cells.**
THP1 cancer cells were cultured in differential R10 medium for 72 hrs and treated with SD70, a pharmacological inhibitor of KDM4C the enzyme that demethylates H3K9 or with DMSO. qRT-PCR shows that *ASS1* upregulation in response to arginine starvation (black) from baseline (arginine-sufficient medium; red) is completely abolished in the presence of SD70 (grey). Bars represent mean with standard deviation derived from triplicate measurements. Expression was relative to the housekeeping gene *GAPDH*. *** denotes $p<0.001$, ns denotes not significant ($p>0.05$).

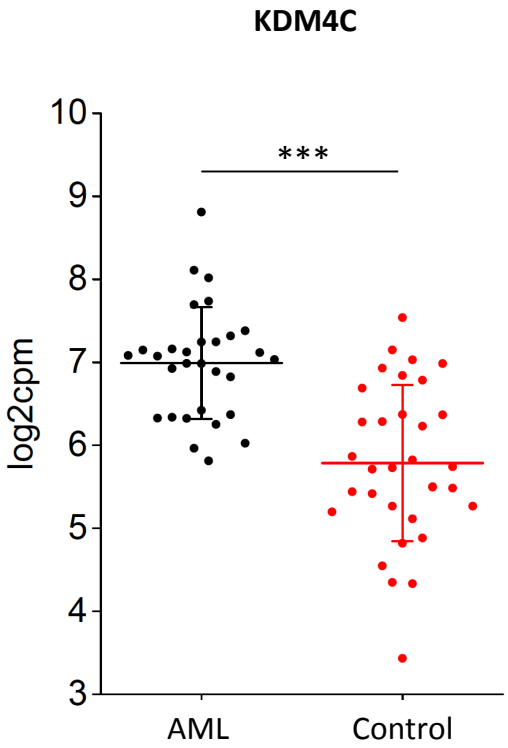



**Figure 5 - 18. KDM4C is overexpressed in AML blasts from patients compared to myeloid cell populations from healthy controls.**
RNA-seq analysis shows that *KDM4C* is expressed at significantly higher levels in AML patient blasts (black) compared to myeloid cells from healthy individuals (red). Bars represent mean and standard deviation. *** $p < 0.001$.

## 5.8 ATF4 might cooperate with CEBPβ to bind to the ASS1 enhancer and regulate ASS1 expression

Given that CEBPβ had previously been suggested to be a binding partner of ATF4 [371, 372, 375-377] and our earlier finding of the two transcription factors sharing multiple common binding sites across the genome **(Figure 5-6)**, we decided to investigate whether CEBPβ has a role to play in cooperating with ATF4 for binding to the *ASS1* intronic enhancer. Thus, we questioned whether an ATF4/CEBPβ binding motif was present at the site of the *ASS1* intronic enhancer. Using bioinformatics methods, more specifically a Deep Neural Network model known as 'deepbind', in collaboration with Dr Hashem Koohy, we analysed the *ASS1* locus looking for binding motifs for transcription factors

focusing mainly on the gene promoter and the intronic enhancer identified in our work earlier. We established that the transcription factors ATF4, CEBPβ, Xbp1 and RUNX2 all have specific binding sites within the *ASS1* enhancer **(Figure 5-19)** whereas the transcription factors MYC and Xbp1 had specific binding sites within the *ASS1* promoter **(Figure 5-20)**. The binding scores for each transcription factor were evaluated by comparisons between specific motifs at the enhancer, promoter, and random regions in the genome as shown in **Figure 5-21**.

More importantly, we showed that the specific binding site for ATF4 coincided with that for CEBPβ within the *ASS1* enhancer **(Figure 5-19)**. Our sequence analysis identified an ATF4/CEBPβ binding motif (TGATGCAA) at the same location **(Figure 5-22)** suggesting that ATF4 and CEBPβ might potentially regulate ASS1 expression in synergy. This specific binding region was confirmed by ATF4 and CEBPβ ChIP-seq providing further evidence that the two transcription factors co-localise at the same region and potentially cooperate in order to regulate *ASS1* expression in response to nutritional stresses such as arginine starvation **(Figure 5-22, panels 1-2)**. As already shown earlier **(Figure 5-7, panels 4-5)**, we could only detect significant CEBPβ binding at the *ASS1* intronic enhancer in THP1 cells but not T-cells, similar to ATF4.

Guided by the results of our CEBPβ ChIP-seq and transcription factor Deepbind bioinformatics analysis at the *ASS1* locus, we tested CEBPβ binding further. Firstly, we confirmed CEBPβ binding at the *ASS1* intronic enhancer by ChIP-qPCR and observed that this binding might be stronger in THP1 cells compared to T-cells both at basal levels and following arginine starvation **(Figure 5-23, shaded box)**. Furthermore, we showed that upon arginine starvation CEBPβ binding increased at the ASS1 enhancer in THP1 cells but not in T-cells, following the same pattern as ATF4 binding **(Figure 5-23, shaded box)**. CEBPβ binding at other ATF4 bindings sites of other relevant genes such as *ASNS,*

*SLC7A1, SLC715* and *SLC7A5* did not differ significantly between T-cells and THP1 cells in the presence or absence of arginine **(Figure 5-23)**. Interestingly, our mutant THP1 cells, in which the ATF4-binding motif within the *ASS1* intronic enhancer had been deleted, showed not only complete abolition of ATF4 binding at this site but also abolition of CEBPβ binding **(Figure 5-24)**. Similar to ATF4, this mutation eliminated CEBPβ binding only at *ASS1*, but not at *SLC7A1* **(Figure 5-24)**. Given that CEBPβ follows a similar pattern to ATF4 in terms of its binding with specific enhancement at the *ASS1* intronic enhancer upon arginine starvation in THP1 but not in T-cells, further investigation is warranted on a functional level to understand the importance of its cooperation with ATF4 in regulating target gene expression.

Finally, our transcription factor Deepbind analysis revealed that the specific binding sites for MYC and Xbp1 at the *ASS1* promoter coincided, suggesting that these two transcription factors might cooperate at the promoter of the gene **(Figure 5-20)**. Given that Xbp1 is involved in cellular responses to external stress and can bind both the enhancer and promoter of the *ASS1* gene, there is a possibility that it might link the two regions through genome looping to allow epigenetic regulation of transcription. This is beyond the scope of this work but warrants further investigation.

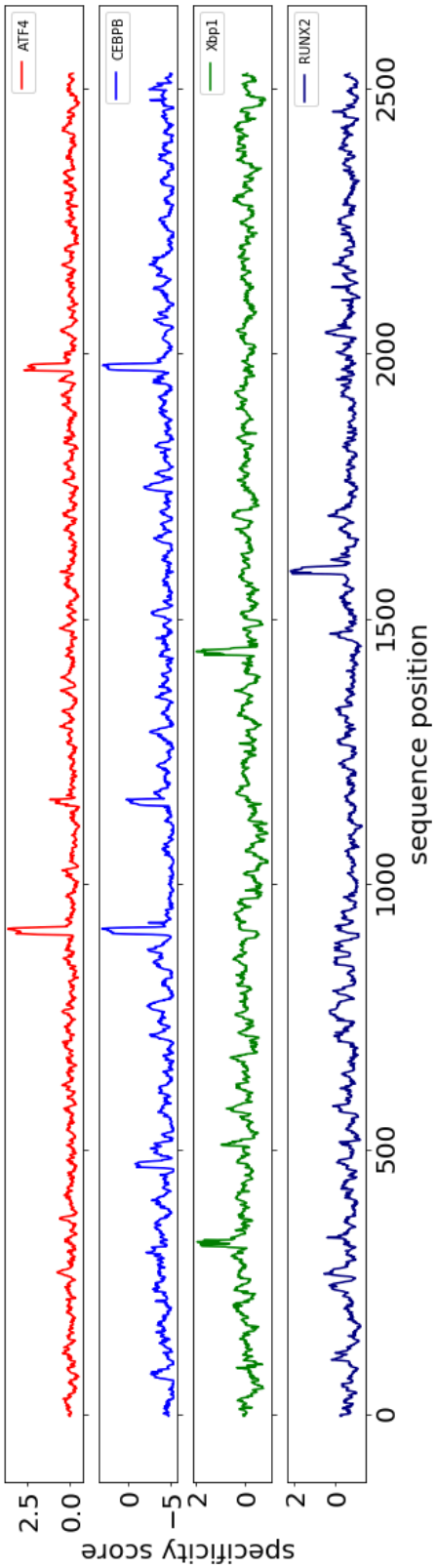



**Figure 5 - 19. The transcription factors ATF4, CEBPβ, Xbp1 and RUNX2 have specific binding sites within the *ASS1* enhancer.**
Deepbind analysis reveals binding motifs for transcription factors ATF4 (red), CEBPβ (blue), Xbp1 (green) and RUNX2 (purple) within the *ASS1* enhancer. ATF4 and CEBPβ share their binding sites confirming their cooperative partnership.

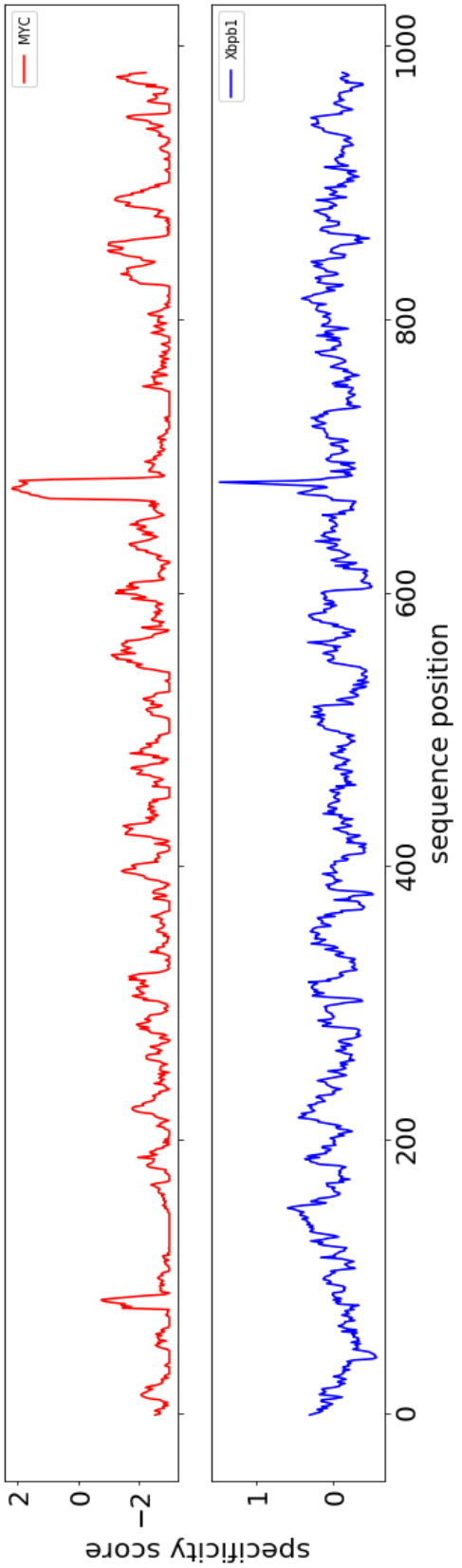
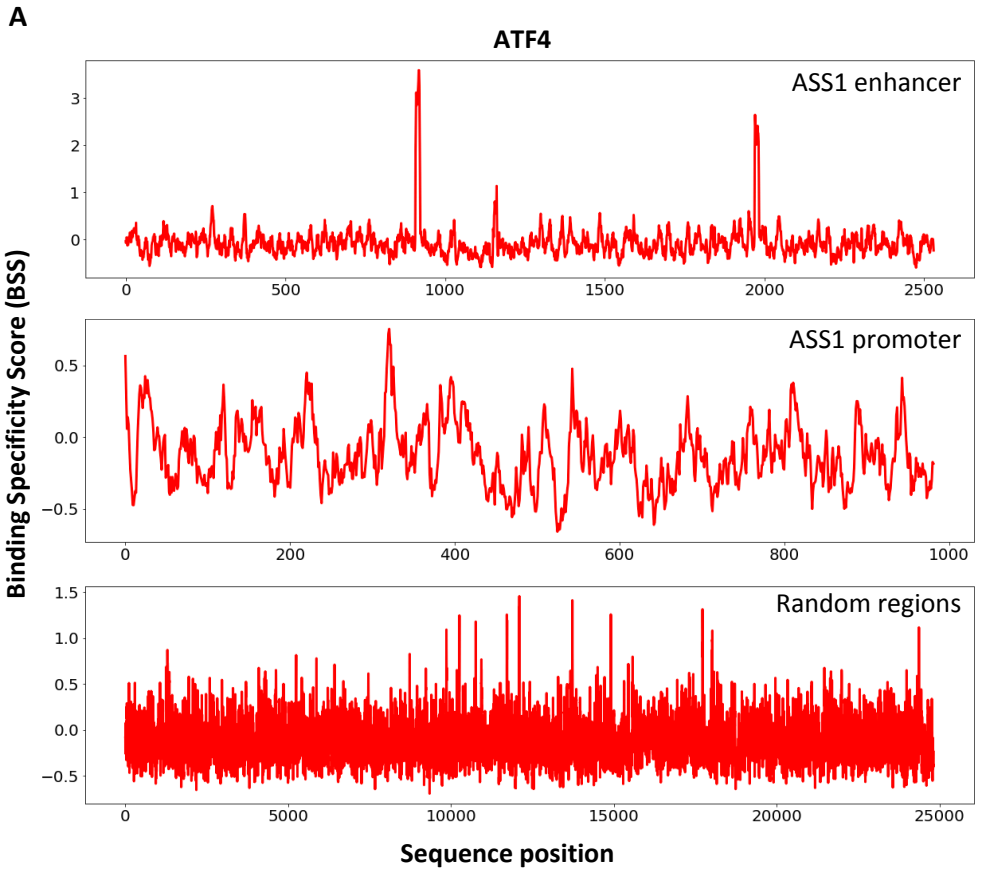
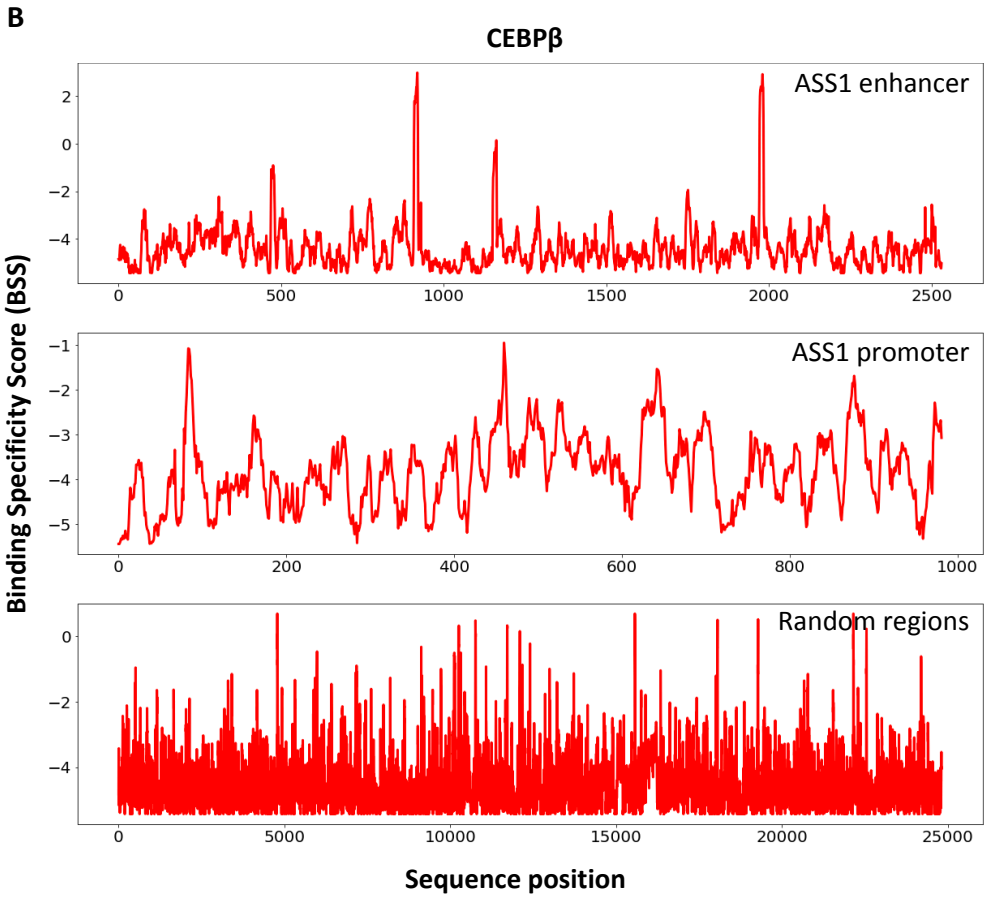
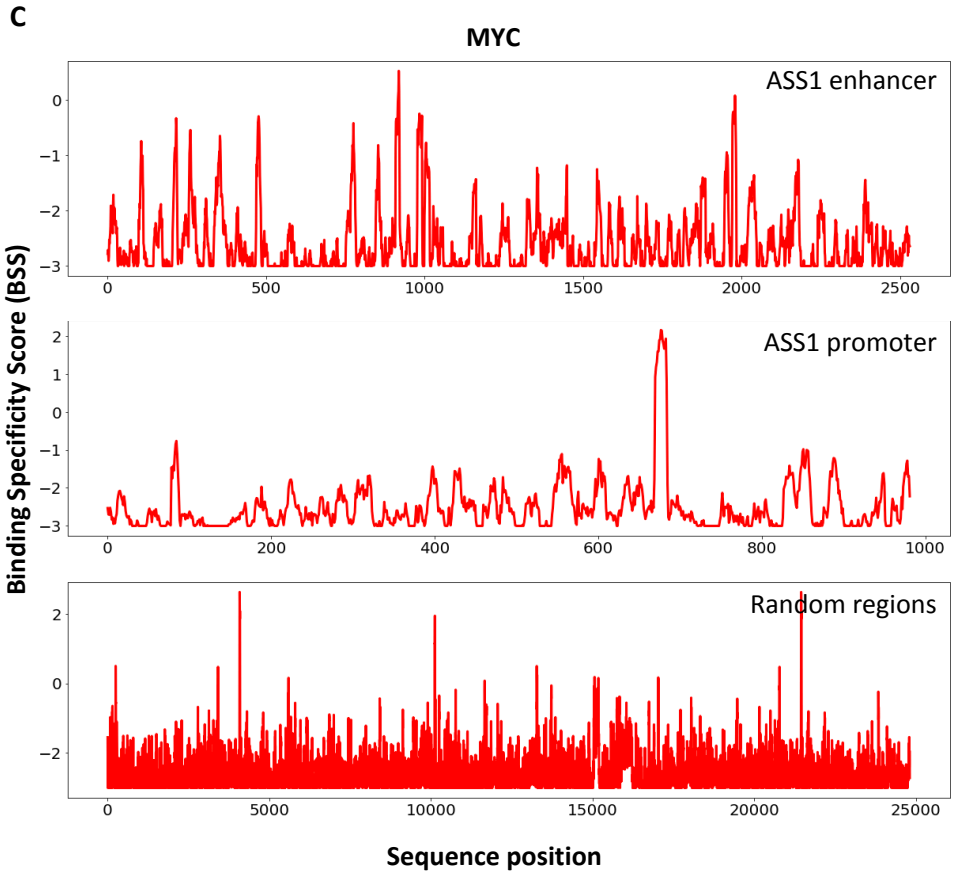
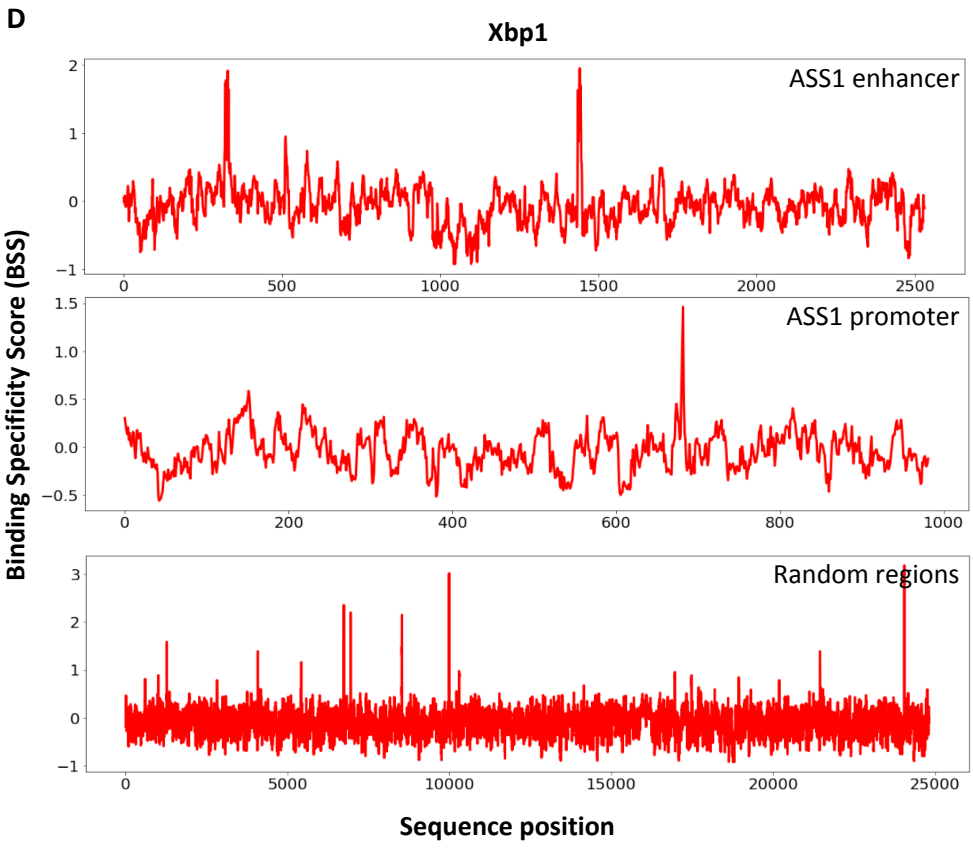



**Figure 5 - 20. The transcription factors MYC and Xbp1 have specific binding sites within the *ASS1* promoter.**
Deepbind analysis reveals binding motifs for transcription factors c-MYC (red) and Xbp1 (blue), which seem to coincide suggesting potential binding partnership.


A
ATF4
ASS1 enhancer
ASS1 promoter
Random regions
Binding Specificity Score (BSS)
Sequence position


B
CEBPβ
ASS1 enhancer
ASS1 promoter
Random regions
Binding Specificity Score (BSS)
Sequence position


C
MYC
ASS1 enhancer
ASS1 promoter
Random regions
Binding Specificity Score (BSS)
Sequence position


D
Xbp1
ASS1 enhancer
ASS1 promoter
Random regions
Binding Specificity Score (BSS)
Sequence position

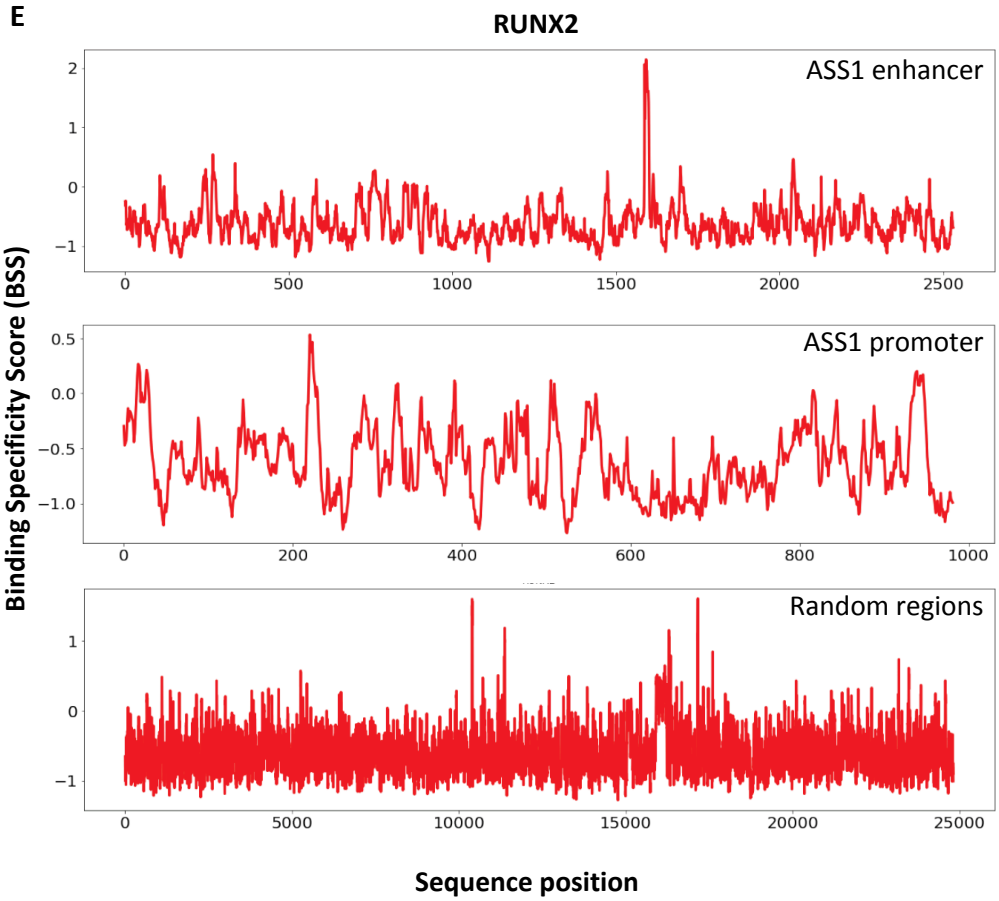



**Figure 5 - 21. Binding Specificity Score (BSS) analysis confirms strong binding signal for transcription factors ATF4, CEBPβ, Xbp1 and RUNX2 within the *ASS1* enhancer and strong biding signal for transcription factors c-MYC and Xbp1 within the ASS1 promoter.**
BSS was used to measure and compare the strength of binding of each of the transcription factors (A) ATF4, (B) CEBPβ, (C) Xbp1, (D) c-MYC and (E) RUNX2 at the *ASS1* enhancer, the *ASS1* promoter and random regions within the *ASS1* gene.

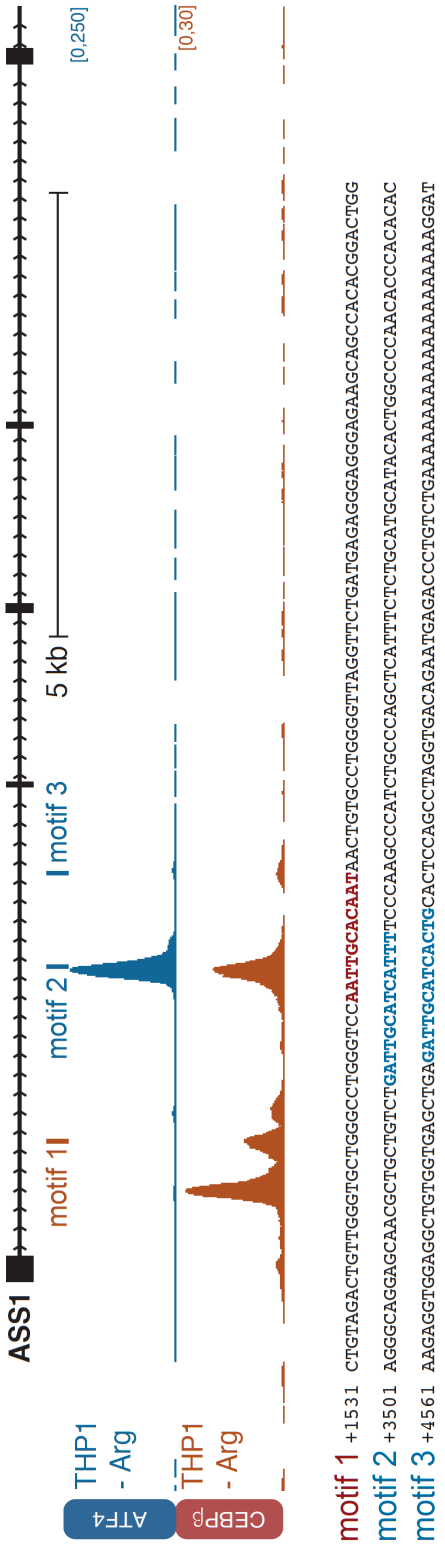



**Figure 5 - 22. Sequence analysis confirms an ATF4/CEBPβ binding motif within the *ASS1* intronic enhancer at the exact region where ATF4 and CEBPβ ChIP-seq reveal an overlapping binding site for the two transcription factors.**
Sequence analysis discloses an ATF4/CEBPβ binding motif (TGATGCAA) at the same location as the common binding site for ATF4 (blue) and CEBPβ (red) revealed by ChIP-seq at the *ASS1* intronic enhancer.

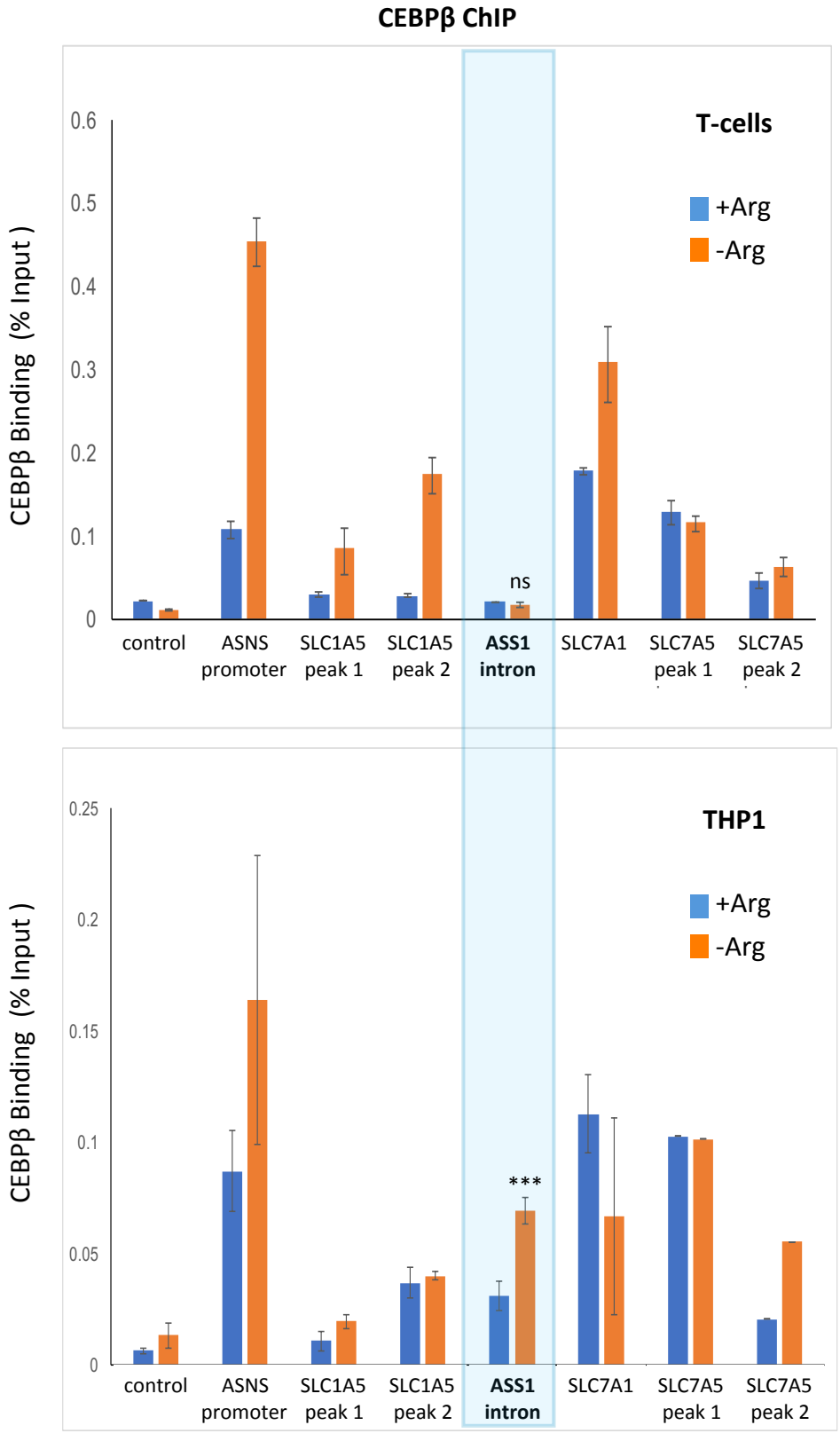



**Figure 5 - 23. CEBPβ ChIP-qPCR shows that CEBPβ binding at the ASS1 intronic enhancer only occurs in THP1 cells but not T-cells and is augmented in response to arginine starvation.**
ChIP-qPCR was performed for CEBPβ binding at various genes in THP1 and T-cells in sufficient arginine conditions (blue) and following exposure to arginine deficiency

(yellow). In contrast to ATF4/CEBPβ binding sites in enhancers or promoters of the *ASNS*, *SLC1A5*, *SLC7A1* and *SLC7A5* genes, CEBPβ binding at the ASS1 intronic enhancer is only detected in THP1 cells in which it is significantly augmented upon arginine starvation (highlighted area). T-cells display no CEBPβ binding at the ASS1 enhancer at neither baseline conditions nor following arginine starvation. Amongst the ATF4/CEBPβ binding sites analysed, the ASS1 intronic enhancer was the only one displaying this dichotomy in CEBPβ binding between THP1 and T-cells. These findings are in line with our earlier results suggesting that THP1 cells express significant ASS1 and upregulate expression further in response to arginine starvation whereas T-cells fail to do so and display negligible ASS1 expression. Bars represent mean with standard deviation derived from triplicate measurements. *** denotes $p<0.001$, ns denotes not significant ($p>0.05$).

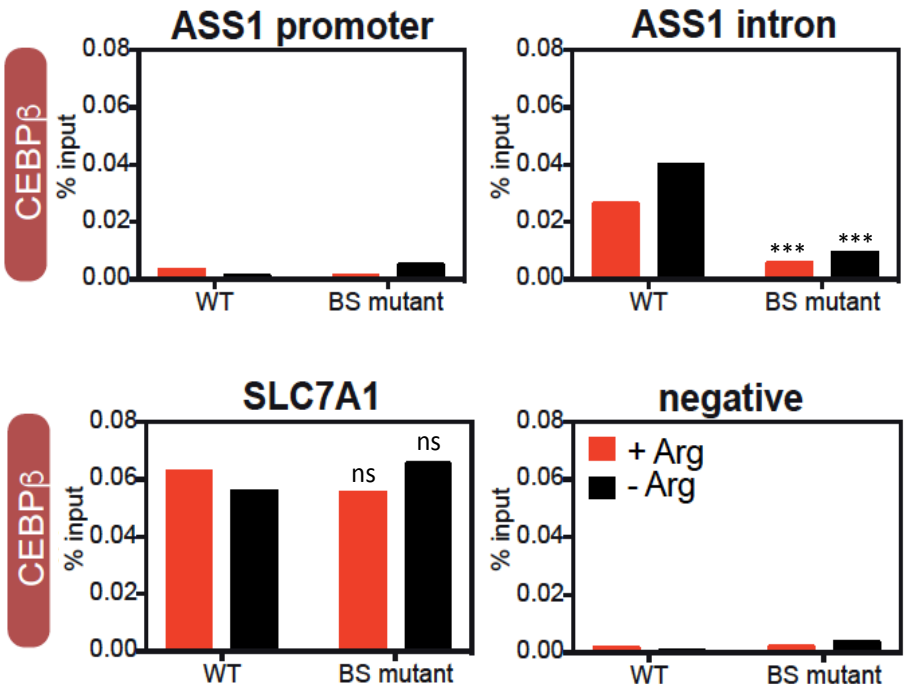



**Figure 5 - 24. Deletion of the ATF4/ CEBPβ-binding motif sequence in the ASS1 intronic enhancer in THP1 cells abolishes CEBPβ binding in a similar manner that ATF4 binding was abolished.**

The ATF4/CEBPβ-binding site (BS) motif within the ASS1intronic enhancer was deleted by CRISPR technology in THP1 cells so that wild-type (WT) and BS mutant cells could be compared. (B) CEBPβ ChIP-qPCR was performed at various regions of interest across the genome in WT and BS mutant THP1 cells in conditions of arginine sufficiency (red) and arginine deficiency (black). There is no CEBPβ binding detected at the ASS1 promoter in either cell type with no impact following exposure to arginine starvation (top left panel) reflecting a similar pattern to our negative control gene (HoxC8; bottom right panel). Significant CEBPβ binding is measured at the ATF4/CEBPβ binding site near the SLC7A1 promoter (our positive control) at baseline in both WT and BS mutant THP1 cells without difference (bottom left panel). CEBPβ binding is enhanced upon arginine starvation in both cell types (bottom left panel). In contrast, CEBPβ binding at the ASS1 intronic enhancer is only detected in WT THP1 cells in which it is significantly augmented

upon arginine starvation (top right panel). CEBPβ binding at the ASS1 enhancer is completely abolished in BS mutant THP1 cells compared to WT THP1 cells both at baseline and in conditions of arginine starvation (top right panel). Bars represent mean with standard deviation derived from triplicate measurements. Statistical comparisons were made for WT vs BS mutant cells in +Arg or –Arg. *** denotes $p<0.001$, ns denotes not significant ($p>0.05$).

## 5.9 Epigenetically-regulated ATF4 binding at the ASS1 intronic enhancer might be a phenomenon present in many cancers including solid tumours and in response to various types of nutritional stress

In Chapter 4 we showed that the ATF4-dependent ASS1 upregulation observed in THP1 is also observed in multiple other cancer cell lines including HeLa cells **(Figure 4-15)**. We also proved that ATF4 knockdown in HeLa cells abrogated ASS1 upregulation in response to arginine starvation and thus abolished the ability to utilize citrulline in order to proliferate in arginine-free environments **(Figure 5-3)**. Given these results, we investigated the possibility that epigenetic regulation at the level of the ASS1 intronic enhancer in HeLa cancer cells is analogous to that in THP1 cancer cells. Indeed, ChIP-seq analysis of HeLa cells revealed binding of ATF4 at the ASS1 intron not only upon arginine depletion but also in response to starvation of tryptophan (an amino acid which also induces upregulation of ATF4; [301] **(Figure 5-25, panel 2)**. ATF4 ChIP-seq in HeLa cells at the loci of other metabolic genes such as SLC7A1 **(Figure 5-8A, panel 2)** and ASNS **(Figure 5-8B, panel 2)** also showed an identical ATF4 binding profile to that observed in THP1 cell.

This suggests that the proposed mechanism of epigenetically-regulated ATF4 binding is not THP1-restricted but rather might be a common mechanism to regulate the expression of ASS1, and possibly other metabolic genes, in many cancer cells including solid tumours in response to nutritional stress. It likely represents an acquired characteristic of many

tumour cells, and may determine the difference in growth potential between T-cells and cancer cells. Our results might also suggest that starvation of amino acids other than arginine, such as the essential amino acid tryptophan, causes a similar nutritional stress response by inducing ATF4-dependent phenomena governed by similar mechanisms of epigenetic regulation.

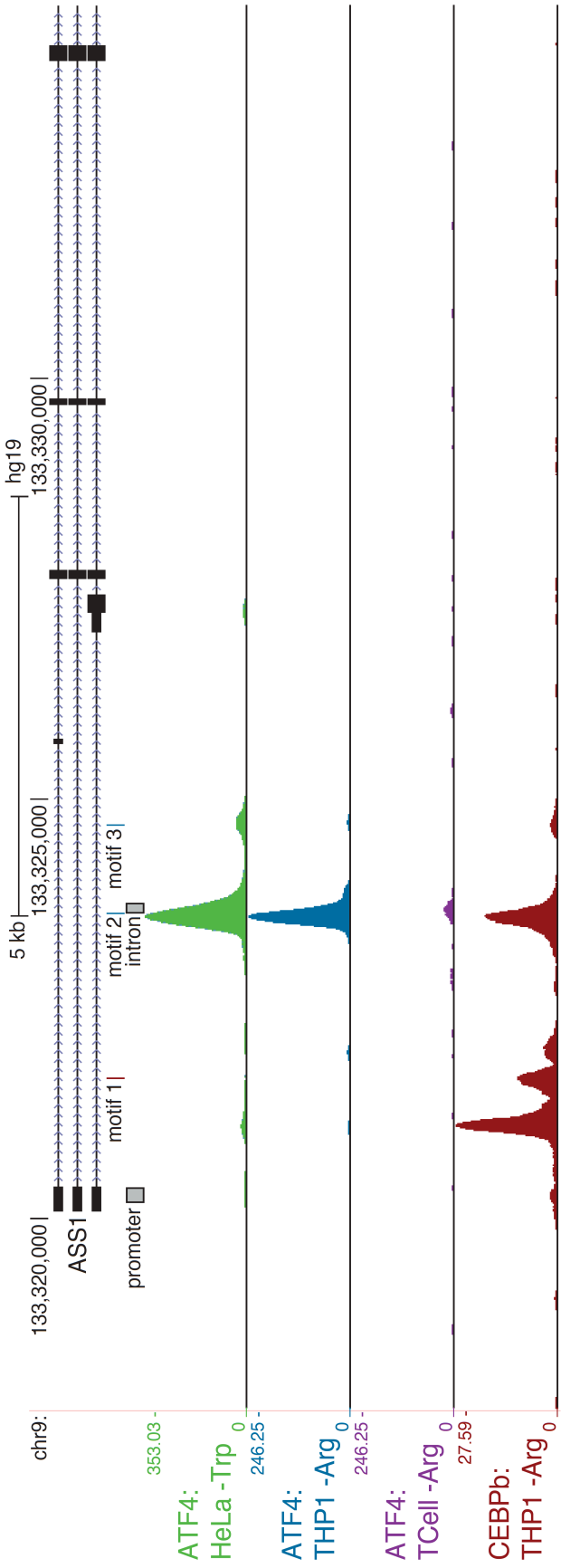

hg19
133,330,000
133,325,000
5 kb
133,320,000
chr9:
ASS1
promoter
motif 1
motif 2
intron
motif 3
353.03
ATF4:
HeLa -Trp
0
246.25
ATF4:
THP1 -Arg
0
246.25
ATF4:
TCell -Arg
0
27.59
CEBPb:
THP1 -Arg
0

**Figure 5 - 25. ATF4 binding at the *ASS1* enhancer is a phenomenon observed not only in THP1 but also HeLa cancer cells and occurs in response to tryptophan starvation in addition to arginine starvation.**
ChIP-seq analysis of HeLa cells (panel 1) reveals binding of ATF4 at the *ASS1* intronic enhancer not only upon arginine deprivation but also in response to starvation of tryptophan. These findings suggest that ATF4-dependent *ASS1* expression might be a general response to nutritional stress in multiple liquid and solid cancer cells lines.

## 5.10 The epigenetic regulation of ASS1 appears to be a cancer-specific attribute rather than a lineage-related effect

We had earlier shown that the significant discrepancy between THP1 cells and T-cells in their ability to upregulate *ASS1* in response to arginine starvation is a cancer-specific feature rather than a lineage-specific feature as CD14+ monocytes from healthy donors behaved in the same way as T-cells, i.e. significantly less able to upregulate *ASS1* compared to THP1 cells **(Figure 4.11)**. In this section, we investigated whether the ATF4 binding at the *ASS1* intronic enhancer and the epigenetic regulation of this binding are also different between CD14+ monocytes and THP1 cells (in collaboration with Dr Mashiko Setshedi and Dr Nicholas Crump). Using ChIP-qPCR, we showed that, in CD14+ monocytes cultured for 48 hours under arginine starvation conditions, neither ATF4 nor CEBPβ binding could be detected at the *ASS1* intronic enhancer, although both were significantly bound at the *SLC7A1* promoter **(Figure 5-26, panels 1, 2)**. This was accompanied by high levels of repressive H3K9me3 **(Figure 5-26, panel 3)**, similar to those shown earlier for T-cells **(Figure 5-13)**. These results prove that the *ASS1* intronic enhancer in healthy monocytes has similar repressive epigenetic modifications as in healthy T-cells at and as such, is non-permissive to ATF4 (or CEBPβ) binding at that region leading to the inability of both cell types to perform ATF4-dependent *ASS1* upregulation in response to arginine starvation. All in all, these results indicate that the

ability of THP1 cells to upregulate *ASS1* is not a lineage-specific property but most likely a cancer-specific property acquired during the cellular transformation process.

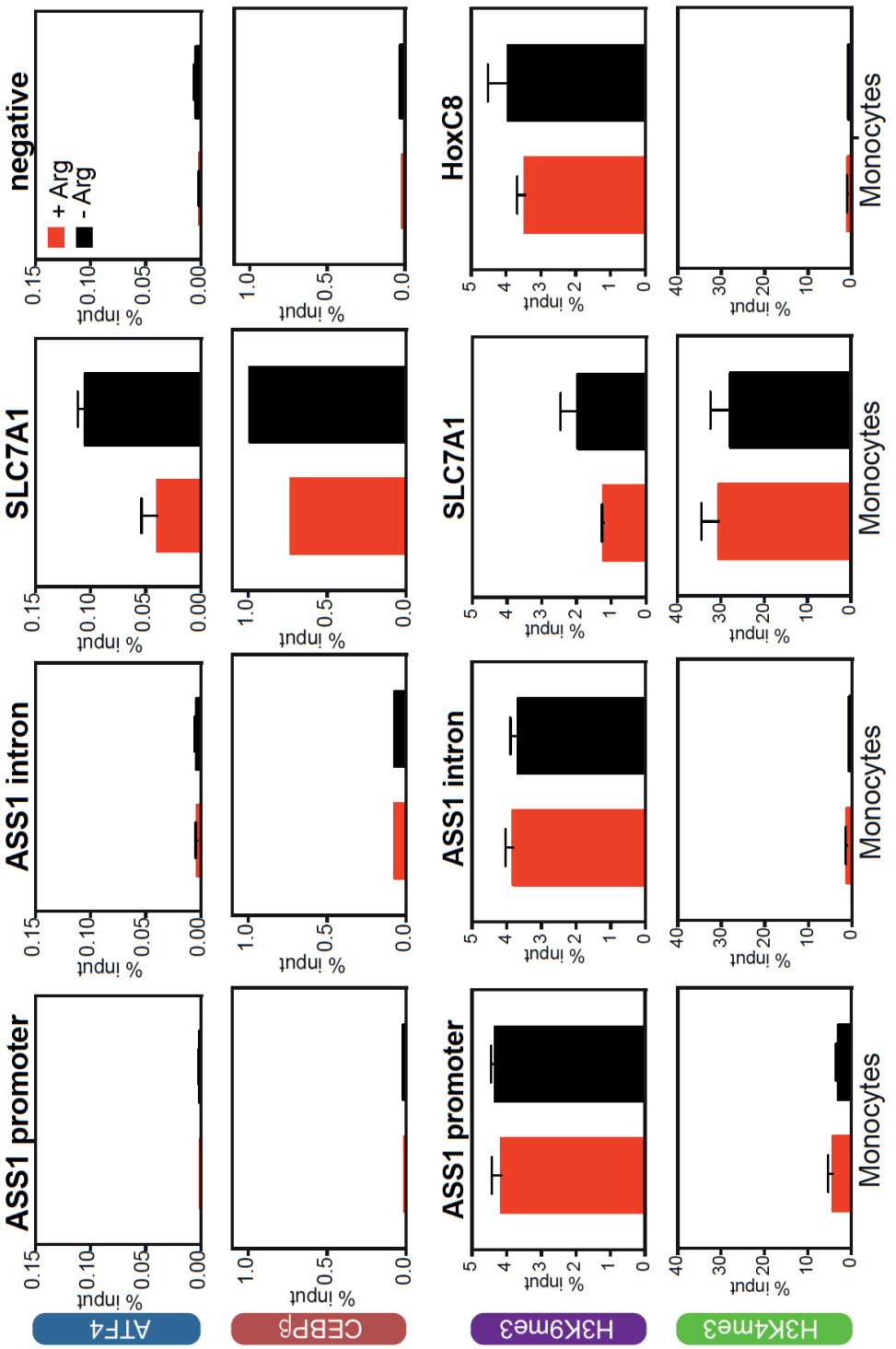


**Figure 5 - 26. The epigenetic regulation of ASS1 through ATF4/CEBPβ seems to be a cancer-specific attribute rather than a lineage-related effect as monocytes show the same features as T-cells rather than THP1 cancer cells.**
ChIP-qPCR for ATF4 (first row) and CEBPβ (second row) binding in monocytes shows similar pattern to T-cells. ATF4 and CEBPβ binding is negligible at both the *ASS1* promoter and the *ASS1* enhancer with levels similar to the negative control gene *HoxC8* and is unaffected by arginine starvation. Significant ATF4 and CEBPβ binding occurs at the *SLC7A1* promoter (positive control) with slight increase upon arginine starvation. Histone modification ChIP in monocytes/macrophages for the repressive H3K9me3 (third row) and the activating H3K4me3 (fourth row) reveals a similar pattern to T-cells with the existence of a repressive chromatin environment at the *ASS1* locus. H3K9me3 is enriched in monocytes at both the *ASS1* promoter and intronic enhancer whereas, at the same sites, the levels of H3K4me3 are negligible. Both histone modifications at these regions showed similar levels to the negative control *HoxC8* (a silent gene) suggesting the presence of repressive heterochromatin. In contrast, lower H3K9me3 and higher H3K4me3 levels were detected at the ATF4/CEBPβ binding region in the *SLC7A1* promoter, again mimicking the in T-cells. Bars represent mean with standard deviation derived from triplicate measurements.

## 5.11 The upregulation of citrulline transporters SLC1A5 and SLC7A5 upon arginine starvation in THP1 cancer cells might also be regulated by ATF4/CEBPβ binding at internal enhancers

Having shown in Chapter 4 that SLC1A5 (ASCT2) and SLC7A5 (LAT1) might be the crucial transporters allowing entry of extracellular citrulline into the cell for conversion to arginine in cancer cells, we decided to look at their regulation more closely. We had already established by qRT-PCR that, in response to arginine starvation, THP1 cells are able to transcriptionally upregulate *SLC1A5* and *SLC7A5* **(Figure 4-19A)**. This finding was in line with earlier results from our microarray suggesting that arginine depletion induced *SLC1A5* and *SLC7A5* upregulation in both THP1 cells and T-cells, although the effect was more pronounced in the former cell type **(Figure 5-5)**. We were also guided by our observations and previous findings in our lab suggesting that cellular ATF4 knockdown abolished *SLC1A5* upregulation in response to tryptophan or arginine starvation [1, 301]. Thus, we decided to investigate the epigenetic regulation of the

transcription of *SLC7A5* and *SLC1A5* and asked whether or not ATF4 and CEBPβ directly bind to these genes. Using ChIP-seq, we showed that both ATF4 and CEBPβ do indeed bind to one and the same intronic region within the *SLC1A5* locus **(Figure 5-27, panels 1, 2)** and one and the same intronic region within the *SLC7A5* locus **(Figure 5-28, panels 1, 2)**. By mapping the histone profile at those regions, we established that they are both active enhancers in light of the typical flanking by H3K4 monomethylation and H3K27 acetylation **(Figure 5-27, panels 6-8 and Figure 5-28, panels 6-8)**.

Having identified ATF4-binding sites in both of our proposed citrulline transporter genes, we used ChIP-qPCR to show that arginine starvation increased ATF4 binding at both the *SCL1A5* and *SLC7A5* intronic enhancer in THP1 cells **(Figure 5-29)**. As a positive control, we used ASNS, a gene known to be involved in amino acid metabolism, having previously shown that it is bound to its promoter by ATF4 **(Figure 5-8B)**. Intriguingly, although in THP1 cells arginine starvation enhanced ATF4 binding in all 3 genes, in T-cells, ATF4 binding was only significantly enhanced at the ASNS promoter and the SLC7A5 enhancer **(Figure 5-29)**. In the case of the SLC1A5 intronic enhancer, arginine starvation had negligible effect on ATF4 binding in T-cells unlike THP1 cells where ATF4 binding was significantly enhanced **(Figure 5-29)**. Overall, although the ATF4 binding levels at the *SLC1A5* and *SLC7A5* introns did not significantly differ between THP1 and T-cells, the former cell type showed more plasticity in response to arginine starvation with a more pronounced gene upregulation effect suggesting better adaptability to nutritional stress **(Figure 5-29)**. Using ATAC-seq in THP1 cells, we showed that DNA at the *SLC7A5* intronic enhancers was widely accessible to transcription factors irrespective of the arginine concentration **(Figure 5-28, panels 3-5)**. Contrary to this, in the case of the *SLC1A5*, low or absent arginine THP1 conditions significantly enhanced DNA accessibility at the enhancer region when compared to normal arginine levels **(Figure 5-**

**27, panels 3-5)**. This finding potentially explains the increase in ATF4 binding observed at the *SLC1A5* but not the *SLC7A5* enhancer in THP1 cells and again supports the case of epigenetic modifications and governing the regulation of gene expression via transcription factor binding facilitation or obstruction.

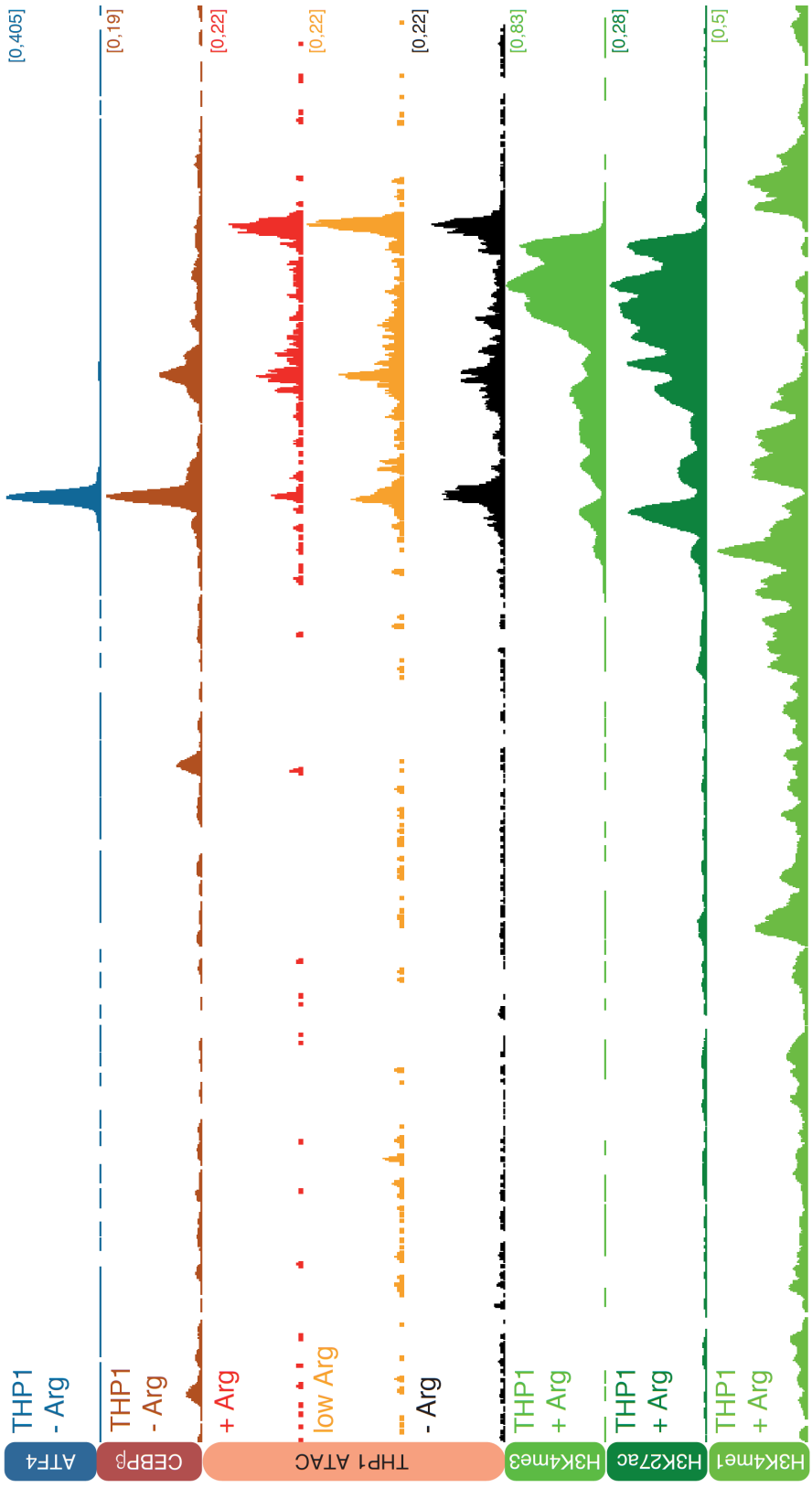

SLC1A5
10 kb
[0,405]
[0,19]
[0,22]
[0,22]
[0,22]
[0,83]
[0,28]
[0,5]
THP1 - Arg
THP1 - Arg
+ Arg
low Arg
- Arg
THP1 + Arg
THP1 + Arg
THP1 + Arg
ATF4
CEBPβ
THP1 ATAC
H3K4me3
H3K27ac
H3K4me1

**Figure 5 - 27. ATF4/CEBPβ ChIP-seq, ATAC-seq for chromatin accessibility and histone modification analysis in THP1 cells reveal the presence of an arginine-sensitive intronic enhancer near the promoter of the *SLC1A5* gene locus.**
A ChIP-seq was performed for ATF4 and its potential binding partner CEBPβ in THP1 cancer cells under conditions of arginine starvation (panels 1-2). This revealed the presence of an ATF4/CEBPβ binding site with strong signal in the first intron of the *SLC1A5* locus. Assay for Transposase-Accessible Chromatin using sequencing (ATAC-Seq) shows that chromatin accessibility at the intronic enhancer, where the ATF4 and CEBPβ transcription factors bind, is significantly enhanced upon arginine deprivation or complete starvation in THP1 cells (panels 3-4), an effect not observed at the promoter of the same gene. Analysis of histone modifications discloses that this binding site is flanked by peaks of Histone 3, lysine 4, monomethylation (H3K4me1) and enriched with Histone 3, lysine 27, acetylation (H3K27ac), epigenetic features that are characteristic of an active enhancer (panels 7-8). Additionally, the gene promoter was rich in Histone 3, lysine 4, trimethylation (H3K4me3) an epigenetic mark typical of promoter regions (panel 6). These results are in line with the *SLC1A5* upregulation observed in response to arginine starvation in cancer cells.

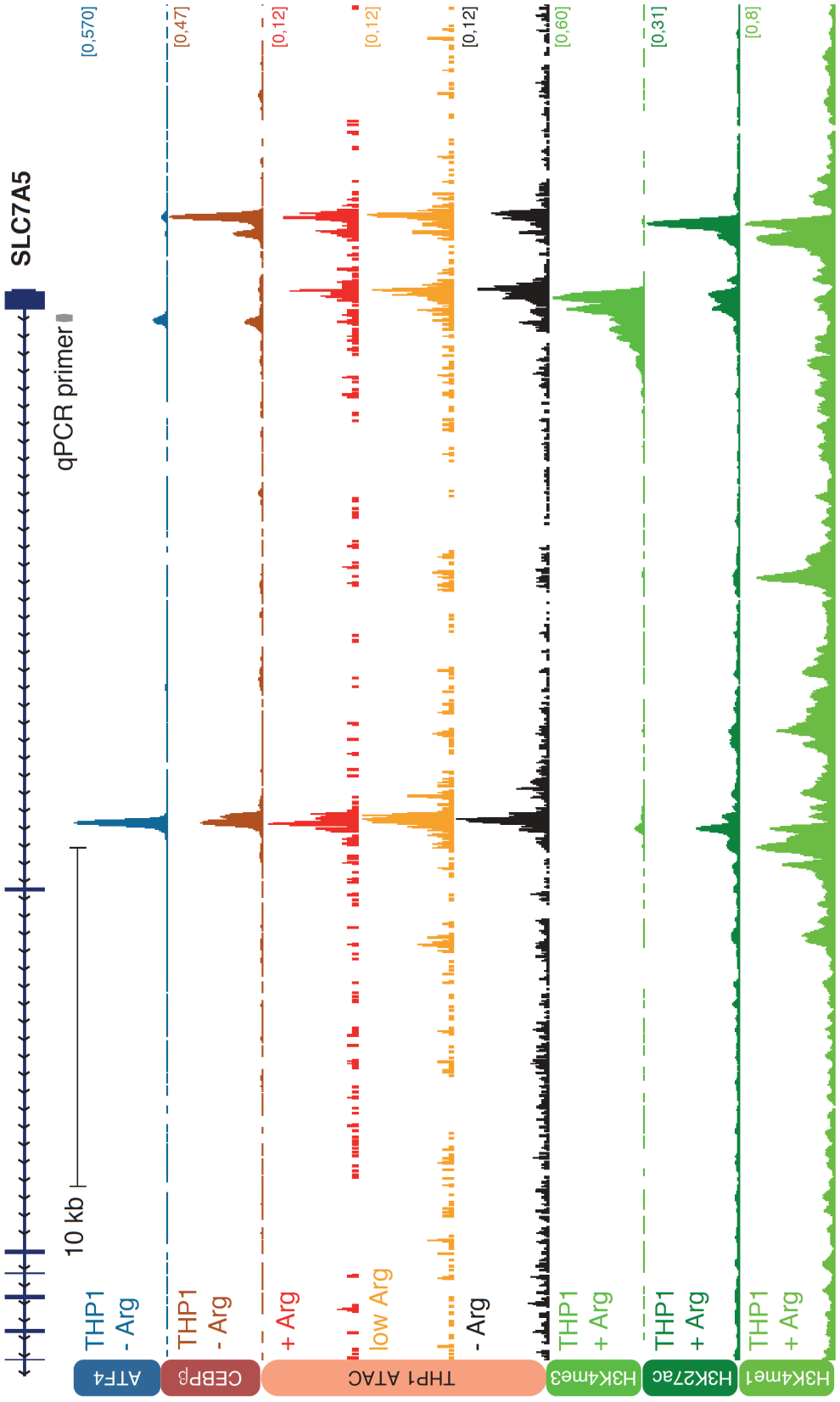

SLC7A5
qPCR primer
10 kb
[0,570]
[0,47]
[0,12]
[0,12]
[0,12]
[0,60]
[0,31]
[0,8]
THP1 - Arg
THP1 - Arg
+ Arg
low Arg
- Arg
THP1 + Arg
THP1 + Arg
THP1 + Arg
ATF4
CEBPβ
THP1 ATAC
H3K4me3
H3K27ac
H3K4me1

**Figure 5 - 28. ATF4/CEBPβ ChIP-seq, ATAC-seq for chromatin accessibility and histone modification analysis in THP1 cells reveal the presence of an arginine-sensitive intronic enhancer near the promoter of the *SLC7A5* gene locus.**
A ChIP-seq was performed for ATF4 and its potential binding partner CEBPβ in THP1 cancer cells under conditions of arginine starvation (panels 1-2). This revealed the presence of an ATF4/CEBPβ binding site with strong signal in the first intron of the *SLC7A5* locus. Assay for Transposase-Accessible Chromatin using sequencing (ATAC-Seq) shows that chromatin accessibility at the promoter and at the intronic enhancer, where the ATF4 and CEBPβ transcription factors bind, is significantly high irrespective of the levels of extracellular arginine (panels 3-4), an effect not observed at the promoter of the same gene. Analysis of histone modifications discloses that this binding site is flanked by peaks of Histone 3, lysine 4, monomethylation (H3K4me1) and enriched with Histone 3, lysine 27, acetylation (H3K27ac), epigenetic features that are characteristic of an active enhancer (panels 7-8). Additionally, the gene promoter was rich in Histone 3, lysine 4, trimethylation (H3K4me3) an epigenetic mark typical of promoter regions (panel 6).

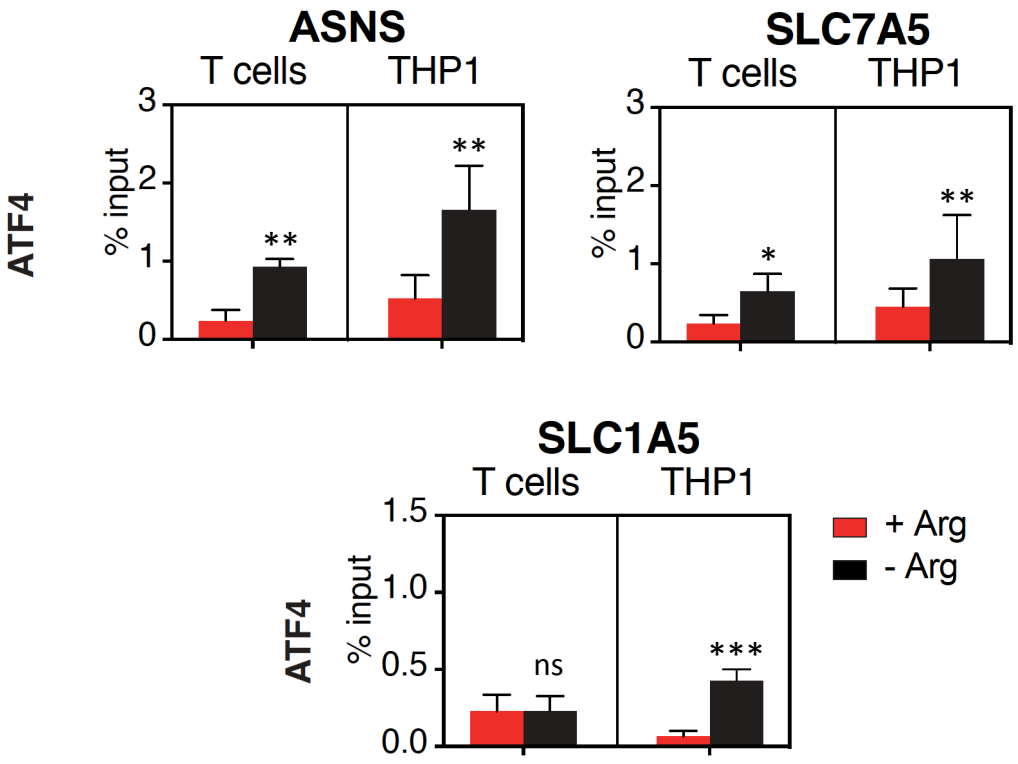



**Figure 5 - 29. ATF4 ChIP-qPCR shows that ATF4 binding at the *ASNS* promoter and at the *SLC7A5* and *SLC1A5* intronic enhancers occurs in both THP1 cells and T-cells and but is stronger and more significantly augmented in response to arginine starvation in the former.**
ChIP-qPCR was performed for ATF4 binding in THP1 and T-cells in sufficient arginine conditions (red) and following exposure to arginine deficiency (black). ATF4 binding at the ASNS promoter (top left panel) and the SLC7A5 intronic enhancer (top right panel) is detected in both cell types at baseline and further enhanced by the absence of arginine.

Significant ATF4 binding is also detected at the SLC1A5 intronic enhancer (bottom panel) in both cell types at baseline but enhanced binding upon arginine starvation only occurs in THP1 cells. These results are in line with our observations that both cell types are able to express these genes but upregulation in response to arginine starvation is either lower or absent in T-cells when compared to THP1 cells. Bars represent mean with standard deviation derived from triplicate measurements. *** denotes $p<0.001$, ** denotes $p<0.01$, * denotes $p<0.05$, ns denotes not significant ($p>0.05$).

## 5.12 Discussion

In the previous chapter we showed that ASS1, the key enzyme in the conversion of citrulline to arginine, is upregulated in cancer cells but not T-cells in response to arginine depletion. This discrepancy gave rise to a functional dichotomy whereby arginine-starved cancer cells were able to utilize exogenous citrulline to proliferate in arginine-free media, an ability not shared by T-cells who failed to proliferate under such conditions. Furthermore, we showed that this dichotomy was not the result of lack of sensing of arginine deprivation in T-cells, as we had previously shown that T-cells could shut down the mTOR pathway in response to Arginase treatment or arginine starvation, and additionally, both THP1 and T-cells upregulated ATF4, the master transcription factor regulating the integrated cellular response to stress, when cultured in arginine-free conditions.

In this chapter, we firstly confirmed that ASS1 is necessary and at least partially sufficient for the conversion of citrulline to arginine and cell proliferation in arginine-depleted environments. Knockdown of *ASS1* in the THP1 cell line abolished the ability of cancer cells to proliferate in arginine-free, citrulline-supplemented medium whereas T-cells that were genetically engineered to overexpress *ASS1* gained the ability to proliferate in arginine-free medium by using citrulline. The latter is particularly important when considering possibilities for adaptive T-cell transfer therapy in the context of cancer. The

importance of arginine in tumour-specific T-cell responses has been recently demonstrated in a study where it was deemed to be necessary in enhancing the survival and anti-tumour capacity of stimulated T-cells [366]. Rapid uptake and turnover was observed upon T-cell activation suggesting that arginine is crucial in the metabolism of stimulated T-cells [366]. In line with the findings of this study we had shown earlier in Chapter 4 that, although upon stimulation T-cells upregulate *ARG2,* this effect is reversed upon exposure to arginine-depleted conditions in which *ARG2* is in fact downregulated.

Furthermore, we showed that ASS1 transcription is dependent on ATF4. ATF4 knockdown in THP1 cells inhibited their ability to upregulate ASS1 in response to arginine starvation and abolished their functional proliferation advantage. The same effect was observed when ATF4 was knocked down in HeLa cells suggesting a regulatory mechanism of ASS1 that is not THP1- specific, but rather cancer-specific. All in all, inhibition of either ASS1 or ATF4 abrogated the aforementioned adaptation mechanism and caused cessation of cancer cell proliferation in arginine-depleted environments supplemented with citrulline. More importantly, a question arose from our findings; given that ATF4 regulates expression of ASS1 at the transcription level, and both THP1 and T-cells are able to upregulate ATF4 upon sensing arginine deprivation, how does ASS1 only get upregulated in THP1 but not T-cells in response to arginine starvation? We hypothesized that this dichotomy has its roots down to epigenetic modifications that differ between cancer cells and T-cells. Using ChIP-seq, we demonstrated that ATF4 binds an intronic region (1$^{st}$ intron), but not the promoter, of the *ASS1* gene in THP1 cells but not T-cells. Furthermore, we showed by ChIP-qPCR that this ATF4 binding is enhanced in the absence of arginine in THP1 cells but not T-cells in which it remains negligible. By analysing the histone modifications surrounding this 1$^{st}$ intron region in the *ASS1* locus, we showed that it is an active enhancer flanked by the characteristic H3K4-monomethylation and H3K27-acetylation.

Interestingly, upon deleting the identified ATF4-binding motif within the enhancer in THP1 cells using CRISP-Cas9, *ASS1* upregulation and the ability to proliferate in arginine-free conditions by utilising citrulline were completely abrogated. This elegantly confirmed the crucial role of ATF4 (and potentially CEBPβ) in regulating *ASS1* expression and thus, the adaptation response to arginine starvation.

Moreover, we showed that ATF4 binding is also induced in HeLa cells in response to tryptophan depletion thus providing further evidence that the mechanism we are studying is globally applicable in various solid and liquid cancers but also in response to starvation of other amino acids in addition to arginine.

We also demonstrated that ATF4 binds to intronic enhancers in the *SLC1A5* and *SLC7A5* gene loci in both THP1 and T-cells, albeit more strongly in the cancer cells, especially under arginine starvation conditions, a finding that perhaps explains the higher extent of upregulation of these transporters in THP1 cells compared to T-cells.

Given the previously reported cooperation between the transcription factors ATF4 and CEBPβ [371, 372, 375-377], we carried out a bioinformatics analysis of the enhancer region and identified ATF4 and CEBPβ binding motifs in close proximity. We confirmed that, similar to ATF4, CEBPβ also binds to the *ASS1* enhancer in cancer cells but not T-cells, with enhanced intensity in the absence of arginine.

Having identified the mechanism that leads to the dichotomy observed between cancer cells and T-cells in upregulating *ASS1*, we aimed at understanding the factors controlling it. In order to do that, we evaluated the level of transcription factor accessibility at the ASS1 intronic enhancer for ATF4 and CEBPβ binding, using ATAC-seq. We measured significantly higher accessibility in THP1 cells compared to T-cells, a finding that could be explained by two possible hypotheses; either certain epigenetic features most prominent in

THP1 cells promote ATF4 (and CEBPβ) binding or certain epigenetic features most prominent in T-cells inhibit ATF4 (and CEBPβ) binding.

To address these hypotheses, we assessed histone and DNA modifications that might affect accessibility to transcription factors. We showed that the heterochromatic repressive histone marks H3K27me3, H3K9me2 and H3K9me3 are more prominent at the *ASS1* enhancer in T-cells compared to THP1 cells. In line with this, DNA methylation, another repressive epigenetic modification often associated with H3K9-methylation [373], was shown by bisulfite sequencing to be significantly higher in T-cells than THP1 cells at the upstream portion of the *ASS1* enhancer, which interestingly incorporates the ATF4 consensus motif and binding site.

Taken together, our findings argue that *ASS1* expression is regulated by the ability of ATF4 to access its internal enhancer. In T-cells, the *ASS1* enhancer exists in an environment of repressive chromatin, with higher levels of H3K9, H3K27 and DNA methylation and reduced accessibility, which prevents ATF4 binding and so blocks gene induction. In THP1 cells, this repressive environment is absent, allowing an accessible chromatin structure to facilitate ATF4 binding and gene activation. The precise mechanisms by which repressive chromatin prevents transcription factor accessibility are unclear. However, the concept has recently been demonstrated, with one study suggesting that increasing levels of the repressive mark H3K27me3 can directly disrupt transcription factor binding [378]. Although the mechanism underlying this observation is not completely understood, it provides a possible paradigm for the idea that a repressive chromatin environment can disrupt transcription factor binding by reducing access to the binding site.

Furthermore, there is some evidence that DNA methylation itself can also directly affect the binding of transcription factors [379-381]. Surprisingly, binding of ATF4-CEBPβ

heterodimers to the sequence TGACGCAA has been shown to increase by methylation of the central CpG dinucleotide [376]. However, the ATF4/CEBPβ motif within the *ASS1* intronic enhancer is TGATGCAA, lacking the modifiable CpG. This argues that the disruption of ATF4 binding at the *ASS1* enhancer observed in T-cells is not a direct consequence of changes in transcription factor affinity for DNA, but rather an indirect effect of decreased chromatin accessibility. This is also consistent with the reduced ATAC signal and increased H3K9 methylation observed in T-cells.

As far the *ASS1* promoter is concerned, in contrast to previous reports of the gene being silenced by promoter DNA methylation in a number of tumours [227, 230, 233], we found that the CpG-rich promoter of *ASS1* is almost exclusively non-methylated in both THP1 and T-cells. This indicates that this is not the mechanism for differential regulation between the two cell types further supporting the hypothesis of an ATF4/CEBPβ-modulated enhancer regulating the expression of *ASS1*. It also argues that the balance between binding of the c-MYC activator and the HIF-1α repressor at the ASS1 promoter, previously reported to regulate ASS1 transcription, is probably necessary but not sufficient for ASS1 expression [217, 382]. In addition to proving that ATF4 and CEBPβ can bind the *ASS1* intronic enhancer and modify *ASS1* expression, in this work we also confirmed c-MYC as a transcription factor that can bind the *ASS1* promoter and furthermore, identified Xbp1, another transcription factor that responds to endoplasmic reticulum stress, to be able to bind to both the *ASS1* promoter and enhancer and RUNX2 as able to bind the *ASS1* enhancer only. In reality, the regulation of *ASS1* transcription is probably more complex with input from both promoter and enhancer, as recent evidence suggests epigenetic modifications occur at the *ASS1* promoter too, with the HDAC2-mediated histone deacetylation allowing a PHD2-driven proteasomal complex to degrade the HIF-1α repressor and reactivating *ASS1* expression [382].

One of the questions arising from our findings is how H3K9 di- and tri-methylation at the *ASS1* intronic enhancer comes about. Interestingly, one model by which ATF4 has been proposed to promote expression of its target genes is by recruiting the histone H3K9 demethylase KDM4C to alleviate repressive modifications at target gene promoters [374]. However, we did not see evidence for KDM4C recruitment or H3K9me3 reduction at target genes, including the *ASS1* enhancer, upon arginine starvation in neither THP1 nor T-cells. Whilst we disclosed that *KDM4C* is upregulated in AML blasts, and levels are higher in THP1 cells than T-cells, suggesting that it may have a role in establishing a more open chromatin environment at *ASS1*, this state seems to be established prior to arginine starvation. We would therefore argue that H3K9 methylation and/or DNA methylation at the ASS1 intronic enhancer determines the potential for ATF4 binding (prior to ATF4 activation), whereby the presence of these repressive marks in T-cells prevents ATF4 access to, and therefore transcription of, the *ASS1* gene. The possibility of KDM4C having a role in shaping the H3K9me2/3 mark is still possible, as suggested by inhibition of ATF4 binding at the enhancer and abrogation of *ASS1* upregulation in THP1 cells by the KDM4C inhibitor SD70, but this is likely to occur at baseline, without any links to arginine starvation-mediated ATF4 activation.

Finally, we also proved that all the effects and mechanisms described above are cancer-specific rather than lineage specific as they hold true for both THP1 and HeLa cells but not primary activated monocytes/macrophages or T-cells.

Taken together, the results presented in this chapter show for the first time that both ASS1 and ATF4 are essential for arginine-starved cancer cells to utilize citrulline and proliferate in environments lacking arginine. They also explain the dichotomy between cancer cells and T-cells in this adaptation mechanism. This is down to DNA and H3K9 and H3K27 methylation, repressive epigenetic modifications that are more prominent in T-cells

compared to THP1 cells and prevent ATF4 (and other synergistic transcription factors) from binding to the ASS1 enhancer and inducing transcription of the gene. To our knowledge this is the first time this dichotomy is reported and the first time such a metabolic phenomenon is justified by cancer-specific, dynamic epigenetic features that can be modified by amino acid availability. It is a finding that bridges the transformation of cancer cells to their ability to escape tumour-specific immunity by modulation of amino acid metabolism and adaptation to altered conditions through targeted epigenetic modifications. Our results could have significant implications for cancer immunotherapy and complement recent findings of T-cell epigenetic reprogramming in response to environmental factors; firstly in tumour-infiltrating lymphocytes exposed to tumour microenvironment (in melanoma and lung cancer) to adjust chromatin accessibility in non-promoter regions of the PD1 gene leading to T-cell dysfunction [383] and secondly in normal activated CD8+ T-cells exposed to high levels of hypoxia-induced 2-S-hydroxyglutarate to modulate histone/DNA marks and alter T-cell differentiation and functional fate [384].

# Chapter 6: Summary and Conclusions

Although cancer immunology is a relatively new field, there is clear evidence that tumours are able to withstand and escape the host immune response in order to continue to grow and metastasize. The generation of an immunosuppressive tumour microenvironment is considered to be one of the main strategies employed by cancer cells in order to evade the immune system, particularly CD4 and CD8 T-cells, the main arms of the tumour-specific defensive response.

Amongst the various ways in which cancer cells induce an immunosuppressive microenvironment is the creation of nutritional stress through depletion of nutrients that are essential for the function of immune cells. Amongst such nutrients are amino acids such as glutamine, cysteine, tryptophan and, most relevant to this work, arginine. In principle, this starvation effect can be achieved by increased uptake of the amino acid by tumour cells or by enhanced breakdown by amino acid degrading enzymes that are overexpressed or released by cancer cells. The role of arginine in immune regulation has been shown in various settings such as infections, pregnancy and autoimmune diseases but it is not well established in the context cancer-specific immune responses. Furthermore, the mechanisms by which cancer cells resist the detrimental effects of amino acid starvation remain elusive.

Our study focused on arginine metabolism at the interphase of cancer-immune cell interactions and as such, had two overarching aims. Firstly, we investigated whether cancer cells, particularly AML blasts, exploit arginine-degrading enzymes, such as Arginase, to deplete arginine from T-cells within the local tumour microenvironment or systemic circulation and suppress their activity. Secondly, given that cancer cells, unlike T-cells,

seem to be able to withstand the nutritional stress generated by the deprivation of arginine (or other amino acids), we wanted to test the hypothesis that cancer cells, but not T-cells, can adapt to low levels of arginine in order to survive and continue to proliferate and furthermore, study the molecular mechanisms that underpin this.

In summary, our results have revealed that Arginase-2 is released in the bloodstream of AML patients to breakdown and deplete systemic arginine to suppress T-cell proliferation and effector function whereas cancer cells, including AML blasts are able to adapt to arginine starvation by importing extracellular citrulline and producing arginine de novo through the initiation of an epigenetically-regulated, ATF4-dependent reprogramming of various amino acid transporters and synthetic enzymes, including ASS1, the enzyme that regulates the rate-limiting step in the conversion of citrulline to arginine.

Furthermore, we showed that the release of Arginase-2 is in the bloodstream of AML patients is an effect that can be reproduced in AML mouse models with the associated systemic arginine depletion and was proportional to disease burden. Importantly, we showed that these Arginase-specific immunosuppression effects can be abrogated by the use of Arginase-specific small molecule inhibitors tested as part of this work suggesting potential therapeutic avenues to tackle the immunosuppressive tumour microenvironment as part of cancer immunotherapy.

Additionally, our results have demonstrated that Arginase starvation induces a dramatic reprogramming of the cellular transcriptomic profile that differs between cancer cells and T-cells. One of the main differences is the ATF4-dependent upregulation of ASS1, the enzyme that drives the rate-limiting step in the conversion of citrulline to arginine, in cancer cells but not T-cells. We have shown that although both cell types can sense and respond to arginine deprivation by upregulating ATF4, the transcription factor governing the cellular response to metabolic stress, strikingly, only cancer cells were able to

upregulate ASS1. Consequently, cancer cells were able to utilize extracellular citrulline, in order to generate arginine de novo and proliferate in arginine-free conditions. This functional adaptation advantage could be abrogated by deleting ASS1 or ATF4 or by inhibiting SLC1A5 and SLC7A5, the citrulline transporters proposed in our study. Our inferences were confirmed by gain-of-function experiments in which T-cells were genetically modified to express ASS1, an action that allowed them to utilize citrulline and proliferate in arginine-free conditions. We extended our findings to show that this adaptation is a global phenomenon in a variety of cancers including multiple types of leukaemias and solid tumour cell lines. This also suggests that it is a cancer-specific feature, likely rising following cell transformation, rather than a lineage-related ability, an inference confirmed by the inability of macrophages and monocytes from healthy individuals to upregulate ASS1 in response to arginine starvation, thus, behaving in a similar manner to T-cells. Moreover, we showed that citrulline levels in the plasma of AML patients is higher than that of healthy donors and identified SLC1A5 and SLC7A5 as the potential transporters of citrulline accounting for both a plausible source and a plausible uptake mechanism of extracellular citrulline for cancer cells to convert to arginine. We also demonstrated that arginine starvation in cancer cells, not only prevented proliferation but also reversed the Warburg effect, driving the cancer cell metabolic profile away from glycolysis, an effect that again was reversed by the utilization of extracellular citrulline to synthesize arginine intracellularly.

Finally, we established the epigenetic mechanism regulating ATF4-dependent ASS1 upregulation and showed that discrepancies in this mechanism can explain the dichotomy observed between cancer cells and T-cells. Having shown that ATF4 regulates ASS1 upregulation at the transcription level, we identified an intronic enhancer region within the ASS1 locus that is absolutely necessary for the effect as its deletion abolished the

functional advantage observed in cancer cells. We showed that ASS1 transcription requires ATF4 and its binding partner CEBPβ, to adequately bind this enhancer. We established that ATF4 and CEBPβ binding at the ASS1 enhancer failed at T-cells, but not cancer cells as a result of reduced DNA accessibility in the former cell type. We identified the reason for this discrepancy to be the presence of repressive histone modifications including H3K9me2, H3K9me3 and H3K27me3, and associated repressive DNA methylation to create a closed or repressive chromatin state, that is non-permissive for transcription factor binding in T-cells. Cancer cells had significantly lower repressive chromatin marks, higher DNA accessibility and stronger ATF4/CEBPβ binding at the ASS1 enhancer compared to T-cells at baseline. To a certain extent, exposure to arginine starvation induced a reduction in the repressive histone modifications and an increase in DNA accessibility and ATF4 binding in cancer cells whereas T-cells showed no such response. We identified KDM4C, a H3K9 demethylase, to be the potential regulator of this response as it was upregulated in cancer cells more than T-cells upon arginine depletion and was expressed at higher levels in AML patient blasts compared to myeloid cells from healthy controls. Indeed, the pharmacological inhibition of KDM4C abrogated ASS1 upregulation in cancer cells but nevertheless, further experiments are required to establish how important its role is in regulating ATF4 binding.

To finish off, it is worth mentioning that we also showed that ATF4 binding occurred at the ASS1 enhancer in response to tryptophan depletion too, also in HeLa cells. This finding argues that the epigenetic regulatory network controlling ASS1 upregulation was not only true for arginine depletion but also tryptophan depletion and for more than one cancer cell types. This in turn suggests that we have in fact discovered a mechanism that might regulate the global response to nutritional stress in multiple settings and triggers

with the possibility that ASS1 is just one of the key players involved in an ATF4-dependent manner to allow cells to adapt to changing metabolic conditions.

Although further work is necessary, especially in vivo and in the clinical setting, our results potentially have significant biological and clinical implications. The identification of this adaptation mechanism creates immense and broad opportunities for cancer therapy. Abolition of this strategy in cancer cells would render them vulnerable to the suppressive microenvironment that they themselves create. ASS1, ATF4, KDM4C, SLC1A5 and SLC7A5 are all potential therapeutic targets that can be inhibited to stop the cancer cells from adapting to arginine depletion as seen in our proposed functional model **(Figure 6-1)**. Furthermore, understanding the role of ASS1 in recycling arginine and surviving in low-arginine environments can open the door to gene therapy and adoptive T-cell transfer therapies for cancer patients. Another possible therapeutic avenue arising from our results is the blockade of the enzymatic action of Arginase in the context of tumours and liquid cancers to relieve the immunosuppression imposed on T-cells and other immune cells. In line with this, we have identified promising Arginase-specific small molecule inhibitors through this work. Finally, we believe that our results are exciting and extremely relevant in the modern era of cancer immunotherapy given the fact that despite the advent of anti-PD1, anti-CTLA4 and other checkpoint inhibitors, only a minority of patients shows satisfactory responses, and even amongst those, a significant proportion relapses. Therefore, there is a tremendous need to address the immunosuppressive tumour microenvironment, which might be key in securing novel cancer immunotherapies, that can be used alone or most likely as part of combination treatment with checkpoint inhibitors. The therapeutic targets identified in our work would not only work for cancer cells (solid tumours and leukaemias) but also for cancer-associated stromal and immune cells, such as cancer-associated fibroblasts, TAMs and MDSCs that work against the host

tumour-specific immune response. There is already evidence that these cell populations utilize Arginase as a way to induce immunosuppression in the context of cancer and it is likely that they function and adapt in a similar manner to the cancer cells described in this work. It remains to be seen through future work whether this is the case.

Our next step is to perform ChIP and ATAC-seq on AML blasts, CD8 and CD4 T-cells extracted from AML patients to establish whether the findings we have in vitro can be reproduced ex vivo. This will be followed by examination of the same principles in vivo in AML mouse models where potential therapeutic targets will also be tested. Finally, we will investigate whether the epigenetic dichotomy revealed in this work between cancer cells and T-cells is down to the induction of intracellular immunometabolites following the absence of arginine.

In conclusion, this work provides insights into the way cancer cells hijack arginine metabolism to create an immunosuppressive tumour microenvironment by inducing arginine starvation and the strategies that permit cancer cells but not T cells to endure local and systemic arginine. In doing so, this work emphasizes the crucial role of de novo amino acid biosynthesis and transport in the process of immune evasion and identifies potential therapeutic targets for cancer immunotherapy. This work begins with a clinical observation only to move on and investigate the functional implications of this clinical observation, reveal its effects at the cellular level and identify its mechanism at a genetic and molecular level. Nevertheless, further work is required ex vivo and in vivo to confirm the applicability of our results before they can be taken further to clinical work in order to have a positive impact for patients.

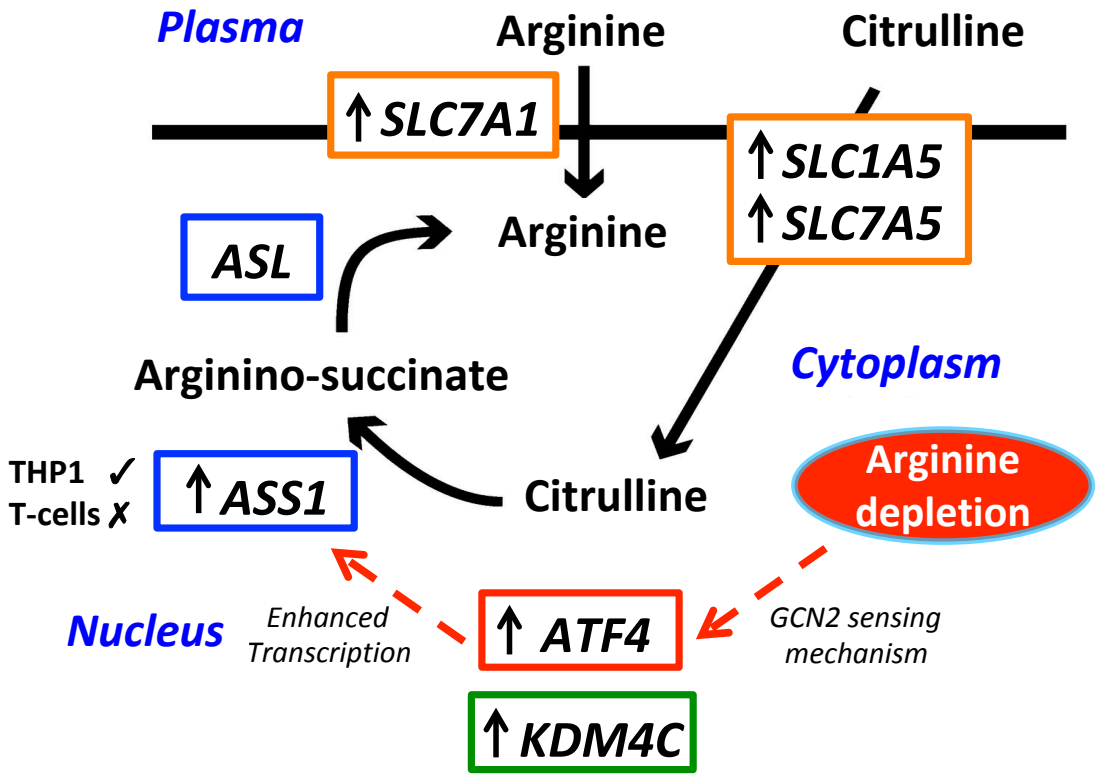



**Figure 6 - 1. Proposed model of the ATF4-dependent cellular response to arginine depletion in the tumour microenvironment**
Arginine breakdown in the extracellular environment leads to reduced arginine uptake in the cells and as a result low arginine levels are sensed intracellularly by GCN2 and mTOR signalling cascades within the cytoplasm and sub-cellular structures including ribosomes and lysosomes. In response to arginine depletion cells upregulate the transcription factor ATF4 via the GCN2 pathway which in turn leads to enhanced transcription of various metabolic genes including the enzyme ASS1 and the amino acid transporters SLC7A1, SLC1A5 and SLC7A5. SLC7A1 allows any extracellular arginine to enter the cell whereas SLC1A5 and SLC7A5 allow extracellular citrulline to be taken up. ASS1, the rate limiting enzyme of the process, converts citrulline to arginine-succinate and the latter is turned directly to arginine by ASL. Although most of these proteins are upregulated in both cancer cells (THP1) and T-cells, the upregulation is much stronger in the former cell type. More importantly, ASS1 is only upregulated in cancer cells but not T-cells, making it the key player in the dichotomy observed between the two cell types in adapting to arginine starvation or low-arginine conditions. This discrepancy might be explained by repressive histone modifications (such as H3K9me2/3) at the ASS1 enhancer that prevent ATF4 binding at that region and are present at much higher levels in T-cells. KDM4C is a H3K9 demethylase that potentially functions in cancer cells but not T-cells permitting removal of these repressive chromatin marks and allowing ATF4 binding and ASS1 transcription in cancer cells but not T-cells. Overall, it seems that cancer cells have a tremendous functional advantage over T-cells in recycling citrulline to arginine and withstanding the detrimental effects of arginine starvation in the tumour microenvironment. Red boxes denote transcription factors, green boxes denote nuclear histone-modifying enzymes, blue boxes denote cytoplasmic amino acid biosynthetic enzymes and orange boxes denote cell membrane amino acid transporters.

# References


1. Timosenko E, Hadjinicolaou AV, Cerundolo V. Modulation of cancer-specific immune responses by amino acid degrading enzymes. *Immunotherapy* 9(1), 83-97 (2017).
2. Parkin J, Cohen B. An overview of the immune system. *Lancet* 357(9270), 1777-1789 (2001).
3. Iwasaki A, Medzhitov R. Control of adaptive immunity by the innate immune system. *Nature immunology* 16(4), 343-353 (2015).
4. Cooper MD, Alder MN. The evolution of adaptive immune systems. *Cell* 124(4), 815-822 (2006).
5. Glusman G, Rowen L, Lee I *et al*. Comparative genomics of the human and mouse T cell receptor loci. *Immunity* 15(3), 337-349 (2001).
6. Dzopalic T, Rajkovic I, Dragicevic A, Colic M. The response of human dendritic cells to co-ligation of pattern-recognition receptors. *Immunologic research* 52(1-2), 20-33 (2012).
7. Dunn GP, Old LJ, Schreiber RD. The immunobiology of cancer immunosurveillance and immunoediting. *Immunity* 21(2), 137-148 (2004).
8. Kim R, Emi M, Tanabe K. Cancer immunoediting from immune surveillance to immune escape. *Immunology* 121(1), 1-14 (2007).
9. Galon J, Costes A, Sanchez-Cabo F *et al*. Type, density, and location of immune cells within human colorectal tumours predict clinical outcome. *Science* 313(5795), 1960-1964 (2006).
10. Swann JB, Smyth MJ. Immune surveillance of tumours. *The Journal of clinical investigation* 117(5), 1137-1146 (2007).
11. Ilyas S, Yang JC. Landscape of Tumour Antigens in T Cell Immunotherapy. *Journal of immunology (Baltimore, Md. : 1950)* 195(11), 5117-5122 (2015).
12. Dunn GP, Bruce AT, Ikeda H, Old LJ, Schreiber RD. Cancer immunoediting: from immunosurveillance to tumour escape. *Nature immunology* 3(11), 991-998 (2002).
13. Dunn GP, Old LJ, Schreiber RD. The three Es of cancer immunoediting. *Annual Review of Immunology* 22 329-360 (2004).
14. Shankaran V, Ikeda H, Bruce AT *et al*. IFNgamma and lymphocytes prevent primary tumour development and shape tumour immunogenicity. *Nature* 410(6832), 1107-1111 (2001).
15. Hanahan D, Weinberg RA. Hallmarks of cancer: the next generation. *Cell* 144(5), 646-674 (2011).
16. Algarra I, Cabrera T, Garrido F. The HLA crossroad in tumour immunology. *Hum Immunol* 61(1), 65-73 (2000).
17. Davies M. New modalities of cancer treatment for NSCLC: focus on immunotherapy. *Cancer management and research* 6 63-75 (2014).
18. Dunn GP, Old LJ, Schreiber RD. The immunobiology of cancer immunosurveillance and immunoediting. *Immunity* 21(2), 137-148 (2004).
19. Johnsen AK, Templeton DJ, Sy M, Harding CV. Deficiency of transporter for antigen presentation (TAP) in tumour cells allows evasion of immune

surveillance and increases tumourigenesis. *Journal of immunology (Baltimore, Md. : 1950)* 163(8), 4224-4231 (1999).
20. Marincola FM, Jaffee EM, Hicklin DJ, Ferrone S. Escape of human solid tumours from T-cell recognition: molecular mechanisms and functional significance. *Advances in immunology* 74 181-273 (2000).
21. Restifo NP, Esquivel F, Kawakami Y *et al*. Identification of human cancers deficient in antigen processing. *The Journal of experimental medicine* 177(2), 265-272 (1993).
22. Rotem-Yehudar R, Groettrup M, Soza A, Kloetzel PM, Ehrlich R. LMP-associated proteolytic activities and TAP-dependent peptide transport for class 1 MHC molecules are suppressed in cell lines transformed by the highly oncogenic adenovirus 12. *The Journal of experimental medicine* 183(2), 499-514 (1996).
23. Wang IM, Mehta V, Cook RG. Regulation of TL antigen expression. Analysis of the T18d promoter region and responses to IFN-gamma. *Journal of immunology (Baltimore, Md. : 1950)* 151(5), 2646-2657 (1993).
24. Prendergast GC. Immune escape as a fundamental trait of cancer: focus on IDO. *Oncogene* 27(28), 3889-3900 (2008).
25. Leach DR, Krummel MF, Allison JP. Enhancement of antitumour immunity by CTLA-4 blockade. *Science* 271(5256), 1734-1736 (1996).
26. Nishimura H, Nose M, Hiai H, Minato N, Honjo T. Development of lupus-like autoimmune diseases by disruption of the PD-1 gene encoding an ITIM motif-carrying immunoreceptor. *Immunity* 11(2), 141-151 (1999).
27. Watanabe N, Gavrieli M, Sedy JR *et al*. BTLA is a lymphocyte inhibitory receptor with similarities to CTLA-4 and PD-1. *Nature immunology* 4(7), 670-679 (2003).
28. Blank C, Brown I, Peterson AC *et al*. PD-L1/B7H-1 inhibits the effector phase of tumour rejection by T cell receptor (TCR) transgenic CD8(+) T cells. *Cancer research* 64(3), 1140-1145 (2004).
29. Blank C, Gajewski TF, Mackensen A. Interaction of PD-L1 on tumour cells with PD-1 on tumour-specific T cells as a mechanism of immune evasion: implications for tumour immunotherapy. *Cancer immunology, immunotherapy : CII* 54(4), 307-314 (2005).
30. Dong H, Strome SE, Salomao DR *et al*. Tumour-associated B7-H1 promotes T-cell apoptosis: a potential mechanism of immune evasion. *Nat Med* 8(8), 793-800 (2002).
31. Wang G, Lu X, Dey P *et al*. Targeting YAP-Dependent MDSC Infiltration Impairs Tumour Progression. *Cancer Discov* 6(1), 80-95 (2016).
32. Hamid O, Robert C, Daud A *et al*. Safety and tumour responses with lambrolizumab (anti-PD-1) in melanoma. *The New England journal of medicine* 369(2), 134-144 (2013).
33. Hodi FS, O'day SJ, Mcdermott DF *et al*. Improved survival with ipilimumab in patients with metastatic melanoma. *The New England journal of medicine* 363(8), 711-723 (2010).
34. Topalian SL, Hodi FS, Brahmer JR *et al*. Safety, activity, and immune correlates of anti-PD-1 antibody in cancer. *The New England journal of medicine* 366(26), 2443-2454 (2012).
35. Wolchok JD, Kluger H, Callahan MK *et al*. Nivolumab plus ipilimumab in advanced melanoma. *The New England journal of medicine* 369(2), 122-133 (2013).

36. Bronte V, Brandau S, Chen SH *et al*. Recommendations for myeloid-derived suppressor cell nomenclature and characterization standards. *Nature communications* 7 12150 (2016).
37. Wang Z, Pratts SG, Zhang H *et al*. Treg depletion in non-human primates using a novel diphtheria toxin-based anti-human CCR4 immunotoxin. *Molecular oncology* 10(4), 553-565 (2016).
38. Zhou G, Levitsky HI. Natural regulatory T cells and de novo-induced regulatory T cells contribute independently to tumour-specific tolerance. *Journal of immunology (Baltimore, Md. : 1950)* 178(4), 2155-2162 (2007).
39. Marvel D, Gabrilovich DI. Myeloid-derived suppressor cells in the tumour microenvironment: expect the unexpected. *The Journal of clinical investigation* 125(9), 3356-3364 (2015).
40. Bauer CA, Kim EY, Marangoni F, Carrizosa E, Claudio NM, Mempel TR. Dynamic Treg interactions with intratumoural APCs promote local CTL dysfunction. *The Journal of clinical investigation* 124(6), 2425-2440 (2014).
41. Curiel TJ, Coukos G, Zou L *et al*. Specific recruitment of regulatory T cells in ovarian carcinoma fosters immune privilege and predicts reduced survival. *Nat Med* 10(9), 942-949 (2004).
42. Facciabene A, Motz GT, Coukos G. T-regulatory cells: key players in tumour immune escape and angiogenesis. *Cancer research* 72(9), 2162-2171 (2012).
43. Facciabene A, Santoro S, Coukos G. Know thy enemy: Why are tumour-infiltrating regulatory T cells so deleterious? *Oncoimmunology* 1(4), 575-577 (2012).
44. Gabrilovich DI, Ostrand-Rosenberg S, Bronte V. Coordinated regulation of myeloid cells by tumours. *Nature reviews. Immunology* 12(4), 253-268 (2012).
45. Ostrand-Rosenberg S, Sinha P. Myeloid-derived suppressor cells: linking inflammation and cancer. *Journal of immunology (Baltimore, Md. : 1950)* 182(8), 4499-4506 (2009).
46. Ugel S, De Sanctis F, Mandruzzato S, Bronte V. Tumour-induced myeloid deviation: when myeloid-derived suppressor cells meet tumour-associated macrophages. *The Journal of clinical investigation* 125(9), 3365-3376 (2015).
47. Munn DH, Bronte V. Immune suppressive mechanisms in the tumour microenvironment. *Curr Opin Immunol* 39 1-6 (2016).
48. Rabinovich GA, Gabrilovich D, Sotomayor EM. Immunosuppressive strategies that are mediated by tumour cells. *Annu Rev Immunol* 25 267-296 (2007).
49. Rabinovich GA, Gabrilovich D, Sotomayor EM. Immunosuppressive strategies that are mediated by tumour cells. In: *Annual Review of Immunology*, 267-296 (2007).
50. Wang TH, Niu GL, Kortylewski M *et al*. Regulation of the innate and adaptive immune responses by Stat-3 signaling in tumour cells. *Nature Medicine* 10(1), 48-54 (2004).
51. Cubillos-Ruiz JR, Bettigole SE, Glimcher LH. Tumourigenic and Immunosuppressive Effects of Endoplasmic Reticulum Stress in Cancer. *Cell* 168(4), 692-706 (2017).
52. Uyttenhove C, Pilotte L, Theate I *et al*. Evidence for a tumoural immune resistance mechanism based on tryptophan degradation by indoleamine 2,3-dioxygenase. *Nat Med* 9(10), 1269-1274 (2003).
53. Vacchelli E, Aranda F, Eggermont A *et al*. Trial watch: IDO inhibitors in cancer therapy. *Oncoimmunology* 3(10), e957994 (2014).

54. Morris SM, Jr. Arginine: beyond protein. *The American journal of clinical nutrition* 83(2), 508s-512s (2006).
55. Bouchet A, Lairion F, Disalvo EA. Role of guanidinium group in the insertion of l-arginine in DMPE and DMPC lipid interphases. *Biochimica et biophysica acta* 1798(3), 616-623 (2010).
56. Tong BC, Barbul A. Cellular and physiological effects of arginine. *Mini reviews in medicinal chemistry* 4(8), 823-832 (2004).
57. Evoy D, Lieberman MD, Fahey TJ, 3rd, Daly JM. Immunonutrition: the role of arginine. *Nutrition (Burbank, Los Angeles County, Calif.)* 14(7-8), 611-617 (1998).
58. Barbul A, Rettura G, Levenson SM, Seifter E. Wound healing and thymotropic effects of arginine: a pituitary mechanism of action. *The American journal of clinical nutrition* 37(5), 786-794 (1983).
59. Smith PA, Sakura H, Coles B, Gummerson N, Proks P, Ashcroft FM. Electrogenic arginine transport mediates stimulus-secretion coupling in mouse pancreatic beta-cells. *The Journal of physiology* 499 ( Pt 3) 625-635 (1997).
60. Papapetropoulos A, Rudic RD, Sessa WC. Molecular control of nitric oxide synthases in the cardiovascular system. *Cardiovascular research* 43(3), 509-520 (1999).
61. Calbet JA, Maclean DA. Plasma glucagon and insulin responses depend on the rate of appearance of amino acids after ingestion of different protein solutions in humans. *The Journal of nutrition* 132(8), 2174-2182 (2002).
62. Tarry WC, Makhoul RG. L-arginine improves endothelium-dependent vasorelaxation and reduces intimal hyperplasia after balloon angioplasty. *Arteriosclerosis and thrombosis : a journal of vascular biology / American Heart Association* 14(6), 938-943 (1994).
63. Morris SM, Jr. Regulation of enzymes of the urea cycle and arginine metabolism. *Annual review of nutrition* 22 87-105 (2002).
64. Wu G, Morris SM, Jr. Arginine metabolism: nitric oxide and beyond. *The Biochemical journal* 336 ( Pt 1) 1-17 (1998).
65. Dhanakoti SN, Brosnan JT, Herzberg GR, Brosnan ME. Renal arginine synthesis: studies in vitro and in vivo. *The American journal of physiology* 259(3 Pt 1), E437-442 (1990).
66. Dhanakoti SN, Brosnan ME, Herzberg GR, Brosnan JT. Cellular and subcellular localization of enzymes of arginine metabolism in rat kidney. *The Biochemical journal* 282 ( Pt 2) 369-375 (1992).
67. Yu JG, Ishine T, Kimura T, O'brien WE, Lee TJ. L-citrulline conversion to L-arginine in sphenopalatine ganglia and cerebral perivascular nerves in the pig. *The American journal of physiology* 273(5 Pt 2), H2192-2199 (1997).
68. Bernard AC, Mistry SK, Morris SM, Jr. *et al*. Alterations in arginine metabolic enzymes in trauma. *Shock (Augusta, Ga.)* 15(3), 215-219 (2001).
69. Luiking YC, Poeze M, Dejong CH, Ramsay G, Deutz NE. Sepsis: an arginine deficiency state? *Critical care medicine* 32(10), 2135-2145 (2004).
70. Bronte V, Zanovello P. Regulation of immune responses by L-arginine metabolism. *Nature reviews. Immunology* 5(8), 641-654 (2005).
71. Boger RH, Sydow K, Borlak J *et al*. LDL cholesterol upregulates synthesis of asymmetrical dimethylarginine in human endothelial cells: involvement of S-adenosylmethionine-dependent methyltransferases. *Circulation research* 87(2), 99-105 (2000).

72. Peters H, Border WA, Ruckert M, Kramer S, Neumayer HH, Noble NA. L-arginine supplementation accelerates renal fibrosis and shortens life span in experimental lupus nephritis. *Kidney international* 63(4), 1382-1392 (2003).
73. Closs EI, Simon A, Vekony N, Rotmann A. Plasma membrane transporters for arginine. *The Journal of nutrition* 134(10 Suppl), 2752S-2759S; discussion 2765S-2767S (2004).
74. Ash DE. Structure and function of arginases. *The Journal of nutrition* 134(10 Suppl), 2760S-2764S; discussion 2765S-2767S (2004).
75. Jenkinson CP, Grody WW, Cederbaum SD. Comparative properties of arginases. *Comparative biochemistry and physiology. Part B, Biochemistry & molecular biology* 114(1), 107-132 (1996).
76. Morris SM, Jr. Recent advances in arginine metabolism: roles and regulation of the arginases. *British journal of pharmacology* 157(6), 922-930 (2009).
77. Munder M, Choi BS, Rogers M, Kropf P. L-arginine deprivation impairs Leishmania major-specific T-cell responses. *European journal of immunology* 39(8), 2161-2172 (2009).
78. Spector EB, Kiernan M, Bernard B, Cederbaum SD. Properties of fetal and adult red blood cell arginase: a possible prenatal diagnostic test for arginase deficiency. *American journal of human genetics* 32(1), 79-87 (1980).
79. Gotoh T, Araki M, Mori M. Chromosomal localization of the human arginase II gene and tissue distribution of its mRNA. *Biochemical and biophysical research communications* 233(2), 487-491 (1997).
80. Sparkes RS, Dizikes GJ, Klisak I *et al*. The gene for human liver arginase (ARG1) is assigned to chromosome band 6q23. *American journal of human genetics* 39(2), 186-193 (1986).
81. Dizikes GJ, Grody WW, Kern RM, Cederbaum SD. Isolation of human liver arginase cDNA and demonstration of nonhomology between the two human arginase genes. *Biochemical and biophysical research communications* 141(1), 53-59 (1986).
82. Kim PS, Iyer RK, Lu KV *et al*. Expression of the liver form of arginase in erythrocytes. *Molecular genetics and metabolism* 76(2), 100-110 (2002).
83. Mori M. Regulation of nitric oxide synthesis and apoptosis by arginase and arginine recycling. *The Journal of nutrition* 137(6 Suppl 2), 1616s-1620s (2007).
84. Munder M. Arginase: an emerging key player in the mammalian immune system. *British journal of pharmacology* 158(3), 638-651 (2009).
85. Chang CI, Zoghi B, Liao JC, Kuo L. The involvement of tyrosine kinases, cyclic AMP/protein kinase A, and p38 mitogen-activated protein kinase in IL-13-mediated arginase I induction in macrophages: its implications in IL-13-inhibited nitric oxide production. *Journal of immunology (Baltimore, Md. : 1950)* 165(4), 2134-2141 (2000).
86. Corraliza IM, Soler G, Eichmann K, Modolell M. Arginase induction by suppressors of nitric oxide synthesis (IL-4, IL-10 and PGE2) in murine bone-marrow-derived macrophages. *Biochemical and biophysical research communications* 206(2), 667-673 (1995).
87. Louis CA, Mody V, Henry WL, Jr., Reichner JS, Albina JE. Regulation of arginase isoforms I and II by IL-4 in cultured murine peritoneal macrophages. *The American journal of physiology* 276(1 Pt 2), R237-242 (1999).

88. Modolell M, Corraliza IM, Link F, Soler G, Eichmann K. Reciprocal regulation of the nitric oxide synthase/arginase balance in mouse bone marrow-derived macrophages by TH1 and TH2 cytokines. *European journal of immunology* 25(4), 1101-1104 (1995).
89. Munder M, Eichmann K, Modolell M. Alternative metabolic states in murine macrophages reflected by the nitric oxide synthase/arginase balance: competitive regulation by CD4+ T cells correlates with Th1/Th2 phenotype. *Journal of immunology (Baltimore, Md. : 1950)* 160(11), 5347-5354 (1998).
90. Mayer AK, Bartz H, Fey F, Schmidt LM, Dalpke AH. Airway epithelial cells modify immune responses by inducing an anti-inflammatory microenvironment. *European journal of immunology* 38(6), 1689-1699 (2008).
91. Munder M, Eichmann K, Moran JM, Centeno F, Soler G, Modolell M. Th1/Th2-regulated expression of arginase isoforms in murine macrophages and dendritic cells. *Journal of immunology (Baltimore, Md. : 1950)* 163(7), 3771-3777 (1999).
92. Munder M, Mollinedo F, Calafat J *et al*. Arginase I is constitutively expressed in human granulocytes and participates in fungicidal activity. *Blood* 105(6), 2549-2556 (2005).
93. Pesce J, Kaviratne M, Ramalingam TR *et al*. The IL-21 receptor augments Th2 effector function and alternative macrophage activation. *The Journal of clinical investigation* 116(7), 2044-2055 (2006).
94. Boucher JL, Custot J, Vadon S *et al*. N omega-hydroxyl-L-arginine, an intermediate in the L-arginine to nitric oxide pathway, is a strong inhibitor of liver and macrophage arginase. *Biochemical and biophysical research communications* 203(3), 1614-1621 (1994).
95. Hecker M, Nematollahi H, Hey C, Busse R, Racke K. Inhibition of arginase by NG-hydroxy-L-arginine in alveolar macrophages: implications for the utilization of L-arginine for nitric oxide synthesis. *FEBS letters* 359(2-3), 251-254 (1995).
96. Reczkowski RS, Ash DE. Rat liver arginase: kinetic mechanism, alternate substrates, and inhibitors. *Archives of biochemistry and biophysics* 312(1), 31-37 (1994).
97. Deves R, Boyd CA. Transporters for cationic amino acids in animal cells: discovery, structure, and function. *Physiological reviews* 78(2), 487-545 (1998).
98. Cox JD, Cama E, Colleluori DM *et al*. Mechanistic and metabolic inferences from the binding of substrate analogues and products to arginase. *Biochemistry* 40(9), 2689-2701 (2001).
99. Schapira RM, Wiessner JH, Morrisey JF, Almagro UA, Nelin LD. L-arginine uptake and metabolism by lung macrophages and neutrophils following intratracheal instillation of silica in vivo. *American journal of respiratory cell and molecular biology* 19(2), 308-315 (1998).
100. Gallardo-Soler A, Gomez-Nieto C, Campo ML *et al*. Arginase I induction by modified lipoproteins in macrophages: a peroxisome proliferator-activated receptor-gamma/delta-mediated effect that links lipid metabolism and immunity. *Molecular endocrinology (Baltimore, Md.)* 22(6), 1394-1402 (2008).
101. Matthiesen S, Lindemann D, Warnken M, Juergens UR, Racke K. Inhibition of NADPH oxidase by apocynin inhibits lipopolysaccharide (LPS) induced up-

regulation of arginase in rat alveolar macrophages. *European journal of pharmacology* 579(1-3), 403-410 (2008).
102. Gotoh T, Sonoki T, Nagasaki A, Terada K, Takiguchi M, Mori M. Molecular cloning of cDNA for nonhepatic mitochondrial arginase (arginase II) and comparison of its induction with nitric oxide synthase in a murine macrophage-like cell line. *FEBS letters* 395(2-3), 119-122 (1996).
103. Klasen S, Hammermann R, Fuhrmann M *et al*. Glucocorticoids inhibit lipopolysaccharide-induced up-regulation of arginase in rat alveolar macrophages. *British journal of pharmacology* 132(6), 1349-1357 (2001).
104. Lindemann D, Racke K. Glucocorticoid inhibition of interleukin-4 (IL-4) and interleukin-13 (IL-13) induced up-regulation of arginase in rat airway fibroblasts. *Naunyn-Schmiedeberg's archives of pharmacology* 368(6), 546-550 (2003).
105. Que LG, Kantrow SP, Jenkinson CP, Piantadosi CA, Huang YC. Induction of arginase isoforms in the lung during hyperoxia. *The American journal of physiology* 275(1 Pt 1), L96-102 (1998).
106. Vockley JG, Jenkinson CP, Shukla H, Kern RM, Grody WW, Cederbaum SD. Cloning and characterization of the human type II arginase gene. *Genomics* 38(2), 118-123 (1996).
107. Cederbaum SD, Yu H, Grody WW, Kern RM, Yoo P, Iyer RK. Arginases I and II: do their functions overlap? *Molecular genetics and metabolism* 81 Suppl 1 S38-44 (2004).
108. Liscovsky MV, Ranocchia RP, Gorlino CV *et al*. Interferon-gamma priming is involved in the activation of arginase by oligodeoxinucleotides containing CpG motifs in murine macrophages. *Immunology* 128(1 Suppl), e159-169 (2009).
109. Morris SM, Jr., Bhamidipati D, Kepka-Lenhart D. Human type II arginase: sequence analysis and tissue-specific expression. *Gene* 193(2), 157-161 (1997).
110. Deignan JL, Livesay JC, Yoo PK *et al*. Ornithine deficiency in the arginase double knockout mouse. *Molecular genetics and metabolism* 89(1-2), 87-96 (2006).
111. Iyer RK, Yoo PK, Kern RM *et al*. Mouse model for human arginase deficiency. *Molecular and cellular biology* 22(13), 4491-4498 (2002).
112. Crombez EA, Cederbaum SD. Hyperargininemia due to liver arginase deficiency. *Molecular genetics and metabolism* 84(3), 243-251 (2005).
113. Choi S, Park C, Ahn M, Lee JH, Shin T. Immunohistochemical study of arginase 1 and 2 in various tissues of rats. *Acta histochemica* 114(5), 487-494 (2012).
114. Iyer RK, Bando JM, Jenkinson CP *et al*. Cloning and characterization of the mouse and rat type II arginase genes. *Molecular genetics and metabolism* 63(3), 168-175 (1998).
115. Xia Y, Dawson VL, Dawson TM, Snyder SH, Zweier JL. Nitric oxide synthase generates superoxide and nitric oxide in arginine-depleted cells leading to peroxynitrite-mediated cellular injury. *Proceedings of the National Academy of Sciences of the United States of America* 93(13), 6770-6774 (1996).
116. Romero MJ, Platt DH, Tawfik HE *et al*. Diabetes-induced coronary vascular dysfunction involves increased arginase activity. *Circulation research* 102(1), 95-102 (2008).

117. Shin WS, Berkowitz DE, Ryoo SW. Increased arginase II activity contributes to endothelial dysfunction through endothelial nitric oxide synthase uncoupling in aged mice. *Experimental & molecular medicine* 44(10), 594-602 (2012).
118. Yepuri G, Velagapudi S, Xiong Y *et al*. Positive crosstalk between arginase-II and S6K1 in vascular endothelial inflammation and aging. *Aging cell* 11(6), 1005-1016 (2012).
119. Chicoine LG, Paffett ML, Young TL, Nelin LD. Arginase inhibition increases nitric oxide production in bovine pulmonary arterial endothelial cells. *American journal of physiology. Lung cellular and molecular physiology* 287(1), L60-68 (2004).
120. Cayatte AJ, Palacino JJ, Horten K, Cohen RA. Chronic inhibition of nitric oxide production accelerates neointima formation and impairs endothelial function in hypercholesterolemic rabbits. *Arteriosclerosis and thrombosis : a journal of vascular biology / American Heart Association* 14(5), 753-759 (1994).
121. Maarsingh H, Zaagsma J, Meurs H. Arginase: a key enzyme in the pathophysiology of allergic asthma opening novel therapeutic perspectives. *British journal of pharmacology* 158(3), 652-664 (2009).
122. Satriano J. Arginine pathways and the inflammatory response: interregulation of nitric oxide and polyamines: review article. *Amino acids* 26(4), 321-329 (2004).
123. Shearer JD, Richards JR, Mills CD, Caldwell MD. Differential regulation of macrophage arginine metabolism: a proposed role in wound healing. *The American journal of physiology* 272(2 Pt 1), E181-190 (1997).
124. Hey C, Boucher JL, Vadon-Le Goff S, Ketterer G, Wessler I, Racke K. Inhibition of arginase in rat and rabbit alveolar macrophages by N omega-hydroxy-D,L-indospicine, effects on L-arginine utilization by nitric oxide synthase. *British journal of pharmacology* 121(3), 395-400 (1997).
125. Wang WW, Jenkinson CP, Griscavage JM *et al*. Co-induction of arginase and nitric oxide synthase in murine macrophages activated by lipopolysaccharide. *Biochemical and biophysical research communications* 210(3), 1009-1016 (1995).
126. Boutard V, Havouis R, Fouqueray B, Philippe C, Moulinoux JP, Baud L. Transforming growth factor-beta stimulates arginase activity in macrophages. Implications for the regulation of macrophage cytotoxicity. *Journal of immunology (Baltimore, Md. : 1950)* 155(4), 2077-2084 (1995).
127. Pesce JT, Ramalingam TR, Mentink-Kane MM *et al*. Arginase-1-expressing macrophages suppress Th2 cytokine-driven inflammation and fibrosis. *PLoS pathogens* 5(4), e1000371 (2009).
128. Gordon S. Alternative activation of macrophages. *Nature reviews. Immunology* 3(1), 23-35 (2003).
129. Morris SM, Jr., Kepka-Lenhart D, Chen LC. Differential regulation of arginases and inducible nitric oxide synthase in murine macrophage cells. *The American journal of physiology* 275(5 Pt 1), E740-747 (1998).
130. Mussai F, De Santo C, Abu-Dayyeh I *et al*. Acute myeloid leukemia creates an arginase-dependent immunosuppressive microenvironment. *Blood* 122(5), 749-758 (2013).
131. Chakravortty D, Hensel M. Inducible nitric oxide synthase and control of intracellular bacterial pathogens. *Microbes and infection / Institut Pasteur* 5(7), 621-627 (2003).

132. Das P, Lahiri A, Lahiri A, Chakravortty D. Modulation of the arginase pathway in the context of microbial pathogenesis: a metabolic enzyme moonlighting as an immune modulator. *PLoS pathogens* 6(6), e1000899 (2010).
133. Lahiri A, Das P, Chakravortty D. Arginase modulates Salmonella induced nitric oxide production in RAW264.7 macrophages and is required for Salmonella pathogenesis in mice model of infection. *Microbes and infection / Institut Pasteur* 10(10-11), 1166-1174 (2008).
134. Qualls JE, Murray PJ. Immunometabolism within the tuberculosis granuloma: amino acids, hypoxia, and cellular respiration. *Seminars in immunopathology* 38(2), 139-152 (2016).
135. Bussiere FI, Chaturvedi R, Cheng Y *et al*. Spermine causes loss of innate immune response to Helicobacter pylori by inhibition of inducible nitric-oxide synthase translation. *The Journal of biological chemistry* 280(4), 2409-2412 (2005).
136. Gobert AP, Mersey BD, Cheng Y, Blumberg DR, Newton JC, Wilson KT. Cutting edge: urease release by Helicobacter pylori stimulates macrophage inducible nitric oxide synthase. *Journal of immunology (Baltimore, Md. : 1950)* 168(12), 6002-6006 (2002).
137. El Kasmi KC, Qualls JE, Pesce JT *et al*. Toll-like receptor-induced arginase 1 in macrophages thwarts effective immunity against intracellular pathogens. *Nature immunology* 9(12), 1399-1406 (2008).
138. Scharton-Kersten TM, Yap G, Magram J, Sher A. Inducible nitric oxide is essential for host control of persistent but not acute infection with the intracellular pathogen Toxoplasma gondii. *The Journal of experimental medicine* 185(7), 1261-1273 (1997).
139. Abdallahi OM, Bensalem H, Augier R, Diagana M, De Reggi M, Gharib B. Arginase expression in peritoneal macrophages and increase in circulating polyamine levels in mice infected with Schistosoma mansoni. *Cellular and molecular life sciences : CMLS* 58(9), 1350-1357 (2001).
140. Oza SL, Tetaud E, Ariyanayagam MR, Warnon SS, Fairlamb AH. A single enzyme catalyses formation of Trypanothione from glutathione and spermidine in Trypanosoma cruzi. *The Journal of biological chemistry* 277(39), 35853-35861 (2002).
141. Aoki MP, Guinazu NL, Pellegrini AV, Gotoh T, Masih DT, Gea S. Cruzipain, a major Trypanosoma cruzi antigen, promotes arginase-2 expression and survival of neonatal mouse cardiomyocytes. *American journal of physiology. Cell physiology* 286(2), C206-212 (2004).
142. Duleu S, Vincendeau P, Courtois P *et al*. Mouse strain susceptibility to trypanosome infection: an arginase-dependent effect. *Journal of immunology (Baltimore, Md. : 1950)* 172(10), 6298-6303 (2004).
143. Namangala B, De Baetselier P, Noel W, Brys L, Beschin A. Alternative versus classical macrophage activation during experimental African trypanosomosis. *Journal of leukocyte biology* 69(3), 387-396 (2001).
144. Iniesta V, Carcelen J, Molano I *et al*. Arginase I induction during Leishmania major infection mediates the development of disease. *Infection and immunity* 73(9), 6085-6090 (2005).
145. Iniesta V, Gomez-Nieto LC, Corraliza I. The inhibition of arginase by N(omega)-hydroxy-l-arginine controls the growth of Leishmania inside macrophages. *The Journal of experimental medicine* 193(6), 777-784 (2001).

146. Cao W, Sun B, Feitelson MA, Wu T, Tur-Kaspa R, Fan Q. Hepatitis C virus targets over-expression of arginase I in hepatocarcinogenesis. *International journal of cancer. Journal international du cancer* 124(12), 2886-2892 (2009).
147. Fitzpatrick JM, Fuentes JM, Chalmers IW *et al*. Schistosoma mansoni arginase shares functional similarities with human orthologs but depends upon disulphide bridges for enzymatic activity. *International journal for parasitology* 39(3), 267-279 (2009).
148. Mcgee DJ, Radcliff FJ, Mendz GL, Ferrero RL, Mobley HL. Helicobacter pylori rocF is required for arginase activity and acid protection in vitro but is not essential for colonization of mice or for urease activity. *Journal of bacteriology* 181(23), 7314-7322 (1999).
149. Mcgee DJ, Zabaleta J, Viator RJ, Testerman TL, Ochoa AC, Mendz GL. Purification and characterization of Helicobacter pylori arginase, RocF: unique features among the arginase superfamily. *European journal of biochemistry / FEBS* 271(10), 1952-1962 (2004).
150. Roberts SC, Tancer MJ, Polinsky MR, Gibson KM, Heby O, Ullman B. Arginase plays a pivotal role in polyamine precursor metabolism in Leishmania. Characterization of gene deletion mutants. *The Journal of biological chemistry* 279(22), 23668-23678 (2004).
151. Rodriguez PC, Zea AH, Desalvo J *et al*. L-arginine consumption by macrophages modulates the expression of CD3 zeta chain in T lymphocytes. *Journal of immunology (Baltimore, Md. : 1950)* 171(3), 1232-1239 (2003).
152. Kropf P, Baud D, Marshall SE *et al*. Arginase activity mediates reversible T cell hyporesponsiveness in human pregnancy. *European journal of immunology* 37(4), 935-945 (2007).
153. Munder M, Schneider H, Luckner C *et al*. Suppression of T-cell functions by human granulocyte arginase. *Blood* 108(5), 1627-1634 (2006).
154. Zea AH, Rodriguez PC, Atkins MB *et al*. Arginase-producing myeloid suppressor cells in renal cell carcinoma patients: a mechanism of tumour evasion. *Cancer research* 65(8), 3044-3048 (2005).
155. Rodriguez PC, Quiceno DG, Ochoa AC. L-arginine availability regulates T-lymphocyte cell-cycle progression. *Blood* 109(4), 1568-1573 (2007).
156. Ichihara F, Kono K, Sekikawa T, Matsumoto Y. Surgical stress induces decreased expression of signal-transducing zeta molecules in T cells. *European surgical research. Europaische chirurgische Forschung. Recherches chirurgicales europeennes* 31(2), 138-146 (1999).
157. Rodriguez PC, Zea AH, Culotta KS, Zabaleta J, Ochoa JB, Ochoa AC. Regulation of T cell receptor CD3zeta chain expression by L-arginine. *The Journal of biological chemistry* 277(24), 21123-21129 (2002).
158. Taheri F, Ochoa JB, Faghiri Z *et al*. L-Arginine regulates the expression of the T-cell receptor zeta chain (CD3zeta) in Jurkat cells. *Clinical cancer research : an official journal of the American Association for Cancer Research* 7(3 Suppl), 958s-965s (2001).
159. Fallarino F, Grohmann U, You S *et al*. The combined effects of tryptophan starvation and tryptophan catabolites down-regulate T cell receptor zeta-chain and induce a regulatory phenotype in naive T cells. *Journal of Immunology* 176(11), 6752-6761 (2006).
160. Xu L, Hilliard B, Carmody RJ *et al*. Arginase and autoimmune inflammation in the central nervous system. *Immunology* 110(1), 141-148 (2003).

161. Corraliza I, Moncada S. Increased expression of arginase II in patients with different forms of arthritis. Implications of the regulation of nitric oxide. *The Journal of rheumatology* 29(11), 2261-2265 (2002).
162. Wu H, Zhen Y, Ma Z *et al*. Arginase-1-dependent promotion of TH17 differentiation and disease progression by MDSCs in systemic lupus erythematosus. *Science translational medicine* 8(331), 331ra340 (2016).
163. Fujii W, Ashihara E, Hirai H *et al*. Myeloid-derived suppressor cells play crucial roles in the regulation of mouse collagen-induced arthritis. *Journal of immunology (Baltimore, Md. : 1950)* 191(3), 1073-1081 (2013).
164. Weiner CP, Knowles RG, Stegink LD, Dawson J, Moncada S. Myometrial arginase activity increases with advancing pregnancy in the guinea pig. *American journal of obstetrics and gynecology* 174(2), 779-782 (1996).
165. Elahi S, Ertelt JM, Kinder JM *et al*. Immunosuppressive CD71+ erythroid cells compromise neonatal host defence against infection. *Nature* 504(7478), 158-162 (2013).
166. Edinger AL, Thompson CB. Antigen-presenting cells control T cell proliferation by regulating amino acid availability. *Proceedings of the National Academy of Sciences of the United States of America* 99(3), 1107-1109 (2002).
167. Dunand-Sauthier I, Irla M, Carnesecchi S *et al*. Repression of arginase-2 expression in dendritic cells by microRNA-155 is critical for promoting T cell proliferation. *Journal of immunology (Baltimore, Md. : 1950)* 193(4), 1690-1700 (2014).
168. Chang CI, Liao JC, Kuo L. Macrophage arginase promotes tumour cell growth and suppresses nitric oxide-mediated tumour cytotoxicity. *Cancer research* 61(3), 1100-1106 (2001).
169. Gannon PO, Godin-Ethier J, Hassler M *et al*. Androgen-regulated expression of arginase 1, arginase 2 and interleukin-8 in human prostate cancer. *PloS one* 5(8), e12107 (2010).
170. Singh R, Pervin S, Karimi A, Cederbaum S, Chaudhuri G. Arginase activity in human breast cancer cell lines: N(omega)-hydroxy-L-arginine selectively inhibits cell proliferation and induces apoptosis in MDA-MB-468 cells. *Cancer research* 60(12), 3305-3312 (2000).
171. Suer Gokmen S, Yoruk Y, Cakir E, Yorulmaz F, Gulen S. Arginase and ornithine, as markers in human non-small cell lung carcinoma. *Cancer biochemistry biophysics* 17(1-2), 125-131 (1999).
172. Tate DJ, Jr., Vonderhaar DJ, Caldas YA *et al*. Effect of arginase II on L-arginine depletion and cell growth in murine cell lines of renal cell carcinoma. *Journal of hematology & oncology* 1 14 (2008).
173. Bronte V, Kasic T, Gri G *et al*. Boosting antitumour responses of T lymphocytes infiltrating human prostate cancers. *The Journal of experimental medicine* 201(8), 1257-1268 (2005).
174. Mumenthaler SM, Yu H, Tze S *et al*. Expression of arginase II in prostate cancer. *International journal of oncology* 32(2), 357-365 (2008).
175. Wu CW, Chi CW, Tsay SH *et al*. The effects of arginase on neoplasm. I. The role of arginase in the immunosuppressive effects of extract from gastric cancer. *Zhonghua Minguo wei sheng wu ji mian yi xue za zhi = Chinese journal of microbiology and immunology* 20(4), 279-289 (1987).

176. Wu CW, Chung WW, Chi CW *et al*. Immunohistochemical study of arginase in cancer of the stomach. *Virchows Archiv : an international journal of pathology* 428(6), 325-331 (1996).
177. Wu CW, Wang SR, Chang TJ *et al*. Content of glucocorticoid receptor and arginase in gastric cancer and normal gastric mucosal tissues. *Cancer* 64(12), 2552-2556 (1989).
178. Wu CW, Chi CW, Lin EC, Lui WY, P'eng F K, Wang SR. Serum arginase level in patients with gastric cancer. *Journal of clinical gastroenterology* 18(1), 84-85 (1994).
179. Porembska Z, Luboinski G, Chrzanowska A, Mielczarek M, Magnuska J, Baranczyk-Kuzma A. Arginase in patients with breast cancer. *Clinica chimica acta; international journal of clinical chemistry* 328(1-2), 105-111 (2003).
180. Adams JL, Smothers J, Srinivasan R, Hoos A. Big opportunities for small molecules in immuno-oncology. *Nature reviews. Drug discovery* 14(9), 603-622 (2015).
181. Bronte V, Apolloni E, Cabrelle A *et al*. Identification of a CD11b(+)/Gr-1(+)/CD31(+) myeloid progenitor capable of activating or suppressing CD8(+) T cells. *Blood* 96(12), 3838-3846 (2000).
182. Bronte V, Serafini P, De Santo C *et al*. IL-4-induced arginase 1 suppresses alloreactive T cells in tumour-bearing mice. *Journal of immunology (Baltimore, Md. : 1950)* 170(1), 270-278 (2003).
183. Gabrilovich DI, Velders MP, Sotomayor EM, Kast WM. Mechanism of immune dysfunction in cancer mediated by immature Gr-1+ myeloid cells. *Journal of immunology (Baltimore, Md. : 1950)* 166(9), 5398-5406 (2001).
184. Ino Y, Yamazaki-Itoh R, Oguro S *et al*. Arginase II expressed in cancer-associated fibroblasts indicates tissue hypoxia and predicts poor outcome in patients with pancreatic cancer. *PloS one* 8(2), e55146 (2013).
185. Rodriguez PC, Ernstoff MS, Hernandez C *et al*. Arginase I-producing myeloid-derived suppressor cells in renal cell carcinoma are a subpopulation of activated granulocytes. *Cancer research* 69(4), 1553-1560 (2009).
186. Rodriguez PC, Quiceno DG, Zabaleta J *et al*. Arginase I production in the tumour microenvironment by mature myeloid cells inhibits T-cell receptor expression and antigen-specific T-cell responses. *Cancer research* 64(16), 5839-5849 (2004).
187. Kusmartsev S, Nefedova Y, Yoder D, Gabrilovich DI. Antigen-specific inhibition of CD8+ T cell response by immature myeloid cells in cancer is mediated by reactive oxygen species. *Journal of immunology (Baltimore, Md. : 1950)* 172(2), 989-999 (2004).
188. Mazzoni A, Bronte V, Visintin A *et al*. Myeloid suppressor lines inhibit T cell responses by an NO-dependent mechanism. *Journal of immunology (Baltimore, Md. : 1950)* 168(2), 689-695 (2002).
189. Vasquez-Dunddel D, Pan F, Zeng Q *et al*. STAT3 regulates arginase-I in myeloid-derived suppressor cells from cancer patients. *The Journal of clinical investigation* 123(4), 1580-1589 (2013).
190. Rutschman R, Lang R, Hesse M, Ihle JN, Wynn TA, Murray PJ. Cutting edge: Stat6-dependent substrate depletion regulates nitric oxide production. *Journal of immunology (Baltimore, Md. : 1950)* 166(4), 2173-2177 (2001).

191. Rodriguez PC, Hernandez CP, Quiceno D *et al*. Arginase I in myeloid suppressor cells is induced by COX-2 in lung carcinoma. *The Journal of experimental medicine* 202(7), 931-939 (2005).
192. De Boniface J, Mao Y, Schmidt-Mende J, Kiessling R, Poschke I. Expression patterns of the immunomodulatory enzyme arginase 1 in blood, lymph nodes and tumour tissue of early-stage breast cancer patients. *Oncoimmunology* 1(8), 1305-1312 (2012).
193. Jacobsen LC, Theilgaard-Monch K, Christensen EI, Borregaard N. Arginase 1 is expressed in myelocytes/metamyelocytes and localized in gelatinase granules of human neutrophils. *Blood* 109(7), 3084-3087 (2007).
194. Balkwill F, Charles KA, Mantovani A. Smoldering and polarized inflammation in the initiation and promotion of malignant disease. *Cancer Cell* 7(3), 211-217 (2005).
195. Bingle L, Brown NJ, Lewis CE. The role of tumour-associated macrophages in tumour progression: implications for new anticancer therapies. *The Journal of pathology* 196(3), 254-265 (2002).
196. Pollard JW. Tumour-educated macrophages promote tumour progression and metastasis. *Nature reviews. Cancer* 4(1), 71-78 (2004).
197. Pucci F, Venneri MA, Biziato D *et al*. A distinguishing gene signature shared by tumour-infiltrating Tie2-expressing monocytes, blood "resident" monocytes, and embryonic macrophages suggests common functions and developmental relationships. *Blood* 114(4), 901-914 (2009).
198. Lissbrant IF, Stattin P, Wikstrom P, Damber JE, Egevad L, Bergh A. Tumour associated macrophages in human prostate cancer: relation to clinicopathological variables and survival. *International journal of oncology* 17(3), 445-451 (2000).
199. Pekarek LA, Starr BA, Toledano AY, Schreiber H. Inhibition of tumour growth by elimination of granulocytes. *The Journal of experimental medicine* 181(1), 435-440 (1995).
200. Rodriguez PC, Ochoa AC. T cell dysfunction in cancer: role of myeloid cells and tumour cells regulating amino acid availability and oxidative stress. *Seminars in cancer biology* 16(1), 66-72 (2006).
201. Sinha P, Clements VK, Ostrand-Rosenberg S. Reduction of myeloid-derived suppressor cells and induction of M1 macrophages facilitate the rejection of established metastatic disease. *Journal of immunology (Baltimore, Md. : 1950)* 174(2), 636-645 (2005).
202. Haines RJ, Pendleton LC, Eichler DC. Argininosuccinate synthase: at the center of arginine metabolism. *International journal of biochemistry and molecular biology* 2(1), 8-23 (2011).
203. Goto M, Omi R, Miyahara I, Sugahara M, Hirotsu K. Structures of argininosuccinate synthetase in enzyme-ATP substrates and enzyme-AMP product forms: stereochemistry of the catalytic reaction. *The Journal of biological chemistry* 278(25), 22964-22971 (2003).
204. Cohen NS. Intracellular localization of the mRNAs of argininosuccinate synthetase and argininosuccinate lyase around liver mitochondria, visualized by high-resolution in situ reverse transcription-polymerase chain reaction. *J Cell Biochem* 61(1), 81-96 (1996).

205. Cohen NS, Kuda A. Argininosuccinate synthetase and argininosuccinate lyase are localized around mitochondria: an immunocytochemical study. *J Cell Biochem* 60(3), 334-340 (1996).
206. Flam BR, Hartmann PJ, Harrell-Booth M, Solomonson LP, Eichler DC. Caveolar localization of arginine regeneration enzymes, argininosuccinate synthase, and lyase, with endothelial nitric oxide synthase. *Nitric oxide : biology and chemistry* 5(2), 187-197 (2001).
207. Fulton D, Babbitt R, Zoellner S *et al*. Targeting of endothelial nitric-oxide synthase to the cytoplasmic face of the Golgi complex or plasma membrane regulates Akt- versus calcium-dependent mechanisms for nitric oxide release. *The Journal of biological chemistry* 279(29), 30349-30357 (2004).
208. Forstermann U, Munzel T. Endothelial nitric oxide synthase in vascular disease: from marvel to menace. *Circulation* 113(13), 1708-1714 (2006).
209. Gao HZ, Kobayashi K, Tabata A *et al*. Identification of 16 novel mutations in the argininosuccinate synthetase gene and genotype-phenotype correlation in 38 classical citrullinemia patients. *Human mutation* 22(1), 24-34 (2003).
210. Kobayashi K, Jackson MJ, Tick DB, O'brien WE, Beaudet AL. Heterogeneity of mutations in argininosuccinate synthetase causing human citrullinemia. *The Journal of biological chemistry* 265(19), 11361-11367 (1990).
211. Saheki T, Kobayashi K, Iijima M *et al*. Adult-onset type II citrullinemia and idiopathic neonatal hepatitis caused by citrin deficiency: involvement of the aspartate glutamate carrier for urea synthesis and maintenance of the urea cycle. *Molecular genetics and metabolism* 81 Suppl 1 S20-26 (2004).
212. Guei TR, Liu MC, Yang CP, Su TS. Identification of a liver-specific cAMP response element in the human argininosuccinate synthetase gene. *Biochemical and biophysical research communications* 377(1), 257-261 (2008).
213. Husson A, Brasse-Lagnel C, Fairand A, Renouf S, Lavoinne A. Argininosuccinate synthetase from the urea cycle to the citrulline-NO cycle. *European journal of biochemistry / FEBS* 270(9), 1887-1899 (2003).
214. Anderson GM, Freytag SO. Synergistic activation of a human promoter in vivo by transcription factor Sp1. *Molecular and cellular biology* 11(4), 1935-1943 (1991).
215. Jinno Y, Matuo S, Nomiyama H, Shimada K, Matsuda I. Novel structure of the 5' end region of the human argininosuccinate synthetase gene. *J Biochem* 98(5), 1395-1403 (1985).
216. Jinno Y, Nomiyama H, Matuo S, Shimada K, Matsuda I, Saheki T. Structure of the 5' end region of the human argininosuccinate synthetase gene. *Journal of inherited metabolic disease* 8(3), 157-159 (1985).
217. Tsai WB, Aiba I, Lee SY, Feun L, Savaraj N, Kuo MT. Resistance to arginine deiminase treatment in melanoma cells is associated with induced argininosuccinate synthetase expression involving c-Myc/HIF-1alpha/Sp4. *Mol Cancer Ther* 8(12), 3223-3233 (2009).
218. Goodwin BL, Solomonson LP, Eichler DC. Argininosuccinate synthase expression is required to maintain nitric oxide production and cell viability in aortic endothelial cells. *The Journal of biological chemistry* 279(18), 18353-18360 (2004).
219. Su Y, Block ER. Hypoxia inhibits L-arginine synthesis from L-citrulline in porcine pulmonary artery endothelial cells. *The American journal of physiology* 269(5 Pt 1), L581-587 (1995).

220. Xie L, Gross SS. Argininosuccinate synthetase overexpression in vascular smooth muscle cells potentiates immunostimulant-induced NO production. *The Journal of biological chemistry* 272(26), 16624-16630 (1997).
221. Davis TA, Fiorotto ML, Reeds PJ. Amino acid compositions of body and milk protein change during the suckling period in rats. *The Journal of nutrition* 123(5), 947-956 (1993).
222. Brosnan ME, Brosnan JT. Renal arginine metabolism. *The Journal of nutrition* 134(10 Suppl), 2791S-2795S; discussion 2796S-2797S (2004).
223. Nasrallah F, Feki M, Kaabachi N. Creatine and creatine deficiency syndromes: biochemical and clinical aspects. *Pediatric neurology* 42(3), 163-171 (2010).
224. Davis PK, Wu G. Compartmentation and kinetics of urea cycle enzymes in porcine enterocytes. *Comparative biochemistry and physiology. Part B, Biochemistry & molecular biology* 119(3), 527-537 (1998).
225. Ensor CM, Holtsberg FW, Bomalaski JS, Clark MA. Pegylated arginine deiminase (ADI-SS PEG20,000 mw) inhibits human melanomas and hepatocellular carcinomas in vitro and in vivo. *Cancer research* 62(19), 5443-5450 (2002).
226. Fiedler T, Strauss M, Hering S *et al*. Arginine deprivation by arginine deiminase of Streptococcus pyogenes controls primary glioblastoma growth in vitro and in vivo. *Cancer biology & therapy* 16(7), 1047-1055 (2015).
227. Syed N, Langer J, Janczar K *et al*. Epigenetic status of argininosuccinate synthetase and argininosuccinate lyase modulates autophagy and cell death in glioblastoma. *Cell death & disease* 4 e458 (2013).
228. Liu Q, Stewart J, Wang H *et al*. Reduced expression of argininosuccinate synthetase 1 has a negative prognostic impact in patients with pancreatic ductal adenocarcinoma. *PloS one* 12(2), e0171985 (2017).
229. Ohshima K, Nojima S, Tahara S *et al*. Argininosuccinate Synthase 1-Deficiency Enhances the Cell Sensitivity to Arginine through Decreased DEPTOR Expression in Endometrial Cancer. *Sci Rep* 7 45504 (2017).
230. Nicholson LJ, Smith PR, Hiller L *et al*. Epigenetic silencing of argininosuccinate synthetase confers resistance to platinum-induced cell death but collateral sensitivity to arginine auxotrophy in ovarian cancer. *International journal of cancer. Journal international du cancer* 125(6), 1454-1463 (2009).
231. Szlosarek PW, Steele JP, Nolan L *et al*. Arginine Deprivation With Pegylated Arginine Deiminase in Patients With Argininosuccinate Synthetase 1-Deficient Malignant Pleural Mesothelioma: A Randomized Clinical Trial. *JAMA oncology* 3(1), 58-66 (2017).
232. Kobayashi E, Masuda M, Nakayama R *et al*. Reduced argininosuccinate synthetase is a predictive biomarker for the development of pulmonary metastasis in patients with osteosarcoma. *Mol Cancer Ther* 9(3), 535-544 (2010).
233. Phillips MM, Sheaff MT, Szlosarek PW. Targeting arginine-dependent cancers with arginine-degrading enzymes: opportunities and challenges. *Cancer research and treatment : official journal of Korean Cancer Association* 45(4), 251-262 (2013).
234. Delage B, Fennell DA, Nicholson L *et al*. Arginine deprivation and argininosuccinate synthetase expression in the treatment of cancer. *International journal of cancer. Journal international du cancer* 126(12), 2762-2772 (2010).

235. Wheatley DN. Controlling cancer by restricting arginine availability--arginine-catabolizing enzymes as anticancer agents. *Anti-cancer drugs* 15(9), 825-833 (2004).
236. Allen MD, Luong P, Hudson C *et al*. Prognostic and therapeutic impact of argininosuccinate synthetase 1 control in bladder cancer as monitored longitudinally by PET imaging. *Cancer research* 74(3), 896-907 (2014).
237. Changou CA, Chen YR, Xing L *et al*. Arginine starvation-associated atypical cellular death involves mitochondrial dysfunction, nuclear DNA leakage, and chromatin autophagy. *Proceedings of the National Academy of Sciences of the United States of America* 111(39), 14147-14152 (2014).
238. Dillon BJ, Prieto VG, Curley SA *et al*. Incidence and distribution of argininosuccinate synthetase deficiency in human cancers: a method for identifying cancers sensitive to arginine deprivation. *Cancer* 100(4), 826-833 (2004).
239. Mcalpine JA, Lu HT, Wu KC, Knowles SK, Thomson JA. Down-regulation of argininosuccinate synthetase is associated with cisplatin resistance in hepatocellular carcinoma cell lines: implications for PEGylated arginine deiminase combination therapy. *BMC Cancer* 14 621 (2014).
240. Szlosarek PW, Grimshaw MJ, Wilbanks GD *et al*. Aberrant regulation of argininosuccinate synthetase by TNF-alpha in human epithelial ovarian cancer. *International journal of cancer. Journal international du cancer* 121(1), 6-11 (2007).
241. Shan YS, Hsu HP, Lai MD *et al*. Argininosuccinate synthetase 1 suppression and arginine restriction inhibit cell migration in gastric cancer cell lines. *Sci Rep* 5 9783 (2015).
242. Shan YS, Hsu HP, Lai MD, Yen MC, Luo YP, Chen YL. Increased expression of argininosuccinate synthetase protein predicts poor prognosis in human gastric cancer. *Oncol Rep* 33(1), 49-57 (2015).
243. Bateman LA, Ku WM, Heslin MJ, Contreras CM, Skibola CF, Nomura DK. Argininosuccinate Synthase 1 is a Metabolic Regulator of Colorectal Cancer Pathogenicity. *ACS Chem Biol* 12(4), 905-911 (2017).
244. Dong J, Qiu H, Garcia-Barrio M, Anderson J, Hinnebusch AG. Uncharged tRNA activates GCN2 by displacing the protein kinase moiety from a bipartite tRNA-binding domain. *Mol Cell* 6(2), 269-279 (2000).
245. Hinnebusch AG. Translational regulation of GCN4 and the general amino acid control of yeast. *Annual review of microbiology* 59 407-450 (2005).
246. Wek SA, Zhu S, Wek RC. The histidyl-tRNA synthetase-related sequence in the eIF-2 alpha protein kinase GCN2 interacts with tRNA and is required for activation in response to starvation for different amino acids. *Molecular and cellular biology* 15(8), 4497-4506 (1995).
247. Qiu H, Dong J, Hu C, Francklyn CS, Hinnebusch AG. The tRNA-binding moiety in GCN2 contains a dimerization domain that interacts with the kinase domain and is required for tRNA binding and kinase activation. *The EMBO journal* 20(6), 1425-1438 (2001).
248. Qiu HF, Garcia-Barrio MT, Hinnebusch AG. Dimerization by translation initiation factor 2 kinase GCN2 is mediated by interactions in the C-terminal ribosome-binding region and the protein kinase domain. *Molecular and cellular biology* 18(5), 2697-2711 (1998).

249. Romano PR, Garcia-Barrio MT, Zhang X *et al*. Autophosphorylation in the activation loop is required for full kinase activity in vivo of human and yeast eukaryotic initiation factor 2alpha kinases PKR and GCN2. *Molecular and cellular biology* 18(4), 2282-2297 (1998).
250. Dever TE, Feng L, Wek RC, Cigan AM, Donahue TF, Hinnebusch AG. Phosphorylation of initiation factor-2-alpha by protein-kinase GCN2 mediates gene-specific translational control of GCN4 in yeast. *Cell* 68(3), 585-596 (1992).
251. Harding HP, Novoa I, Zhang Y *et al*. Regulated translation initiation controls stress-induced gene expression in mammalian cells. *Mol Cell* 6(5), 1099-1108 (2000).
252. Harding HP, Zhang Y, Zeng H *et al*. An integrated stress response regulates amino acid metabolism and resistance to oxidative stress. *Mol Cell* 11(3), 619-633 (2003).
253. Ye J, Kumanova M, Hart LS *et al*. The GCN2-ATF4 pathway is critical for tumour cell survival and proliferation in response to nutrient deprivation. *Embo Journal* 29(12), 2082-2096 (2010).
254. Thomson AW, Turnquist HR, Raimondi G. Immunoregulatory functions of mTOR inhibition. *Nature reviews. Immunology* 9(5), 324-337 (2009).
255. Sancak Y, Bar-Peled L, Zoncu R, Markhard AL, Nada S, Sabatini DM. Ragulator-Rag complex targets mTORC1 to the lysosomal surface and is necessary for its activation by amino acids. *Cell* 141(2), 290-303 (2010).
256. Sancak Y, Peterson TR, Shaul YD *et al*. The Rag GTPases bind raptor and mediate amino acid signaling to mTORC1. *Science* 320(5882), 1496-1501 (2008).
257. Nicklin P, Bergman P, Zhang B *et al*. Bidirectional transport of amino acids regulates mTOR and autophagy. *Cell* 136(3), 521-534 (2009).
258. Zoncu R, Bar-Peled L, Efeyan A, Wang S, Sancak Y, Sabatini DM. mTORC1 senses lysosomal amino acids through an inside-out mechanism that requires the vacuolar H(+)-ATPase. *Science* 334(6056), 678-683 (2011).
259. Zoncu R, Efeyan A, Sabatini DM. mTOR: from growth signal integration to cancer, diabetes and ageing. *Nature reviews. Molecular cell biology* 12(1), 21-35 (2011).
260. Bonfils G, Jaquenoud M, Bontron S, Ostrowicz C, Ungermann C, De Virgilio C. Leucyl-tRNA synthetase controls TORC1 via the EGO complex. *Mol Cell* 46(1), 105-110 (2012).
261. Chantranupong L, Scaria SM, Saxton RA *et al*. The CASTOR Proteins Are Arginine Sensors for the mTORC1 Pathway. *Cell* 165(1), 153-164 (2016).
262. Han JM, Jeong SJ, Park MC *et al*. Leucyl-tRNA synthetase is an intracellular leucine sensor for the mTORC1-signaling pathway. *Cell* 149(2), 410-424 (2012).
263. Rebsamen M, Pochini L, Stasyk T *et al*. SLC38A9 is a component of the lysosomal amino acid sensing machinery that controls mTORC1. *Nature* 519(7544), 477-+ (2015).
264. Rebsamen M, Superti-Furga G. SLC38A9: A lysosomal amino acid transporter at the core of the amino acid-sensing machinery that controls MTORC1. *Autophagy* 12(6), 1061-1062 (2016).

265. Wang H, Ji Y, Wu G *et al*. l-Tryptophan Activates Mammalian Target of Rapamycin and Enhances Expression of Tight Junction Proteins in Intestinal Porcine Epithelial Cells*. The Journal of nutrition* 145(6), 1156-1162 (2015).
266. Wang SY, Tsun ZY, Wolfson RL *et al*. Lysosomal amino acid transporter SLC38A9 signals arginine sufficiency to mTORC1*. Science* 347(6218), 188-194 (2015).
267. Wolfson RL, Chantranupong L, Saxton RA *et al*. Sestrin2 is a leucine sensor for the mTORC1 pathway*. Science* 351(6268), 43-48 (2016).
268. Beretta L, Gingras AC, Svitkin YV, Hall MN, Sonenberg N. Rapamycin blocks the phosphorylation of 4E-BP1 and inhibits cap-dependent initiation of translation*. The EMBO journal* 15(3), 658-664 (1996).
269. Brown EJ, Schreiber SL. A signaling pathway to translational control*. Cell* 86(4), 517-520 (1996).
270. Yang H, Jiang X, Li B *et al*. Mechanisms of mTORC1 activation by RHEB and inhibition by PRAS40*. Nature* 552(7685), 368-373 (2017).
271. Klysz D, Tai X, Robert PA *et al*. Glutamine-dependent alpha-ketoglutarate production regulates the balance between T helper 1 cell and regulatory T cell generation*. Science signaling* 8(396), ra97 (2015).
272. Cesar-Razquin A, Snijder B, Frappier-Brinton T *et al*. A Call for Systematic Research on Solute Carriers*. Cell* 162(3), 478-487 (2015).
273. Schlessinger A, Yee SW, Sali A, Giacomini KM. SLC classification: an update*. Clinical pharmacology and therapeutics* 94(1), 19-23 (2013).
274. Lin DY, Huang S, Chen J. Crystal structures of a polypeptide processing and secretion transporter*. Nature* 523(7561), 425-430 (2015).
275. He L, Vasiliou K, Nebert DW. Analysis and update of the human solute carrier (SLC) gene superfamily*. Human genomics* 3(2), 195-206 (2009).
276. Lin L, Yee SW, Kim RB, Giacomini KM. SLC transporters as therapeutic targets: emerging opportunities*. Nature reviews. Drug discovery* 14(8), 543-560 (2015).
277. Hediger MA, Romero MF, Peng JB, Rolfs A, Takanaga H, Bruford EA. The ABCs of solute carriers: physiological, pathological and therapeutic implications of human membrane transport proteins - Introduction*. Pflugers Archiv-European Journal of Physiology* 447(5), 465-468 (2004).
278. Durante W, Liao L, Reyna SV, Peyton KJ, Schafer AI. Transforming growth factor-beta(1) stimulates L-arginine transport and metabolism in vascular smooth muscle cells: role in polyamine and collagen synthesis*. Circulation* 103(8), 1121-1127 (2001).
279. Verrey F, Closs EI, Wagner CA, Palacin M, Endou H, Kanai Y. CATs and HATs: the SLC7 family of amino acid transporters*. Pflugers Archiv-European Journal of Physiology* 447(5), 532-542 (2004).
280. Yeramian A, Martin L, Serrat N *et al*. Arginine transport via cationic amino acid transporter 2 plays a critical regulatory role in classical or alternative activation of macrophages*. Journal of immunology (Baltimore, Md. : 1950)* 176(10), 5918-5924 (2006).
281. White MF. The transport of cationic amino acids across the plasma membrane of mammalian cells*. Biochimica et biophysica acta* 822(3-4), 355-374 (1985).
282. Thompson RW, Pesce JT, Ramalingam T *et al*. Cationic amino acid transporter-2 regulates immunity by modulating arginase activity*. PLoS pathogens* 4(3), e1000023 (2008).

283. Wanasen N, Macleod CL, Ellies LG, Soong L. L-arginine and cationic amino acid transporter 2B regulate growth and survival of Leishmania amazonensis amastigotes in macrophages. *Infection and immunity* 75(6), 2802-2810 (2007).
284. Werner A, Amann E, Schnitzius V *et al*. Induced arginine transport via cationic amino acid transporter-1 is necessary for human T-cell proliferation. *European journal of immunology* 46(1), 92-103 (2016).
285. Hosokawa H, Sawamura T, Kobayashi S, Ninomiya H, Miwa S, Masaki T. Cloning and characterization of a brain-specific cationic amino acid transporter. *The Journal of biological chemistry* 272(13), 8717-8722 (1997).
286. Kim JW, Closs EI, Albritton LM, Cunningham JM. Transport of cationic amino acids by the mouse ecotropic retrovirus receptor. *Nature* 352(6337), 725-728 (1991).
287. Macleod CL, Finley KD, Kakuda DK. y(+)-type cationic amino acid transport: expression and regulation of the mCAT genes. *The Journal of experimental biology* 196 109-121 (1994).
288. Chang J, Nicolas E, Marks D *et al*. miR-122, a mammalian liver-specific microRNA, is processed from hcr mRNA and may downregulate the high affinity cationic amino acid transporter CAT-1. *RNA biology* 1(2), 106-113 (2004).
289. Colas C, Ung PM, Schlessinger A. SLC Transporters: Structure, Function, and Drug Discovery. *MedChemComm* 7(6), 1069-1081 (2016).
290. Kanai Y, Hediger MA. The glutamate/neutral amino acid transporter family SLC1: molecular, physiological and pharmacological aspects. *Pflugers Archiv-European Journal of Physiology* 447(5), 469-479 (2004).
291. Kanai Y, Segawa H, Miyamoto K, Uchino H, Takeda E, Endou H. Expression cloning and characterization of a transporter for large neutral amino acids activated by the heavy chain of 4F2 antigen (CD98). *Journal of Biological Chemistry* 273(37), 23629-23632 (1998).
292. Mastroberardino L, Spindler B, Pfeiffer R *et al*. Amino-acid transport by heterodimers of 4F2hc/CD98 and members of a permease family. *Nature* 395(6699), 288-291 (1998).
293. Rossier G, Meier C, Bauch C *et al*. LAT2, a new basolateral 4F2hc/CD98-associated amino acid transporter of kidney and intestine. *The Journal of biological chemistry* 274(49), 34948-34954 (1999).
294. Segawa H, Fukasawa Y, Miyamoto K, Takeda E, Endou H, Kanai Y. Identification and functional characterization of a Na+-independent neutral amino acid transporter with broad substrate selectivity. *The Journal of biological chemistry* 274(28), 19745-19751 (1999).
295. Verrey F. System L: heteromeric exchangers of large, neutral amino acids involved in directional transport. *Pflugers Archiv-European Journal of Physiology* 445(5), 529-533 (2003).
296. Cormerais Y, Massard PA, Vucetic M *et al*. The glutamine transporter ASCT2 (SLC1A5) promotes tumour growth independently of the amino acid transporter LAT1 (SLC7A5). *The Journal of biological chemistry* 293(8), 2877-2887 (2018).
297. Fenczik CA, Zent R, Dellos M *et al*. Distinct domains of CD98hc regulate integrins and amino acid transport. *The Journal of biological chemistry* 276(12), 8746-8752 (2001).

298. Yanagida O, Kanai Y, Chairoungdua A *et al*. Human L-type amino acid transporter 1 (LAT1): characterization of function and expression in tumour cell lines*. Biochimica et biophysica acta* 1514(2), 291-302 (2001).
299. Boado RJ, Li JY, Nagaya M, Zhang C, Pardridge WM. Selective expression of the large neutral amino acid transporter at the blood-brain barrier*. Proceedings of the National Academy of Sciences of the United States of America* 96(21), 12079-12084 (1999).
300. Pochini L, Scalise M, Galluccio M, Indiveri C. Membrane transporters for the special amino acid glutamine: structure/function relationships and relevance to human health*. Frontiers in chemistry* 2 61 (2014).
301. Timosenko E, Ghadbane H, Silk JD *et al*. Nutritional Stress Induced by Tryptophan-Degrading Enzymes Results in ATF4-Dependent Reprogramming of the Amino Acid Transporter Profile in Tumour Cells*. Cancer research* 76(21), 6193-6204 (2016).
302. Broer A, Wagner C, Lang F, Broer S. Neutral amino acid transporter ASCT2 displays substrate-induced Na+ exchange and a substrate-gated anion conductance*. The Biochemical journal* 346 Pt 3 705-710 (2000).
303. Oburoglu L, Tardito S, Fritz V *et al*. Glucose and glutamine metabolism regulate human hematopoietic stem cell lineage specification*. Cell stem cell* 15(2), 169-184 (2014).
304. Kobayashi T, Shimabukuro-Demoto S, Yoshida-Sugitani R *et al*. The histidine transporter SLC15A4 coordinates mTOR-dependent inflammatory responses and pathogenic antibody production*. Immunity* 41(3), 375-388 (2014).
305. Kurian MA, Zhen J, Cheng SY *et al*. Homozygous loss-of-function mutations in the gene encoding the dopamine transporter are associated with infantile parkinsonism-dystonia*. The Journal of clinical investigation* 119(6), 1595-1603 (2009).
306. Wojtal KA, Eloranta JJ, Hruz P *et al*. Changes in mRNA Expression Levels of Solute Carrier Transporters in Inflammatory Bowel Disease Patients*. Drug Metabolism and Disposition* 37(9), 1871-1877 (2009).
307. Parks SK, Cormerais Y, Marchiq I, Pouyssegur J. Hypoxia optimises tumour growth by controlling nutrient import and acidic metabolite export*. Mol Aspects Med* 47-48 3-14 (2016).
308. Edinger AL. Controlling cell growth and survival through regulated nutrient transporter expression*. The Biochemical journal* 406(1), 1-12 (2007).
309. Pakos-Zebrucka K, Koryga I, Mnich K, Ljujic M, Samali A, Gorman AM. The integrated stress response*. EMBO reports* 17(10), 1374-1395 (2016).
310. Pavlova NN, Thompson CB. The Emerging Hallmarks of Cancer Metabolism*. Cell metabolism* 23(1), 27-47 (2016).
311. Timmerman LA, Holton T, Yuneva M *et al*. Glutamine sensitivity analysis identifies the xCT antiporter as a common triple-negative breast tumour therapeutic target*. Cancer Cell* 24(4), 450-465 (2013).
312. Srivastava MK, Sinha P, Clements VK, Rodriguez P, Ostrand-Rosenberg S. Myeloid-derived suppressor cells inhibit T-cell activation by depleting cystine and cysteine*. Cancer research* 70(1), 68-77 (2010).
313. Ishimoto T, Nagano O, Yae T *et al*. CD44 variant regulates redox status in cancer cells by stabilizing the xCT subunit of system xc(-) and thereby promotes tumour growth*. Cancer Cell* 19(3), 387-400 (2011).

314. Lu Y, Wang W, Wang J *et al*. Overexpression of arginine transporter CAT-1 is associated with accumulation of L-arginine and cell growth in human colorectal cancer tissue. *PloS one* 8(9), e73866 (2013).
315. Nicklin P, Bergman P, Zhang B *et al*. Bidirectional Transport of Amino Acids Regulates mTOR and Autophagy. *Cell* 136(3), 521-534 (2009).
316. Fuchs BC, Bode BP. Amino acid transporters ASCT2 and LAT1 in cancer: Partners in crime? *Seminars in cancer biology* 15(4), 254-266 (2005).
317. Sakata T, Ferdous G, Tsuruta T *et al*. L-type amino-acid transporter 1 as a novel biomarker for high-grade malignancy in prostate cancer. *Pathology international* 59(1), 7-18 (2009).
318. Wang Q, Hardie RA, Hoy AJ *et al*. Targeting ASCT2-mediated glutamine uptake blocks prostate cancer growth and tumour development. *The Journal of pathology* 236(3), 278-289 (2015).
319. Furuya M, Horiguchi J, Nakajima H, Kanai Y, Oyama T. Correlation of L-type amino acid transporter 1 and CD98 expression with triple negative breast cancer prognosis. *Cancer Sci* 103(2), 382-389 (2012).
320. Van Geldermalsen M, Wang Q, Nagarajah R *et al*. ASCT2/SLC1A5 controls glutamine uptake and tumour growth in triple-negative basal-like breast cancer. *Oncogene* 35(24), 3201-3208 (2016).
321. Fukumoto S, Hanazono K, Fu DR *et al*. A new treatment for human malignant melanoma targeting L-type amino acid transporter 1 (LAT1): a pilot study in a canine model. *Biochemical and biophysical research communications* 439(1), 103-108 (2013).
322. Wang Q, Beaumont KA, Otte NJ *et al*. Targeting glutamine transport to suppress melanoma cell growth. *International journal of cancer. Journal international du cancer* 135(5), 1060-1071 (2014).
323. Shimizu A, Kaira K, Kato M *et al*. Prognostic significance of L-type amino acid transporter 1 (LAT1) expression in cutaneous melanoma. *Melanoma research* 25(5), 399-405 (2015).
324. Hassanein M, Hoeksema MD, Shiota M *et al*. SLC1A5 Mediates Glutamine Transport Required for Lung Cancer Cell Growth and Survival. *Clinical Cancer Research* 19(3), 560-570 (2013).
325. Kaira K, Oriuchi N, Imai H *et al*. l-type amino acid transporter 1 and CD98 expression in primary and metastatic sites of human neoplasms. *Cancer Sci* 99(12), 2380-2386 (2008).
326. Kaira K, Oriuchi N, Imai H *et al*. Prognostic significance of L-type amino acid transporter 1 expression in resectable stage I-III nonsmall cell lung cancer. *Br J Cancer* 98(4), 742-748 (2008).
327. Huang F, Zhao Y, Zhao J *et al*. Upregulated SLC1A5 promotes cell growth and survival in colorectal cancer. *Int J Clin Exp Pathol* 7(9), 6006-6014 (2014).
328. Chen L, Cui H. Targeting Glutamine Induces Apoptosis: A Cancer Therapy Approach. *International journal of molecular sciences* 16(9), 22830-22855 (2015).
329. Arber DA, Orazi A, Hasserjian R *et al*. The 2016 revision to the World Health Organization classification of myeloid neoplasms and acute leukemia. *Blood* 127(20), 2391-2405 (2016).
330. Shafer D, Grant S. Update on rational targeted therapy in AML. *Blood reviews* 30(4), 275-283 (2016).

331. Austin R, Smyth MJ, Lane SW. Harnessing the immune system in acute myeloid leukaemia. *Critical reviews in oncology/hematology* 103 62-77 (2016).
332. Barrett AJ, Le Blanc K. Immunotherapy prospects for acute myeloid leukaemia. *Clin Exp Immunol* 161(2), 223-232 (2010).
333. Behl D, Porrata LF, Markovic SN *et al*. Absolute lymphocyte count recovery after induction chemotherapy predicts superior survival in acute myelogenous leukemia. *Leukemia* 20(1), 29-34 (2006).
334. Muller CI, Trepel M, Kunzmann R, Lais A, Engelhardt R, Lubbert M. Hematologic and molecular spontaneous remission following sepsis in acute monoblastic leukemia with translocation (9;11): a case report and review of the literature. *European journal of haematology* 73(1), 62-66 (2004).
335. Gambacorti-Passerini C, Grignani F, Arienti F, Pandolfi PP, Pelicci PG, Parmiani G. Human CD4 lymphocytes specifically recognize a peptide representing the fusion region of the hybrid protein pml/RAR alpha present in acute promyelocytic leukemia cells. *Blood* 81(5), 1369-1375 (1993).
336. Graf C, Heidel F, Tenzer S *et al*. A neoepitope generated by an FLT3 internal tandem duplication (FLT3-ITD) is recognized by leukemia-reactive autologous CD8+ T cells. *Blood* 109(7), 2985-2988 (2007).
337. Greiner J, Ono Y, Hofmann S *et al*. Mutated regions of nucleophosmin 1 elicit both CD4(+) and CD8(+) T-cell responses in patients with acute myeloid leukemia. *Blood* 120(6), 1282-1289 (2012).
338. Makita M, Azuma T, Hamaguchi H *et al*. Leukemia-associated fusion proteins, dek-can and bcr-abl, represent immunogenic HLA-DR-restricted epitopes recognized by fusion peptide-specific CD4+ T lymphocytes. *Leukemia* 16(12), 2400-2407 (2002).
339. Martner A, Thoren FB, Aurelius J, Hellstrand K. Immunotherapeutic strategies for relapse control in acute myeloid leukemia. *Blood reviews* 27(5), 209-216 (2013).
340. Lichtenegger FS, Krupka C, Haubner S, Kohnke T, Subklewe M. Recent developments in immunotherapy of acute myeloid leukemia. *Journal of hematology & oncology* 10(1), 142 (2017).
341. Quek L, Otto GW, Garnett C *et al*. Genetically distinct leukemic stem cells in human CD34- acute myeloid leukemia are arrested at a hemopoietic precursor-like stage. *The Journal of experimental medicine* 213(8), 1513-1535 (2016).
342. Booth CaG, Barkas N, Neo WH *et al*. Ezh2 and Runx1 Mutations Collaborate to Initiate Lympho-Myeloid Leukemia in Early Thymic Progenitors. *Cancer Cell* 33(2), 274-291.e278 (2018).
343. Bereshchenko O, Mancini E, Moore S *et al*. Hematopoietic stem cell expansion precedes the generation of committed myeloid leukemia-initiating cells in C/EBPalpha mutant AML. *Cancer Cell* 16(5), 390-400 (2009).
344. Kirstetter P, Schuster MB, Bereshchenko O *et al*. Modeling of C/EBPalpha mutant acute myeloid leukemia reveals a common expression signature of committed myeloid leukemia-initiating cells. *Cancer Cell* 13(4), 299-310 (2008).
345. Mortensen M, Soilleux EJ, Djordjevic G *et al*. The autophagy protein Atg7 is essential for hematopoietic stem cell maintenance. *The Journal of experimental medicine* 208(3), 455-467 (2011).

346. Riffelmacher T, Clarke A, Richter FC *et al*. Autophagy-Dependent Generation of Free Fatty Acids Is Critical for Normal Neutrophil Differentiation. *Immunity* 47(3), 466-480.e465 (2017).
347. Ritchie ME, Phipson B, Wu D *et al*. limma powers differential expression analyses for RNA-sequencing and microarray studies. *Nucleic Acids Res* 43(7), e47 (2015).
348. Subramanian A, Tamayo P, Mootha VK *et al*. Gene set enrichment analysis: a knowledge-based approach for interpreting genome-wide expression profiles. *Proceedings of the National Academy of Sciences of the United States of America* 102(43), 15545-15550 (2005).
349. Li H, Handsaker B, Wysoker A *et al*. The Sequence Alignment/Map format and SAMtools. *Bioinformatics* 25(16), 2078-2079 (2009).
350. Mccarthy DJ, Chen Y, Smyth GK. Differential expression analysis of multifactor RNA-Seq experiments with respect to biological variation. *Nucleic Acids Res* 40(10), 4288-4297 (2012).
351. Demaison C, Parsley K, Brouns G *et al*. High-level transduction and gene expression in hematopoietic repopulating cells using a human immunodeficiency [correction of imunodeficiency] virus type 1-based lentiviral vector containing an internal spleen focus forming virus promoter. *Human gene therapy* 13(7), 803-813 (2002).
352. Lee HH, Kim DJ, Ahn HJ, Ha JY, Suh SW. Crystal structure of T-protein of the glycine cleavage system. Cofactor binding, insights into H-protein recognition, and molecular basis for understanding nonketotic hyperglycinemia. *The Journal of biological chemistry* 279(48), 50514-50523 (2004).
353. Hsu PD, Lander ES, Zhang F. Development and applications of CRISPR-Cas9 for genome engineering. *Cell* 157(6), 1262-1278 (2014).
354. Chen J-L, Morgan AJ, Stewart-Jones G *et al*. Ca2+ Release from the Endoplasmic Reticulum of NY-ESO-1-Specific T Cells Is Modulated by the Affinity of TCR and by the Use of the CD8 Coreceptor. *Journal of Immunology* 184(4), 1829-1839 (2010).
355. Chen JL, Dunbar PR, Gileadi U *et al*. Identification of NY-ESO-1 peptide analogues capable of improved stimulation of tumour-reactive CTL. *Journal of Immunology* 165(2), 948-955 (2000).
356. Chen JL, Stewart-Jones G, Bossi G *et al*. Structural and kinetic basis for heightened immunogenicity of T cell vaccines. *Journal of Experimental Medicine* 201(8), 1243-1255 (2005).
357. Milne TA, Zhao K, Hess JL. Chromatin immunoprecipitation (ChIP) for analysis of histone modifications and chromatin-associated proteins. *Methods in molecular biology (Clifton, N.J.)* 538 409-423 (2009).
358. Wilkinson AC, Ballabio E, Geng H *et al*. RUNX1 is a key target in t(4;11) leukemias that contributes to gene activation through an AF4-MLL complex interaction. *Cell Rep* 3(1), 116-127 (2013).
359. Alipanahi B, Delong A, Weirauch MT, Frey BJ. Predicting the sequence specificities of DNA- and RNA-binding proteins by deep learning. *Nat Biotechnol* 33(8), 831-838 (2015).
360. Buenrostro JD, Giresi PG, Zaba LC, Chang HY, Greenleaf WJ. Transposition of native chromatin for fast and sensitive epigenomic profiling of open chromatin, DNA-binding proteins and nucleosome position. *Nat Methods* 10(12), 1213-1218 (2013).

361. Buenrostro JD, Wu B, Chang HY, Greenleaf WJ. ATAC-seq: A Method for Assaying Chromatin Accessibility Genome-Wide. *Current protocols in molecular biology* 109 21.29.21-29 (2015).
362. Grant CE, Bailey TL, Noble WS. FIMO: scanning for occurrences of a given motif. *Bioinformatics* 27(7), 1017-1018 (2011).
363. Khan A, Fornes O, Stigliani A *et al*. JASPAR 2018: update of the open-access database of transcription factor binding profiles and its web framework. *Nucleic Acids Res* 46(D1), D1284 (2018).
364. Khan A, Fornes O, Stigliani A *et al*. JASPAR 2018: update of the open-access database of transcription factor binding profiles and its web framework. *Nucleic Acids Res* 46(D1), D260-d266 (2018).
365. Khan A, Mathelier A. JASPAR RESTful API: accessing JASPAR data from any programming language. *Bioinformatics* 34(9), 1612-1614 (2018).
366. Geiger R, Rieckmann JC, Wolf T *et al*. L-Arginine Modulates T Cell Metabolism and Enhances Survival and Anti-tumour Activity. *Cell* 167(3), 829-842.e813 (2016).
367. Mussai F, De Santo C, Abu-Dayyeh I *et al*. Acute myeloid leukemia creates an arginase-dependent immunosuppressive microenvironment. *Blood* 122(5), 749-758 (2013).
368. Fuchs BC, Bode BP. Amino acid transporters ASCT2 and LAT1 in cancer: partners in crime? *Seminars in cancer biology* 15(4), 254-266 (2005).
369. Werner A, Koschke M, Leuchtner N *et al*. Reconstitution of T Cell Proliferation under Arginine Limitation: Activated Human T Cells Take Up Citrulline via L-Type Amino Acid Transporter 1 and Use It to Regenerate Arginine after Induction of Argininosuccinate Synthase Expression. *Front Immunol* 8 864 (2017).
370. Kremer JC, Prudner BC, Lange SES *et al*. Arginine Deprivation Inhibits the Warburg Effect and Upregulates Glutamine Anaplerosis and Serine Biosynthesis in ASS1-Deficient Cancers. *Cell Rep* 18(4), 991-1004 (2017).
371. Podust LM, Krezel AM, Kim Y. Crystal structure of the CCAAT box/enhancer-binding protein beta activating transcription factor-4 basic leucine zipper heterodimer in the absence of DNA. *The Journal of biological chemistry* 276(1), 505-513 (2001).
372. Tominaga H, Maeda S, Hayashi M *et al*. CCAAT/enhancer-binding protein beta promotes osteoblast differentiation by enhancing Runx2 activity with ATF4. *Molecular biology of the cell* 19(12), 5373-5386 (2008).
373. Rose NR, Klose RJ. Understanding the relationship between DNA methylation and histone lysine methylation. *Biochimica et biophysica acta* 1839(12), 1362-1372 (2014).
374. Zhao E, Ding J, Xia Y *et al*. KDM4C and ATF4 Cooperate in Transcriptional Control of Amino Acid Metabolism. *Cell Rep* 14(3), 506-519 (2016).
375. Liang G, Hai T. Characterization of human activating transcription factor 4, a transcriptional activator that interacts with multiple domains of cAMP-responsive element-binding protein (CREB)-binding protein. *The Journal of biological chemistry* 272(38), 24088-24095 (1997).
376. Mann IK, Chatterjee R, Zhao J *et al*. CG methylated microarrays identify a novel methylated sequence bound by the CEBPB|ATF4 heterodimer that is active in vivo. *Genome Res* 23(6), 988-997 (2013).

377. Vallejo M, Ron D, Miller CP, Habener JF. C/ATF, a member of the activating transcription factor family of DNA-binding proteins, dimerizes with CAAT/enhancer-binding proteins and directs their binding to cAMP response elements. *Proceedings of the National Academy of Sciences of the United States of America* 90(10), 4679-4683 (1993).
378. Petruk S, Cai J, Sussman R *et al*. Delayed Accumulation of H3K27me3 on Nascent DNA Is Essential for Recruitment of Transcription Factors at Early Stages of Stem Cell Differentiation. *Mol Cell* 66(2), 247-257.e245 (2017).
379. Bird A. The essentials of DNA methylation. *Cell* 70(1), 5-8 (1992).
380. Maurano MT, Wang H, John S *et al*. Role of DNA Methylation in Modulating Transcription Factor Occupancy. *Cell Rep* 12(7), 1184-1195 (2015).
381. Medvedeva YA, Khamis AM, Kulakovskiy IV *et al*. Effects of cytosine methylation on transcription factor binding sites. *BMC genomics* 15 119 (2014).
382. Tsai WB, Long Y, Chang JT *et al*. Chromatin remodeling system p300-HDAC2-Sin3A is involved in Arginine Starvation-Induced HIF-1alpha Degradation at the ASS1 promoter for ASS1 Derepression. *Sci Rep* 7(1), 10814 (2017).
383. Philip M, Fairchild L, Sun L *et al*. Chromatin states define tumour-specific T cell dysfunction and reprogramming. *Nature* 545(7655), 452-456 (2017).
384. Tyrakis PA, Palazon A, Macias D *et al*. S-2-hydroxyglutarate regulates CD8(+) T-lymphocyte fate. *Nature* 540(7632), 236-241 (2016).